Deliverable No. D1.6

Public summary report of WP1

Grant Agreement no.:	945253
Project Title:	**Advanced PTS Analysis for LTO**
Contractual Submission Date:	30/09/2021
Actual Submission Date:	20/12/2021
Responsible partner:	P6: TECNATOM

Grant agreement no.	945253
Project full title	Advanced PTS Analysis for LTO

Deliverable number	**D1.6**
Deliverable title	**Public summary report of WP1**
Type[1]	R
Dissemination level[2]	PU
Work package number	WP1
Work package leader	P6 - TECNATOM
Author(s)	Carlos Cueto-Felgueroso (Tecnatom), Vladislav Pistora (UJV), Szabolcs Szavai (BZN), Maksym Zarazovskii (IPP-CENTRE), Ivor Clifford (PSI), Pavel Kral (UJV)
Keywords	Pressurised Thermal Shock (PTS), reactor pressure vessel (RPV), integrity assessment, Thermal-hydraulics (TH), Human interactions, warm pre-stress (WPS), residual stresses, fracture toughness, fracture mechanics, probabilistic fracture mechanics, Monte Carlo, FORM, SORM, Long Term Operation (LTO).

The author is solely responsible for its content, it does not represent the opinion of the European Commission and the Commission is not responsible for any use that might be made of data appearing therein.

---

[1] **Type**: Use one of the following codes (in consistence with the Description of the Action):
    R: Document, report (excluding the periodic and final reports)
    DEM: Demonstrator, pilot, prototype, plan designs
    DEC: Websites, patents filing, press & media actions, videos, etc.
    OTHER: Software, technical diagram, etc.

[2] **Dissemination level**: Use one of the following codes (in consistence with the Description of the Action)
    PU: Public, fully open, e.g. web
    CO: Confidential, restricted under conditions set out in the Model Grant Agreement
    CI: Classified, information as referred to in Commission Decision 2001/844/EC

Table of Contents

1 Abbreviations

ASME	American Society of Mechanical Engineers
ATLAS+	Advanced Structural Integrity Assessment Tools for Safe Long Term Operation (Horizon 2020 project)
BC	Boundary condition
BEPU	Best estimate plus uncertainty
CCA	Compact Crack Arrest
CCSF	Countercurrent Stratified Flow
CF	Cool–Fracture
CFD	Computational Fluid Dynamics
CMFD	Computation Multi-Fluid Dynamics
CPI	Conditional probability of initiation
CPTWC	Conditional probability of through-wall cracking
CRS	Cladding residual stress
CT	Compact Tension specimen
CTB	Critical temperature of brittleness
CTE	Coefficient of thermal expansion
CV	Coefficient of Variation
CVCS	Chemical and Volume Control System (in PWRs)
DC	Downcomer
DCC	Direct contact condensation
DEFI-PROSAFE	Definition of reference case studies for harmonized Probabilistic evaluation of Safety margins in integrity assessment for long-term operation of reactor pressure vessel (NUGENIA+ project)
DES	Detached Eddy Simulation
DN	Nominal diameter of a pipe
DNS	Direct Numerical Simulation
ECC	Emergency Core-Cooling
ECCS	Emergency Core-Cooling System
ENIQ	European Network for Inspection & Qualification
ENSI	Swiss Federal Nuclear Safety Inspectorate
EOL	End of Life
EOP	Emergency Operating Procedures
FAVOR	Fracture Analysis of Vessels–Oak Ridge (software)

FEA	Finite Element Analysis	
FEM	Finite Element Model	
FM	Fracture Mechanics	
FWLB	Feed Water Line Break	
HAZ	Heat affected zone	
HPIS	High Pressure Injection System	
HPSI	High Pressure Safety Injection	
I&C	Instrumentation and Control	
IAEA	International Atomic Energy Agency	
IF-LOCA	Interface Loss of Coolant Accident	
IVMR	In-Vessel Melt Retention	
ISI	In-Service Inspection	
KTA	Nuclear Safety Standards Commission (German standard)	
LB-LOCA	Large Break Loss of Coolant Accident	
LCF	Load–Cool–Fracture	
LIF	Laser Induced Fluorescence	
LOFT	Loss of Fluid Test	
LPIS	Low Pressure Injection System	
LEFM	Linear-Elastic Fracture Mechanics	
LES	Large Eddy Simulation	
LOCA	Loss of Coolant Accident	
LPTUF	Load–Partial Transient Unload–Fracture	
LPUCF	Load–Partial Unload–Cool–Fracture	
LSTF	Large-Scale Test Facility	
LTO	Long Term Operation	
LTOP	Low Temperature Overpressure Protection	
LTUF	Load–Transient Unload–Fracture	
LUCF	Load–Unload–Cool–Fracture	
MC	Monte Carlo	
MSLB	Main Steam Large Break	
NDT	Non-Destructive Testing	
NPP	Nuclear Power Plant	
NTD AME	Normative Technical Documentation of Association of Mechanical Engineers (Czech standard)	
NUGENIA	Nuclear Generation II & III Alliance	

NURESIM	NUclear REactor SIMulation (6th Framework Programme project)
ORNL	Oak Ridge National Laboratory
PFM	Probabilistic Fracture Mechanics
PIRT	Phenomena Identification and Ranking Tables
PIV	Particle Image Velocimetry
PORV	Power-Operated Relief Valve
PRA/PSA	Probabilistic Risk Assessment/ Probabilistic Safety Assessment
PRISE	Primary to secondary leak
PRZ	Pressurizer
PRZ SV	Pressurizer Safety Valve
PTS	Pressurised Thermal Shock
PWHT	Post-weld heat treatment
PWR	Pressurized Water Reactor
RANS	Reynold-Averaged Navier-Stokes
RCP	Reactor Coolant Pump
ROSA	Rig-of-Safety Assessment
RPV	Reactor Pressure Vessel
RS	Residual stresses
SA	Sensitivity Analysis
SB-LOCA	Small-Break Loss-Of-Coolant-Accident
SD	Standard deviation
SDA	Steam Dump to Atmosphere
SE	Standard error
SENB	Single Edge Notched Bend specimen
SI	Safety injection
SIF	Stress intensity factor
SG	Steam Generator
SOV	Stuck-Open Valve
SS	Surveillance specimen
SSCs	Structures, Systems and Components
SUSA	Software for Uncertainty and Sensitivity Analyses
TDA	Température descente annulaire
TH	Thermal Hydraulic
TP	Tangent Point approach for RPV brittle fracture assessment
TSO	Technical Support Organisation

TWCF	Through-wall crack frequency
UCC	Underclad cracking
UQ	Uncertainty quantification
UPTF	Upper Plenum Test Facility
US NRC	U.S. Nuclear Regulatory Commission
WP	Work Package
WPS	Warm Pre-Stress
WRS	Welding residual stress
WWER / VVER	Water Cooled Water Moderated Power Reactor

2   Introduction

The reactor pressure vessel (RPV) represents a key component of a nuclear power plant (NPP) and its integrity must be ensured throughout its entire operating time in accordance with applicable regulations.

The dominant and expected type of damage in the RPV is embrittlement under neutron irradiation of the RPV, especially in the core (beltline) area. If in an embrittled RPV a flaw of critical size existed and if certain severe system transients occurred, the flaw could propagate very rapidly through the vessel, possibly resulting in a through-wall crack and challenging the integrity of the RPV.

The Pressurized Thermal Shock (PTS) analysis is a part of RPV structural integrity assessment. PTS is characterized by a rapid cooling (i.e., thermal shock) of the downcomer and internal RPV surface, followed sometimes by re-pressurization of the RPV. Thus, a PTS event poses a potentially significant challenge to the structural integrity of the RPV in pressurized water reactors (PWRs) and water cooled water moderated energy reactors (WWERs).

In the European Union, currently used PTS analyses are based on deterministic assessment and conservative boundary conditions. This type of PTS analyses is reaching its limits in demonstrating the safety for PWRs and WWERs facing Long Term Operation (LTO) and need to be enhanced. However, inherent safety margins exist and several LTO improvements and advanced methods are intended to increase the safety margins of PTS analysis. Additionally, the quantification of safety margins in terms of risk of RPV failure by advanced probabilistic assessments becomes more and more important as the probabilistic methods ensure more comprehensive assessment in PTS analysis and enable the quantification of uncertainties of results.

To address that challenge, the APAL project (Advanced PTS Analyses for LTO) has been launched in October 2020 with funding from EURATOM Work Programme 2019-2020 and with a duration of four years. The main objectives of the APAL project are the development of advanced probabilistic PTS assessment method, quantification of safety margins for LTO improvements and the development of best-practice guidance. The project will address multidisciplinary and multi-physics challenges related to RPV safety assessment of PTS. The planned work to achieve these objectives is divided into six technical work packages (WPs).

The first part (WP1 *LTO improvements relevant for PTS analysis*) consists of an extensive literature review and collection of experience to identify the state-of-the-art of LTO improvements (hardware and software) that may have an either beneficial or adverse impact on the results of PTS analysis. This includes the identification of technology gaps and the definition of possible improvements. Furthermore, the human factor relevant during a PTS event will be identified (and quantified) based on available operator experience and expert judgement.

After establishing the LTO improvements, thermal-hydraulic (TH) calculations will be performed including also uncertainty quantification relevant to the PTS assessment (WP2). The impact of both LTO improvements and human factor on the results of TH analysis will be quantified and later assessed by subsequent structural and fracture mechanics benchmarks within WP3 and WP4.

The third work package (WP3) will consist in performing deterministic structural and fracture mechanics analyses to quantify the safety margins related to both LTO improvements and uncertainties in TH analysis. The analyses to be used for deterministic margin assessment will be carried out based on a common deterministic benchmark.

In the fourth work package (WP4), probabilistic margin assessment based on probabilistic fracture mechanics analysis will be performed. The assessment will allow the quantification of safety margins in terms of risk of RPV failure. An advanced probabilistic PTS assessment will be performed by considering the TH uncertainties in the subsequent structural mechanics and probabilistic fracture mechanics analyses. An appropriate benchmark for the probabilistic fracture mechanics analysis will be defined in accordance with the benchmark performed for deterministic margin assessment.

The fifth work package (WP5) will gather recommendations and conclusions from performed work to define the best-practices for an advanced PTS analysis for LTO. Close cooperation with Advisory Board (AB), regulatory bodies and end-users (NPP owners, suppliers, etc.) during the project will help to increase the acceptance of the best-practice guidance. For that purpose, several workshops will be organized (WP6) to discuss the best-practice guidance with regulatory bodies and main end-users in order to analyse potential barriers, integrate feedback and obtain broad acceptance of the best-practice guidance for an advanced PTS analysis for LTO within the nuclear community.

The interaction of WPs within APAL is shown in the diagram below:
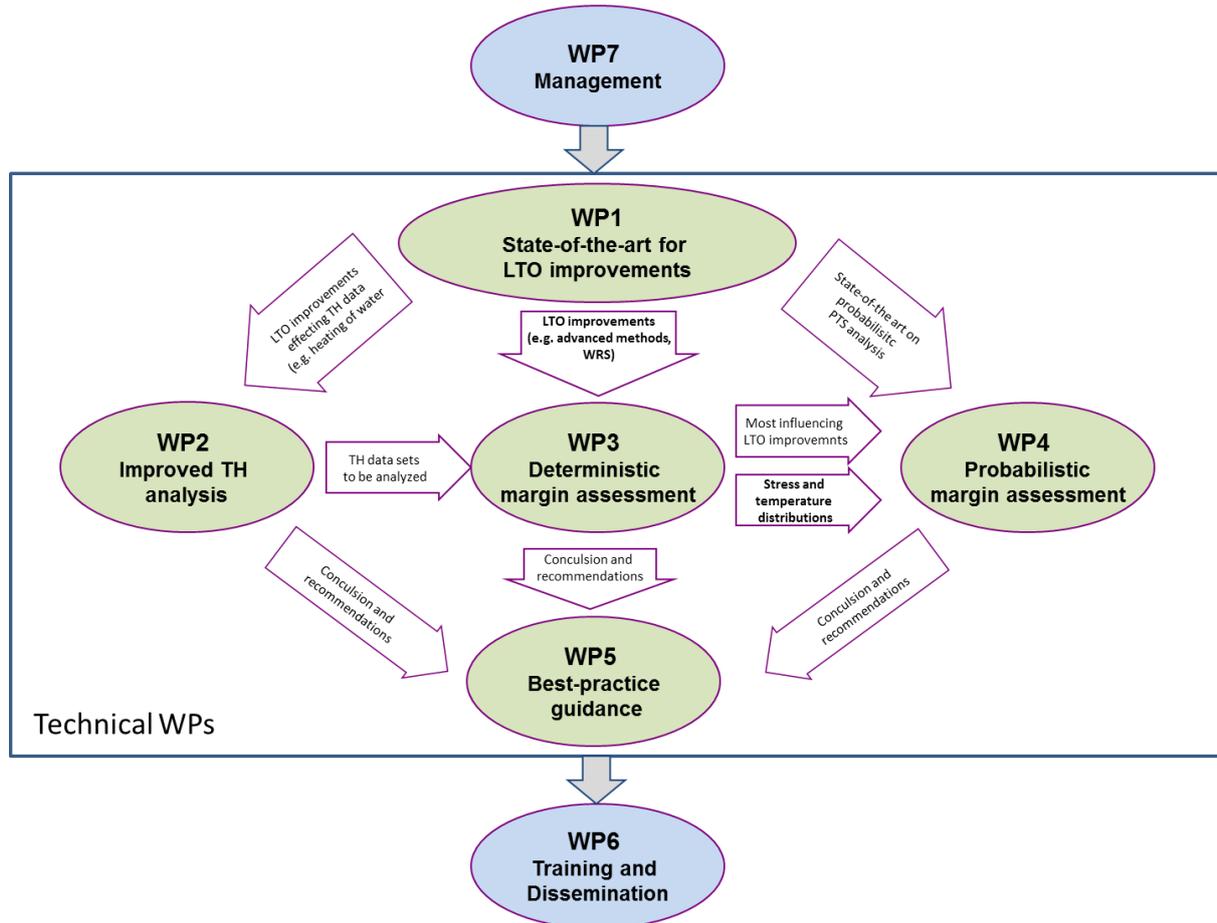
This report summarizes the main results from the activities in WP1.

Four LTO improvements have been defined a-priori to be reviewed/investigated in more detail, resulting in the following subtasks in WP1:

- Residual stress distributions for welds (WRS) and cladding (Task 1.1).
- Warm pre-stress (WPS) approach applied in PTS (Task 1.2).
- Thermal-hydraulic (TH) analysis (including definition of human factor) (Task 1.3).
- Probabilistic PTS analysis (Task 1.4).

In addition, another subtask (Task 1.5) is dedicated to the investigation of further potential LTO improvements relevant for PTS analysis.

Within each subtask, an extensive literature review and collection of experience from APAL partners were performed to identify the state-of-the-art of LTO improvements. The state-of-the-art reviews include:

- Collection of existing solutions/approaches for assessment of LTO improvements.
- Collection of existing assessments.
- Identification of gaps and possible improvements.

The process was carried out through the preparation of technical questionnaires covering relevant issues for every task. Involved partners had to complete the questionnaires based on their experience in the analysis carried out in their countries. In addition, additional information from some partners was provided to get a better understanding of specific assessments or LTO improvements. Based on the compilation of answers, additional information and discussions during various task meetings, the state-of-the-art of the investigated LTO improvements have been summarized. Moreover, common understanding of best-practice on some topics have been agreed between the partners. Besides, some gaps and conclusions were collected to be assessed in WP2, WP3 and WP4.

3   Objective and methodology

The objective of this deliverable is to summarize in a public document the results of WP1, identifying the gaps, and to expose main conclusions and recommendations to be incorporated in the best-practice document for PTS analysis (WP5).

4   State-of-the-art on weld residual stress (WRS)

The relevance of residual stresses (RS) for both welds and cladding and also for heat affected zone (HAZ) should be evaluated in PTS analyses. Weld residual stress (WRS) distributions are generally based on measurements on specimens in absence of cracks and on calculations. Proposed WRS distributions and calculation methodologies in the literature, as well as the relevance of the potential WRS relaxation when a crack develops in the RPV wall, were investigated in Task 1.1.

The results of the Task 1.1 *State-of-the-art for weld residual stress* are summarized in this section.

4.1   Overview

Pressurized thermal shock (PTS) is one of the most important issues in assessing the structural integrity of reactor pressure vessel (RPV). During the analyses, it is requested to evaluate residual stresses in the seam welds in the RPV beltline zone, in the austenitic cladding and in the heat affected zones, and to identify the effects of residual stress on fracture mechanics analysis in order to assess the RPV structural integrity.

Temperature and stress distributions in the RPV wall during PTS transients are also needed to assess the RPV integrity.

4.2   Description of Activities

To achieve the objectives of Task 1.1, a questionnaire was prepared, discussed among the partners and distributed among them for their response. This questionnaire focuses on the following points:

- collection of existing residual stress (RS) approaches/models for RPV brittle fracture assessment in PTS events/analyses,
- collection of existing experimental data,
- analysis of the existing RS approaches/models,
- identification of gaps and possible improvements.

The work was built upon national approaches, standards, and existing knowledge from project partners.

In total, 11 responses to the questionnaire were obtained, which are summarised in this section. The responding countries, persons and partners are listed below:

Country	Partner	Contributing Author
Czech Republic	UJV	Vladislav Pistora
Germany	Framatome	Florian Obermeier
Switzerland	PSI	Diego Mora
Ukraine	IPP-CENTRE	Maksym Zarazovskii and Yaroslav Dubyk
Sweden	KIWA	Daniel Mångård and Jens Gunnars
Spain	Tecnatom	Carlos Cueto-Felgueroso
Hungary	BZN	Judit Dudra and Szabolcs Szávai
Slovenia	JSI	Oriol Costa
France	IRSN	Christophe Blain
Japan	JAEA	Jinya Katsuyama
USA	OCI	B. Richard Bass and Paul T. Williams

Blank of the RS questionnaire can be found in Annex A *Task 1.1 Partner Questionnaire*

The main conclusions drawn from the evaluation of the answers are summarised in Section 4.4.

4.3 Main topics

4.3.1 Critical locations

To demonstrate the RPV integrity under conditions leading to a pressurized thermal shock (PTS), it is common practice to postulate flaws at critical locations and to perform a brittle fracture analysis. This requires determining the stress intensity factor of the postulated flaw that is driven by internal pressure, thermal loading and residual stresses and compare it to the fracture toughness of the material.

During the assessment of a PTS scenario, different locations of the RPV are considered. Postulated flaws are placed in regions with high crack tip loading (e.g., nozzle corners) and regions with the highest fluence (beltline zone / core weld).

The purpose of this section is to summarise the critical locations identified, where, according to the participants, residual stresses should be considered, and to present the most suitable methodologies to determine RS.

4.3.1.1 Reactor pressure vessel weld residual stresses

The beltline region of an RPV is fabricated using either forged-ring or rolled-plate segments. RPVs made with forgings have only girth (circumferential) welds, and plate-type vessels have both girth and longitudinal (axial) welds, as shown in **Figure *1***. The vessels are typically constructed of special pressure vessel ferritic steels. The heavy-section steel wall is lined with an internal cladding of stainless steel. After welding and cladding, the RPV is heat treated, partially relieving weld residual stresses.

The main factors that affect the level of the weld residual stress (WRS) are:

- welding technology and materials,
- welding sequence and the location of the weld root,
- stress relieving heat treatment, namely temperature and time of tempering.

The level of the maximum residual stress depends on the parameters of the stress relieving heat treatment (temperature and time of tempering) and the material properties of the weld.

Residual stresses can influence the fracture mechanics assessment results depending on their magnitude and the way how they are treated within the analyses. Over the recent years, there has been a major progress in better understanding of weld residual stresses, in particular, due to the availability of advanced weld residual stress modelling tools.

4.3.1.2 Cladding residual stresses

To protect the reactor pressure vessel (RPV) - made of ferritic low-alloy steel - from primary water corrosion, the inner surface is frequently coated with a thin layer of corrosion resistant material, for which austenitic steel cladding is widely practiced.

In principle, one or multiple layers are used for cladding. The effects of cladding can be different for different types of reactors, e.g., PWR (pressurized water-reactor), BWR (boiling water-reactor) or WWER (water cooled and water moderated energy reactor), which is the consequence of different welding processes, different values of thermal expansion coefficient of austenitic cladding and ferritic material and also due to different tensile and toughness properties.

In the case of two-layer cladding, both cladding layers have different chemical compositions and also different tensile and toughness properties. Properties of both layers are also affected by neutron irradiation even though to smaller extent than RPV ferritic materials.

Based on the above, it can be stated that cladding residual stresses have to be considered during the analyses. One way to do this is to apply an approximate description using a stress-free temperature (T_{sf}), which should be chosen to produce appropriate levels of residual stress at room temperature.

The value of stress-free temperature depends on material properties, the manufacturing procedure, and the influence of the hydro test.

When measured data of cladding residual stresses are available (experimental data) they can be considered in defining the stress distribution in the cladding.
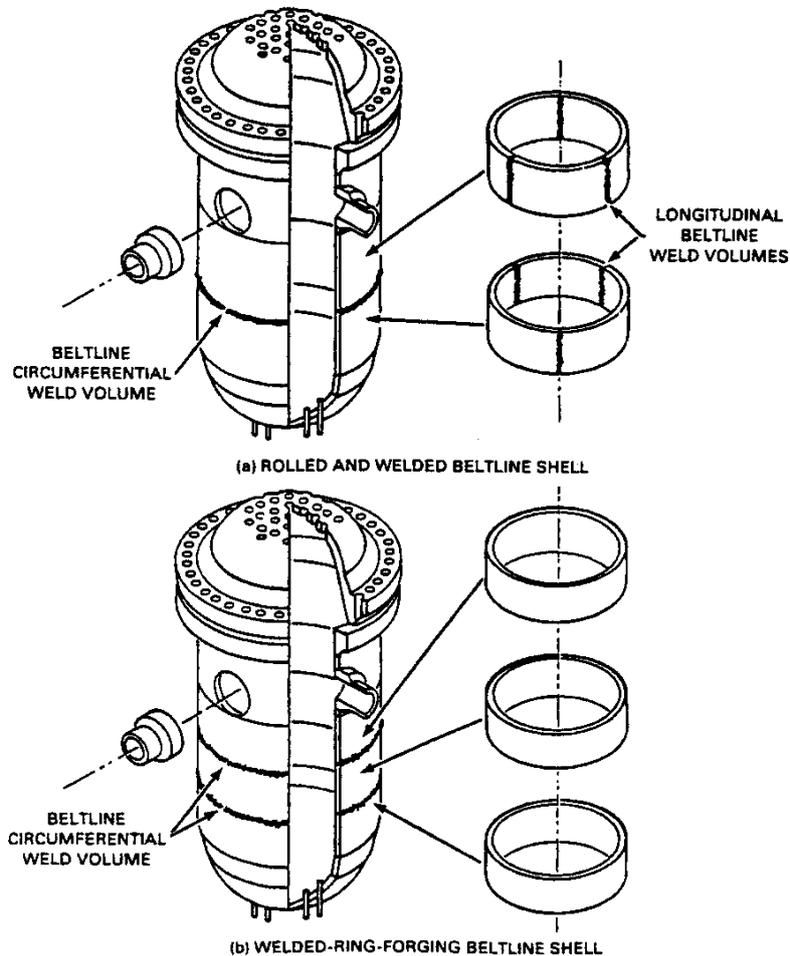
Figure 1: Fabrication configurations of PWR beltline: (a) rolled-plate construction with longitudinal and circumferential welds and (b) ring-forging construction with circumferential welds only.

4.3.2   PTS analyses in which RS should be considered.

In addition to the critical location, it is also important to define the operating conditions where residual stresses should be applied to demonstrate the RPV integrity. The partners' practices should be investigated in relation to

- The consideration of residual stresses not only for emergency and faulted conditions but also for normal operation,
- The treatment of residual stresses for brittle fracture and for ductile tearing assessments.

4.3.3   Methodologies to determine RS

There are three main methodologies to determine RS, which differ in the level of difficulty to obtain them:

- Take RS from standards,
- Calculate RS from a detailed FEM analysis,
- Determine RS based on measurements.

A short explanation of each method is provided below.

4.3.3.1   RS taken from standards or other literature

In order to provide a reasonable and practical way to deal with RS in the case of RPV assessments, several standards and codes solutions for RS profiles in welds and cladding are available. These distributions were in general obtained in the absence of crack(s).

Czech Republic

RS for assessment of RPV resistance against fast (brittle) fracture are taken from the Czech standard NTD-AME Section IV [8]. Its approach to RS is based on Russian standard MRKR–SKhR–2004 [25]. The paper by V. I. Kostylev and B. Z. Margolin [29] contains the technical basis for this RS distribution.

Basic assumptions:

RS magnitude in cladding is taken as 390 MPa (at room temperature). Weld residual stress profile through the RPV wall thickness is considered as cosine with adjustment for HAZ. RS profile through the RPV wall thickness in base metal is considered as stepwise with adjustment for HAZ (see **Figure 2**).

a)   b)
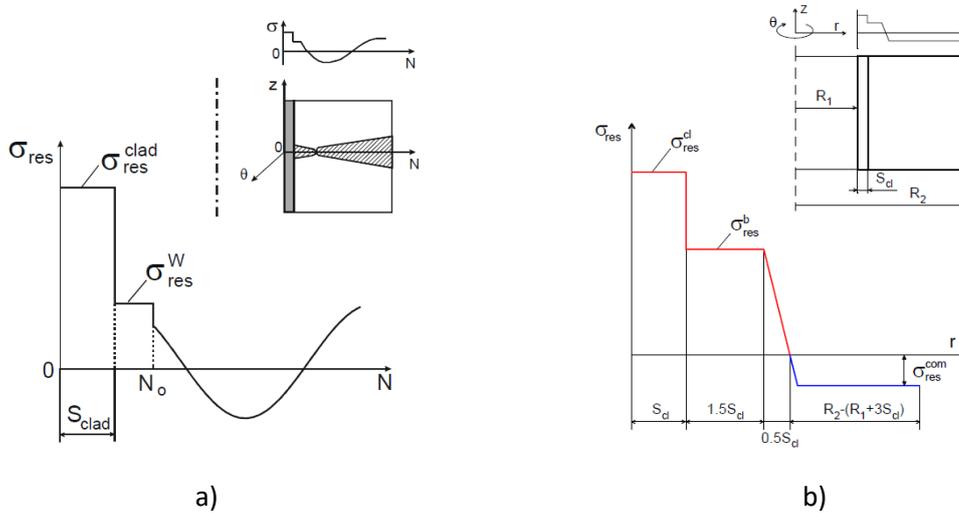
Figure 2: RS profile through the RPV wall thickness in a) weld, b) base metal.

Inputs:

The magnitude of RS in HAZ due to cladding and in weld is taken based on diagrams in the standard in dependency on duration and temperature of tempering (see **Figure 3**).
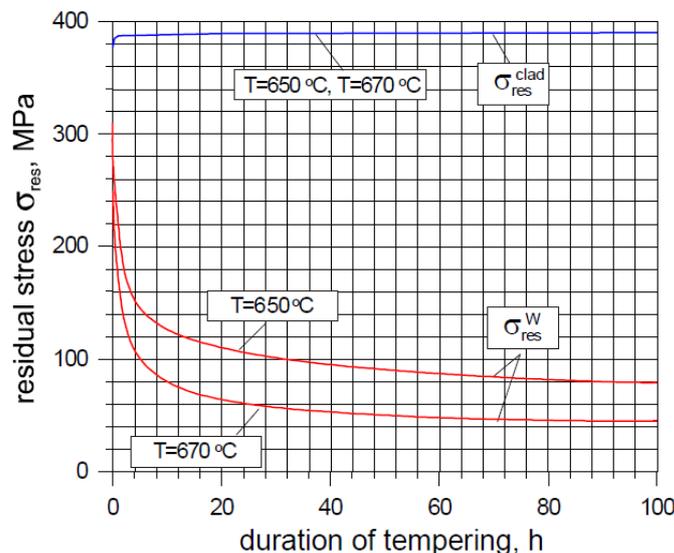
Figure 3: Dependency of RS magnitude on duration and temperature of tempering.

Introducing of RS based on measurement or based on detailed calculation is acceptable by the Czech standard, but no detailed procedure for the calculation is provided in the Czech standard. The detailed calculation of RS has not been applied in practice yet.

RS redistribution due to pressure test and/or operational load:
The RS are introduced (by introducing initial strains which produce the required RS) at the beginning of the calculation process. Subsequently, hydrotest is modelled, which can redistribute the residual strains and stresses. Subsequently, PTS is simulated.

RS are considered as deterministic parameters even in probabilistic PTS assessment. No uncertainties for RS are considered. RS taken according to the standard are supposed to be conservative.

Germany
According to the German KTA standard [9] the weld residual stress shall be considered by applying a constant value of $56\ MPa$ across the wall thickness in parallel to the weld if no other value can be determined. The irregular distribution transversal to the weld may be considered by means of the following equation:

$$\sigma_{eigen(x,t)} = 56\ MPa * \cos\left(2\pi x/t\right)$$

with x being the current coordinate along the path through the wall and t being the wall thickness without cladding.

The consideration of residual stresses resulting from the cladding procedure is not explicitly described in the KTA. For residual stresses in the cladding itself, it is common practice in Germany to consider the operating temperature as a stress-free temperature for the cladding in the FEA if no detailed information is available. Therefore, the stresses due to different thermal expansion coefficients of base and clad material lead to a conservative stress generation during the thermal transients. Residual stress in the HAZ is considered in the analysis if the material properties are available (Young's modulus, strain-stress curve, RT_{NDT}).

Basic assumptions:
The simplified approach given in the KTA standard is based on work published by D.A. Ferrill, P.B. Juhl and D.R. Miller in 1966 [30]. They measured residual stresses on a ferritic plate (ASTM A302 Gr. B) before and after post weld heat treatment (PWHT). The two halves of the plate with a thickness of 5 inch (127 mm) each were welded together using the submerged arc welding technique. This setup was assumed to be representative for a RPV girth weldment, but it did not consider the overlay cladding. The subsequent PWHT was performed at 620 °C for 6 hours. Afterwards, residual stresses were measured by strain gauges placed in several drilled holes in the specimen. These gauges were used to measure the relaxation during sawing of the weldment into prismatic bars. They concluded that the maximum residual stresses at room temperature were reduced from tensile yield strength level before PWHT down to $8000\ psi$ ($\sim 56\ MPa$) after PWHT.

Inputs:
The simple analytical formulation given in the KTA standard requires only the wall thickness as input.

RS redistribution due to pressure test and/or operational load:
The stresses and strains calculated during the WRS simulation are used as input parameters for the pressure test or operational load calculations. These can be simulated as additional steps within the WRS simulation or by transferring the results to a new finite element analysis. If the WRS simulation was performed as a 2D axisymmetric analysis the results can be transformed and transferred into a 3D RPV model.

Uncertainty distributions:
No uncertainties for RS are usually considered but the scatter due the methodology adopted to estimate the RS (the measurement) as well as the calculation has been reduced due to advances in knowledge. Another point is the scatter (non-symmetrical) in RS distribution (azimuthal direction of RPV in case of two forgings welded together), which is usually not considered.

The used method is validated by taking part in round robin projects [31] or by comparison with actual measurements.

Switzerland

RS were considered based on the IAEA-TECDOC-1627 [6] and the residual stresses were determined using the FAVOR code (see below).

Basic assumptions:

The WRS is determined as $\sigma_R = 56 \cdot \cos(2\pi x/t)\ MPa$ and in FAVOR code as $\sigma_R = 44 \cdot \cos(2\pi x/t)\ MPa$. This value is prescribed in a finite element simulation in ABAQUS based on the radial and circumferential coordinates of the point of analysis. During the calculations, RS are assumed deterministic and correspond to the values in FAVOR code according to the reference [32].

Inputs:

For welds, the stress is initialized in the model according to the previous equations at room temperature and a subsequent analysis step allows the stress to self-equilibrate. The magnitude of RS is kept constant in time.

For cladding, in FAVOR, it is assumed that the residual stress at room temperature is $146.9\ MPa$. Stress-free temperature is set to $280.3\ °C$. Temperature dependent material properties are used.

US, Slovenia, Spain (RS approach in FAVOR code)

Basic assumptions:

The residual stresses implemented in FAVOR were obtained experimentally and with numerical analyses of a RPV shell segment with a structural weld from a cancelled pressurized water reactor plant in the US.

The RS profile through the RPV wall thickness in welds available in FAVOR is shown in **Figure 4**. At the inner surface, a $6.5\ ksi\ (\sim 45\ MPa)$ tensile stress is observed. This stress profile, which does not include the cladding RS described above, is re-scaled in the wall-thickness direction to adapt the profile to the studied RPV wall thickness.
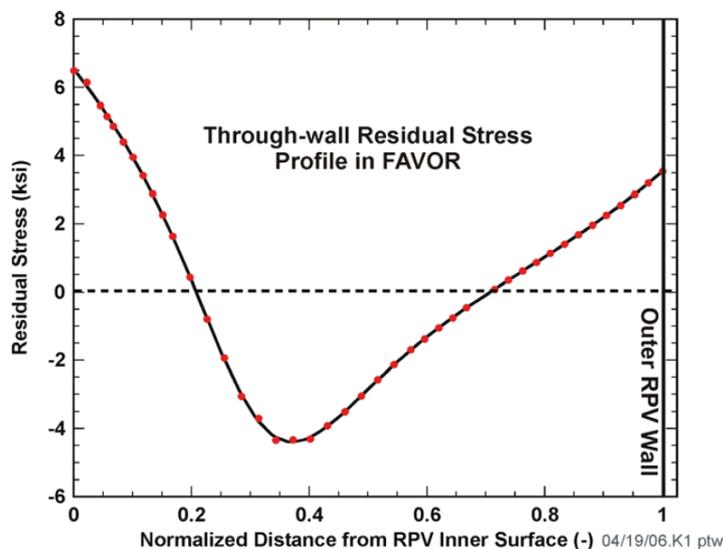
Figure 4: Welding residual stresses in FAVOR 16.1 [13].

In the FAVOR code, the specification of a selected stress-free temperature (T_{sf}) allows the user to include the effects of an initial difference in thermal expansion coefficients between the cladding and base materials (i.e., cladding RS). Thus, the cladding RS are introduced by thermal strains mismatch between the cladding and base materials. With a T_{sf} equal to $488\ °F\ (\sim 253\ °C)$, a reference temperature (T_{ref}) equal to $70°F\ (\sim 21°C)$ and temperature dependent material properties, the through-cladding average tensile stress of about $21.3\ ksi\ (\sim 147\ MPa)$ is obtained. Because T_{sf} and

19

T_{ref} usually differ, the thermal expansion coefficient is re-scaled within FAVOR to assure the strain free condition at T_{sf}.

These residual stresses can have a significant impact on the probability of cleavage initiation of shallow surface flaws under normal operational loading of the RPV (see subsections 4.4.4.2 and 4.4.5).

Inputs:
The values that influence the cladding RS are T_{sf} and T_{ref}. The shape and magnitude of the WRS profile shown in the **Figure 4** are fixed.

Uncertainty distributions:
The uncertainty distributions were not derived/considered in the development of the FAVOR RS. Within the code, the RS are assumed deterministic in both deterministic and probabilistic calculations.

Ukraine
RS for assessment of RPV resistance against brittle fracture are taken from Ukrainian standard PM-T.0.03.415-16 [33] which refers to the IAEA recommendation [7] ($\sigma_R = 60 \cdot \cos(2\pi x/t) \ MPa$).

Basic assumptions:
RS stress profile through the weld is considered to be a cosine. RS profile due to cladding is considered as a step function.

Inputs:
In case of using IAEA recommendation [7] no other inputs are needed. From the other hand, according to clause G.3 of Annex G of SOY NAEK 177:2019 [34] RS distribution is allowed to be defined in result of simulation.

The strain field is inserted to the FEM model for further elastic-plastic fracture mechanics calculations. During the calculation ANSYS mechanical software was used.

RS redistribution due to pressure test and/or operational load:
Only the stress-free temperature is adjusted. In case of FEM calculation of RS the redistribution due to hydrotest is calculated.

Sweden
RS are taken from standards if there is a representative reference available for the case in question.

The reference must be representative in terms of geometry, material, groove, passes and heat input. It is assumed that the reference is based on a common combination of these, and the current analysis case must be sufficiently similar (no significant deviation from the assumed common parameters), e.g., neighbouring weld within characteristic distance and welding performed with multiple coincident start/stop positions (as opposed to axisymmetry).

Hungary
The residual stress distribution in welds has been taken as follows [19]:

$$\sigma_R = \sigma_{Rmax} \cdot \cos(2\pi x/t),$$

where $\sigma_{Rmax} = 60 \ MPa$, x is the coordinate in weld thickness direction starting from the cladding/weld metal interface, and t is weld thickness (without cladding).

The cladding residual stresses have been taken into account, applying a stress-free temperature (T_{sf}), which has been chosen equal to the operating temperature of the corresponding component. Calculations and measurements were performed to show that this is a conservative assumption.

France
Predefined residual stress profiles were proposed by industrials (see **Figure 5**) based on a literature study including engineering, R&D measurements and international standards. The proposed RS profiles were verified by FEM analysis using Code_Aster. Measurements will further be performed by industrials to validate the FEM analysis and to confirm the conservativeness of the proposed RS profiles.
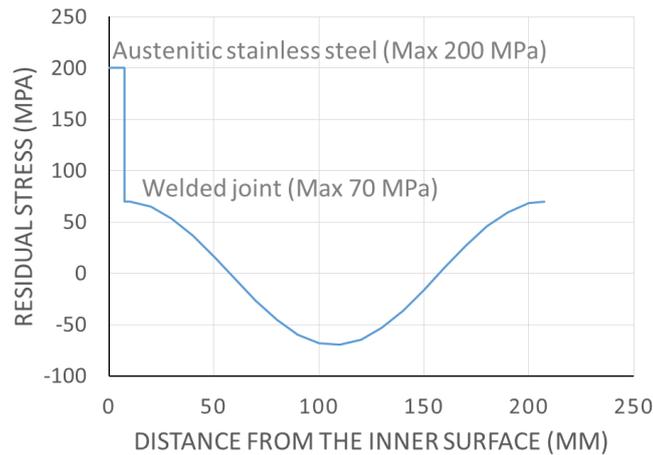
Figure 5: RS profiles as a function of distance from the inner surface.

The RS is postulated in the post weld heat treatment state of the RPV. The impact of pressure test (hydro-test) is taken into account in the evaluation of RS (FEM analysis). Thereafter, eventual evolution of RS caused by in-service loadings is neglected.

Japan
There is no description of RS distribution to be used in PTS assessment of RPV in Japanese codes, but the technical basis of RS distribution used in the assessment shall be justified.

4.3.3.2   RS calculations

Another way to determine RS is throughout detailed FEM calculations. This RS numerical simulation is still a challenging task since a lot of input data is required:

- Material (stress-strain curves, creep curves, mechanical and thermal properties in a wide range of temperatures, phase transformation),
- Welding processes information (welding conditions, bead dimensions, heat profiles),
- Post weld heat treatment (temperature, time, heating and cooling rates),
- Hydro-pressure test (pressure and time duration).

As a rule of thumb, commercial FEA codes (like ABAQUS) or specific codes focussed on welding simulations (like SYSWELD) are usually used. For direct FE simulation the following assumptions and simplifications are often used: 2D axisymmetrical model and weld is modelled as a moving heat source. That it is why weld simulations are still used in science field rather than in industrial applications. General workflow for RS evaluation is presented in **Figure 6**.
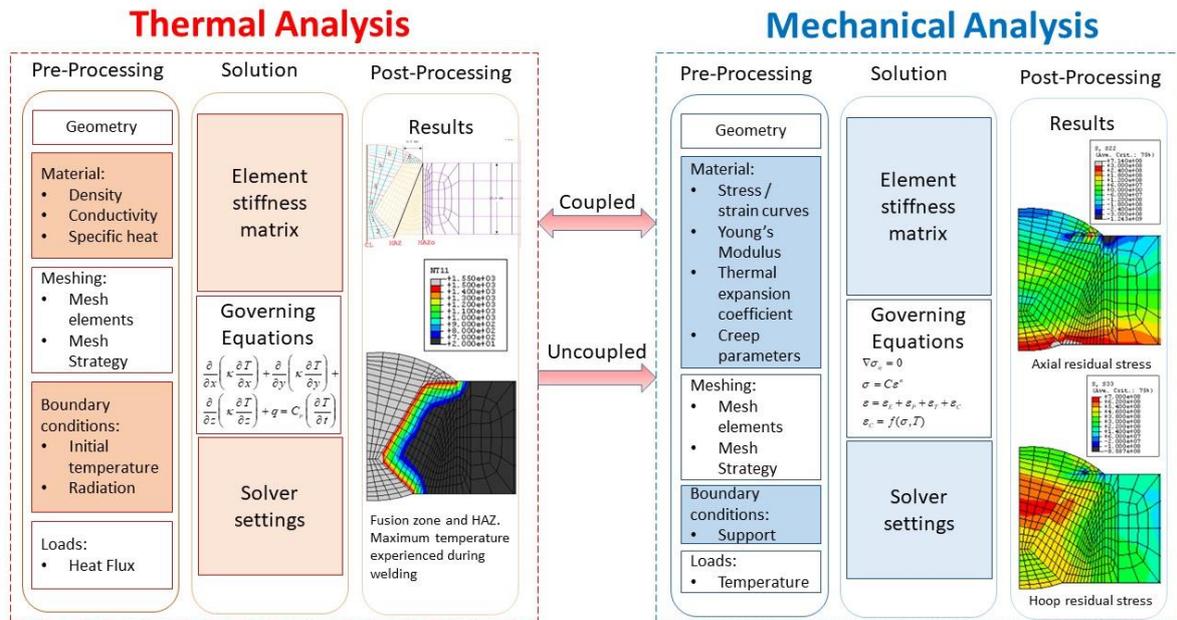
Figure 6: General scheme for RS calculation using FEM.

4.3.3.3   RS determination based on measurements

Reliable information regarding magnitude and distribution of residual stress in both welds and cladding is important for RPV integrity assessment and decisions concerning continued safe operation. One valuable method for characterization of the residual stresses is measurements performed on a reference component to collect empirical data for application on similar components. Measurements are also used to validate numerical models used for predicting the residual strain and stress states for specific components and welding conditions, including effects of pressure tests and operational loads.

The reference component may be a cut-out piece from an actual pressure vessel (never operated or decommissioned) or a representative mock-up. Aspects such as whether an actual cut-out piece has been in service or not, post-weld heat treatment, pressure test, and operational conditions could potentially imply a significant difference. Mock-ups will most likely correspond to cut-out pieces if realistic boundary conditions can be successfully imposed during manufacture. Conditions from events after the as-welded state and post-weld heat treatment will always be difficult to include. There may also be a deviation in actual material properties unless archived original material is available. Inadequate documentation may constitute uncertainty concerning the actual procedures during manufacturing decades ago.

There are several different residual stress measurement techniques available which are generally classified into destructive, semi-destructive and non-destructive. Destructive and semi-destructive techniques measure the effect from relieving residual strain which requires material removal, whereas non-destructive techniques are based on the interaction between strain/stress, physical and crystallographic characteristics of the material. All these techniques have both practical limitations and physical characteristics requiring considerations of e.g., geometry, location of the specimen, resolution, uncertainty, penetration depth, stress triaxiality, gradients, sampling volume and stress-free samples. Transportability and size of the specimen may reduce the number of available measurement techniques depending on the portability and size of the device.

The experience from residual stress measurements among the project organisations are indicated below.

UJV:

RS measurements were performed in frame of Phare Project "VVER Cladded Reactor Pressure Vessel Integrity Evaluation with Respect to Pressurised Thermal Shock Events", PHARE project service contract N° ZZ02NUS-02-02-0001, in 2006.

The specimens of base metal with cladding from the cylindrical part of RPV from the decommissioned (never operated) VVER 440 NPP Nord were tested.

The geometry of the mock-ups was the following:

- Beam thinning method – 35x200x10 mm specimens (35 mm was through wall thickness, including 9 mm cladding)
- Hole drilling method - 85x690x40 mm and 85x200x200 mm specimens (85 mm was through wall thickness, including 9 mm cladding).

RS was measured by beam thinning method and (shallow) hole drilling method. The more reliable results were obtained by the beam thinning method. The stress-free temperature approach (used at that time for modelling RS in cladding) with $T_{sf} = 350\,°C$ seemed to be in good accordance with measured residual stresses by the beam thinning method.

Framatome:

Currently only the X-Ray method is used to measure the residual stresses. The technique used is limited to a maximum measurement depth of ~10 mm, depending on the geometry of the specimen.

Experimental experience:

Cladding mock-ups intended to represent the RPV shell and measurements on cut-out pieces of reactor pressure vessel heads. One decommissioned pressure vessel and one that has never seen operational conditions were used for this purpose. The whole work was part of customer-related projects.

The mock-up was manufactured with a SA-508 Class 3 base material and a two-layer Alloy 182 cladding. After a first series of measurements a third cladding layer was applied. Residual stresses were measured before and after PWHT.

RS was measured by deep hole drilling technique and ring core method. The results from the cladding of the decommissioned RPV head, which was exposed to service conditions and the results from the cladding of the head that has not been in service show a similar trend that is in agreement with the general experience from other cladding residual stress measurements. However, there is a significant difference in the peaks of the stresses. After exposure to test pressure and service conditions the maximum values at room temperature appear significantly lower.

The mock-up measurements demonstrated that a PWHT significantly reduces the stresses on the ferritic side, however, the residual stresses on the austenitic side show only a minor decrease.

KIWA:

RS are determined based on measurement in combination with RS calculations. This may be specifically challenging considering that the RPVs are usually in service, i.e., it is not possible to perform measurements on site and therefore it is hard to achieve the relevant mock-ups. Measurements on identical or similar enough decommissioned RPVs may serve as highly valuable alternatives.

The measurement technique applied must be well suited, verified and validated for the measurement. Some measurements require inputs for evaluation, e.g., Young's modulus for calculating the stresses from strains (shape deviations). In case of Young's modulus, this may be anisotropically dependent on the weld geometry and solidification structure and therefore difficult to quantify. Assumptions of biaxial stress states in the evaluation may not always be fulfilled and this may lead to an (unknown?) influence on the results. If a mock-up is manufactured and used for the measurements, applying the correct mechanical boundary conditions is often of most importance.

Experimental experience:

23

Tested structures:

- RPV cladding (square RPV plate clad with 9 strips.)
- RPV core shroud support leg attachment (RPV plate with buttering, leg and supporting BC-frame)

RS was measured:

- With incremental deep hole drilling (iDHD/DHD), incremental centre hole drilling (iCHD) and ring coring – all performed by Veqter Ltd. UK.
- 32 channel thermocouple measurements were performed on the square RPV plate clad with 9 strips.

In conclusion, RPV core shroud support leg attachment: the numerical simulation results corresponded very well to the experimentally measured WRS.

BZN:
Measurements and FEM calculations for RS in cladding:

- Specimens were manufactured for the measurements using similar material properties and manufacturing processes to the ones used for the RPV. The hole drilling method (performed in Brno) did not give consistent results. The instrumented hardness tests gave more reliable results, but due to its limits could not validate the whole scope of FEM calculations.
- FEM calculations in which the effect of the first pressure tests was taken into account confirmed the assumption: taking into account stress-free temperature at normal operating temperature is conservative enough. However, results of comparison between FEM calculations and measurements showed that using lower stress-free temperature than the normal operating temperature is not recommended.

IRSN:
Within the framework of a planned project which will take few years, measurements will be taken by industrials by trying to reproduce as much as possible the welding and heat treatment conditions of the welded joint between the two RPV core shells.

OCI:
Weld Residual Stress
The through-wall WRS distribution currently used in FAVOR was derived in the HSST program from a combination (see [13] [115] [116]) of two sources:

- experimental measurements taken from an RPV shell segment made available from a cancelled pressurized-water reactor plant and
- finite-element thermal and stress analyses

Experimental data required for calculation of residual stresses incorporated into FAVOR were obtained by:
- cutting a radial slot in the longitudinal weld found in a shell segment from an RPV and
- measuring the deformation of the slot width after cutting
- the measured slot openings were assumed to be the sums of the openings due to (1) the clad-base material differential thermal expansion (DTE) and (2) the fabrication WRS.

Specific details of the procedure include the following:

- Slot opening measurements were made during the machining of full-thickness clad beam specimens with two-dimensional flaws. The blanks measured 137 cm (54 inches) long (circumferential direction), 23 cm (9 inches) wide (longitudinal direction), and 23 cm (9 inches) thick (radial direction). The blanks were cut so as to have a segment of a longitudinal seam weld from the original RPV at the mid-length of the blank.
- Using the wire-EDM process, a slot was cut along the weld centreline in a radial direction from the inside (clad) surface of the blank.

24

- Measurements were made on three specimens having final slot depths of 1.14 mm (0.045 inches), 23 mm (0.90 inches), or 115 mm (4.50 inches), respectively.
- After machining, the widths of the slots were measured along each radial face of the blanks.
- Finite-element analyses were used to develop a through-thickness stress distribution that gave a deformation profile matching the measured values.

A three-step analysis procedure was developed [13] [115] [116] to produce the estimated WRS profile applied in FAVOR.

Step 1. – As discussed above, the first step was to measure the width of a machined slot (flaw) cut into the axial weld, which was contained in a full-thickness beam taken from the RPV shell segment. The measured slot openings in the clad beam specimens are the result of relaxing the residual stresses from (1) the clad-/base-material differential thermal expansion (DTE) and (2) the residual stress generated by the structural welding process, which were not completely relaxed by post-weld heat treatment. Therefore, the measured slot width is assumed to be the superposition of the deformation due to DTE and the deformation due to the WRS.

Step 2. – Next, an ABAQUS finite-element analysis was performed to simulate the cooling of the clad beam from a stress-free state. The opening displacement of the notch resulting from this analysis is caused by DTE of the clad and base-material properties. The clad beam specimen was cooled uniformly from an assumed stress-free temperature of 315.6 °C (600 °F) to room temperature at 22 °C (72 °F). The difference between the slot displacement from the cooldown and the total measured slot width is then assumed to be caused by the WRS alone.

Step 3. – The third step was to determine the through-wall stress distribution in the clad beam caused by the WRS. An ABAQUS finite-element stress analysis was performed to impose the displacements from the WRS on the crack plane. The resulting stress distribution is the estimated through-wall residual stress distribution.

Clad Residual Stress

In the study [117], finite element analysis was used to compare the stresses and stress-intensity factors (SIF) during a cool-down transient for two cases: (1) the existing SFT model of FAVOR, and (2) directly applied RPV clad residual stress (CRS) distribution obtained from empirical (hole-drilling) measurements made at room temperature on an RPV that was never put into service.

The clad residual stress data used in the study were measured in an RPV vessel wall by FRAMATOME (now AREVA) at 21 °C using hole-drilling technique; that work that was performed in support of the NESC-IV European Network Project [110]. Specific details include the following:

- Radial variation of room temperature clad residual stresses was determined at positions in and near cladding/base interface.
- A ring-core technique was used to obtain axial, hoop, and shear stresses through inner 14 mm (0.55 in.) of vessel thickness.
- The CRS profiles are assumed to be introduced at the time of manufacture and before the vessel is placed in service.
- The stress profiles were used as input to finite-element models developed for the study.

JAEA:

Thick plates with weld-overlay cladding by submerged arc welding and electroslag welding were tested. JAEA used plate test specimen the dimensions of which were 500x500x120 mm^3, with a cladding thickness of 5 mm. Through-thickness distributions of RS were measured by sectioning and deep hole drilling (DHD) techniques and applied.

In conclusion, a high tensile stress comparable to the yield stress is produced in the cladding after PWHT. This high tensile residual stress is due to the difference in the thermal expansion coefficients between the cladding and base materials. The phase transformation that occurs during welding and PWHT should be considered in order to obtain highly accurate results for the residual stress

distribution. In order to appropriately assess the structural integrity of RPVs, the WRS near the cladding should be considered.

4.4 Conclusions

4.4.1 Critical locations where RS should be considered

There is a common understanding among the APAL partners that residual stresses should be considered in deposited cladding as well as in welded joints, especially in the beltline region of the RPV. However, there are differences in the consideration of residual stresses in the corresponding HAZs.

A unified approach should be discussed within the framework of APAL regarding the treatment of residual stresses in welds and cladding HAZs.

4.4.2 Operating conditions where RS should be applied

There is a common understanding among APAL partners that residual stresses should be considered in the brittle fracture analysis of emergency conditions. The treatment of residual stresses in ductile tearing evaluation should be discussed in the framework of this project and documented in WP5.

Some partners propose to consider RS for all operating conditions not just for emergency and upset ones. Consideration of residual stresses also for normal operating conditions would be physically correct. Furthermore, for normal operating conditions with low thermal stresses and low pressure (in some cases) the relative effect of residual stresses on the stress intensity factor might be even higher and therefore more important compared to emergency conditions. By considering RS in the assessment of normal operating conditions an adjustment of the safety factor that is applied to the K_{IC} curve should also be considered. This proposal should be further discussed in the framework of this project and documented in WP5.

4.4.3 Methodologies to determine RS

RS taken from standards

A fair similarity has been observed between the WRS distributions proposed in the standards and technical literature for RPV assessments. The shape of WRS is often assumed to be cosinusoidal with an amplitude between $45\ MPa$ and $56\ MPa$ for PWRs, and of $60\ MPa$ for WWER vessels according to the IAEA recommendation [6].

The cladding residual stresses are generally approximated using a stress-free temperature (T_{sf}), which should be chosen to produce appropriate levels of residual stress at room temperature. The value of stress-free temperature depends on material properties, the manufacturing procedure and the influence of the hydro test.

A more detailed procedure can be found in the Russian Standard MRKR-SKhR-2004 [25] which contains recommendations on how to perform the calculation of residual stresses for WWERs due to welding and cladding manufacturing processes and heat treatment. The RS profile through the RPV wall thickness in base metal is considered as stepwise with adjustment for the cladding HAZ. The magnitude of RS in HAZ due to cladding and in weld is taken based on diagrams in the standard in dependency on the duration and the temperature of tempering. The standard contains also recommendations on how to define the residual stresses in the cladding after the hydrotest.

Due to the similarities observed in the RS distributions currently proposed in the different codes and technical literature, solution based on common understanding should be selected for using in APAL project.

Existing RS distributions in the different codes and technical literature are based on measurements on cancelled plants that never entered into operation or on mock-ups or on FEM calculations. A topic to investigate regarding PTS analyses for LTO includes the possible RS relaxations during operation. For

this purpose, RS measurements, ideally on materials from decommissioned RPVs, should be performed.

RS calculation

Another way to determine RS is throughout detailed FEM calculations. This RS numerical simulation is still a challenging task since a lot of input data is required as indicated in the subsection 4.3.3.2.

Performing detailed FE calculation of RS is out of the scope of the APAL project. Nevertheless, some sensitivity studies focussed on the effect of RS magnitudes on the PTS results are recommended for WP3 and WP4.

For future work and possible projects, it is recommended to consider detailed FE calculations of RS. Also, it would be useful to organize a benchmark for residual stress calculations for several RPV weld types and to perform the appropriate sensitivity studies.

RS determination based on measurements

Strain relieving methods appear to account for most of the experimental experience among the project participants, although X-ray and neutron-based methods receive increasing attention. Examples of other recent experimental results are contained in references [168] [169] [170].

The reported experimental experience mainly involves cut-out pieces and mock-ups made from plate/shell base materials of different classes/grades of SA-508 and SA-533 covered by single or multi-layered cladding of nickel-based Alloy 182 or austenitic stainless steel. The components are primarily free from weldments in the ferritic steel, although specimens including circumferential and longitudinal shell welds exist.

Weld residual stress distributions are generally extracted along paths starting at the cladding surface and extending through the thickness with varying depths. These results can be very detailed along the selected path but lack field information regarding variations in directions away from the path. This means that measurement results depend on the selected location, e.g., bead centre or bead-overlap.

There is significant experimental evidence that post-weld heat treatment (PWHT) effectively reduces residual stress in the ferritic material. This is not the case for the cladding since these materials are much more heat resistant. Different values of thermal expansion coefficient result in compressive stress within the cladding at the typical PWHT temperatures.

On the other hand, residual stress in the cladding appears to be significantly reduced during hydrostatic pressure testing after PWHT. This is not expected for the ferritic material because of the already reduced residual stress levels.

In summary, at room temperature after PWHT and pressure test, a significant level of residual stress remains in the cladding while residual stress in the ferritic metal is usually greatly reduced overall. It is possible to have a remaining local compressive state immediately underneath the cladding/base metal interface, depending on the thermodynamical process and chemical composition of the ferritic steel.

It is common to relate the resulting residual stress profiles to a stress-free temperature. This piece-wise linear function, which is an approximate description of the residual stress state at room temperature, is determined from the different values of thermal expansion coefficient and the thicknesses of the cladding and base metal. This description does not account for any variation of the residual stresses in the cladding transverse and longitudinal directions, although different stress states are expected at e.g., mid-width of beads, and in the bead overlap region. Residual stress profiles from this approximation lack information regarding the HAZ, which is automatically captured in experimental measurements and numerical simulations.

General recommendations:

The process of extracting a cut-out piece potentially introduces deformation due to releasing restraints imposed by the pressure vessel structure. This can result in strain relieving bending components as

well as edge effects and needs to be acknowledged. Measuring the deformation during cut-out and manufacture of blanks makes it possible to assess the influence either by estimates or numerically.

The manufacture of a mock-up should account for the actual structural boundary conditions to limit any potential deviation between measurements and the true state and location of the corresponding real component. Although a numerical simulation may not be relevant or planned during the experimental program, such an investigation may be requested later. It is therefore recommended that thermal response is measured at several strategic points for validation of thermal simulations.

It is recommended to prepare weld micrographs since these contain valuable information regarding the fusion and heat affected zone as well as the microstructure in areas exposed to elevated temperatures. Hardness testing may be suggested depending on the microstructure. Extracting samples from the weld gives the possibility of performing e.g., tensile testing or impact resonance testing.

The result from strain relief methods relies on reliable information regarding elastic properties since they are based on quantification by direct proportional relationship between residual stress and residual strain. Neutron based techniques require the configuration of a stress-free reference samples and are sensitive to grain size and texture. Parameters and assumptions which are required for the evaluation of an experimental measurement must be carefully considered. Correction for plasticity effects during strain relieving may be necessary.

The ferritic materials differ between many experimental programs, which means different chemical compositions and thus different thermodynamic behaviour. This could potentially influence the stress state in the HAZ immediately below the cladding depending on the potential presence and amount of martensite. Such an influence would typically introduce strong gradients over short distances which may be difficult to capture accurately without very high measurement resolution.

Experimental methods to some extent always include uncertainties. Validation of experimental measurement methods is important, often by comparison to results from numerical simulations. At some stages of the evaluation and analysis of experimental data, numerical methods are often used.

The use of different and complementing techniques may form a basis for validation of the measurement results as well as numerical predictions.

4.4.4   Consideration of RS for RPV integrity assessment in case of PTS

In simplified PTS analyses (using linear elastic fracture mechanics) RS can be treated separately from other loads resulting from PTS. In advanced nonlinear FEM analyses, RS are included into the model together with the loads resulting from PTS. In this case, some partners use direct introduction of residual stresses (according to methods described in [1]); other partners use introduction of strains corresponding to RS. The approach is dependent on capabilities of the used FEM software. In the case of introduction of strains, checking of resulting stresses (calculated before application of loads resulting from PTS on FEM model with "closed" crack) shall be performed. As far as RS due to cladding are concerned, some partners introduce this type of RS by using different thermal expansion coefficients of base/weld material and cladding and by selection of the appropriate stress-free-temperature.

Elastic-plastic FEM calculations with introduction of relevant RS before PTS loading either by direct introduction of the stresses or by introduction of strains as initial load are recommended as a good practice.

4.4.4.1   Consideration of RS effect for ageing

RS serve as important input data when predicting the safety margins which may be limited by the fracture toughness, which may be reduced over time (e.g., due to radiation or thermal ageing).

The partners do not consider the effect of RS on RPV ageing. Another topic can be the effect of RPV operational loads on potential RS changing.

In general, the operational temperature is low enough for neglecting the creep relaxation effects.

The PWHT process during RPV fabrication, the pressure tests and also operational conditions can cause residual stress relaxation and redistribution. However, even after several years of operation certain residual stresses remain. The residual stress relaxation during operation is not clear and was not examined so far.

4.4.4.2 RS effect on crack initiation, propagation, arrest and stable crack growth

The partners who perform PTS analyses including crack propagation and crack arrest consider RS in the same manner as for crack initiation. There is no need for distinguishing between the different phases from the point of view of RS.

4.4.4.3 Methods for taking into consideration the uncertainties of residual stresses in case of probabilistic PTS calculations (Statistical distribution for residual stress magnitude or spatial distribution)

It is well-known that numerical evaluation of the RS requires a lot of input data and simplifications or special experiment, moreover RS depends on type of processing and heat treatment. Therefore, it is logical to assume that in probabilistic PTS RS should be treated as a stochastic variable.

However, almost all partners consider RS as deterministic value for both deterministic and probabilistic calculations, due to the lack of data. In this field some research programmes are ongoing, but an extensive work is expected in near future.

Thus, it is recommended to consider RS as a deterministic value at present, both for probabilistic and deterministic calculations.

4.4.4.4 Overall point of view concerning role of residual stress in LTO focusing on RPV and PTS

It can be stated that residual stresses can impact the safe long-term operation of the RPV and should be part of every RPV safety (PTS) assessment, especially in the view of LTO.

All partners consider including residual stresses (both in the weld and due to the cladding) into PTS assessment as important and relevant. The RS increase the PTS loadings in the welds which are usually the most embrittled regions of RPVs and where presence of a flaw is more likely than in the base metal. This means that the RS may have an impact on the integrity of welded joints during PTS event.

The consideration of residual stresses in reactor pressure vessel safety assessments is mandatory according to several codes and guidelines, since RS can affect the stress intensity factor at the crack front of a postulated or existing crack.

Moreover, much of what is discussed is of general relevance to other RPV welds (outside of the beltline, e.g., dissimilar metal welds of RPV nozzles) and also can be relevant to other reactor pressure boundary components.

General recommendation:

Including of RS into the PTS assessment is mandatory according to most standards. Determining of more precise residual stress profiles is recommended especially for PTS assessment for LTO, where the margins against fast fracture diminish and using overconservative values of RS can lead to unnecessary reduction of the RPV lifetime.

Relaxation of RS during long term operation is not clear and its investigation is recommended, e.g., by measurements on decommissioned RPVs.

4.4.5 Completed projects related to RS

UJV:
RS measurements were performed in the frame of Phare Project "VVER Cladded Reactor Pressure Vessel Integrity Evaluation with Respect to Pressurised Thermal Shock Events", PHARE project service contract N° ZZ02NUS-02-02-0001, in 2006 (see details in Section 4.3.3.3).

Framatome:

Completed projects are as follows:

- NRC Weld residual stress round robin 2011 [112]
- EN Power [113]

KIWA:

KIWA has developed a defect tolerance analysis procedure for the Swedish nuclear plants in which RS is always accounted for as default. The procedure is applied when determining the inspection intervals.

JSI:

The MULTIMETAL project (EC, 7th FP, 2012-2015) focused on RS characterisation and calculations, as well as on mechanical and fracture properties measurements of dissimilar metal welded pipes.

OCI:

A major study (see [110]) performed by ORNL staff (including current OCI staff) for the US NRC analysed a range of RPV geometries subjected to postulated transients that follow normal cool-down limit curves using the FAVOR code. The objective of those studies was to determine trends for conditional probability of initiation (CPI) and the conditional probability of vessel failure (CPF) as a function of initial flaw depth for postulated circumferential, surface-breaking flaws on the inner surface of the RPV. Those cool-down transients were developed using standard procedures that define pressure-temperature (P-T) limits as specified by the American Society of Mechanical Engineers (ASME) Boiler and Pressure Vessel Code, Section XI, Nonmandatory Appendix G [114].

The ORNL studies [110] demonstrated that stresses in the HAZ region of the clad-base metal interface, induced by DTE, constitute an important loading component that can have a major impact on the probability of cleavage initiation of shallow surface flaws under normal operational loading of the RPV. Specifically, these analyses produced two results:

> Result 1. Very shallow surface-breaking flaws dominate the RPV failure probability. This result was unanticipated because, in previous analyses of pressurized thermal shock (PTS) transients, shallow surface-breaking flaws were observed to be small contributors to the total estimated probability of vessel failure.

> Result 2. Very shallow surface-breaking flaws exhibit CPI and CPF values that exceed by orders of magnitude those for the 1⁄4 t flaw referenced in the ASME Code, Section XI, Appendix G. This result was unanticipated because the much deeper flaw is expected to pose a greater risk to the integrity of the vessel when evaluated in terms of the CPI/CPF metrics.

Figure 7 depicts the P-T versus time limit curves computed according to the ASME Code procedure [114] for a pressurized water reactor RPV at 60 effective-full-power-years (EFPY) at a cool-down rate of 50 °F/hr. These P-T versus time curves were used as input to PFM analyses performed with the FAVOR code to determine the mean CPI as a function of normalized flaw depth for circumferentially oriented, inner-surface flaws. Three flaws shown in **Figure 8** (Flaw 1: $a/t = 0.03$, Flaw 2: $a/t = 0.05$, Flaw 3: $a/t = 0.25$) are of particular interest in the latter analyses. The normalized flaw depth, a/t, is defined as the initial flaw depth, a, normalized by the vessel's total (cladding plus base metal) wall thickness, t.
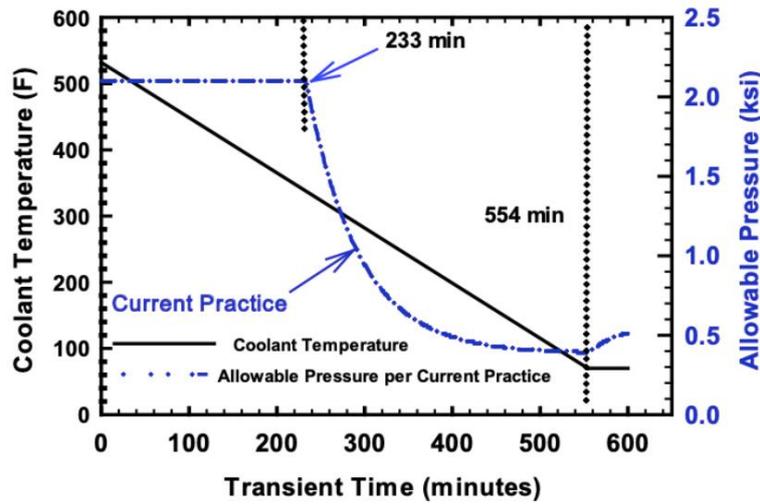
Figure 7: Prescribed pressure-temperature limits for normal cool-down transients determined using standard ASME code procedures. Results are shown for Vessel A at 60 EFPY with a cool-down rate of 27.8 °C (50 °F/hr).
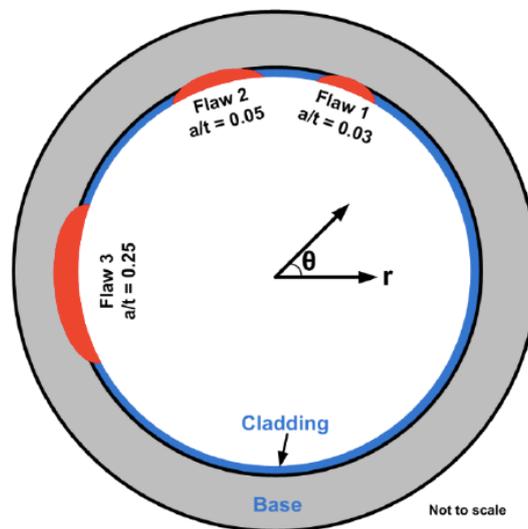
Figure 8: Schematic of three inner-surface breaking flaws of interest with varying depth and constant aspect ratio of flaw length to depth (figure not to scale).

These analyses demonstrated trends in *CPI* and *CPF* for ID surface-breaking flaws that vary nonmonotonically with flaw depth, reaching a global maximum for very shallow flaws just penetrating through the stainless-steel cladding and into the ferritic RPV steel wall. This outcome is caused by the additional crack driving force generated for shallow flaws due to the mismatch in coefficient of thermal expansion (CTE) between cladding and base material, which elevates the thermally induced stresses. The CTE contribution diminishes rapidly as flaw depth increases.

Current understanding of OCI is that this so-called "shallow-flaw issue" apparently remains unresolved within the U.S. Nuclear Regulatory Commission.

As shown in **Figure 9** the predicted mean *CPI* trends from FAVOR for these flaws vary non-monotonically with initial flaw depth. The initial flaw depth corresponds to the depth of the assumed pre-existing, surface-breaking, semi-elliptic flaw before the initiation of any subsequent flaw growth that could occur due to thermal-mechanical loading. More specifically, the mean *CPI* exhibits a global minimum for very shallow flaws over an interval of normalized flaw depths from 0.03 to 0.06 and a global maximum as the flaw depth approaches the clad/base metal interface. The mean *CPI* for Flaw 1 with $a/t = 0.03$ in **Figure 9**, subjected to the postulated cool-down transient of **Figure 7**, is estimated

31

to be 3.57×10^{-5}, compared to the global minimum mean CPI value of $6.58 \cdot 10^{-11}$ observed for the slightly deeper Flaw 2 at $a/t = 0.05$. The CPI value for the shallowest flaw (Flaw 1) shown in **Figure 9** significantly exceeds that computed for the ASME ¼ t flaw, designated as Flaw 3.
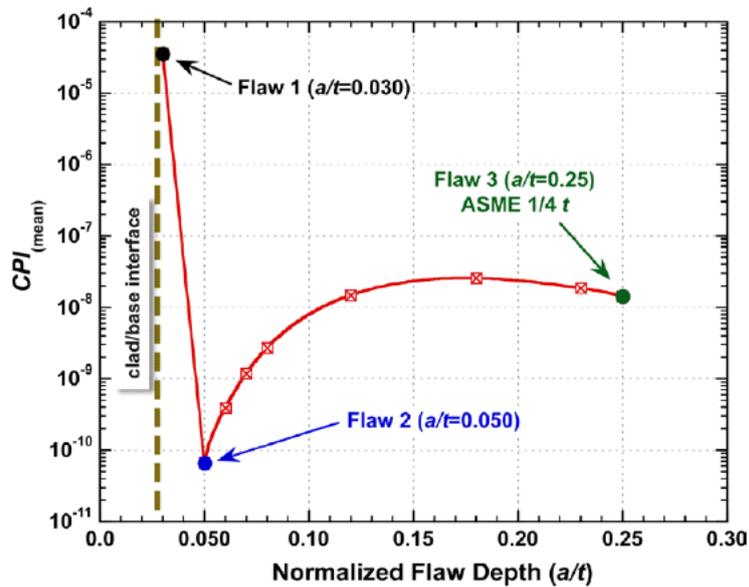
Figure 9: CPI for circumferentially oriented, inner-surface flaws exhibiting non-monotonic behavior with flaw depth for Vessel A subject to the pressure and temperature limits determined from the standard ASME code procedure and shown in Figure 7, the latter is based on 60 EFPY and cool-down rate of 50 °F/hr [110].

4.4.6   Ongoing projects related to RS

PSI:

PSI is currently conducting a project, named as "PROACTIV", the goal of which is to deal with probabilistic leak before break analysis of nozzles and piping in the context of active degradation and ageing mechanism. In association with this project, it is of great significance to investigate the effect of WRS on the failure probabilities of piping with dissimilar metal welds to evaluate the safety and reliability of nuclear power plants.

4.4.7   Planned projects related to RS

UJV:

Within a contract with ČEZ company (owner of the Czech NPPs) for assessment and lifetime management of RPV and reactor internals for NPP Dukovany and Temelín for $2021 - 2025$, large work package for determination of RS in RPV welds is planned. Measurements on large specimens from decommissioned VVER 440 RPV and on artificially fabricated mock-up of VVER 1000 seam weld are planned using neutron diffraction method and deep hole drilling method. Calculations of RS by SYSWELD or ABAQUS codes are planned for both the specimens with RS measurements (for validation purpose) and for real VVER 440 and VVER 1000 RPVs.

4.5 Gaps

4.5.1   Gaps in computer simulation of weld RS

Simplifications are needed in RS simulations due to the long computational times required, the lack of input data on the involved parameters and the complex (material) phenomena occurring during welding. The applied material models and their influence on the obtained WRS may require further investigations for the analysis of cyclic (welding) thermo-mechanical transients with a subsequent PTS (cooldown) transient, circumstances that could have an impact on small/shallow flaw assessment.

Nevertheless, the "shallow flaw issue" (see subsection 4.4.5) in RPV under PTS loads, in this case due to the thermal expansion mismatch between cladding and base material, has been also identified.

4.5.2   Gaps in experimental RS measurements

Scatter of weld RS measurements has been reduced over the years by constant improvement of the techniques available, participation in round robin exercises and validation efforts with improved computational modelling. On the other hand, PTS integrity assessments could benefit from additional and more accurate RS measurements on decommissioned RPV. This seems to be the goal particularly of the completed and planned projects by UJV in the Czech Republic, and of other research projects. Additional experimental gaps listed by the participants include the impact of RS on material embrittlement and on toughness measurements of specimens containing residual stresses.

4.5.3   Gaps in the inclusion of RS in computer codes, analyses and RS applicability in integrity assessment

The axisymmetric WRS assumption may not be accurate at start/stop points of welding and local repair locations. Several partners also agree with the possibility of RS redistribution and relaxation during crack growth, which could affect the way RS are treated in the analyses. It has also been pointed out that the interrelation between underclad cracking (UCC), cladding RS and RS relaxation could benefit from further study.

Overall, all these gaps seem to result in a current lack of guidance for consideration of RS in the integrity assessment. This results in RS profiles with severe magnitudes being typically utilized, and possibly leading to additional conservatism in the integrity assessment outcome.

4.6   Recommendations

For APAL project

Future studies could evaluate the RS influence on PTS margin assessments with deterministic and probabilistic approaches, the latter intended to review the impact of RS on probabilities of crack initiation and RPV failure. The outcomes could clearly benefit from the consideration of different crack sizes in the analyses to assess the "shallow flaw issue".

The outcome of PTS margin assessment could be strengthened with a sensitivity analysis involving RS available in the literature, from APAL partners experience and/or RS accepted by regulatory authorities. The aim of this analysis would be to study the influence of RS variability in the PTS analysis results.

For future research projects

To support national projects planned to date, future international research could be directed towards several topics identified above. These include more accurate RS measurements on decommissioned RPV, to study the RS impact on material embrittlement and on toughness measurements, as well as the interrelation between UCC, cladding RS and RS relaxation. Numerical and experimental evaluation of local RS variations due to cladding deposition, start/stop points of welding and local repairs could be beneficial to assess whether these could have an impact on RPV integrity assessment, both deterministically and probabilistically.

General recommendation

Future research should be aimed towards assisting in the development of improved guidance for the consideration of RS in the integrity assessment of RPV under PTS loads. Furthermore, evaluating uncertainties in RS is also recommended, maybe by RS calculations for varying input data based on some estimated uncertainties.

5   State-of-the-art for Warm pre-stress (WPS)

The inclusion of warm pre-stress (WPS) effect in RPV assessment can reduce over-conservatism and enable more accurate evaluations of the safety margins against limiting conditions, which may occur at PTS events. However, the inclusion of WPS effect in PTS analyses is currently not uniform across the different European countries, nor is the position of national regulators regarding its acceptance. A review of existing WPS approaches and limitations was performed in Task 1.2, and recommendations were proposed for assessments in WP2, WP3, WP4 and eventually will be incorporated in the best-practice documents for PTS analysis (WP5). Moreover, the consideration of WPS effect has an impact on the transient selection for PTS assessment.

The objective of this chapter is to summarize the results of *Task 1.2 State-of-the-art for warm pre-stress approach*.

5.1   Overview

One of the items considered in the evaluation of reactor system response to the PTS event is the effect of the relatively cold emergency core coolant on the hot reactor pressure vessel. The resulting temperature gradients induce thermal stresses. Under "worst case" conditions, analyses of the thermal stresses that could occur due to the thermal shock, in combination with the internal pressure in RPV and assumed small flaws on the inner surface of the vessel, lead to the prediction that the flaws will initiate. Fortunately, there exists a combination of circumstances during a PTS, whereby the crack tip region of an assumed flaw is subjected to warm prestress (WPS), a phenomenon that can preclude crack initiation, when it otherwise would have been predicted.

To describe the warm prestress effect, once a crack is loaded while the material is very tough, no rapid extension will occur during subsequent combined cooling and unloading. This applies even if the imposed stress intensity factor (SIF), K_I, which is a function of stress and flaw severity, exceeds the fracture toughness during the cooldown-unloading. Linear Elastic Fracture Mechanics (LEFM), without consideration of the effects of warm prestressing, predicts rapid extension (initiation) of a crack when the K_I becomes equal to the fracture toughness of the material, K_{Ic}. Thus, it is necessary to have verified procedures for evaluating the initiation and propagation of flaws in reactor pressure vessel steels under realistic PTS conditions with inclusion of the warm prestress phenomenon.

The WPS effect can be attributed to four main mechanisms which can be expected to have different impacts, depending on the load path and the pre-load level. All the mechanisms are related to the level of applied load and straining during the pre-load in the ductile regime.

The four main mechanisms contributing to WPS are (see detailed description in the subsequent paragraphs):

- Introduction of a beneficial compressive residual stress field in front of the crack tip, due to local plastic deformation from the preloading and unloading. The interaction of WPS and WRS is addressed in Section 5.5.1 of this report.
- Change of yield properties due to lowering of temperature.
- Deactivation of cleavage initiation sites by pre-straining.
- Blunting of the crack tip.

5.1.1   Introduction of beneficial compressive residual stress field

During the unloading phase of a PTS transient, a compressive residual stress field around the macroscopic crack tip will arise due to the plastic deformation created during the pre-loading. After unloading the structure, the material will attempt to return to its origin state but since the macroscopic crack tip has undergone high plastic deformation it will not return to its undeformed state. This causes the surrounding material to compress the highly plastically deformed region near the macroscopic crack tip, resulting in a compressive residual stress field around the macroscopic crack tip. This compressive residual stress field remains as the temperature is lowered. When the specimen (or RPV)

is reloaded in the brittle lower-shelf region the compressive residual stress field will reduce the opening stress around the macroscopic crack tip. By lowering the opening stress near the crack tip, the volume in which the stresses are high enough to initiate cleavage fracture is reduced and thus the probability of cleavage fracture is also reduced. **Figure 10** illustrates how the residual stress field affects the opening stress in front of the macroscopic crack tip.
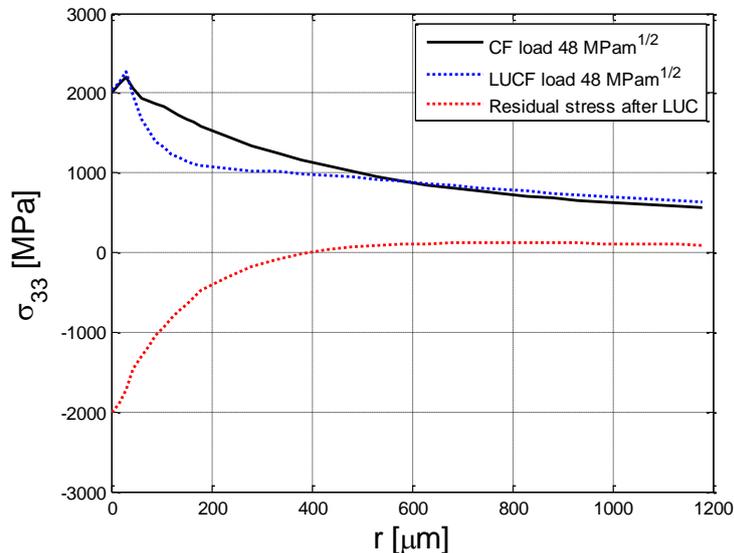
Figure 10: Opening stress in front of the macroscopic crack tip for a Cool-Fracture (CF) cycle and a Load-Unload-Cool-Fracture (LUCF) load cycle after cooling and reloading.

When reloading the specimen in the brittle lower-shelf region, the material will deform plastically at the crack tip of the macroscopic crack. The active plastic zone will therefore start at the crack tip and then grow as the load is increased. This yields a high stress gradient at the border of the active plastic zone. This means that a volume which experiences a low stress due to the residual stress field can quickly change into a high stress state when entering the active plastic zone.

5.1.2   Change of yield properties due to lowering of temperature

The yield stress of a material increases as the temperature decreases and vice versa. This means that a structure loaded in the ductile region will experience more plastic strains than if it were loaded in the brittle region with the same external force.

Now assume that the structure, loaded in the ductile upper-shelf region, is moved to the brittle lower-shelf region by changing the temperature in such a way that the stress field is unchanged. By lowering the temperature, the yield strength will increase, and the yield surface will expand. Hence, the elastic and plastic strains will not change and therefore the stress field also remains unchanged. This means that the specimen loaded in the ductile region and then moved to the brittle region will experience a lower stress field than the specimen directly loaded in the brittle region even if the specimens are exposed to the same external load. This is illustrated below in **Figure 11**.

This means that the structure loaded in the ductile region cannot theoretically fracture by only lowering the temperature. Cleavage fracture can only occur if the load at an initiation point is increased. Nevertheless, a small increase in load during the cooling phase could cause cleavage fracture.

5.1.3   Deactivation of cleavage initiation sites

During the WPS cycle, when the structure is pre-loaded in the ductile upper-shelf region, inclusions near the crack tip can separate from the matrix material and/or fracture due to high strains near the crack tip. The inclusions that do separate and/or fracture during this pre-load do not lead to fracture of the structure. For example, if the inclusions separate from the matrix material a void is created,

which cannot cause cleavage fracture. If the inclusion does not separate and instead fractures and creates a microcrack in the matrix material then the microcrack will blunt, due to the high temperature causing increased plastic dissipation. An arrested microcrack will quickly blunt and generate a void in the material. Hence, all inclusions that fracture in the ductile region during the pre-load can be considered inactive in the cleavage fracture event. These inclusions are called deactivated inclusions. In **Figure 12** two such deactivated inclusions can be seen on the fracture surface of a specimen subjected to a LUCF load transient. The voids that are formed during the pre-load are clearly evident. The SEM image in **Figure 12** is from the experimental work performed in [43]. This study clearly shows that the deactivation of initiation sites is an active and significant mechanism even at lower pre-load levels.
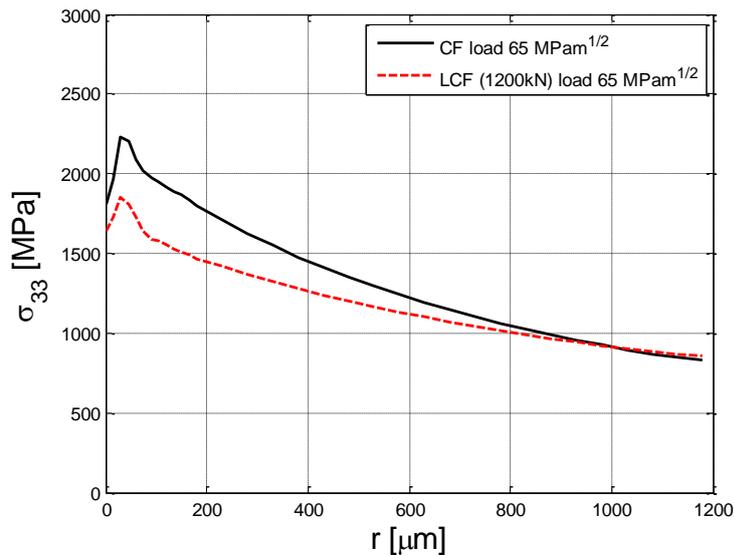
Figure 11: Opening stress in front of the macroscopic crack tip for a CF load cycle and a LCF load cycle.
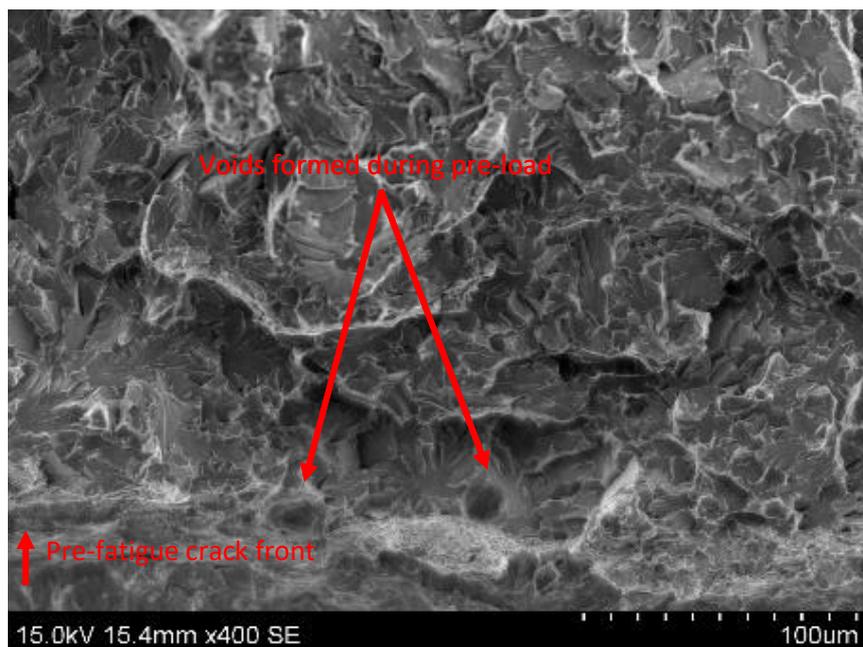
Figure 12: SEM picture with magnification of 400 times, fracture specimen subjected to a LUCF load transient [43].

5.1.4   Blunting of the crack tip

Since the pre-loading is performed in the ductile region, cleavage fracture cannot occur and a higher load can be applied without experiencing structural failure. This gives a large plastic region and plastic strains around the crack tip. The plastic strains will blunt the sharp crack tip and the theoretic stress singularity will be lost. The stress field around the vicinity of the crack tip will therefore be reduced which makes smaller the region, in which the stress is high enough to cause cleavage fracture, reducing thus the probability of cleavage fracture.

5.2 Description of activities

To define the state of the art for WPS, a questionnaire was prepared and discussed among the partners and then it was distributed among them for their response. Based on the feedback of the questionnaire of Task 1.2, the work was divided into three main parts:

- description of the WPS model/approach or standard, limitation of the WPS applicability, connection with the other PTS topics,
- identification and discussion of the WPS open issues,
- analysis of the considered WPS approaches/models in terms of their predictive capability:

    o based on the experimental data provided by the UJV (whose ownership is the Czech Republic represented by the State Office for Nuclear Safety and were provided for research purposes within the APAL project) and IPP,
    o based on the results of the RPV brittle fracture margin calculations using the representative PTS transients provided by UJV and IPP.

In total, 12 responses to the questionnaire were obtained, which are summarised in this section. The responding countries, persons and partners are listed below:

Country	Partner	Contributing Author
Czech Republic	UJV	Vladislav Pistora and Dana Lauerova
Germany	Framatome	Florian Obermeier
Switzerland	PSI	Diego Mora
Ukraine	IPP-CENTRE / SSTC-NRS	Maksym Zarazovskii and Yaroslav Dubyk / Oleksii Shugailo
Sweden	KIWA	Tobias Bolinder
Spain	Tecnatom	Carlos Cueto-Felgueroso
Hungary	BZN	Judit Dudra and Szabolcs Szávai
Slovenia	JSI	Oriol Costa
France	IRSN	Christophe Blain
Finland	LUT	Markku Puustinen
Japan	JAEA	Jinya Katsuyama
USA	OCI	B. Richard Bass and Paul T. Williams

Blank of the WPS questionnaire can be found in Annex B *Task 1.2 Partner Questionnaire*

The main conclusions drawn from the evaluation of the answers are summarised in Section 5.4 and include APAL overall point of view concerning the role of WPS in LTO focusing on RPV and PTS, recommendations regarding the WPS models/approaches and recommendations for further WP2 WP3 and WP4 related to the TH analysis, deterministic and probabilistic RPV brittle fracture assessment.

5.3 Main topics

5.3.1 Collection of existing WPS models/approaches or standards, limitation of the WPS applicability and connection with the other PTS topics

This section provides an overview of the different approaches and models used in the national standards to determine the effect of warm pre-stressing. Usually, such an implementation of the WPS effect into national standards and the decision which approach to use is based on experimental investigations that have been carried out. These experiments will be explained in detail in chapter 5.3.2.

Czech Republic

In the Czech Republic WPS is acceptable for both monotonical and non-monotonical unloading (no need for distinguishing). Level of 90% (which is applied as safety margin) of the global maximum of K_I (denoted as K_I^{max}) is the basis for the integrity assessment (see the point denoted as "A" in the **Figure 13** which is the point corresponding to the lowest temperature on the level $0.9 \cdot K_I^{max}$). Below 90% of K_I^{max} the increased fracture toughness curve (so called Case 1) is used according to the modified Wallin approach as follows:

Establish $\qquad [K_{IC}]^{Case\_1} = \sqrt{[K_{IC}] \cdot (0.9 \cdot K_I^{max} - K_I^{min})} + K_I^{min}$

Where,

$[K_{IC}]^{Case\_1}$ is the temperature dependence of fracture toughness affected by WPS for Case 1,

$[K_{IC}]$ is the "conventional" temperature dependence of fracture toughness (without considering WPS, based either on critical temperature of brittleness or on Master Curve reference temperature),

K_I^{max} is the global maximum of K_I trajectory during the PTS transient (WPS approach can be applied only after reaching the global maximum K_I^{max}),

K_I^{min} is the local minimum of K_I trajectory (during the PTS transient) reached in that part of the trajectory following point A (see **Figure 13**), or conservatively using the global minimum of the K_I trajectory.

The condition

$$K_I \leq [K_{IC}]^{Case\_1}$$

must be fulfilled below 90% of K_I^{max}. If there are several local minima of K_I trajectory, this condition has to be met for each of them.

The WPS approach according to NTD AME [8] is illustrated in the **Figure 13**.

Since the WPS approach implemented in NTD AME is based on the modified Wallin model, complemented with an additional safety factor 0.9, it may be described by the following equations:

If $K_{IC} \leq 0.9 \cdot K_{max} - K_2$, then

$$K_{FRAC}{}^{pred} = \sqrt{K_{IC} \cdot (0.9 \cdot K_{max} - K_2)} + K_2 \qquad\qquad \text{(Case 1)}$$

If $K_{IC} < 0.9 \cdot K_{max} < K_{IC} + K_2$, then

$$K_{FRAC}{}^{pred} = 0.9 \cdot K_{max} \qquad\qquad \text{(Case 2)}$$

If $K_{IC} \geq 0.9 \cdot K_{max}$, then

$$K_{FRAC}{}^{pred} = K_{IC} \qquad\qquad \text{(Case 3)}$$

where K_2 is the "unloading" value, i.e., $K_2 = K_{min}$ as far as condition for Case 1 (with $K_2 = K_{min}$) is being fulfilled, and if this condition is no longer fulfilled, then $K_2 = 0.9 \cdot K_{max}$ (Case 2 occurs). $K_{FRAC}{}^{pred}$ means here the predicted value of fracture toughness (at re-load).
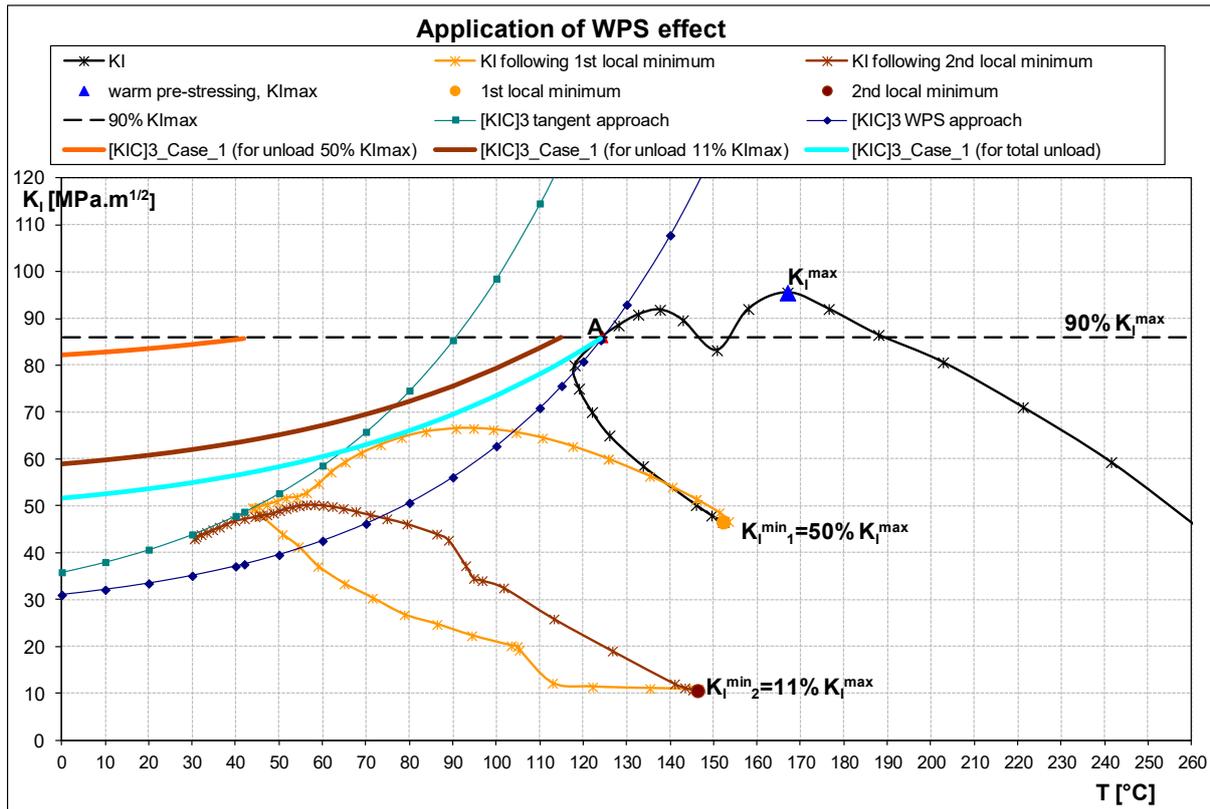
Figure 13: Illustration of the procedure for WPS approach application according to NTD AME.

Germany

In Germany the WPS approach in KTA 3201.2 [9] is divided in the effect on the loading side (crack tip loading) and the effect on the material side. *"Upon warm pre-stressing of the crack front and in the case of a monotonously decreasing stress intensity factor (specimen cooling under sustained load), i.e., at $dK/dt \leq 0$, crack initiation is to be excluded"*. This statement holds even if the load reaches the material's fracture toughness during unloading and cooling.
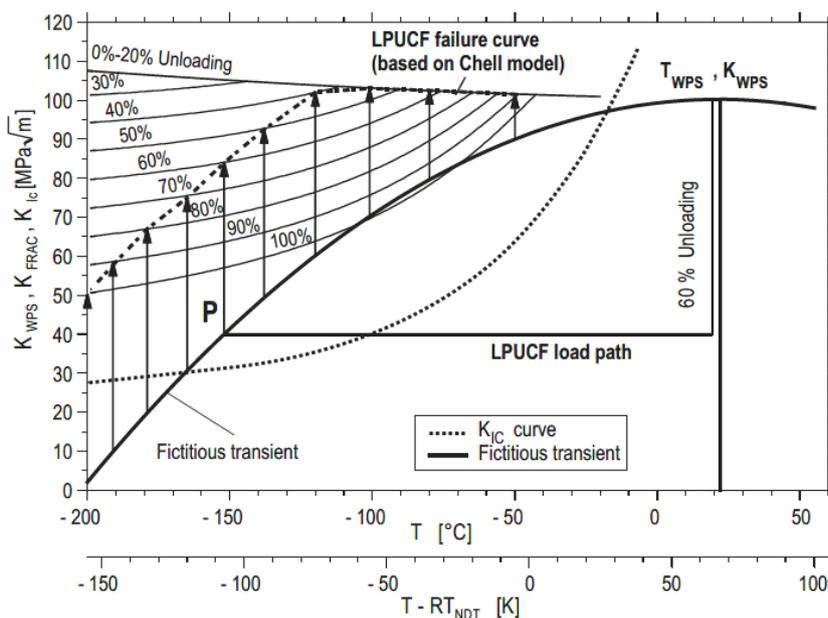
Figure 14: Principle sketch to show the determination of the fracture toughness K_{FRAC} upon warm pre-stressing.

The KTA also allows taking the increase of the apparent fracture toughness into account to exclude crack initiation in case of a sudden increase of the stress intensity factor (reloading at lower temperature). In such cases, it is advised to determine the apparent fracture toughness K_{FRAC} after a warm pre-loading that is also depending on the unloading before the rise of the stress intensity factor. **Figure 14** shows the determination of the fracture toughness K_{FRAC} upon warm pre-stressing for the complete unloading range of a fictious transient.

The approach described within the KTA is basically the approach proposed in 1980 by G. G. Chell [10]. German R&D results were used to verify its application. The results can be found in references [171] [172] [173] [174] [175].

It is important to note that besides the described approach the KTA also allows using other models to determine the fracture toughness upon warm pre-stressing. In this context it refers to the method used in the British Standard BS 7910 [11] as an example.

Ukraine
The National general approach [12] to determination of RPV brittle fracture margin using WPS approach is described below.

The calculated fracture mechanics parameter (for example stress intensity factor (SIF)) and maximum allowable critical temperature of brittleness (CTB, T_{ka}) are defined for postulated defects and for any transient with PTS.

Allowable CTB for transient accident mode corresponds to minimum CTB along the crack front for which allowable SIF function touches the calculated SIF curve (tangent approach).

Maximum allowable critical temperature of brittleness (T_{ka}) for given accident corresponds to minimum of obtained values of allowable CTB for all calculated variants (scenarios) of the accidents.

Difference between T_{ka} and critical temperature of brittleness (T_k) of RPV metal defines margin of brittle fracture ΔT_{ka}.

In case that SIF curve decreases monotonically after reaching its global maximum K_{WPS}, it is allowed to determine T_{ka} based on approach of warm prestressing with using tangent point method in the SIF range $K_I = [0.9 \cdot K_{WPS}; K_{WPS}]$.

In case of repeated loading (after reaching the global maximum of SIF curve K_{WPS}), using of WPS approach is allowed provided that the following two conditions are met:

- repeated loading occurs at lower temperature T_2 than is the temperature of pre-load T_{WPS}, i.e., $T_2 < T_{WPS}$;
- maximum SIF over the repeated loading K_{max} must not exceed $0.9 \cdot K_{WPS}$, i.e. $K_{max} < 0.9 \cdot K_{WPS}$.

If these two conditions are met, T_{ka} may also be determined using the tangent point method in the range $K_I = [0.9 \cdot K_{WPS}; K_{WPS}]$.

In cases where at least one of these two conditions is not met (see examples on **Figure 15**), the WPS approach is prohibited, and the tangent point approach must be used for the part of SIF curve following the K_{WPS} value.
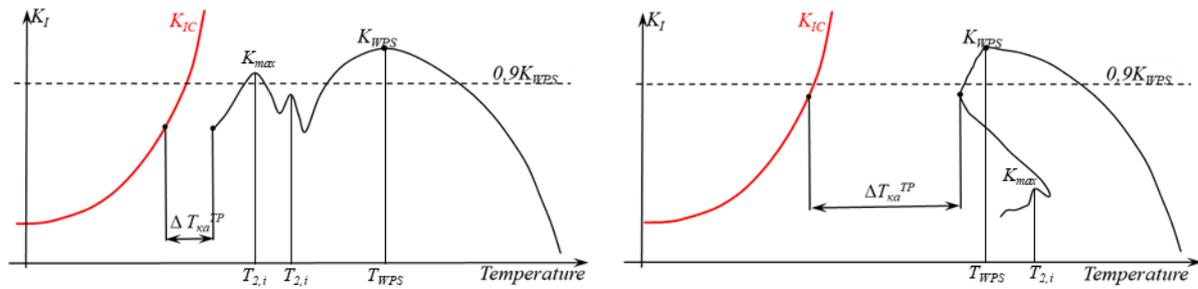
Figure 15: PTS examples for which WPS is not applicable according to the Ukrainian rules [12] (TP denotes tangent point method).

WPS approach in FAVOR PFM (used in the US, Slovenia, Spain and Switzerland)

In FAVOR, a fundamental requirement to apply the WPS model is that the flaw is not propagating into the RPV wall. This requirement is satisfied for two states: 1) the pre-existing flaw has not experienced its first initiation or 2) the flaw is in a state of crack arrest after propagating to some depth within the RPV wall.

Note 1: Crack propagation occurs instantaneously; time, τ, is frozen until the crack either 1) initiates a pre-existing flaw at $\tau = 0$ or 2) re-initiates upon leaving the arrest state.

Note 2: When the crack is in a state of arrest, the temperature and applied crack driving force, K_I, at the crack tip continue to evolve over time. The starting time for the WPS model is the elapsed time for the transient at the time of entering crack arrest. The transient "clock" is turned "off" at the point of initiation or re-initiation and turned back "on" (but not reset to 0) when the crack arrests.

Requirements for Entering into a WPS State

A flaw can enter into a state of WPS when all of the following requirements are met:

> Enter Condition 1: $K_I(\tau) > K_{Ic(min)} = a_{K_{Ic}}$; the crack is within the K_{Ic} probability space

> Enter Condition 2: $dK_I(\tau)/d\tau \leq 0$; a falling K_I field with respect to time, τ

Requirements for Exiting a WPS State

The WPS models implemented in FAVOR can be designated by combinations of the following three conditions to exit a WPS state:

> Exit Condition 1. $K_I(\tau) > K_{Ic(min)} = a_{K_{Ic}}$; the crack is within the K_{Ic} probability space

> Exit Condition 2. $dK_I(\tau)/d\tau > 0$; a rising K_I field with respect to time, τ

> Exit Condition 3. $K_I(\tau) \geq \alpha \cdot K_{I(max)}$

To satisfy Exit Condition 3, the K_I at the flaw tip must exceed some fraction, α, of the previously established maximum, $K_{I(max)}$, experienced by the flaw up to the point in time under consideration. The value for α is sampled from a prescribed distribution within the range of $0 \leq \alpha \leq 1.5$ (See **Figure 16**).

Table 1 *lists the three WPS models currently implemented in the FAVOR code[3]. All three models require the conventional LEFM condition, where Enter Condition 1 is a necessary, but not sufficient, condition for crack initiation. Thus, the three WPS models in*

Table 1 *adopt the additional condition that the driving force must also increase with time for cleavage crack re-initiation to be possible (Exit Condition 2). Where the WPS models differ is in how the crack exits the WPS state and then re-initiates, i.e., the treatment of the flaw when K_I is increasing with time $(dK_I/d\tau > 0)$ after there has been some previous time when $(dK_I/d\tau \leq 0)$.*

Table *1* summarizes the conditions required for crack re-initiation for the three WPS models. In addition to the Conventional LEFM model, all three WPS models in

---

3 Note that the FAVOR analysis results generated for the USNRC PTS Reevaluation Project (leading to the Alternative PTS Rule) were based on use of the "Conservative Principle WPS" in

Table *1*; however, the FAVOR code has implemented all WPS models in

Table *1*.

Table 1 are available to the NPP licensee for inclusion in their submission to the USNRC requesting a license extension.
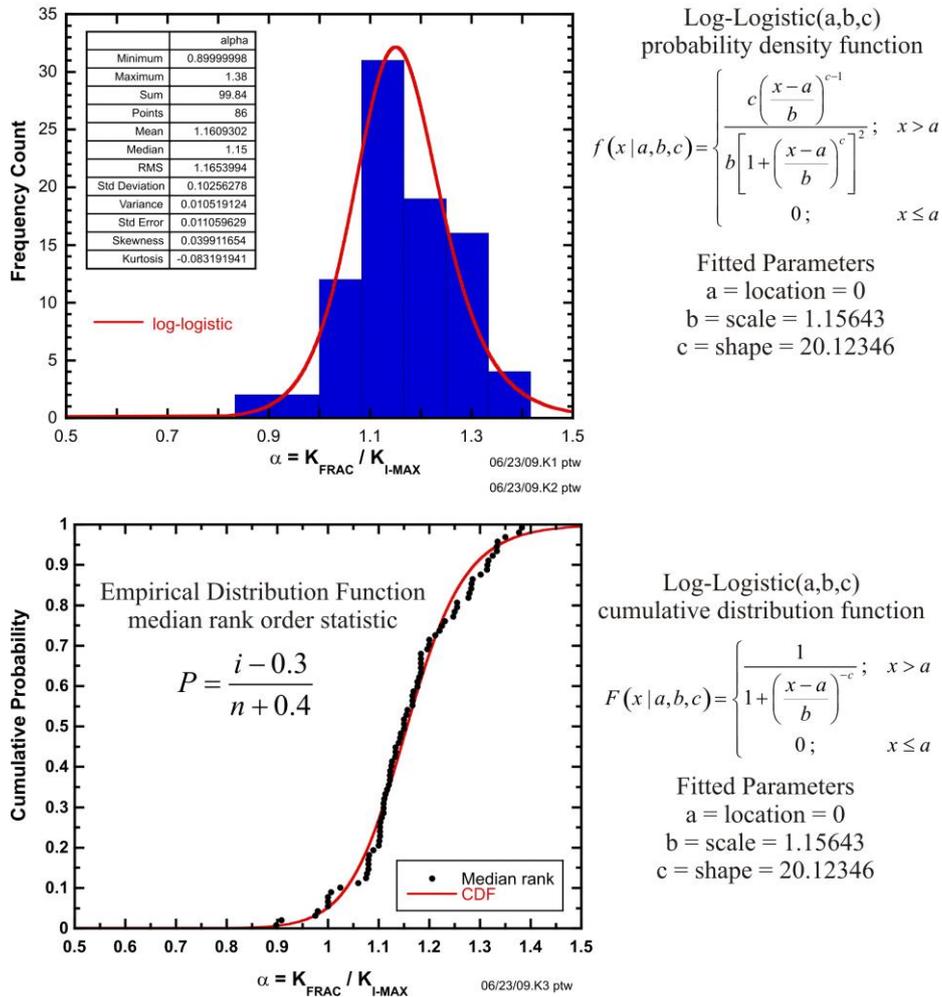
Figure 16: Example of warm prestressing: log-logistic distribution fitted to data obtained from Moinereau et al. [16] for a parameter in Best-Estimate Model for warm-prestress model implemented in FAVOR.

Reference [15] describes a study comparing the effects of conventional LEFM and the three WPS models summarized in

Table 1 on the computed RPV failure risks that are calculated by the FAVOR code. Analyses of the "Best Estimate WPS" model utilize data produced by the European Commission NESC-VII "SMILE" project and published by Moinereau and colleagues in 2007 [16].

Table 1: Summary of Criteria for Crack Re-Initiation Imposed by Different Models*.*

WPS?	Model ID	Conditions required for CPI>0
No	Conventional LEFM	Only condition 1.
Yes	Conservative Principle WPS	Condition 1 and 2.
	FAVOR WPS	Condition 1, 2, and 3, $\alpha = 1$.
	Best Estimate WPS	Condition 1, 2, and 3 α is sampled **from** distribution

For the conditions presented in **Figure 17** through **Figure 19**, the crack tip is static; it does not propagate.
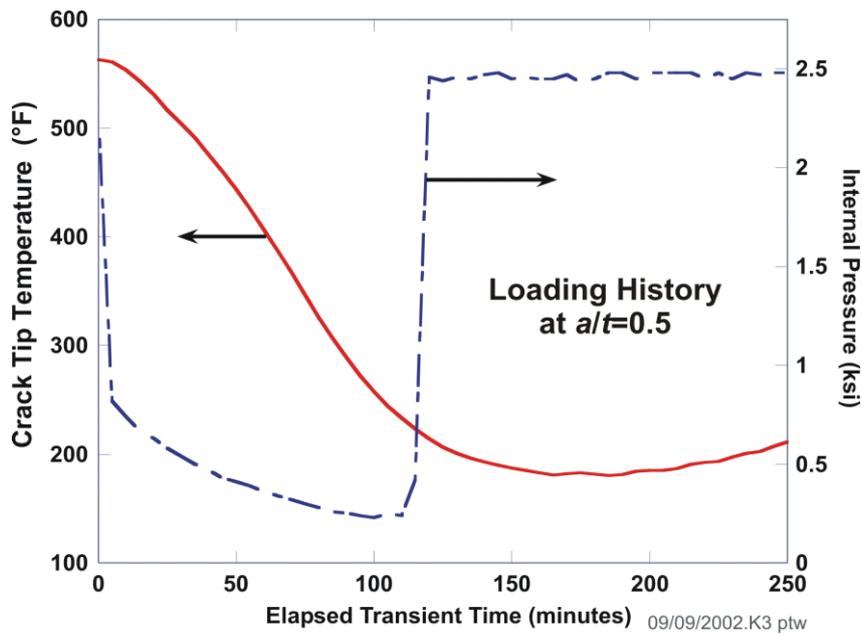
Figure 17: Example of warm prestressing: loading history with pressure applied to the inner surface and the temperature at the crack tip.
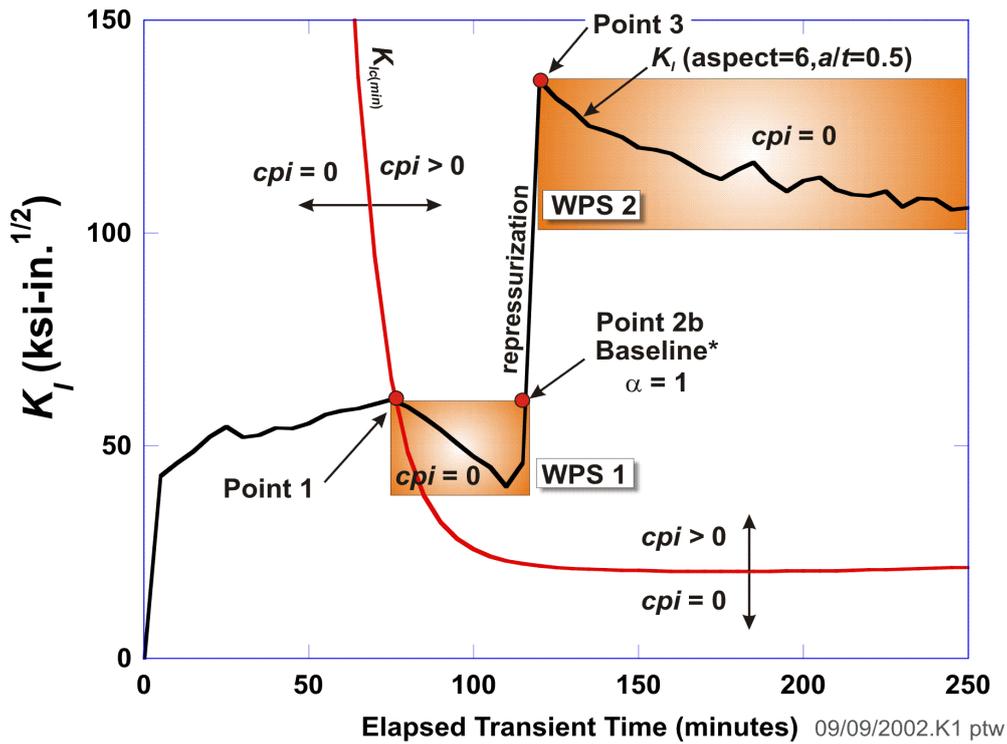
Figure 18: Example of warm prestressing: load path for a flaw showing two WPS regions. (cpi is the instantaneous conditional probability of initiation.
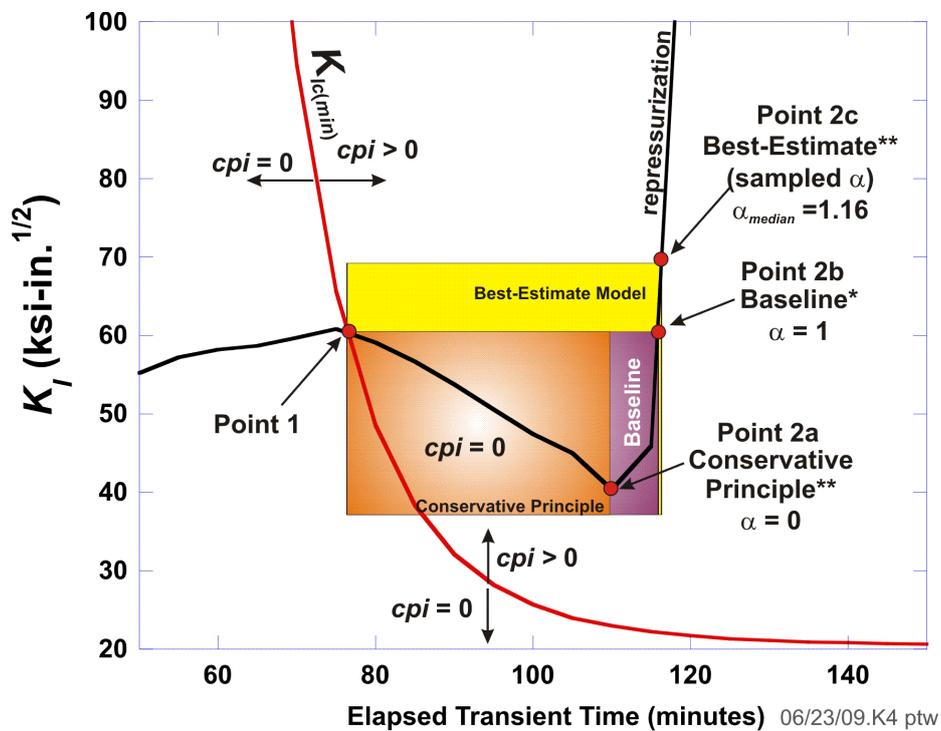
*Baseline WPS model implemented in FAVOR v02.4
**Conservative Principle and Best Estimate models
implemented in FAVOR v09.1

Figure 19: Example of warm prestressing: three options implemented in FAVOR for a flaw leaving the warm-prestress state allowing re-initiation. (cpi is the instantaneous conditional probability of initiation).

Hungary

In Hungary the effect of Warm Pre-Stress (WPS) can be taken into account for transients in which the vessel is not re-pressurized. When using WPS approach, the 90% value of the stress intensity factor at the local maximum point just before the reloading (understood in the K_I-time diagram) is used instead of the value at the given time as K_{Ic}. This method might be used also for irradiated materials (without further limitations).

France

In France the ACE methodology for WPS is used (see **Figure 20**). The allowable value of toughness K_{ACE} in cold conditions is given by the formula:

$$K_{ACE} = max\{K_{IC}; min(K_{WPS}; K_2 + K_{WPS}/2)\}$$

where K_{IC} is value given by the toughness curve (RCC-M code ZG 6000) and,

$$K_{WPS} = \max_{0 \to \tau} K_J(T)$$

$$K_2 = \min_{\tau_{max} \to \tau} K_J(T)$$

τ_{max} is the time at maximum K_J between 0 and τ; T is the crack tip temperature at τ.

Japan

In Japan for deterministic evaluations prescribed in JEAC4206-2016 [22], crack initiation cannot occur during $dK_I/d\tau \le 0$, here K_I and τ represent the stress intensity factor and time, respectively. On the other hand, WPS model, named ACE (Areva-CEA-EDF) model, is prescribed in JEAG4640-2018 [23] for probabilistic calculations.
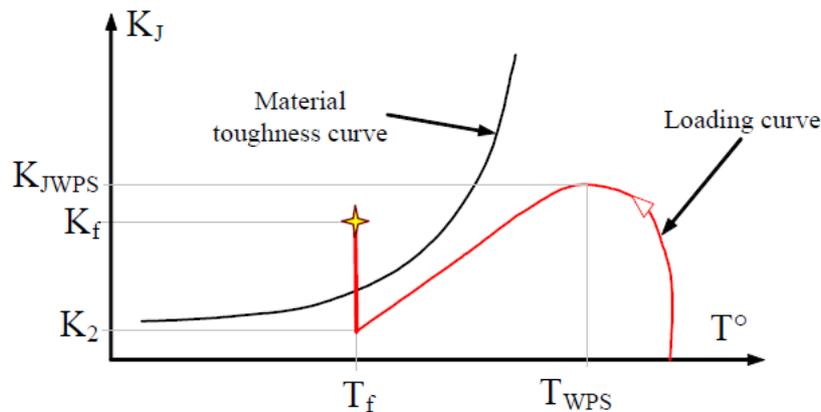
Figure 20: Interaction of the applied K_I time history and the Weibull K_{Ic} statistical model.

Russian Federation

According to the Russian standard [25] the strength condition is considered as satisfied if at any time point during the PTS event the following condition is satisfied for any point of the postulated defect front located in base and/or weld metal:

$$(K_I)_i = n_i \cdot K_I \le K_{IC} \tag{A4.1}$$

where for accident conditions ($i = 4$) the safety factor $n_i = 1.1$.

The condition (A4.1) is analysed for all time points when the following ratio is met:

$$(K_I)_i \ge 0.9 \cdot \Phi_i \tag{A4.2}$$

In the ratio (A4.2) Φ_i is function of time. For the time point τ, $\Phi_i(\tau)$ is equal to the maximum $(K_I)_i$ value for the time period from 0 to τ (see **Figure 21**), herein within the time range from 0 to $\tau_{max}^{(1)}$,

$\Phi_i(\tau) = 0$; where $\tau_{max}^{(1)}$ is the time point corresponding to the first maximum of $(K_I)_i$ dependence on τ.

As evident from **Figure 21**, within the range $0 \leq \tau < \tau_{max}^{(3)}$, $max(K_I)_i = K_{max}^{(1)}$. Therefore, within the range $\tau_{max}^{(1)} \leq \tau < \tau_{max}^{(3)}$, $\Phi_i(\tau)_i = K_{max}^{(1)}$. Within the range $0 \leq \tau < \tau_{max}^{(4)}$, $max(K_I)_i = K_{max}^{(3)}$. Therefore, within the range $\tau_{max}^{(3)} \leq \tau < \tau_{max}^{(4)}$, $\Phi_i(\tau) = K_{max}^{(3)}$.

5.3.2 Collection of existing experimental data

The previous chapter provides an overview of the different approaches and models used in the national standards to determine the effect of warm pre-stressing. Usually, such an the implementation of the WPS effect into national standards and the decision on which approach to use is based on experimental investigations that have been carried out. The purpose of this section is to briefly summarize the experiments related to WPS effect that have supported the respective implementations into national codes and standards.

Experiments that are explicitly investigating the WPS effect or experiments that consider the WPS effect besides other effects have been carried out for many years. Tests have been performed from large scale specimens down to small 10x10 SENB specimens, on base and weld metals in unirradiated, artificially aged and irradiated conditions.

In the Czech Republic a large experimental programme was performed in 2006–2008 within a research project focussed on WPS. This project was funded by the Czech Regulatory Body. WPS tests were performed on non-irradiated, artificially aged and irradiated (in research reactor) materials. Base materials of WWER-440 and WWER-1000 RPVs were tested. Both Charpy size SENB specimens and 1T CT specimens were tested. The total number of specimens was about 600. Different WPS-type tests like LCF, LUCF, LPUCF, LTUF, LPTUF were performed. Various test conditions (temperature and load at preloading and temperature at fracture) were used. Results of the project were used for preparation of the requirements for the WPS approach implementation in "Unified Procedure for Lifetime Assessment of Components and Piping in WWER NPPs–VERLIFE", which was later converted to Normative Technical Documentation of Association of Mechanical Engineers, Section IV (NTD AME).
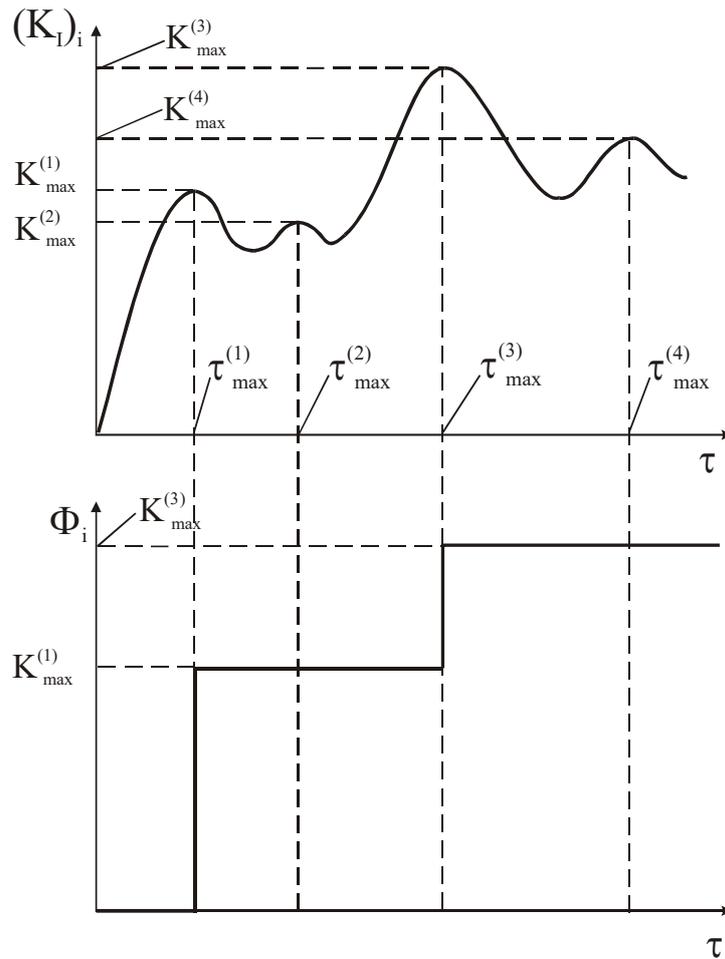
Figure 21: Scheme illustrating the $\Phi_i(\tau)$ function determination based on a known $(K_I)_i$ dependence on time τ [25].

Currently, a large project funded by ČEZ Company (owner of the Czech NPPs) is running, in frame of which the WPS tests are being performed with the goal to support application of WPS approach in PTS evaluations in accord with the NTD AME standard. Within this project, surveillance specimens irradiated (to various levels of fluence) directly in WWER-440 and WWER-1000 reactors are tested. Both base and weld materials are tested. Approximately 1600 specimens have been tested to date.

In Germany a large experimental program (>100 specimens) was performed that covered different loading cycles (LCF–LUCF) different specimen sizes (C(T)25 up to C(T)235), different materials with properties ranging from beginning of life to beyond end-of-life (references [171] [172] [173] [174] [175]). There is a national program ongoing, partly funded by the German ministry for economic affairs and energy and partly by NPP companies.

Experimental work has been performed in Sweden [43] and is ongoing in a joint research project with organisations from Sweden and Finland. These two projects are intended to give the authorities enough knowledge to better judge the applicability of the WPS effect.

At the end of the last century the WPS project was conducted in Ukraine, which include $1500\ mm$ thick specimens made from artificially aged WWER-440 and WWER-1000 materials, but the results themselves did not lead to the WPS implementation in Ukraine.

It should be mentioned that the European Commission funded an extensive investigation of WPS effect within SMILE project [16]. A study of WPS conditions (e.g., Load-Cool-Fracture, Load-Unload-Cool-Fracture, Load-Transient-Fracture, etc.) was performed using three nuclear pressure vessel grade ferritic steels. Data from a total of 86 experiments were reported and summarized in Table 3 of [13]. One outcome from these experiments is the ratio of the K_I at fracture, designated K_{I-FRAC}, to K_{I-MAX}

which is the maximum K_I that had occurred previously during the transient. This ratio quantifies the degree of re-loading that can occur before crack re-initiation again becomes possible.

5.3.3   WPS and constraint effect

Currently, constraint effect (shallow crack effect and/or biaxial loading effect) is not included in almost any national standard in terms of interaction with the WPS.

However, it should be noted that some investigations related to the study of the WPS effect at biaxial loading were performed within the NESC VII project, which included large-scale cruciform specimens (refs. [49] and [50]). The main result of the project is that WPS effect takes place also at biaxial loading and experimental results confirmed the applicability of considered WPS models (Chell, Chell & Haigh, Wallin and ACE) models to predict the WPS effect in case of biaxial loading with an acceptable level of accuracy. In conclusion, biaxial loading does not restrict the WPS effect.

Shallow crack effect is only included in the Russian standard MRKR–SKhR –2004 [25]. The technical basis of this methodology is contained in the references [47] [48]. The shallow crack effect can be applied in combination with the WPS model of MRKR–SKhR –2004 standard.

5.3.4   WPS and crack arrest

Section 5.3.1 deals with the applicability of WPS effect in the PTS assessment following national standards. In this section, this topic is extended to the simultaneous application of WPS effect and crack arrest. Thus, the focus of this section is to supplement the answers in Section 5.3.1 with the consideration of crack arrest, taking into account that an initiated crack could arrest, and its re-initiation may depend on WPS effect being (or not) considered simultaneously.

The answers provided in this section reveal that, in general, crack arrest is not considered in PTS assessments for WWER PTS applications. Crack arrest is not considered in France, Sweden and Japan either.

The German safety standards do not exclude explicitly consideration of WPS in combination with crack arrest. If a crack initiates brittle fracture even after taking WPS into account, the same mechanism should apply as in case without WPS. It is just stated "*If the stress intensity $K_I(\tau,T)$ is less than the crack arrest toughness $K_{Ia}(\tau,T)$ an unstable crack is arrested*". An issue may be the fact that the energy stored in the structure and released could be significantly higher since WPS effect altered the fracture toughness to higher values. This leads to potentially higher crack speeds and may therefore not be assessable with the static K_{Ia} concept. This issue should be investigated and clarified.

In the FAVOR code, the crack arrest and WPS models are applied independently. There is a possibility for crack initiation/arrest/re-initiation to occur with or without consideration of WPS. With WPS turned off, the crack initiation/arrest/re-initiation event sequence is also available, where the criterion for re-initiation is that the local applied K_I exceeds the local fracture toughness, K_{Ic}. WPS is not considered during the cleavage crack propagation phase, but only for crack initiation or re-initiation. In the case of the assessment of crack re-initiation (after the crack has arrested), WPS is considered separately only for re-initiation phase.

5.3.5   Application of the WPS to irradiated zones of RPV

Larger number of experimental studies of the WPS effect was carried-out on unirradiated materials than on the irradiated ones. However, based on the responses of the partners, it is concluded that the WPS approach is applicable for irradiated materials as well and there are no limits for its applicability in terms of level ductility, embrittlement or fluence for practical cases.

5.3.6   Analysis of the WPS aspect for RPV brittle fracture assessment

This subsection is a summary of Section 3.3 of Deliverable 1.2 [2] dedicated to the two following WPS aspects:

- analysis of the WPS experimental background, as provided by APAL partners as well as literature data, in terms of assessing the benefit of warm pre-stressing (material fracture toughness increasing) and in terms of determining the predictive capability of the modern WPS models
- analysis of the impact of the application of WPS models/approaches to the RPV brittle fracture margin for real PTS provided by the APAL partners

The calculations are performed based on the APAL partners' feedback to the questions presented below.

Data from national experimental projects (WPS tests) were provided by partners UJV and IPP.

Data for PTS scenarios (K_I in dependence on temperature for selected points of postulated cracks) were provided by UJV and IPP.

5.3.6.1   Analysis of the available WPS experimental data

5.3.6.1.1   Benefit of the pre-stressing

During years 2006 – 2008, warm pre-stressing tests on small (Charpy size) specimens were performed at UJV Rez [118] (some publicly available results are shown in [28] [46]). The specimens were made from WWER-440 and WWER-1000 RPV materials in unirradiated (as-received), thermally treated (artificially aged) and irradiated conditions, the last two conditions simulating the end-of-life state of the RPV.

In what follows, WPS effect on fracture toughness is evaluated in terms of the ratio of enhanced fracture toughness K_{Frac} (at re-load, after WPS) to fracture toughness of virgin material K_{IC} (without pre-load), as obtained from the experimental data of the Czech large experimental programme.

This ratio represents the increase of fracture toughness due to WPS effect and is expressed as follows:

$$K_{Frac}/K_{IC}$$

Since K_{IC} is of stochastic nature, for evaluation of the WPS effect (as objectively as possible) the value of K_{IC} relevant to 50% of fracture probability was selected.

In Ukraine the experimental studies of the WPS were performed at the end of the 80's – beginning of the 90's of the last century in G.S. Pisarenko Institute for Problems of Strength of the National Academy of Sciences of Ukraine. The results of these works were summarized in the paper [119]. The base metal and weld materials of WWER-440 and WWER-1000 RPVs in artificially aged state were tested. The effect of warm pre-stressing on fracture toughness characteristics has been most extensively studied on 25 mm and 50 mm thick specimens of WWER-440 RPV materials. Specimens of 150 mm thickness were tested after the 1T and 2T specimen test results had been analysed in order to confirm the most important conclusions obtained from that analysis and also to obtain the best experimentally substantiated data that could be applied to real structures.

Available experimental data (in numeric format) were taken from reference [120]. The CT1T and CT2T specimens were made from two WWER-440 RPV forgings and one weldment (total 19 specimens were tested for examination of the WPS effect).

As mentioned above, evaluations of WPS effect are determined relatively to the 50% confidence level of fracture toughness. Similar evaluation could be performed also for 95% confidence level of fracture toughness. The results of such evaluation are contained in Section 3.3.1 and section A2.1 of Annex 2 of Deliverable D1.2 [2]. These results can be summarized as follows:

- relative to the $K_{IC,50\%}$ the WPS effect led to an increase of fracture toughness in 579 cases from 593 experiments that is equal 97.6%.
- relative to the $K_{IC,95\%}$ the WPS effect led to an increase of fracture toughness in 480 cases from 593 experiments that is equal 80,9%.

Thus, it can be concluded that WPS inherent beneficial effect may be considered confirmed. This conclusion is based on increased material fracture toughness after WPS compared to the 50% and 95% fracture toughness confidence levels of virgin material (material to which WPS was not applied).

If the above evaluation of the effect of WPS is performed separately for irradiated or aged specimens and for unirradiated specimens, the following quantitative evaluation of the WPS effect is obtained:

- relative to the $K_{IC,50\%}$, the WPS effect for irradiated or aged specimens led to an increase of fracture toughness in 314 from 315 cases (99,7%) while for unirradiated specimens the WPS effect led to an increase of fracture toughness in 265 from 278 cases (95,3%)
- relative to the $K_{IC,95\%}$, the WPS effect for irradiated or aged specimens led to an increase of fracture toughness in 271 from 315 cases (86,0%) while for unirradiated specimens the WPS effect led to an increase of fracture toughness in 209 from 278 cases (78,9%).

This result witnesses in favour of the fact that beneficial WPS effect takes place for irradiated materials in the same manner as for the unirradiated ones.

It is also interesting to evaluate the material fracture toughness increase compared to the level of the pre-stressing at elevated temperature, i.e., to examine the ratio:

$$K_{Frac}/K_{WPS}$$

Summarized results of this ratio evaluation based on the Czech and Ukrainian WPS data as well as on the results from international project SMILE are presented in the chapter A2.2 of Annex 2 of Deliverable 1.2 [2]. Within SMILE project the WPS effect was experimentally studied on two unirradiated materials: heat-treated 17MoV8-4 mod. steel (in order to simulate the end-of-life state of RPV material) and 18MND5 steel (fully representative of initial state of RPV steel)) [14] [16]. These data from SMILE project served as the basis for establishing the parameter in Best-Estimate Model for warm pre-stress model implemented in FAVOR, see Figure 16.

These data (from all 3 projects presented - Czech, Ukrainian and SMILE - show that in 31 cases (4.6%) $K_{Frac} \leq K_{WPS}$. Thus, approximately in 95% cases pre-stressing leads to material fracture toughness increase to values higher than the pre-stressing level. It has to be noted that the distribution of parameter K_{Frac}/K_{WPS} depends on selection of WPS regimes and conditions (temperatures, loads) of the WPS tests in the database.

5.3.6.1.2   Analysis of the predictive capability of the modern WPS models

Based on the Czech project [118] WPS data, the calculation of predictions of fracture toughness values using the considered modern WPS models was performed[4]. In the calculations reported in subsection 3.3.1.2 of Deliverable 1.2 [2], the fracture toughness values (K_{IC}) were taken as 5% confidence level values (determined using 3-parametric Weibull distribution of the corresponding experimental data for the virgin material [118]) of the elastic parts of K_{JC}. Also, the K_{WPS} values and experimental K_{Fract} values are the elastic parts of the fracture toughness. The same approach was applied to the Ukrainian WPS data [120].

Based on the predictive results relatively to the 5% fracture toughness data, it can be seen that application of modified Wallin, Chell & Haigh and ACE models lead to conservative results in respect to the experimental data. The predictive results of the Wallin model [44] are slightly less conservative in respect to experimental data, and therefore application of this model in PTS assessments could lead to overestimation of the RPV brittle fracture margin. Modification of Wallin model proposed by UJV [46] enhances conservativeness of the Wallin model to a sufficient level. Concerning Chell & Haigh model, its application in PTS assessments may be associated with some technical difficulties.

---

[4] The data used for the validation of WPS effect are the ownership of the Czech Republic represented by the State Office for Nuclear Safety and were provide for research purposes within the APAL project.

Thus, application of ACE, modified Wallin and Chell & Haigh models may be considered more preferable from point of view of their usage in deterministic and probabilistic RPV brittle fracture assessments and it can be recommended for the analysis within WP3 and WP4.

Application of the Wallin model could be considered for probabilistic applications (it is relevant, if the whole fracture toughness distribution is used).

Considering the predictive results obtained relative to the 50% fracture toughness data, it can be seen that for this fracture toughness confidence level the predictions by modified Wallin, Chell & Haigh and ACE models are conservative in respect to the experimental data. But as it was mentioned above, the 50% fracture toughness curve is not used in the RPV integrity assessments (in deterministic formulation), and therefore results of this type of evaluation are not directly related to performing the PTS assessments.

5.3.6.2   WPS impact on the determination of RPV brittle fracture margin in PTS evaluations

In order to determine the influence of different WPS models (or WPS procedures) application on determination of RPV brittle fracture margin in PTS evaluations, seven model PTS transients were selected and provided by UJV and IPP.

UJV regimes are as follows:

- Regime 1 "Loss of Coolant Accident (LOCA) with break equivalent diameter 200 mm in hot leg of WWER-440 NPP"
- Regime 2 "Small Break Loss of Coolant Accident (SBLOCA) with break equivalent diameter 32 mm in cold leg of WWER-1000 NPP"

IPP regimes are as follows (all for WWER-1000 NPP):

- Regime 3 "False PRZ SV opening with maximum configuration of the ECCS, followed by closing after 2570 s in the "hot shutdown" state and operator actions to turn off the TQ14-34D01 pumps"
- Regime 4 "SG's 3 tubes rupture with the maximum configuration of the ECCS in the "hot shutdown" state"
- Regime 5 "Primary leakage DN 32 with maximum ECCS configuration (hot shutdown state)";
- Regime 6 "ECCS HPIS pipeline rupture DN 125 with minimum ECCS configuration (power operating state)"
- Regime 7 "Inadvertent opening of fast acting reducing valve for steam discharge into the condenser with minimum ECCS configuration (hot shutdown state)"

The results of RPV brittle fracture margin assessment for considered model transients with using different WPS models and/or national standards are presented in **Table 2** and **Figure 22**.

The approach "k=0.8, no peaks" presented in **Table 2** was taken from the chapter 8.3 of IAEA-EBP-WWER-08 [121]. According to [121], this approach is applicable only for those transients which are characterized by monotonically decreasing loading path after reaching K_{WPS}, and T_{ka} is defined using TP method within the SIF range $K_I = [0.8 \cdot K_{WPS}; K_{WPS}]$.

Note, that approach "k=0.9, no peaks" is similar (taken from the IAEA-EBP-WWER-08 Rev. 1 [7]), but the only one difference is that T_{ka} is defined using TP method within the SIF range $K_I = [0.9 \cdot K_{WPS}; K_{WPS}]$. In both cases, coefficients 0.8 and 0.9 represent some kind of safety factor.

WPS application according to the IAEA Guidelines [7] and [121] can give benefit for monotonically decreasing loading path transients, which has limited practical benefit. So, it can be recommended not to use these Guidelines in further works within the APAL project.

It can be seen from **Table 2** that in general almost all WPS approaches, except Ukrainian one and Russian one for some cases, lead to the reasonable decreasing of conservativeness in the RPV safety assessment.

It is seen that Ukrainian WPS approach is not applicable almost for any of the representative transients. Therefore, it doesn't provide any practical benefit. Consequently, it is recommended that this approach should be examined more carefully, taking into account the nature of WPS experimental data, or harmonized with some of the physically relevant models, like modified Wallin or ACE models or NTD AME 2020 (VERLIFE-NULIFE) WPS procedure.

Russian approach is similar to the Ukrainian one, but in some cases, it leads even to increasing conservatism relatively to the TP approach (1)[5].

As recommendation for further deterministic and probabilistic RPV brittle fracture assessments within APAL WP3 and WP4 we propose to select some of the (7) – (12) models (see numbering of columns in **Table 2**).

---

[5] It is relevant if we compare with the classic TP approach. But it is not true if we compare with the Russian TP approach where the safety factor 1.1 is also used.

Table 2: Variation of the maximum allowable transition temperature for considered transients depending on the WPS model or standard applied.

Regime	TP	k=0.8, no peaks[1]	k=0.9, no peaks[2]	VERLIFE-2008[3]	UKR	RUS	USA (Baseline model, K_{max} estimated)	USA (all local maximums estimated)	ACE	Wallin	Modified Wallin	NTD AME 2020 (VERLIFE-NULIFE)
	(1)	(2)	(3)	(4)	(5)	(6)	(7)	(8)	(9)	(10)	(11)	(12)
1	119.1	119.1	119.1	119.1	119.1	120.6	141.5	129.98	141.5	141.5	141.5	129.38
2	80.5	80.5	80.5	80.5	80.5	107.6	173.5	91.33	173.5	173.5	173.5	116.87
3	55.7	55.7	55.7	55.7	55.7	49.1	96.7	55.7	55.7	78.0	60.4	55.7
4	80.8	80.8	80.8	80.8	83.6	109.8	154.6	125.5	80.8	139.0	108.2	95.6
5	57.54	71.1	73.36	73.36	67.84	60.44	69.69	69.69	64.38	75.5	75.5	71.5
6	83.34	83.34	83.34	83.34	83.34	83.23	125.32	83.34	87.61	127.4	104.44	94.8
7	97.26	98.94	104.34	104.34	101.54	97.27	124.99	124.99	124.99	125.0	124.99	104.34

Yellow cells indicate that WPS approach is inapplicable according to the corresponding rules.

Gray cells indicate the case when application of the Russian approach results in decreasing the RPV brittle fracture margin in comparison to classic TP approach (it is due to the fact, that according to Russian brittle fracture criterion, SIF is multiplied by safety factor 1.1). This statement is true if we compare the Russian approach (6) with the classic TP approach (1), but it is not true if we compare Russian approach (6) with the "Russian TP approach" where the safety factor of 1.1 is also applied.

Notes:

1) This approach is taken according to the chapter 8.3 of IAEA-EBP-WWER-08 [121], according to which WPS is applicable for those transients which are characterized by continuously decreasing loading path after reaching K_{WPS}. In this case T_{ka} is defined using tangent point method within the range $K_I = [0.8 \cdot K_{WPS}; K_{WPS}]$.
2) This approach is taken according to chapter 7.3 of IAEA-EBP-WWER-08 Rev. 1 [7], according to which WPS is applicable for those transients which are characterized by continuously decreasing loading path after reaching K_{WPS}. In this case T_{ka} is defined using tangent point method within the range $K_I = [0.9 \cdot K_{WPS}; K_{WPS}]$.
3) According to the VERLIFE-2008 [27] in the case with reloading (when the loading path of temperature is not monotonically decreasing), T_{ka} can be determined using the most conservative value from all 90% of local maxima of SIF.
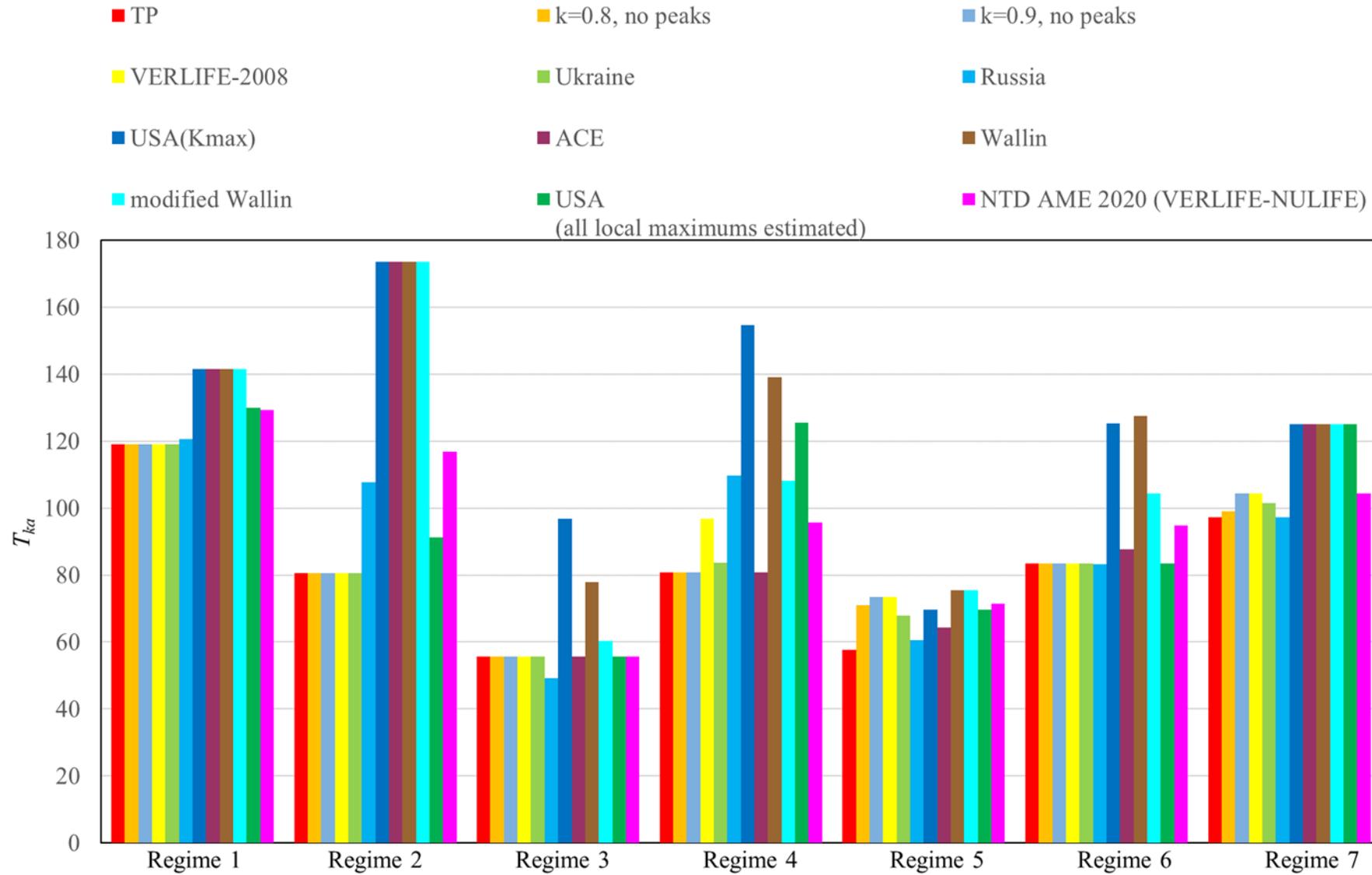
Figure 22: Variation of the maximum allowable transition temperature for considered transients depending on the WPS model applied.

5.4 Conclusions

5.4.1 WPS models/approaches, standards and applicability

As a result of the answers to the Task 1.2 questionnaire, it is concluded that only Sweden, France and Finland have not yet implemented the WPS approach into the RPV PTS assessment.

France and Sweden have performed a lot of experimental research activities in this field, and it is expected that they include WPS approach into RPV integrity assessments. Also, Sweden and Finland have joint ongoing project. It is expected that they include WPS into RPV integrity assessments.

It can be seen that USA, Spain and Slovenia use the US NRC rules. In Germany and Switzerland the KTA WPS rules are specified in the national standards. Czech Republic, Ukraine, Hungary, France and Japan have their own domestic rules.

For those countries where the WPS is not incorporated in the national rules of nuclear industry, it can be recommended to include it since the usage of the WPS is beneficial and corresponds to the best world practice.

Different standards or methodologies are used in participating countries to consider WPS effect in PTS analyses. The main differences consist in the following aspects: possibility of WPS application for monotonical or non-monotonical unloading, consideration of Case 1 in WPS approach, application of different WPS models for Case 1 and application of additional safety margins. The appropriate comparison is shown in **Table *3***.

5.4.2 Experimental data

The WPS effect has been extensively investigated up to this date. Several large national test campaigns (e.g., campaign funded by the Czech Regulatory Body reported by UJV with ~600 tests) supported the implementation of WPS into national codes and standards.

Still efforts are being made to further improve the acceptance and the knowledge of this effect. A large national experimental program funded by ČEZ Company focusing on irradiated materials from surveillance programs is currently ongoing in the Czech Republic. In Germany there is a national program ongoing, partly funded by the German ministry for economic affairs and energy and partly by NPP companies. Companies from Sweden and Finland are involved in a joint research project regarding WPS. This shows that even though the existence and the assessment of the effect itself are commonly accepted, there is still a need for further investigations.

Table *4* provides an overview of the reported national efforts to implement a suitable WPS approach into the respective national standards. Besides these reported projects, several other have been conducted to investigate WPS effect with a lot of published data. Summarizing all these available data and their easy access could further improve the research of the WPS effect and its understanding.

Table 3: Comparison of approaches to WPS application in partner's countries.

Country	Czech R.	Germany	Switzerland	Ukraine	Hungary	France	Japan	Spain	Slovenia	USA	Russia (*)
Partner	UJV	FRA-G	PSI	IPP + SSTC NRS	BZN	IRSN	JAEA	Tecnatom	JSI	OCI	IPP
Standard	NTD AME	KTA	KTA	PM-T.0.03.415-16	HAEA guide is used	RCC-M/RSE-M	JEAC/JEAG	US NRC			RD EO 0606 – 2005 (MRKR – SKhR – 2004)
WPS for monotonical	+	+		+	+	+ / +	+ / +	+			+
WPS for non-monotonical	+	+		+	+ (always the latest monotonic part is taken in consideration)	- / +	+ / +	+			+
Case 1	+	+		−	+	- / +	+ / +	−			−
WPS model for Case 1	modif. Wallin	Chell, other allowed		−	−	- / ACE	+ / ACE	−			−
Safety factor	0.9	1		0.9	0.9	1	1	1			0.9 (**)
Additional condition	−	−		$T_2 < T_1$ for reload $K_{reload} < 0.9\ K_{WPS}$	$K_{reload} < 0.9\ K_{WPS}$	−	−	Necessary conditions for a flaw to initiate: $K_{applied} > K_{Ic(min)}$ $dK_{applied}/d\tau > 0$ $K_{applied}(\tau) \geq \alpha \cdot \max_{0 \leq t \leq \tau} K_{applied}(t),$			−

* Despite the fact that there is no Russian representative among the APAL partners it is relevant to include the Russian approach into order the table to be consistent in terms of the world-wide experience

** Before application of the safety factor 0.9 for WPS the PTS loading path (SIF) must be multiplied by 1.1

Table 4: Experimental WPS data in partner's countries.

Participant	National test program	Materials	Conditions	Type of specimen	WPS regime	Number of tests	Comments
UJV	YES	different VVER base materials	unirradiated, artificially aged and irradiated / different temperatures and load level	Charpy sized SEN(B), 1T C(T)	LCF, LUCF, LPUCF, LTUF, LPTUF	~600	Currently ongoing project with ~ 1600 specimens from surveillance programs
FRA-G	YES	different base materials	begin of life - beyond end of life (artificially aged)	C(T)25 up to C(T)235	LCF, LPUCF, LUCF, LCUF, LTUF	> 100	Currently ongoing project with unirradiated and irradiated material
PSI	NO	n.l.	n.l.	n.l.	n.l.	n.l.	
IPP and SSTC NRS	YES	WWER-440 RPV: two forgings and one weld seam. WWER-1000 one forging and one weld seam	artificially aged for EOL	1T C(T) 2T C(T) SEN(B) T=150mm	LCF, LUCF, LPUCF	19 15	WPS used according to the IAEA guidelines with taking into account literature experimental data and conclusions of SMILE project
KIWA	YES	18MND5	Test temperature -150 C	3PB, W=50 mm, a/W=0.5	LUCF LU(HT)CF	63	
Tecnatom	NO	n.l.	n.l.	n.l.	n.l.	n.l.	WPS model by US NRC used
BZN	NO	n.l.	n.l.	n.l.	n.l.	n.l.	
JSI	NO	n.l.	n.l.	n.l.	n.l.	n.l.	WPS model by US NRC used
IRSN	YES	n.l.	n.l.	n.l.	n.l.	n.l.	
JAEA	YES	A533B Cl.1 steel	unirradiated / different temperatures and load level	1T C(T), 0.4T C(T)	LTTUF, LTPTUF, LUCF	66	Additional tests on the other conditions are ongoing.
OCI	YES	n.l.	n.l.	n.l.	n.l.	n.l.	WPS model by US NRC used

5.4.3   WPS effects

Constraint effect
Currently, constraint effect (shallow crack effect and/or biaxial loading effect) is not included in almost any national standard in terms of interaction with the WPS.

However, it should be noted that some investigations related to the study of the WPS effect at biaxial loading were performed within the NESC VII project indicate that WPS effect takes place also at biaxial loading and experimental results confirmed the applicability of considered WPS models (Chell, Chell & Haigh, Wallin and ACE) to predict WPS effect in case of biaxial loading with an acceptable level of accuracy. Thus, biaxial loading does not restrict the WPS effect.

Shallow crack effect is only included in the Russian standard MRKR–SKhR –2004 [25]. The technical basis of this methodology is contained in the references [47] and [48]. The shallow crack effect can be applied in combination with the WPS model of MRKR–SKhR –2004 standard.

Crack arrest

The answers provided in this section reveal that, in general, crack arrest is not considered in PTS assessments for WWER PTS applications. Crack arrest is not considered in France, Sweden, Switzerland and Japan either.

It can be seen that, besides the USA, also Spain and Slovenia use the US NRC rules, that allows WPS effect and crack arrest to be applied simultaneously.

The German safety standards do not exclude explicitly consideration of WPS in combination with crack arrest. However, Framatome recommends that future experimental work shall be directed to assess whether the static K_{Ia} concept is valid or not under WPS effect (See section 5.3.4).

In summary, the whole spectrum of possible answers is covered by the participants. Thus, a recommendation would be to analyse the possible benefits in terms of margin assessment, based on considering the WPS effect in re-initiation events after crack arrest, both in the deterministic and probabilistic PTS analyses to be performed within APAL.

WPS effect applied to irradiated RPV zones

As a result of the partners´ answers, it can be stated that the WPS approach is also applicable for irradiated materials and there are no limits for its applicability in terms of level of ductility, embrittlement or fluence for practical cases.

5.5 Gaps

5.5.1 Gaps related to the WPS consideration in the RPV PTS assessment

The overall opinion is that the WPS effect is an important subject. Furthermore, most partners have the opinion that the WPS effect is a relevant and, in some cases, required effect to be considered in PTS assessments especially when considering LTO. From the answers above open questions or issues regarding the WPS effect have also been identified. Below the open issues are summarized:

- The possible non- conservative estimation of the WPS effect when the most severe load is estimated with the TH analyses. The reasoning behind this is that the magnitude of the WPS effect is directly connected with the magnitude of the pre-load, a higher pre-load gives a larger WPS effect. Hence, overpredicting the pre-load would lead to over predicting the WPS effect leading to a possible non-conservative result.
- The possibility that important information from the transient is lost when an envelope of the TH analyses is used. The level of margin to fracture given by the WPS effect during the cooling phase of the PTS transient is not known with certainty. Therefore, it is important to know if there exist load disturbances during the transient. If load disturbances exist during the cooling phase the criteria of monotonic decreasing load could be violated. These transients could possibly be analysed with local probabilistic models such as Beremin [51] or Kroon and Faleskog [52].
- The lack of experimental results on realistically pre-loaded irradiated material. The majority of the published experimental results demonstrating the WPS effect are on non-irradiated material where low temperatures are used to mimic the effect of the irradiation on the fracture toughness curve. There exist some published experimental results regarding the WPS effect on irradiated materials, e.g., [28]. But as one partner points out is that all these experiments have been conducted on material that has not been irradiated in loaded condition. It is suggested that material from decommissioned RPV could be used to determine if this could be of importance. This would also increase the available experimental data on irradiated material.

- How to treat residual stresses in regard to the WPS effect in analyses is not fully examined. There is very little published work on this subject. There is ongoing work that suggests that a prior high residual stress field can slightly affect the WPS-effect in both positive and negative direction. Further experimental and numerical research in this field is recommended.
- The interaction between constraint and the WPS effect is also suggested as a topic that could need more studies. The majority of the performed WPS experiments have been conducted on standard high constraint specimens. A situation with low constraint (shallow crack) would lead to a larger plastic zone size during the pre-load. This larger plastic zone size in front of the crack tip could, due to the mechanisms behind the WPS effect, possibly also lead to a larger WPS effect.
- The probabilistic formulation of the WPS models for probabilistic calculations of RPV brittle fracture is an open issue.

5.5.2   Gaps related to the most sophisticated WPS model

Almost all partners support the application of some of the specific WPS models, like Chell, Wallin, modified Wallin or ACE. This fact implicitly means that WPS can be applied also for non-monotonical unloading during PTS. This becomes more important for currently performed PTS analyses which are based on more realistic representations of the TH transients (mixing analyses performed by CFD codes), including consideration of operator's actions (which can lead to re-pressurization of the primary system or to switch off/switch on the Emergency Core-Cooling System, ECCS). In these cases, the time dependent stress intensity factor curve after reaching its maximum exhibits at least small fluctuations or even large unloadings and reloadings. Applicability of WPS for non-monotonical unloading seems necessary in this context.

On the other hand, when applied WPS to non-monotonical unloading, consideration of Case 1 is necessary to maintain sufficient conservativeness. Some methodologies currently in use in participating countries do not consider Case 1, but its relevancy was proven by many WPS tests, when final fracture occurs below K_{WPS}. All the above mentioned WPS models consider Case 1. Chell model was found as rather complicated for practical application. Wallin model was not found as sufficiently conservative for some types of WPS tests, e.g., for LCF tests. Both modified Wallin and ACE models are simple for use and sufficiently conservative. Advantage of ACE model is its independence of K_{IC} value, but this model is rather more conservative than modified Wallin model.

The current TH analyses are focused on most severe cooling at the beginning of PTS, which will enhance preloading (WPS), but unloading phase may not be analysed conservatively enough for WPS. When considering WPS effect in PTS evaluation the attention should be paid to this issue (not to overestimate the pre-load and not to enhance the effect of WPS, See Subsection 5.5.3).

Only KTA (based on Chell), Czech NTD AME (based on modified Wallin) and French RSE-M (based on ACE) standards consider unloading in WPS application. Most approaches do not consider "Case 1" at all and use only K_{WPS} (i.e., maximum approach). Thus, when considering Case 1 sufficiently conservative, unloading during the PTS should be considered.

5.5.3   Gaps related to TH aspects

Although the WPS method can bring benefits to the RPV structural integrity assessment, requirements for TH analyses in case of WPS application are not clearly defined yet. This leads to varied application of WPS in PTS analyses in different countries. The mentioned variation can potentially impact the TH transient selection for PTS analysis and affect the results of the structural integrity assessment of the RPV. Therefore, analysis of applied approaches and development of recommendations (unified approach) for the TH analyses with respect to WPS application is an important aspect of the RPV structural integrity assessment for LTO.

Performed analyses confirmed the absence of a unified methodology not only for WPS approach, but also for the TH aspects of its application.

In the Czech Republic and Ukraine conservative TH calculations should be performed for their further application in structural analyses. At the same time Czech requirements foreseen that the TH analyses should be conservative in relation to K_{min} determination, which does not necessarily correspond to the conservative K_{max} values. Such approach may require performing variant TH calculations.

German regulations do not require performing of conservative TH calculations. Preference is given to variant analyses (several transients need to be investigated), which should demonstrate that leading transient provides lowest maximum allowable transition temperature. Similar position is demonstrated by Finland, which indicated the need to perform TH analyses with varying parameters in case of WPS application.

France (IRSN), Switzerland (PSI), Sweden (KIWA) and Slovenia (JSI) indicated the reasonability to perform sensitivity study or variant calculations in case of WPS approach application.

Applied in Japan (JAEA) WPS approach is based on the conservative methodology and does not require variant TH calculations or uncertainties evaluation.

In the USA (OCI), the WPS approach is linked with a probabilistic fracture mechanic computer program. It is assumed that for the severe PTS transients that dominate risk for RPV, there is a small difference between the conditional probabilities of crack initiation and of through-wall cracking frequency predicted by the different WPS models. Thus, changing the approach for the TH analysis or the variant TH calculations are not foreseen.

Recommendations to APAL WP2, WP3 and WP4 works

It is recommended during TH analysis within WP2 (and subsequent structural analysis within WP3 and WP4) to take into account conservative consideration of maximum loading and maximum unloading during the PTS. The second option is to perform the sensitivity study focused on assessment of these effects.

Based on the performed analysis of the predictive capabilities of the examined WPS models, it is concluded that application of modified Wallin, Chell & Haigh and ACE models leads to conservative results in respect to experimental data (provided by UJV and IPP) and, consequently, also with respect to RPV brittle fracture assessment. The predictive results of the Wallin model are slightly less conservative, and therefore its application could lead to overestimation of the RPV brittle fracture margin in PTS assessment. The NTD AME 2020 procedure is more conservative than the modified Wallin model.

Therefore, application of the NTD AME 2020, ACE and modified Wallin models may be considered more preferable in terms of their usage in deterministic RPV brittle fracture assessments and can be recommended for the analysis within WP3. However, it would be also useful to perform deterministic calculations using TP method, Ukrainian, Russian and Hungarian standards.

WPS effect can be examined in some sensitivity studies within WP4 probabilistic PTS assessments. Application of the Wallin model could be considered in WP4 for probabilistic applications (it is relevant if the whole fracture toughness distribution is used). Besides of models implemented in FAVOR also WPS models considering Case 1 should be examined.

5.5.4   Gaps related to probabilistic brittle fracture and ductile fracture

For the probabilistic formulation of the WPS models in probabilistic calculations of RPV brittle fracture there is not a common answer; thus, this is an open issue.

Regarding to ductile fracture, exceeding the ductile upper shelf limit is not allowed by majority of standards. Nevertheless, the question whether WPS takes place in conditions of preload approaching or slightly exceeding this limit is of interest.

The partners who perform PTS analyses do not contain impose any specific requirements on WPS in the context of ductile tearing during preloading. Usually, they have found it a very hypothetical issue and such a case has not been observed yet, but it could be considered as a hypothetical one and the

reason for this evaluation should be evaluated based on case by case basis. Usually, the codes have no limitation for using WPS approach after preloading to ductile tearing level, however, there is no significant benefit especially in case of the RPV.

5.6   Recommendations

It is recommended during TH analysis within WP2 (and subsequent structural analysis within WP3 and WP4) to take into account conservative consideration of maximum loading and maximum unloading during the PTS. The second option is to perform the sensitivity study focused on assessment of these effects.

Based on the performed analysis of the predictive capabilities of the examined WPS models, it is concluded that application of modified Wallin, Chell & Haigh and ACE models lead to conservative results in respect to experimental data (provided by UJV and IPP) and, consequently, also with respect to RPV brittle fracture assessment. The predictive results of the Wallin model are slightly less conservative, and therefore its application could lead to overestimation of the RPV brittle fracture margin in PTS assessment. The NTD AME 2020 procedure is more conservative than the modified Wallin model.

Therefore, application of the NTD AME 2020, ACE and modified Wallin models may be considered more preferable in terms of their usage in deterministic RPV brittle fracture assessments and can be recommended for the analyses within WP3 and WP4. However, it would be also useful to perform deterministic calculations using TP method, Ukrainian, Russian and Hungarian standards.

Application of the Wallin model could be considered in WP3 and WP4 for probabilistic applications (it is relevant if the whole fracture toughness distribution is used).

WPS effect can be examined in some sensitivity studies within WP4 probabilistic PTS assessments. Besides of models implemented in FAVOR also WPS models considering Case 1 should be examined.

6   State-of-the-art for thermal-hydraulic (TH) analysis

Accurate analysis of loading of the reactor pressure vessel (RPV) and other components of PWRs and WWERs requires knowledge of the local thermal-hydraulic parameters for the scenarios being considered. These parameters are obtained through thermal-hydraulic (TH) analysis. The goal of the thermal-hydraulic (TH) analysis is the determination of the local pressure, temperature, and heat transfer coefficient histories in the downcomer region that affect the RPV wall by thermal and mechanical loading.

The results of Task 1.3 *State-of-the-art for the thermal-hydraulic (TH) analysis* are summarized in this section.

6.1   Overview

A literature review and collection of experience and of current practices have been carried out to define the current state-of-the-art and remaining gaps in thermal-hydraulic analysis for pressurized thermal shock (PTS) scenarios. Experience from the different APAL partners was collected through a questionnaire, which was distributed to the partners. The responses to this questionnaire provide a basis for many of the conclusions in this report. The limits of computer codes used for mixing analysis were discussed. The results of previous projects oriented to TH analysis and uncertainty quantification (UQ) have been collected and summarized, where relevant for PTS analysis. The available experimental TH data for PTS, usable for validation of TH computer codes and in the development of UQ methods, have been gathered. Existing knowledge on human interactions assumed for PTS analysis has also been considered.

6.2   Description of activities

The questionnaire of Task 1.3 State-of-the-art for thermal-hydraulic (TH) analysis focuses on the following points:

- The current methodology employed by each partner for thermal-hydraulics analysis of PTS, and the verification and validation (V&V) status of this work
- The PTS scenarios that have been considered by each partner and the basic simplifying assumptions that are applied for the scenarios
- The partners' capabilities regarding uncertainty quantification and its application to thermal-hydraulics analysis of PTS scenarios, including the availability of relevant model input and boundary conditions uncertainties
- The partners' capabilities regarding the propagation of uncertainties in multi-physics simulations, and in particular their capabilities for modelling the propagation of uncertainties from thermal-hydraulics simulations to subsequent structural mechanics simulations for PTS
- The partners' experience in considering the impact of human interactions (e.g., timing of operator actions, erroneous operator actions) on PTS TH analysis

In total, 14 responses to the questionnaire were received. These have been summarised in this report. The responding countries, partners and persons are listed below:

Country	Partner	Contributing Author
Czech Republic	UJV	Pavel Kral
Germany	Framatome	Richard Trewin
Switzerland	PSI	Ivor Clifford
Ukraine	IPP-CENTRE	Yaroslav Dubyk
Sweden	KIWA	Lukasz Sokolowski
Spain	Tecnatom	Carlos Cueto-Felgueroso
Germany	GRS	Stefan Wenzel
Hungary	BZN	Szabolcs Szávai

Country	Partner	Contributing Author
Slovenia	JSI	Andrej Prošek
France	IRSN	Jérôme Roy
Finland	LUT	Markku Puustinen
Ukraine	SSTC	Maksym Vyshemirskyi
Japan	JAEA	Jinya Katsuyuma
USA	OCI	Richard Bass

6.3   Main topics

This section provides a summary of the main topics included in D1.3 [3] with a specific focus on the literature review that was conducted for each of the topics.

6.3.1   Thermal-hydraulic Phenomena Relevant for PTS

As stated above, PTS accidents are characterized by rapid cooldown of the primary coolant, particularly in the downcomer, and by the subsequent cooldown of the RPV wall leading to thermal stresses in the RPV wall loaded (usually) at the same time by inner pressure. This cooldown is often nonuniform (asymmetric), which causes additional thermal stress and RPV load. The nonuniformity is caused typically by emergency core cooling system (ECCS) injection or/and by rapid asymmetric cooling down via steam generators.

The thermal-hydraulic phenomena and factors important for PTS are described in number of publications and papers. Abstracts from the most important PTS references (relevant to TH phenomena) are given in subsections 2.1.1 through 2.1.4 of Deliverable D1.3 [3] including an overview of evolution of the phenomena identification and ranking table (PIRT). An APAL summary on the topic of TH phenomena relevant to PTS is concluded in the subsection 2.1.5 of Deliverable D1.3 [3]. Those subsections of Deliverable D1.3 are summarized below.

6.3.1.1   International Atomic Energy Agency, 2010. Pressurised Thermal Shock in Nuclear Power Plants: Good Practices for Assessment, IAEA, Austria, IAEA-TECDOC-1627 [6]

6.3.1.1.1   Thermal-hydraulic factors determining PTS load

Selection of the transients for deterministic analysis can be based on analysis and engineering judgment using the design basis accident analysis approach, combined with operational experience. It is important to consider several factors determining thermal and mechanical loading mechanisms in the downcomer during the overcooling events. These factors are:

- Final temperature in the downcomer.
- Temperature decrease rate.
- Nonuniform cooling of the RPV, characterized by cold plumes and their interaction and by the nonuniformity of the coolant-to-wall heat transfer coefficient in the downcomer.
- Level of primary pressure.
- Width of cold plume.
- Initial temperature in downcomer.
- Stratification or stagnation of flow in cold leg.

6.3.1.1.2   Relevant initiating events and phenomena

The aim of setting up a list of initiating events is to ensure a complete analysis of the RPV response to postulated disturbances which may threaten its integrity. At a minimum, the following groups of initiating events should be taken into account. Compilation of the list of initiating events corresponding to each of the following groups is usually based on engineering judgment while assisted with probabilistic consideration available in the Safety Analysis Report (SAR) of the plant, taking into account the design features and implemented modifications of the given nuclear plant.

Loss of coolant accidents

Different sizes of both cold and hot leg loss of coolant accidents (LOCA) which are characterized by rapid cooldown should be considered. Attention should be paid on to the scenarios leading to flow stagnation, which causes faster cooldown rate and cold plumes in the downcomer. Attention should be given to breaks sizes corresponding to existing pipes connected to primary system. Cold re-pressurisation of the reactor vessel is usually prohibited in principle, but the possibility of isolating the leak and the subsequent re-pressurisation have to be considered.

Stuck open pressurizer safety or relief valve

After an overcooling transient caused by a stuck open pressurizer safety or relief valve, a possible reclosure can cause a severe re-pressurisation. Even without the valve reclosing, the system pressure can remain high after having reached the final temperature. The low decay power may further lead to the main loop flow stagnation. In addition, the "feed and bleed" method of mitigation for loss of feedwater should be assessed.

Primary to secondary leakage accidents

Different sizes for both single and multiple steam generator tube ruptures up to the full steam generator collector cover opening should be considered. The risk of re-pressurisation should be taken into account, if the relevant emergency operation procedure contains a requirement to isolate the affected steam generator by closing of main gate valves.

Large secondary leaks

Transients with secondary side de-pressurization caused either by the loss of integrity of the secondary circuit or by the inadvertent opening of a steam dump valve can cause significant cooldown of the primary side. Consequently, start of high-pressure injection due to low primary pressure (and/or low pressurizer level or directly due to low secondary circuit parameters), which leads to re-pressurisation, can be expected. The degree of secondary side de-pressurization is strongly dependent on the plant configurations (mainly the presence of fast acting main steam isolation valves and the criteria for steam line isolation).

6.3.1.1.3   Symmetric cooling

If forced or intensive natural circulation is maintained, homogeneous cooling of the whole primary circuit can be assumed (except for the pressurizer and reactor upper head). In these conditions the cooling of the reactor pressure vessel can be assumed axisymmetric. According to the results of studies performed in the scope of the US PTS re-evaluation (i.e., NUREG-1806 [17] [18]) for US reactor designs, the simplifying assumption of uniform temperatures can be assumed in the downcomer, in the region adjacent to the core. It is only in this region that the vessel is embrittled. The top of the core is approximately 1.5 m (5 feet) below the cold leg. This distance provides a mixing zone for cold fluid entering the downcomer from the cold legs before it reaches the embrittled zone of the reactor vessel.

Symmetrical cooling can also be applied at primary side flow stagnation in case of relatively high cold leg cold water injection rates e.g., for a double-ended guillotine break for German PWRs. The high injection rate leads to a rapid cooling to the cold water temperature, which leads to a symmetrical thermal shock without plumes.

For WWER reactor designs, the downcomer width is less than in western designs, so that mixing of the injected ECCS water is less efficient and the role of plumes may be correspondingly greater.

6.3.1.1.4   Asymmetric cooling

If flow stagnation occurs in the primary system, the cold plumes will exist below the nozzles of legs with cold water injection, plumes will exist below causing a non-uniform temperature distribution. In case of flow stagnation, thermal mixing and plume cooling of the RPV wall occurs when the downcomer and the cold legs are totally filled with water. A cold stream, caused either by ECCS water injection or by an increased heat removal from the primary to the secondary side in affected loops, flows in the cold loop towards the RPV inlet and falls into the downcomer forming a quasi-planar buoyant plume

(**Figure *23***). In case of direct ECCS water injection into the downcomer, as applied in WWER, the plume origin is at the lower edge of the injection nozzle.

Condensation and strip cooling of the RPV wall (**Figure *23***) takes place when the cold legs are partially filled with steam and the collapsed water level in the downcomer is below the lower edge of cold leg. A cold stream caused by ECC water injection flows at the bottom of the cold leg towards the RPV inlet and falls into the downcomer forming a strip directly in contact with the RPV wall. The stripe detaches from the RPV wall when higher cold leg ECC injection rates are applied. In case of direct ECC water injection into the downcomer, the ECC water impinges on the core barrel forming a water film which flows along the core barrel. To account for these effects, sophisticated 3D computer codes that are able to treat two-phase flow phenomena or engineering calculation methods verified on experimental data are needed to account for the associated condensation processes.

The number of plumes depends on the break location and the configuration of the injection system. The most asymmetric situation of plumes around the RPV may be of importance for numerical fracture mechanics simulations.
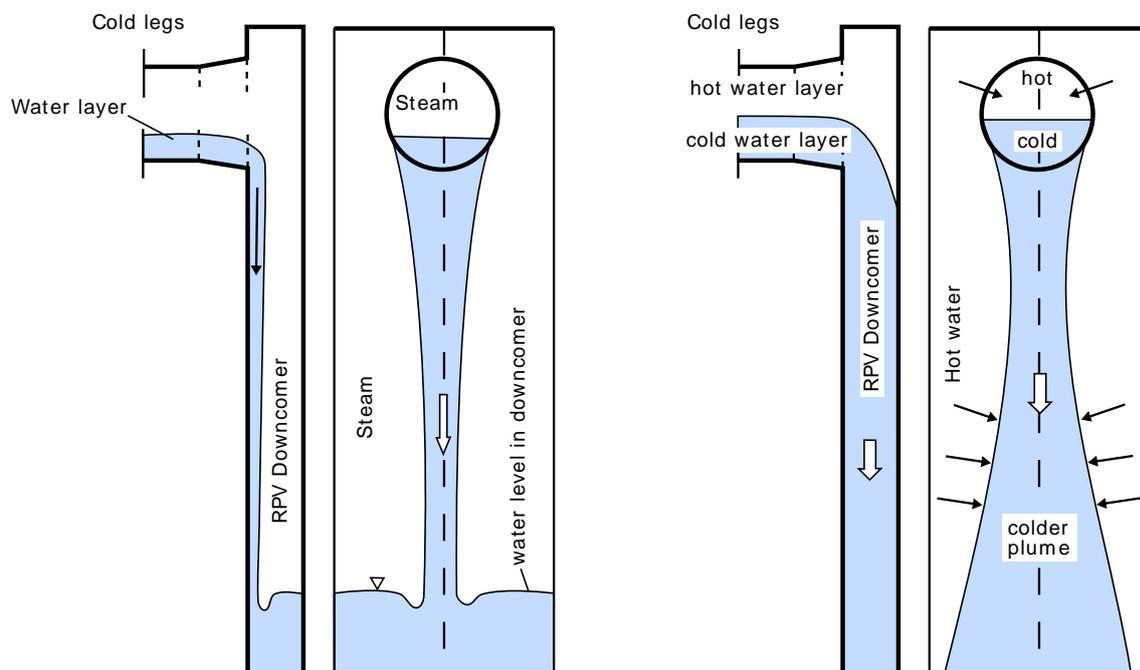
Figure 23: Stripe cooling (left part) and plume cooling (right part) of the RPV inside wall [6].

6.3.1.1.5   Modelling of phenomena

Adequate modelling of natural circulation and validation is important. Fluid flow mixing codes should be able to describe the phenomena like mixing near the injection location, stratification in the cold leg and mixing in the downcomer. An important feature of some PTS transients is flow stagnation in the primary circuit. It occurs when the flow distribution is governed by buoyancy forces (i.e., thermal stratification and mixing of cold high pressure injection water in the cold legs and the downcomer become the dominant effects). These phenomena can also be influenced by the loop seals behaviour. Since these may not be predicted correctly with the existing thermal hydraulic system codes, specific fluid-fluid mixing calculations may be needed.

6.3.1.2   US NRC NUREG-1806, Technical Basis for Revision of the Pressurized Thermal Shock (PTS) Screening Limits in the PTS Rule: Summary Report, 2007 [17]

US NRC revision of PTS Rule project ran in 1998-2009 and led to substantial re-evaluation of the approach to PTS assessment (comparing to original PTS Rule from 1980s). Major features are as follows:

- Probabilistic approach
- No more excluded "thermal only transients" (medium and large LOCA now considered)
- No mixing calculation (temperature asymmetries no more considered)
- More TH sequences modelled (RELAP only)
- Operator actions credited
- External events considered
- Number of changes in integrity assessment

6.3.1.2.1   Transients and their Contributions to PTS Risk

Transients involving primary side faults are the dominant contributors to through-wall cracking frequency (TWCF), while transients involving secondary side faults play a much smaller role.

- The severity of a transient is controlled by a combination of three factors:
    - initial cooling rate, which controls the thermal stress in the RPV wall
    - minimum temperature of the transient, which controls the resistance of the vessel to fracture
    - pressure retained in the primary system, which controls the pressure stress in the RPV wall

- The significance of a transient (i.e., how much it contributes to PTS risk) depends on these three factors and the likelihood that the transient will occur.
- The analysis considered transients in the following classes (as shown in **Table 5**):
    - primary side pipe breaks
    - stuck-open valves on the primary side
    - main steam line breaks
    - stuck-open valves on the secondary side
    - feed-and-bleed
    - steam generator tube rupture
    - mixed primary and secondary initiators

Table 5 provides a qualitative summary of the results for these transient classes in terms of both transient severity and the likelihood that the transient will occur. The color-coding of table entries indicates the contribution (or lack thereof) of these factors to the TWCF of the various classes of transients. This summary indicates that the risk-dominant transients (medium- and large diameter primary side pipe breaks, and stuck-open primary side valves that later reclose) all have multiple factors that, in combination, result in their significant contributions to TWCF.

- For medium- to large-diameter primary side pipe breaks, the fast to moderate cooling rates and low downcomer temperatures (generated by rapid depressurization and emergency injection of low-temperature makeup water directly to the primary) combine to produce a high-severity transient. Despite the moderate to low likelihood that these transients will occur, their severity (if they do occur) makes them significant contributors to the total TWCF.

- For stuck-open primary side valves that later reclose, the re-pressurisation associated with valve reclosure coupled with low temperatures in the primary combine to produce a high severity transient. This, coupled with a high likelihood of transient occurrence, makes stuck open primary side valves that later reclose significant contributors to the total TWCF.

- The small or negligible contribution of all secondary side transients (main steam line break, stuck-open secondary valves) results directly from the lack of low temperatures in the primary system. For these transients, the minimum temperature of the primary for times of relevance is controlled by the boiling point of water in the secondary (212 °F (100 °C) or above). At these temperatures, the fracture toughness of the RPV steel is sufficiently high to resist vessel failure in most cases.

Table 5: Factors contributing to the severity and risk-dominance of various transient classes [17].

Transient Class		Transient Severity			Transient Likelihood	TWCF Contribution
		Cooling Rate	Minimum Temperature	Pressure		
Primary Side Pipe Breaks	Large-Diameter	Fast	Low	Low	Low	Large
	Medium-Diameter	Moderate	Low	Low	Moderate	Large
	Small-Diameter	Slow	High	Moderate	High	~0
Stuck-Open Valves, Primary Side	Valve Recloses	Slow	Moderate	High	High	Large
	Valve Remains Open	Slow	Moderate	Low	High	~0
Main Steam Line Break		Fast	Moderate	High	High	Small
Stuck-Open Valve(s), Secondary Side		Moderate	High	High	High	~0
Feed-and- Bleed		Slow	Low	Low	Low	~0
Steam Generator Tube Rupture		Slow	High	Moderate	Low	~0
Mixed Primary & Secondary Initiators		Slow	Mixed		Very Low	~0
Color Key		Enhances TWCF Contribution	Intermediate		Diminishes TWCF Contribution	

Another important part of the NUREG-1806 was the development of the phenomena identification and ranking table (PIRT) - for description of this process see subsection 6.3.1.4.

6.3.1.3 An Overview of the Pressurized Thermal Shock Issue in the Context of the NURESIM Project, Science and Technology of Nuclear Installations, 2008 [36]

Within the European Integrated Project NURESIM, the simulation of PTS was investigated with focus on PWR accident scenarios caused by Emergency Core Coolant injection into the cold leg. They imply the formation of temperature gradients in the thick vessel walls with consequent localized stresses and the potential for propagation of possible flaws present in the material. The appropriate paper focuses on two-phase conditions that are potentially at the origin of PTS. It summarizes recent advances in the understanding of the two-phase phenomena occurring within the geometric region of the nuclear reactor, that is, the cold leg and the downcomer, where the "PTS fluid-dynamics" is relevant. Available experimental data for validation of two-phase CFD simulation tools are reviewed and the capabilities of such tools to capture each basic phenomenon are discussed. Key conclusions show that several two-phase flow sub-phenomena are involved and can individually be simulated at least at a qualitative level, but the capability to simulate their interaction and the overall system performance is still limited. In the near term, one may envisage a simplified treatment of two-phase PTS transients by neglecting some effects which are not yet well controlled, leading to slightly conservative predictions.

As shown in **Figure 24**, different flow phenomena occur. There are flows with separated surfaces (jet interface, horizontal interface), but also dispersed flows occur due to bubble entrainment (at jet impingement and possibly also in the horizontal flow region by entrainment caused by waves). Since there is a strong thermal non-equilibrium at these interfaces, momentum transfer as well as heat and mass transfer have to be considered. The various two-phase phenomena taking place are strongly coupled, both within the fluids and in regard to the heat transfer to walls. The different phenomena depend on very different characteristic length-scales, from the size of the smallest eddy up to the system scale. Some of the involved phenomena are not yet well understood regarding their physics. The simulations of the whole system during the ECC injection process and then accurate reproduction of the thermal loads on the RPV are thus a considerable challenge.

In detail, the following "geometrical" flow regions or flow patterns connected with the listed single phenomena can be distinguished for the two-phase PTS situation:

    i.   Free liquid jet:

        a.   momentum transfer at the jet interface, including instabilities,

      b. splitting of the jet,

      c. condensation on the jet surface.

ii.   Zone of the impinging jet:

      a. surface deformation by the jet including generation of waves,

      b. steam bubble entrainment,

      c. bubble migration and de-entrainment,

      d. turbulence production below the jet.
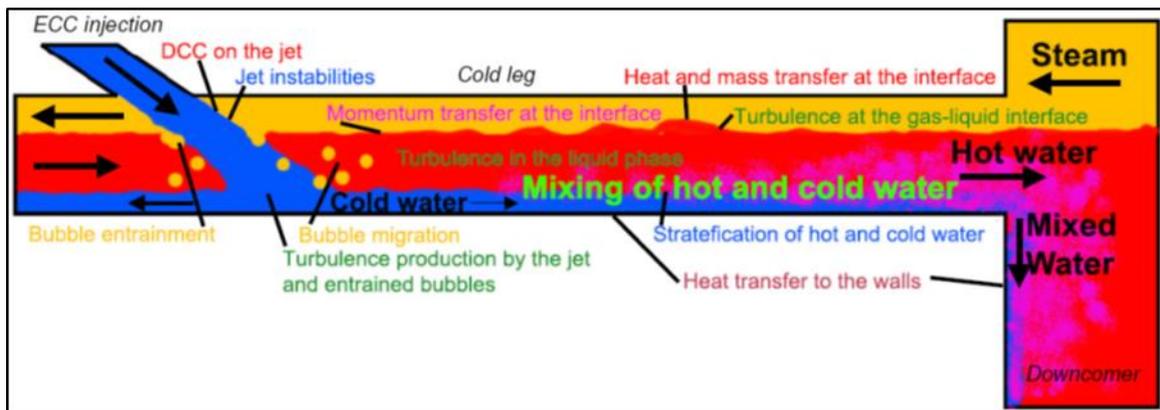
Figure 24: Thermal stratification in cold leg and forming of cold plume in downcomer[36].

iii.   Zone of horizontal flow:

      a. momentum exchange at the gas-liquid interface, including generation of waves and growth or damping of these waves,

      b. heat and mass transfer (condensation) at the gas-liquid interface including its influence on the momentum transfer,

      c. heat transfer to the walls,

      d. turbulence production at the interface,

      e. turbulence production at the walls,

      f. influence of the phase change on turbulence and on wave pattern,

      g. mixing/stratification of hot and cold water streams.

iv.   Flow in the downcomer in the case of a partially filled cold leg:

      a. turbulence production at the walls,

      b. mixing/stratification of hot and cold water,

      c. heat transfer to the walls.

v.   Flow in the downcomer in the case of the water level being below the cold leg nozzle:

      a. separation of the incoming water jet from the downcomer wall or not,

      b. momentum transfer at the jet interface, including instabilities,

      c. splitting of the jet,

      d. phase change at the jet surface,

      e. heat transfer to the walls.

Within the NURESIM project a comprehensive overview of the thermal-hydraulic phenomena (and subphenomena) connected with PTS in pressurized water reactors has been provided, with emphasis given to two-phase conditions. The outline given in relation to single-phase phenomena shows that coupling techniques involving system thermal-hydraulics and CFD codes are mature enough to be used for technological purposes, with main reference to the evaluation of safety margins, though improvements are still needed (as expected when nuclear safety is part of the game) in the area of

convection heat transfer. The detailed analysis performed in relation to the two-phase flow phenomena shows the complexity of those phenomena. Computation techniques are capable to reproduce qualitatively the individual aspects (also called subphenomena) but fail, so far, in the prediction of the interaction among the subphenomena and of the overall system behaviour.

6.3.1.4　Phenomena Identification and Ranking Tables (PIRT)

In the PIRT process, typically the panel of thermal-hydraulic experts discuss and agree to a list of relevant phenomena and then proceed to rank them according to their contribution in determining the final outcome of a specific scenario. In the following, the PIRTs for PTS are shown as they evolve with time, without the description of the identified phenomena (phenomena relevant for PTS are described in subsections 6.3.1.1.1 through 6.3.1.1.5). The first presented is PIRT described in NUREG/CR-5452 [37] from 1999, followed by PIRT described in NUREG/CR-6857 [38] from 2004, PIRT described in NUREG-1809 [39] from 2005, PIRT described in NUREG-1806, Vol. 1 [17] from 2007, and PIRT described in DEFI-PROSAFE [40] from 2018, in which NUREG/CR-6857 and NUREG-1806 have been reviewed.

Subchapters 2.1.4.1, 2.1.4.2, 2.1.4.3, 2.1.4.4 and 2.1.4.5 of Deliverable D1.3 [3] summarize the PIRT process results in NUREG/CR-5452 [37], NUREG/CR-6857 [38], NUREG-1809 [39], NUREG-1806 Vol. 1 [17] and the PIRT described in DEFI-PROSAFE [40] respectively. The following paragraphs summarizes the latter.

Acronym DEFI-PROSAFE means "*DEFInition of reference case studies for harmonized PRObabilistic evaluation of SAFEty margins in integrity assessment for long term operation of reactor pressure vessel*". A methodology has been proposed to assess margin in RPV integrity evaluation accounting for uncertainties propagation. The DEFI-PROSAFE methodology, which is based on the comparison between deterministic and probabilistic assessments, has been detailed. The experience gained from the US Screening Criteria (NUREG-1806 [17][18]) and past projects (ICAS [41][26], PROSIR [42]), and guideline IAEA TECDOC-1627 [6], as well as aspects specific to European deterministic integrity approach have been considered.

The DEFI-PROSAFE methodology considers RPV discontinuity regions (like RPV nozzle) and specific PIRT analysis has been therefore performed for selection of the TH parameters.

For the determination of the leading phenomena and parameters from the TH loading, in a first step, the phenomena identification and ranking table (PIRT) from NUREG/CR-6857 [38] and NUREG-1806 [17] [18] have been reviewed. The leading phenomena have been mostly taken from these earlier PIRTs developed only for application to PTS at the core region of the downcomer and slightly modified for the application of the current PIRT to the cold-leg and hot-leg nozzles as well as the downcomer. The transient class was also changed in the current PIRT to exclude secondary-side accidents. Therefore, the rankings of the phenomena from the earlier PIRTs were changed in the current PIRT.

The most important phenomena and processes identified were:

- Break flow (see "Break flow/size" – rank 1 of Table 1-1 in [38] ((**Table 6** below))
- Re-closure of the pressurizer valve if it is stuck-open (similar to "Time of stuck valve re-closure " – rank 4 of Table 1-1 in [38])
- Safety-injection flow rate (see "ECCS flow rate (Accumulator, HPI, LPI)" – rank 2 of Table 1-1 in [38])
- Accumulator injection rate (see "ECCS flow rate (Accumulator, HPI, LPI)" – rank 2 of Table 1-1 in [38])
- Jet behaviour, flow distribution and mixing (see ranks 15 to 17 of Table 1-1 in [38]), i.e., "ECCS-Reactor coolant system mixing in cold legs", "Flow distribution in downcomer" and "Jet behaviour, cold leg pipe to downcomer");
- Interphase condensation & non-condensables (see "Interphase condensation & non-condensables" – rank 21 of Table 1-1 in [38])

- Time of flow stagnation (similar to parameter "Natural circulation/flow stagnation" for RELAP5 code assessment in [38])
- Liquid/vapor interface in upper downcomer.

The most important boundary conditions were:

- accumulator injection temperature and initial pressure (for temperature see "ECCS temperatures" – rank 9 of Table 1-1 in [38] ((**Table *6*** below))
- high-pressure injection temperature (see "ECCS temperatures" – rank 9 of Table 1-1 in [38])
- safety-injection asymmetry (see " HPI asymmetry", no. 8 of Table K-2 in [39])
- break size (see "Break flow/size" – rank 1 of Table 1-1 in [38])
- time of re-closure if the pressurizer valve is stuck-open (similar to "Time of stuck valve re-closure " – rank 4 of Table 1-1 in [38])
- break location (see "Break location" – rank 6 of Table 1-1 in [38])
- low-pressure injection temperature (see "ECCS temperatures" – rank 9 of Table 1-1 in [38])

The values of these parameters have been assigned statistically (preferably) or conservatively (if necessary) in the benchmark definition in order to include the effect of uncertainties.

Table 6: Phenomena Identification and Ranking Table for Pressurized Thermal Shock in Pressurized Water Reactors (Table 1-1 of [38]).

Old Rank	New Rank	Description	Comments
6	1	Break flow/size (or valve capacity)	Importance of LBLOCA has increased, pressure is less important
1 & 3	2	ECCS flow rate (Accumulator, HPI, LPI)	State on/off, shutoff head of pumps, accumulator initial pressure
	3	Operator actions	Includes operating procedures, RCP trip, HPI throttling, feedwater isolation, etc.
	4	Time of stuck valve re-closure	Pressurizer safety relief valves which re-close after sticking open
9	5	Plant initial state	Hot Full Power vs. Hot Zero Power Operation
	6	Break location	Primary LOCA (hot leg, cold leg), MSLB, (inside/outside containment, upstream/downstream MSIVs), SGTR
	7	Unique plant features/design	Difference in steam generator design, # of loops, vent valves, etc.
	8	Vessel to downcomer fluid heat transfer	Affects the rate at which heat is transferred from the vessel wall to the downcomer fluid
5	9	ECCS temperatures	Seasonal/operational variations
	10	Sump recirculation	ECCS temperature/flow changes after RWST drained
19	11	Feedwater control (or failure)	Post trip main feedwater behaviour for Oconee, steam generator overfeed events
18	12	Feedwater Temperature	Oconee (using emergency feedwater instead of main feedwater during transient)
2	13	Reactor vessel wall heat conduction	In conjunction with vessel to downcomer fluid heat transfer, affects the rate at which heat is transferred from the vessel wall to the downcomer fluid. Important particularly in those situations when heat transfer from the wall is conduction limited
11	14	Loop flow upstream of HPI	Scenario dependent, not as important for LBLOCAs
12	15	ECCS-Reactor coolant system mixing in cold legs	Affects potential for formation of cold plumes in the downcomer. Ranking lowered due to Oregon State University data

Old Rank	New Rank	Description	Comments
4	16	Flow distribution in downcomer	Affects mixing and potential for formation of cold plumes in the downcomer. Ranking lowered due to Oregon State University data
8	17	Jet behaviour, cold leg pipe to downcomer	Ranking lowered due to Oregon State University data
13	18	Loop temperature upstream of the location of the safety injection junction	Scenario dependent, important for MSLB, not for LBLOCA
20	19	Steam generator energy exchange	
21	20	Timing of manual reactor coolant pump trips	
17	21	Interphase condensation & non-condensables	RELAP5 overprediction of condensation
14	22	Downcomer to core inlet bypass	Ranking lowered, less important for LBLOCAs
15	23	Downcomer to upper plenum bypass	Ranking lowered, less important for LBLOCAs
16	24	Upper head HTC under voided conditions	Ranking lowered, less important for LBLOCAs
22		Combined with new #7	
7		HPI temp (replaced with ECCS temperatures)	
10		Combined with old #2	

6.3.1.5 Further Remarks Regarding Thermal-Hydraulic Phenomena and Factors Important for PTS

When studying and assessing the pressurized-thermal shock on RPV, one should distinguish between the inner PTS and outer PTS. The outer PTS could be initiated e.g., by inadvertent flooding of reactor cavity or actuation of In-Vessel Melt Retention (IVMR) system. As the project APAL and this report are focused on the inner PTS, we will not further consider the outer PTS phenomena and deteriorating factors.

6.3.1.5.1 Major Deteriorating TH Factors and Corresponding Phenomena

The most important deteriorating TH factors with respect to inner PTS and corresponding TH phenomena are listed and shortly discussed below. These should be taken into account when selecting the set of initiating events and scenarios to be analysed, selecting the computer codes and models, and specifying the conservative set of initial and boundary conditions for TH analyses.

- Fast and deep temperature decrease in reactor downcomer:
  - Maximal initial temperature in the downcomer
  - Flat temperature profile in the RPV wall (result of assuming adiabatic RPV outer surface boundary conditions)
  - Low final temperature in the downcomer
  - Fast temperature decrease rate

- High primary pressure in the course of accident (a specific case is re-pressurisation due to break isolation)
- Low flow rate or flow stagnation in reactor coolant loops with ECCS injection (enables thermal stratification and creation of cold plumes). Note: It is important to correctly predict potential partitioning of SI cold water flow to reactor and to RCP and further to loop seal. The entrance of cold and heavy water into loop seal could create plug of heavy cold water that can block any further flow in the loop and leads to flow stagnation.
- Non-uniform temperature field in reactor downcomer (cold plumes, cold stripes, cold sectors), when the most adverse is maximal temperature difference between ambient and cold region

- Non-uniform HTC field in reactor downcomer, when the most adverse is high HTC in cold region and low HTC in ambient region
- Form and width of cold plume (stripe, sector), when the most adverse is narrow cold region.
- Stability of cold plume, when the most adverse is stable cold plume (without side-movements)
- Merging of neighbouring cold plumes into one stronger plume
- Position of isolated cold plumes – in case of isolated (not merging) cold plumes the most adverse position is with the cold plumes on the opposite sides of reactor vessel.

Cold plume is typically a result of ECCS injection of cold water, thermal stratification in the cold leg and downflow of this cold water in the reactor downcomer with characteristic "plume" form (see **Figure 23**). Cold plume is nonuniformity in downcomer coolant temperature in both radial and azimuthal direction. The cold water in downcomer could flow down along the inner surface of RPV or along the outer surface of core barrel. In case of multiple cold plumes, they can merge into one plume. The cold plumes could be stable or unstable (side movements due to Kelvin-Helmholtz instability).

Cold sector is typically result of MSLB (asymmetric increase of heat transfer to secondary side) and strong cooldown of one main coolant loop. The cold water flows from affected SG through the whole cross section of the loop (no thermal stratification) and reactor inlet nozzle. The flow is strong – either in forced circulation or strong natural circulation after RCP trip. In case of operation of all RCPs, the cold water flows through the relevant section of the downcomer. Similar flow pattern in downcomer is in case of trip of all RCP, when in the affected loop is strong natural circulation and in the other loops is weak natural circulation or later flow stagnation.

Cold stripe means the input of cold water into the downcomer containing steam. The source of cold water can be ECCS injection into cold leg or direct ECCS injection into reactor downcomer (e.g., accumulators' injection into downcomer in VVER-1000 or APR-1400). The form of cold stripe is different from cold plume (see **Figure 23**).

6.3.1.5.2   Groups of Initiating Events/Scenarios and Relevant Phenomena

The following groups of initiating events shall be considered for inner PTS assessments:

- Loss of coolant accidents (small, medium, large break LOCA)
- Stuck open pressurizer safety or relief valve (risk of reclosure)
- Primary to secondary leakage accidents (PRISE)
- Interfacing LOCA (potential of break isolation)
- Inadvertent actuation of SI
- Large secondary leaks (MSLB, FWLB, SDA open)

The main TH phenomena occurring for individual groups of PTS events are:

- SB-LOCA: high prim. pressure + total cooldown + cold plumes
- MB-LOCA: fast total cooldown + cold plumes (merging)
- LB-LOCA: very fast total cooldown + cold stripes + cold plumes (merging)
- Inadvertent opening of PRZ SV: high prim. pressure (in case of reclosure) + total cooldown + cold plumes
- PRISE: high prim. pressure + total cooldown + cold plumes
- IF-LOCA: high prim. pressure (in case of break isolation) + total cooldown + cold plumes
- Inadvertent actuation of SI: cold over-pressurisation + cold plumes
- Malfunction of CVCS (esp. make-up): cold over-pressurisation
- MSLB (incl. inadvertent steam dump and FWLB): high prim. pressure + total cooldown + cold sectors + cold plumes

6.3.1.5.3   Effect of TH Analysis Assumptions on the Dominant TH Phenomena and PTS

Analysis assumptions can have a large effect on the phenomena that are predicted to occur, which can in turn lead to conservative or non-conservative analysis results. The following should be taken into account in defining PTS scenarios for analysis:

- The assumption of "maximum availability of ECCS" and "minimum availability of ECCS" should be evaluated in the analysis of LOCA, MSLB and other relevant accidents:
  - maximum availability of ECCS leads to the fastest overall cooldown plus maximum primary pressure,
  - minimum availability of ECCS leads to higher injection from one safety injection train and higher asymmetry in reactor downcomer cooldown.

- In MSLB analysis the combination of affected SG and injecting HPSI can lead to different phenomena and results (in case of RCP trip):
  - Injection of HPSI into affected loop (with strong cooldown and natural circulation due to MSLB) leads to mixing of cold water in cold leg and "only" intensifies cold sector type of downcomer cooldown.
  - Injection of HPSI into intact loop (with weak circulation and later flow stagnation) lead to thermal stratification and cold plumes formation in downcomer.

6.3.2   Experimental Activities and Validation

Because of their importance and complexity of modelling, PTS effects have been extensively studied both experimentally and numerically. From the beginning of the 1980's, a large variety of experimental programs have been executed to improve the understanding of mixing phenomena defining the severity of PTS and to provide the required data base for code development and code validation. The available investigations can be subdivided into separate-effect studies and combined-effect/integral system studies. The separate-effect studies deal only with a single aspect of PTS, like free surface flow or generic condensation. The integral system studies are performed in realistic reactor configurations and examine the interaction of all relevant effects. Because of their complexity and cost, only few data on the combined-effect studies are available.

Several separate effects tests were supported by the U.S. Nuclear Regulatory Commission (US NRC) and EPRI in the 1980's to characterize (buoyancy-induced) thermal mixing and stratification of cold high-pressure safety injection water in the cold legs and downcomer. In addition, phenomena related to natural circulation interruptions in the reactor coolant system and oscillations of the single-phase natural circulation were studied. Experiments were performed, for example, at Creare at 1/2 and 1/5 scales, Imatran Voima Oy (IVO) at 2/5 scale with multiple loops, Purdue at 1/2 scale, at HDR Battelle Institute at full scale and at the UPTF KWU Kraftwerk Union at full scale [129]. In addition to their wide variation in scale, these facilities were operated under widely different conditions. They included both solute and/or thermally induced buoyancy and concentration or temperature measurements as an indication of mixing.

The Purdue experiments were run with room temperature water and brine (HPI), and mixing was obtained from concentrations measurements. The Creare-1/5, IVO, and IVO(NRC) experiments were run with solute buoyancy also, but mixing was inferred from temperature measurements. The Creare-1/2, HDR, and UPTF were all run at pressure, i.e., thermally-induced buoyancy and temperature as the tracer. The HDR was a full pressure facility of somewhat reduced scale of downcomer gap (1/2) and cold leg (1/4), the UPTF was a full-scale facility run at reduced pressure, and Creare-1/2 was representative of a combination of both attributes. The IVO(NRC) tests were unique in involving multi-loop injection, i.e., plume interactions in the downcomer (circumferentially 1/2). The HDR and UPTF experiments, on the other hand, involved single loop operation on a whole downcomer.

Theofanous [130] used the separate effects test data to develop a criterion to identify the primary loop flow and HPI flow conditions at which thermal stratification would occur.. The Purdue research team

also developed the REMIX and NEWMIX computer codes to predict the temperature profiles in the cold legs and downcomer [57]. This permitted the complete analysis of an overcooling transient in a short time frame.

In addition to the facilities mentioned above there are many smaller scale separate effects test facilities, where different PTS related phenomena have been studied over the decades. These include, for example, the HAWAC, KAERI&KAIST, LIM, LAOKOON, COSI, Vattenfall, B-MOV facilities (see below).

Combined-effect/integral system PTS tests modelling realistic reactor configurations were done, for example, in the APEX-CE test facility at the Oregon State University (OSU). The research program was sponsored by the US NRC [143].. The thermal hydraulic phenomena of specific interest to the OSU experimental effort were the onset of loop stagnation, the onset of thermal stratification in the cold legs, and characterization of thermal fluid mixing and heat transfer in the downcomer. These phenomena were examined for various primary and secondary side transients in the APEX-CE facility. The purpose of the PTS research conducted at OSU was to obtain test data for transients of potential PTS significance. This data was used to assess the existing thermal hydraulic computer codes and CFD codes that were implemented in an improved PTS thermal hydraulic analysis methodology. Because stagnant loop conditions can be particularly severe with respect to PTS, an assessment of the ability of systems analysis codes to predict the onset of primary loop stagnation was of particular interest. This was one of the motivating factors for the APEX-CE test program.

The OECD ROSA V experiments, which were performed in the Large Scale Test Facility (LSTF) belong also to the combined effect category [131]. The LSTF emulated a Westinghouse-type four-loop 3423 MW thermal power PWR by a full-height and 1/48 volumetrically scaled two-loop system [132]. The goal of the ROSA V experimental program was to investigate temperature stratification under natural circulation conditions, and to provide data for the validation of CFD software.

The Rossendorf Coolant Mixing (ROCOM) test facility at Forschungszentrum Dresden-Rossendorf (FZD) belongs also to the integral test facility category. It was a scaled down Perspex model of the primary circuit of a German (Siemens Konvoi) PWR nuclear reactor. The facility was used for example for flow distribution, boron dilution and PTS scenario studies. Types of experiments included stationary and transient experiments and experiments with ECC water injection [133].

Those above mentioned facilities and few other test facilities used for PTS studies, whose information has been publicly available, are presented in more detail in the sections 2.2.2.1 through 2.2.2.21 of Deliverable D1.3 [3]. A brief summary is presented below:

-   Creare 1/2-Scale [136] [137]. The ½-Scale Test Facility at Creare modelled the loop seal, cold leg, downcomer, and lower plenum of a PWR. The facility could be operated with steady or transient inlet boundary conditions. Extensive instrumentation was provided to measure flow rates, temperatures, and pressure at the facility boundaries and for detailed measurements of temperature, velocity and heat transfer data in the cold leg and downcomer models.
-   Creare 1/5-Scale [138]. An experimental program (MIX3 and MIX4 tests) of fluid mixing experiments was performed at atmospheric pressure in a 1/5-scale, transparent model of a cold leg, downcomer and lower plenum typical of Westinghouse and Combustion Engineering PWRs. The tests were transient cooldown tests in that they simulated an extreme condition of SB-LOCA during which cold HPI fluid was injected into stagnant, hot, primary fluid with complete loss of natural circulation in the loop.
-   IVO Facility [139]. This test facility was constructed at the Hydraulic Laboratory of Imatran Voima Oy (IVO) in Finland to study thermal mixing of cold HPI water with hot primary coolant in a pressurized water reactor during postulated overcooling accidents. The facility was built as a two-fifths scale model of the Loviisa VVER-440 reactor.
-   Purdue's ½-Scale HPI Thermal Mixing Facility [140]. The Purdue's basic experimental facility consisted of a transparent acrylic 1/2-Scale model of a typical PWR cold-leg /downcomer/ lower plenum configuration. The lower portion of the downcomer and of the lower plenum (corresponding to one of the cold legs) were geometrically distorted to keep the overall height

of the facility manageable. Based on this reference configuration, the essential features of three reactor geometries were assembled by making appropriate attachments to the cold leg. These features included, for example, inclined portion of the cold leg and the small diameter HPI line. The inclined portion of the cold leg forces all HPI to flow in the direction of the reactor vessel (as opposed to some diverting towards the pump) while the small diameter HPI line results in a forced jet (as opposed to a buoyant plume) that is strongly deflected in all directions as it impacts the opposite cold leg wall.

- HDR [141] [142]. The thermal mixing tests at the Heissdampfreaktor (HDR) facility allowed the examination of both thermal-hydraulic and structural aspects at once in a truly three-dimensional, rather thick-walled pressure vessel under prototypical system conditions. This additional feature of the test series provided an expanded data base including the inside vessel surface strains and derived stresses as well as the thermal-hydraulic behaviour.
- APEX-CE [143] [144]. The Oregon State University (OSU) Advanced Plant Experiment-Combustion Engineering (APEX-CE) test facility was roughly a one-fourth height integral system model of the Palisades plant. The facility was operated at reduced pressure and on a one-to-one time-scale. The design of the original APEX test facility was based on the Westinghouse AP600.
- Upper Plenum Test Facility (UPTF) [145] [146] [147]. The upper plenum test facility (UPTF) was designed to investigate flow behaviour in the primary system of a PWR during a LOCA. A particular goal was to extend the existing experimental data base to include multidimensional effects under full-scale conditions and to assist in the development and assessment of advanced computer codes. The UPTF was designed and constructed as a full-size simulation of the 1300 MW 4-loop Grafenrheinfeld PWR of Siemens-KWU.
- ROSA/LSTF [131] [132]. The OECD ROSA V experiments, which were performed in the Large Scale Test Facility (LSTF) belong to the separate effect and combined effect category. In the experiments, the three-dimensional temperature field was measured in the cold leg and downcomer under realistic reactor conditions pertaining to PTS.
- ROCOM (e.g., [148] [149]). The influence of density differences on the mixing of the primary loop inventory and ECC water in a PWR was also analysed at the Rossendorf Coolant Mixing (ROCOM) test facility at Forschungszentrum Dresden-Rossendorf (FZD). The ROCOM experimental facility was a quintessential facility, a scaled down Perspex model of the primary circuit of a German (Siemens Konvoi) PWR nuclear reactor. It used a linear scale of 1:5 with respect to the original PWR reactor. Four coolant loops were connected to an RPV mock-up and flow was realized through the cold legs, ECC inlet nozzles, the downcomer, core and finally hot legs. As these components formed a closed flow circuit the ROCOM facility can be thus considered an integral test facility.
- TOPFLOW [134] [135] [151] [152]. The TOPFLOW-PTS facility, located in Helmholz-Zentrum Dresden-Rossendorf (HZDR), is a 1:2.5 scale model of the cold leg and downcomer of the EDF CPY 900 MWe PWR, and it was constructed to study two-phase PTS conditions. The geometry was modelled with some modifications to obtain a more simple/analytical configuration allowing better access for instrumentation and easier results analyses.
- HAWAC [153]. The Horizontal Air/Water Channel (HAWAC) at Forschungszentrum Dresden-Rossendorf (FZD) was dedicated to generic co-current flow experiments at atmospheric pressure and room temperature. A special inlet device offered well-defined inlet boundary conditions by a separate injection of water and air into the test section for comparisons with CFD.
- KAERI & KAIST Facility. Countercurrent Stratified Flow (CCSF) was studied in the KAERI & KAIST test facility [154]. It was designed and constructed such that the condensation rates of the steam along a circular channel could be measured while saturated steam and subcooled water flowed in the opposite direction.
- Facility for OECD/NEA Cold Leg Mixing CFD-UQ Benchmark Exercise [155]. An experimental facility was designed and constructed at Texas A&M University for the OECD/NEA Cold Leg

Mixing CFD-UQ Benchmark exercise to collect measurements of density-driven flow mixing. The test facility consisted of two large transparent vessels connected through a horizontal acrylic pipe. One of the two vessels was designed to incorporate specific geometrical features of the reactor vessel of a typical PWR. In particular, the nozzle of the test facility was constructed to realistically represent the fluid domain of the cold leg nozzle of a PWR vessel.

- LIM [156]. Horizontal co-current smooth and wavy Steam Water Stratified (SWST) flow in a rectangular channel with adiabatic walls was studied in the LIM facility. The dimensions of the rectangular cross section were: 6.35 cm, 30.48 cm and 160.1 cm (height x width x length). Smooth to wavy turbulent, concurrent stratified steam-water flows were obtained by varying the liquid and steam flow rates.

- LAOKOON [36]. Contact condensation in horizontal stratified flows of subcooled water and saturated steam were investigated in the LAOKOON test facility at the University of Munich. The experimental equipment was designed to set up co-current and counter-current flow conditions in a straight channel with adiabatic walls. Available measured data include the water and steam flow rates at the water feed cross section, the inlet water temperature, and the temperature distribution across the water layer at one location, where a vertical array of thermocouples was installed. The pressure level inside the channel and the water layer height were also measured.

- COSI [156] [157] [158]. The COSI test facility at the CEA Grenoble simulated the ECC injection system of a 900 MW Framatome PWR and was scaled 1/100 for volume and power. The tests focused on studying complex condensation phenomena that take place in the area of the ECC injection during a loss of coolant accident in a PWR.

- Vattenfall Mixing Facility. The Vattenfall mixing test facility was a 1:5 scale model of a 3-loop Westinghouse PWR. The lower plenum and the lower 2/3 of the downcomer were made from acrylic glass. Two idle loops were included in the model. The model was run with a maximum flow rate of 127 l/s and at temperatures between 20 and 50°C. Components that can be important for mixing were modelled, for example thermal shields, inlet pipe diffusers, structures in lower plenum, core support plates, and core [159].

- University of Maryland Thermal Hydraulic Loop Facility [160]. The University of Maryland (UM), College Park 2x4 Thermal Hydraulic Loop Facility was a scaled down model of the Three Mile Island Unit 2 Babcock & Wilcox (B&W) PWR. The main components of the model reactor coolant system included a reactor vessel, two hot legs, two once-through steam generators, four cold legs, four reactor coolant pumps, and one pressurizer. Altogether 286 thermocouples were mounted in the downcomer and the lower plenum of the reactor vessel on 11 horizontal planes to trace slug mixing.

- University of Maryland B-MOV Facility [161]. An optically transparent separate-effect facility (referred to as the Boron-Mixing Optical Vessel, or B-MOV) was constructed to conduct the high-resolution boron dilution experiments at the University of Maryland. The facility was scaled by 1:4 in length and 1:500 in volume with respect to the prototypical B&W 2×4 lowered-loop PWR. The B-MOV was a replica of the similarly scaled integral facility at the University of Maryland. It was capable of providing spatially and temporally resolved data concerning the flow in the downcomer.

- Jet Impinging Apparatus of Bonetto and Lahey. Jet impingement on free surface may occur in the PWRs cold legs, in the PTS scenarios where a stratified flow in the cold legs takes place, with a low enough liquid height, when ECC water is injected [36]. The impinging jet flow on a free surface is a particularly challenging case for multiphase models [156].

- Jet Impinging Apparatus of Iguchi et al [162]. Liquid jet influence on a free surface and the effect of gas entrainment on liquid velocity and turbulence characteristics were investigated by Iguchi et al. (1998) using an axisymmetric, turbulent jet impinging orthogonally a free surface, in a cylindrical vessel (diameter = 20 cm, height = 39 cm). The flow reached a statistically steady-state; the fluids were liquid water and air. The liquid velocities were measured in a range of depths below the free surface.

6.3.2.1   Completeness of the Experimental Data Base for TH Analysis of PTS

Thermal hydraulic experiments/analysis related to PTS produce initial and boundary condition data for structural and mechanical analysis. It is therefore important in the studies to cover all the different thermal loading mechanisms in the downcomer during the overcooling events [163]. These loading mechanisms are

- the final temperature in the downcomer (this is the most important parameter)
- the rate of the temperature decrease
- nonuniformity of the temperature fields (cold plumes)
- nonuniformity of the coolant-to-wall heat transfer coefficients in the downcomer

Additionally, the mechanical stresses caused by high primary pressure increase the total stress level.

Significant separate effects thermal fluid-fluid mixing research programs related to PTS were performed in the USA, Germany, Finland, Belgium and Japan in the 1980's. The data obtained from these test facilities were used to benchmark a variety of thermal hydraulic computer codes and mixing models. The primary goals of the separate effects testing programs were to:

- Determine the fluid mixing patterns that are established during HPSI flow into the cold legs for a wide range of PWR geometries and loop flow conditions.
- Measure the loop flow and HPS flow conditions that produce thermal stratification in the cold legs.
- Measure the plume/wall heat transfer coefficients in the downcomer and estimate its importance to downcomer heat transfer.
- Measure the plume temperature decay in the downcomer.

Combined-effect/integral system PTS tests modelling realistic reactor configurations were done, for example, in the APEX-CE, LSTF and ROCOM test facilities. Investigations in these integral facilities covered a wide spectrum of PTS related accident scenarios, such as SB-LOCA, MB-LOCA and MSLB.

The more challenging condition of safety injection into voided or partially voided cold legs was the subject of an international comparative assessment in the late 1990's. The most challenging thermal-hydraulic conditions involve a reduced water level and safety injections into the steam environment.

The steam in the cold leg and downcomer condenses on the surface of the injection flows and water stripe. This type of DCC along with PTS has been identified by the EUROFASTNET project as a key safety related issue [164]. The condensation provides the main heating mechanism for the injected water. High condensation rates will warm up the injected fluid while a reduction in the condensation rate would allow the cold water to make its way into the downcomer at a lower temperature. Factors such as liquid surface area, heat transfer rates, splashing, droplet entrainment, turbulence levels within the liquid and gas, non-condensable gas concentrations, and the water stripe detachment mechanism are all important considerations for this type of modelling [129]. The issue of PTS and DCC modelling was addressed, for example, by the NURESIM (SP2) Thermal-Hydraulics project in 2005-2008 [165]. The focus was on two-phase flow phenomena with an emphasis on modelling needs and areas for improvement. Also, the TOPFLOW PTS experimental program concentrated on two-phase situations. The objective of the programme was to provide a well-documented experimental database for both validation of CFD modelling of the two-phase flow in the cold leg and the downcomer including flow-wall heat transfer, and the improvement of the understanding of key thermal hydraulic phenomena involved [36]. Particularly, the TOPFLOW program contributed to the validation of CFD and CMFD codes by providing precise local void fraction, turbulent quantity and interfacial area measurements.

More recently, PTS related mixing phenomena were studied within the framework of the OECD/NEA Cold Leg Mixing CFDUQ Benchmark exercise, where measurements of the velocity and concentrations of density-driven flow mixing were performed using high-resolution experimental methods. The data produced a unique contribution to the advancement of high-fidelity computer codes currently

employed for nuclear reactor safety and design evaluations. Particularly, the data suit for assessing the performance of CFD tools in predicting mixing in buoyancy-driven flows [155].

Concerning the coverage of all possible PTS related accident scenarios studied in the integral system tests over the decades it can be quite safely said that there is probably nothing to be found with new tests. On the phenomena side the situation is different. Although the experimental data base collected through PTS related investigations is large, there are some phenomena that have been addressed only in one or two test campaigns and geometries.

One such topic is interactions of cold plumes in the downcomer which have been studied only in a couple of test facilities. The IVO (NRC) tests were unique in involving multi-loop injection, i.e., plume interactions in the downcomer (circumferentially 1/2). The APEX-CE facility operated also with multiple loops and allowed investigation of the interaction of the plumes.

Interaction of plumes is one of the key phenomena affecting the mixing processes taking place in the downcomer. The geometry of the downcomer and the placement of hot/cold leg nozzles have a strong effect on the developing flow fields and thus on the interaction of plumes. The fact that there exists only experimental data on multi-loop plume interaction from two different geometries (IVO-NRC, APEX-CE) would possibly justify additional tests on the issue.

All geometrical details of the cold leg and RPV, such as injection pipes, inlet nozzles and curvatures, influence the development of flow fields during the safety injection resulting to complex multidimensional flow phenomena. Furthermore, the neutron shield has a strong impact on the flow development in the downcomer. As system codes cannot model multidimensional effects in all detail, CFD methods are needed in order to predict the 3-dimensional behaviour of the flow in the cold leg and plume oscillation in the downcomer. CFD analysis of for example Qian et al. (2018) [166] has confirmed the highly 3-dimensional behaviour of the plume cooling in the downcomer and the importance of the detailed CFD simulation to precisely capture these phenomena.

3D phenomena have been studied in some experimental programs dealing with PTS. Multidimensional mixing tests were carried out in UPTF. The three-dimensional temperature field was measured in the cold leg and downcomer also in the OECD ROSA V experiments in the LSTF. As the development of flow fields in the cold leg and downcomer is geometry specific and therefore differs from plant design to another, extension of the experiment data base could be considered to be able to validate CFD codes and the 3D models of the system codes for all geometries.

Many efforts have been made to understand PTS but usually these efforts have assumed symmetric reactor cooling injection. An asymmetric cooling injection can occur, for example, if some of the safety injection pumps fail during PTS loading. This failure makes symmetric injection impossible, leading to more serious conditions. The effect of asymmetric reactor cooling was investigated using three-dimensional computational fluid dynamics and the finite element method by Ruan et al. (2021) [167]. The results indicate that the most asymmetric injections provide approximately 30% more serious situations than symmetric injections. Qian et al. (2018) [166] concluded in their study that considering the non-uniform plume cooling effects increases the total failure frequency by more than 1 order of magnitude. For the validation of CFD codes for different asymmetric cooling situations additional experimental data may be needed.

Two-phase PTS is closely connected with DCC. Condensation influences the mixing and the final thermal loads at the RPV walls. Model development and validation on DCC are assessed to have a high priority and must be validated against high-grade experimental data but there are no experimental data on the condensation at the jet itself available [165].

The most important physical phenomenon leading to the mixing is turbulence. There is a turbulence production below the jet caused by shear as well as by interaction with the entrained bubbles. For the stratified flow wall shear and interfacial shear are the most important sources of turbulence. Different approaches to model turbulence have been suggested and these must be validated against

experimental data [165]. Today's sophisticated measurement techniques would allow more detailed information on the physics of turbulence than was obtained in the tests performed earlier.

PTS related tests in the 80's and 90's were done before such sophisticated measurement techniques as Particle Image Velocimetry (PIV) or Laser Induced Fluorescence (LIF) were developed to their maturity. Instead, they mostly relied on traditional temperature and flow rate measurements. With the new techniques high-grade information on the flow regimes and temperature distributions from the locations of interest for PTS could be obtained without intruding the flow.

6.3.3   Thermal-hydraulic Analysis Methodologies

Several options are available for the thermal-hydraulic analysis of the system thermal-hydraulics and detailed flow distribution in the downcomer for PTS scenarios. These include system thermal-hydraulics analysis codes, CFD analysis codes, and mixing codes. The purpose of this subsection is to assess which methods are most commonly used for PTS analysis and whether any special techniques or methodologies have been developed to improve predictions. Finally, this subsection also aims to assess the current state of validation of the different simulation codes.

6.3.3.1   Thermal-hydraulics Systems Analysis Codes

The thermal-hydraulic behaviour of the primary system and portions of the secondary systems of light water reactors have traditionally been modelled using so-called thermal-hydraulics systems analysis codes. Systems codes use a one-dimensional nodalisation of the various components of the reactor's primary and secondary cooling circuits. Examples in the European context are CATHARE (CEA), ATHLET (GRS), Apros (VTT) and the US NRC codes RELAP5 and TRACE. The most recent generation of systems analysis codes implement six equations for the mass, momentum and energy balance for the liquid and vapour phases of the water coolant. The exchange of mass, momentum and energy between the two phases and the solid structures of the reactor are modelled though empirical closure models. The appropriate closure models for different geometries and flow conditions are selected through flow regime maps. These maps estimate the flow regime based on the local phase velocities, void fraction and other parameters. The codes' capabilities are complemented by dedicated models for specialised hydraulic components such as valves and steam separators, as well as basic models for one or two-dimensional heat conduction through the solid structures, e.g., fuel rods and pipe walls. Comprehensive control system and dynamic system modelling capabilities allow the user to mimic the plant and operator responses for complex transients.

The ability of systems codes to adapt to different local flow conditions and yet model the entire primary side and large proportion of the secondary side of LWRs means that they are appropriate for modelling a large variety of transient scenarios, including PTS-relevant scenarios such as LOCA and MSLB. Systems codes have been used extensively in the past to perform screening analyses and obtain boundary conditions for PTS-relevant scenarios; these are then used in combination with thermal-hydraulic mixing codes (see subsection 6.3.3.2) to obtain more resolved distributions in the downcomer. In more recent years, these boundary conditions have been used for downstream CFD analyses [53] [54]. Further examples of systems code analyses for PTS scenarios are provided in the subsections that follow.

By their design, systems codes traditionally had limited success in predicting local flow behaviour where three-dimensional effects are important. In particular, 1D systems codes are unable to predict the temperature stratification occurring in the cold leg during the safety injection. Further, the 3D nature of flow in the downcomer region cannot be captured using 1D components. Code users have opted to model multiple parallel 1D channels for the downcomer region towards capturing the asymmetry in downcomer flow. By design, however, these 1D components are unable to capture the lateral momentum with any accuracy.

In an effort to address these limitations, codes such as CATHARE, ATHLET and TRACE now incorporate dedicated three-dimensional components. One should not confuse this extended capability with modern computational fluid dynamics codes (see subsection 6.3.3.3). The 3D components in systems

codes are based on many of the same simplifying assumptions and flow regime maps used for 1D components. One important limitation is in the modelling of turbulent mixing and dispersion. ATHLET, TRACE and CATHARE-2 do not explicitly model turbulence, suggesting that their ability to accurately capture the complex dynamic behaviour of cold plumes in the downcomer is limited. Despite this limitation, all three codes have been shown to reasonably predict the flow distribution at the core inlet in comparison to CFD simulations for the ROCOM experimental tests [55]. Comparisons dedicated to PTS between standalone TRACE, 2D mixing codes and CFD simulation results for several LOCA scenarios [55] showed that TRACE models using 3D components for the downcomer could reasonably predict the minimum and average coolant temperatures in the downcomer region for larger break sizes. For smaller break sizes, it was found that the inability to the code to predict the temperature stratification in the cold leg led to an overprediction of mixing in the cold leg and downcomer region and therefore an underprediction of the severity of PTS. This non-conservatism was also identified in the DEFI-PROSAFE project [40]. The use of mixing codes and CFD simulations was shown to improve the agreement between experimental and calculated results.

The latest version of the CATHARE family of codes, CATHARE-3, includes dedicated turbulence modelling equations based on the two equations k-epsilon model, potentially providing better predictions of PTS in the downcomer region of PWRs. This advanced functionality has been validated for several experiments focused on flow in rod bundles (e.g., [56]). Dedicated PTS analysis results using CATHARE-3 have not yet been published, however.

The role of the system TH code depends on the overall approach to TH analysis code in the PTS evaluation (see the list of possible approaches at the beginning of chapter 2.3). Also, in frame of one PTS study (for one NPP) more approaches to TH analyses can be applied:

- 1D system TH code + mixing code (or CFD) for transients with prevailing single-phase flow in RCS (SB-LOCA, PRISE, MSLB, etc.)
- 1D system TH code with 2D/3D component for events with strong two-phase flow in RCS (MB-LOCA, LB-LOCA)

Notes and recommendations to systems and components to be modelled in the system TH analysis:

- Comprehensive modelling of reactor coolant system and individual modelling of all reactor coolant loops, 3D model of reactor or at least 2D nodalisation of reactor downcomer applied already in system TH calculation (even coarse prediction of 2D temperature and velocity fields in DC improves prediction of natural circulation in individual loops, flow coast-down and flow stagnation = important for many phenomena relevant to PTS).
- Detailed modelling of ECCS system for injection phase (accumulators + injection lines, SI tanks, SI pumps, discharge lines).
- Complex modelling of SI recirculation phase (modelling of whole SI recirculation circuit: RCS break → containment → sump → heat exchangers → SI suction → SI pumps → RCS)
- Detailed modelling of SG and Main Steam System (important mainly for the MSLB events).

6.3.3.2   Thermal-hydraulic Mixing Codes

Six-equation, thermal-hydraulic system-analysis codes such as TRACE, CATHARE, ATHLET, and RELAP5 do not model the turbulent mixing between two liquid streams within a control volume. Therefore, some of the most important phenomena are simulated by mixing-analysis codes, examples of which are computational fluid dynamics (CFD) programs or mechanistic-model programs. CFD programs solve the conservation equations for mass, momentum, and energy by approximating the differential equations by finite-difference equations. Mechanistic-model programs simplify the conservation equations by the use of boundary-layer approximations or integral methods for solving the differential equations. Both types of programs rely partly on correlations for closure of the conservation equations.

Numerous mechanistic-model programs for performing mixing analyses exist for application to PTS. Some of the early codes were REMIX (Iyer et al. [57]), GRS-MIX (Sonnenburg [58]), KWU-MIX (Hertlein

[59]), COMMIX (Sha et al. [60]), TEMPEST (Eyler and Trent [61]), and SOLA-PTS (Daly and Torrey [62]). The first three of these programs were based on dividing the flow of water into regions or zones where a particular set of the most important phenomena occur. KWU-MIX is a thermal-hydraulic mixing-analysis program for performing analyses of pressurized thermal shock in the wall of the reactor pressure vessel (RPV) of a PWR. KWU-MIX is a fast-running program, so numerous simulations can be performed quickly.

An advantage of the mechanistic-model programs is the speed at which the mixing analyses are performed. The ability to perform hundreds of analyses in a time span on the order of minutes makes it possible to perform best-estimate-plus uncertainty analyses. They are also applicable to probabilistic fracture mechanics (PFM) as described by Cheverton and Shelby [63].

6.3.3.2.1   Other Types of Thermal-Hydraulic Mixing Codes

Concerning French Utility and IRSN mixing codes, a tool is used to determine water temperature at the RPV wall at the highest point of the RPV under irradiation (facing the core), which is the point of mechanical interest. Boundary and initial conditions come from CATHARE outputs. Before the end of forced convection, the water temperature at the RPV wall is equal to the mean temperature at cold legs outputs. After the departure of natural convection, the tool performs mass and enthalpy balances in a volume based on cold legs, downcomer and lower plenum volumes and depending on the water level in the downcomer. The mixing volume used is determined on experimental tests. This tool assumes some conservative and beneficial assumptions[6]. At the end, the mixing tool is considered as reasonably covering the real fluid temperature at the RPV wall.

6.3.3.3   Computational Fluid Dynamics Analysis Codes

Refined calculation of stresses in the reactor vessel requires knowledge of accurate three-dimensional temperature fields. One-dimensional models, for example developed in RELAP5, do not describe complex three-dimensional processes occurring when emergency water enters the downcomer and three-dimensional heat conduction processes in the metal. Detailed prediction of volumetric temperature fields in the reactor pressure vessel is possible using CFD modelling.

6.3.3.3.1   General Aspects of CFD Modelling of PTS

CFD Modelling of Hydrodynamics and Heat Transfer in VVERs Under Thermal Shock

When simulating a transient with a corresponding thermal shock, the following processes should be considered:

- coolant flow and heat transfer in the downcomer between the reactor vessel and core barrel
- thermal conductivity in the reactor vessel and other structural elements
- coolant flow and heat transfer in the core, where the core can be replaced by simplified equivalent domain

When studying the processes in the specified channel, the mathematical model includes the Navier-Stokes, continuity and energy equations.

A number of assumptions are made when solving the problem. Mainly, the coolant is assumed to be single-phase liquid during the whole process of the reactor emergency cooling.

The model includes the coolant domain and the core barrel and RPV metal with cladding layer. In this case, the conditions of ideal thermal contact are set on all interacted surfaces.

---

[6] Assumptions of TDA (Température descente annulaire) tool are: 1) An instantaneous mixing in the volume; 2) All the cold flows are taken into account in the balance; 3) Hot condensation flow is not taken into account in the balance; 4) Solid structures inertia is not considered; 5) Safety injection flow is not heated up by steam in two-phase configurations.

When solving the problem, the temperature dependence of the thermophysical properties of water and construction materials is taken into account (thermal conductivity and heat capacity, density and kinematic viscosity).

The presence of natural convection is taken into account when modelling the flow and heat transfer.

Within the framework of this study, it is of the greatest interest to obtain reliable information on the temporal changes of the three-dimensional temperature field in the reactor vessel. This information serves as the basis for the subsequent fracture mechanics analysis of the RPV. In general, the procedure of the RPV fracture mechanics analysis consists of four stages:

1. The solution of the flow and heat transfer problem in a one-dimensional formulation using RELAP5 thermal hydraulic code.
2. CFD modelling of the flow and heat transfer problem in a three-dimensional formulation using the boundary conditions obtained from the RELAP5 code (stage 1).
3. Finite element calculation of stresses in the reactor vessel using three-dimensional temperature fields obtained by CFD modelling. (The purpose of this calculation is the time and space localization of the maximum stresses in the reactor vessel).
4. Analysis of fracture mechanics by sub-modelling of the regions with maximum stresses. Results of previous calculations of stresses in the RPV are used to set the boundary conditions on these subdomains (stage 3).

It is especially important to construct the high-quality and sufficiently structured computational mesh, particularly in mixing areas and boundary layers.

Computational Domain

When determining the computational domain for 3D CFD modelling of hydrodynamics and heat transfer processes under PTS in VVER-1000 reactors, the following considerations were accounted.

In VVER-1000 reactors, emergency water is supplied according to a slightly different scheme. Here, the branch pipe for supplying of emergency water from the accumulators to the annular gap is not aligned with the cold legs and is located separately on the reactor vessel (Diameter of the emergency water supply pipe is dA = 230 mm).

Accounting this, in the case of VVER-1000 it is necessary to include to the computational model the area of reactor with emergency water supply branches combined both with cold legs and with the vessel directly. As for the outlet branches, they can be excluded from consideration.

It should be noted that the ECCS branches geometry needs to be modelled reasonably accurate, especially taking into account the features of its curvilinear connection with the reactor vessel. This is due to the fact that in this sub- region, the specificity of the jet supply of emergency water forms the further development of the cold plumes in the annular gap. Further, as studies have shown [54], this subdomain contains the so-called critical points corresponding to increased stress levels.

It is also necessary to pay attention to the fact that the computational domain for CFD modelling should take into account the heterogeneity of structural materials, in particular, the presence of a cladding layer on the RPV inner surface.

Initial Conditions

As the initial conditions, the data obtained using the RELAP5 code, which correspond to the time moment before the ECCS is turned on, can be taken. The initial distribution of temperature, velocities and pressures in the computational domain is determined for this time point. This approximation is in line with other studies, e.g., [53] [54] [122], where constant values of the indicated parameters are taken as the initial distribution.

Boundary Conditions

Boundary conditions are also set based on the solution of the problem, obtained using the RELAP5 code. They are dependent on time and set from the initial time moment corresponding to the ECCS switching on to the selected moment of the calculation end.

Regarding the contact interfaces between structural elements (of the type "RPV - cladding layer", "surface of the downcomer - coolant"), here the conditions of ideal thermal contact (the equality of temperatures and heat fluxes at the interfaces) are set as thermal boundary conditions.

The considered length of emergency water supply branches should be enough to ensure the formation of correct velocity and temperature profiles before the junctions with cold legs and RPV.

Constant velocity and temperature profiles can be set at the inlet to these branches. Herewith the turbulence intensity may be assumed to be 3% in analogy to [53].

Velocity profile for developed turbulent flow in a circular channel should be set on the inlet of ECCS tubes to reduce their modelled length.

Thermophysical Properties of Materials

The physical properties of water (thermal conductivity and heat capacity, density and kinematic viscosity) are dependent on temperature. Particularly important is a detailed description of the dependence of water density on temperature, since it largely determines the features of flow and heat transfer in the downcomer associated with the buoyancy presence.

Thermophysical properties of structural elements (thermal conductivity coefficient, heat capacity and density) should also be considered as dependent on temperature.

CFD Modelling of Hydrodynamics and Heat Transfer in PWRs Under Thermal Shock

For PWRs, the accepted computational domain included the reactor, inlet branches and emergency water supply lines from hydraulic accumulators and emergency water injection systems. The water injection lines and lines from the accumulators are connected to the cold legs. In this case, the hot legs were not included in the computational domain, and the outlet boundary was located at the outlet branches of the reactor vessel.

The spatial mesh must be structured and built from hexagonal elements in order to be consistent with the flow field in its main part.

Also, the mesh must be sufficiently detailed in areas directly related to PTS, primarily:

- at the emergency water supply pipe branches
- in the downcomer

A sufficiently detailed mesh should also be provided in the reactor lower head.

Available studies indicate that for PTS modelling in PWR reactors, a spatial mesh of about 5 million cells with its rational irregularity is quite effective. This is confirmed by comparing the results of calculations on such mesh with the data obtained on a coarser mesh consisting of 3.5 million cells [53].

As for the time step, in available studies the solution of PTS problems was implemented with a constant time step of 2.5 milliseconds. Perhaps more rational is the use of an adaptive time step that changes over time.

Turbulence Modelling for PTS Applications

Of primary importance in the modelling of the fluid flow and heat transfer for PTS applications relates to the accurate modelling of the mixing processes between hot and cold coolant within the cold legs and downcomer regions of the reactor. Currently, many approaches to mathematical modelling of turbulent flows have been developed. Among them are Direct Numerical Simulation (DNS), Large Eddy Simulation (LES), and Reynolds-Averaged Navier-Stokes (RANS) solutions. There are also combined

approaches that include certain features of DNS, RANS and LES, for example, Detached Eddy Simulation (DES).

The direct numerical simulation method implies solving the complete (non-stationary and three-dimensional) Navier-Stokes's equations. Under DNS approach, all scales of turbulent motion are resolved. That allows to calculate the amplitude and average characteristics of the flow by averaging over a sufficiently long (statistically representative) time interval. However, the use of DNS requires powerful computational resources, and the possibilities of its application are limited to calculations of flows with a fairly simple geometry and relatively low Reynolds numbers (about 10^3 - 10^4).

The approach based on the solution of Reynolds-Averaged Navier-Stokes equations requires much less computational resources. The RANS simulates the contribution of all turbulence scales to the averaged motion. This method is successfully applied on practice.

The method of pseudo- or quasi- direct numerical simulation (Pseudo or Quasi DNS, PDNS or QDNS), as well as the monotonic method for large eddies modelling (Monotonically Integrated LES, MILES) can also be used. In these methods, subgrid models are not used, and dissipative processes are accounted using specially designed difference schemes [126].

The Unsteady RANS (URANS) approach, which solves the unsteady Reynolds equations, is usually regarded as a generalization of the RANS method. This approach is less computationally expensive and mesh sensitive than LES or DES. However, there is no reliable theoretical basis of URANS applicability for describing the turbulent flow (in the derivation of Reynolds equations used averaging over a time interval which is much higher than the characteristic time of the turbulent fluctuations). Application of the transient Reynolds equations form is justified in the presence of external non-stationary influences (in the case of transient boundary conditions).

1. Calculations using unsteady Reynolds's equations on a relatively fine mesh allow to solve large-scale vortex structures and trace their development in time.
2. Let us consider in more detail the features of modelling the processes occurring in a downcomer based on URANS. First, it should be noted that to approximate the convective terms in the explicit part of the motion equations, it is advisable to use the upwind scheme with quadratic interpolation. Second, for a more accurate description of the non-stationary terms in the explicit part of the equations, a second-order time approximation scheme should be used. As for the procedure of pressure gradient correction, it's advisable to use the PISO algorithm (Pressure-Implicit with Splitting of Operators).
3. These recommendations meet the experience of solving such problems described in the literature, e.g., [127] [53][53] [54] [122].

The choice of a turbulence model for a particular problem is typically made by comparing the results of CFD simulations for various turbulence models with data from corresponding experimental studies. The results of such a comparison for PTS are given in [127]. Several variants of mesh resolution, turbulence model and numerical schemes were considered in this work. Based on the results of these studies, the following conclusions were drawn:

- The SST (shear stress transport) k-ω Menter's turbulence model [128] can be used for similar problems, provided that it takes into account the lifting forces, i.e., using SST k-ω turbulence model in buoyancy modification (variant B)
- The use of standard k-ε turbulence model in the buoyancy modification also provides a satisfactory agreement between experimental and calculated data (variant C)
- The best agreement between the experimental data and simulation results is achieved using multi-parameter Reynolds's stress model RSM (variant G). RSM models are, however, known to be less stable than the two-equation turbulence models and are generally less suited to practical engineering simulations

In most publications devoted to the study of PTS, preference is given to using the SST k-ω turbulence model with the buoyancy modification.

Some examples of CFD applications for TH PTS analysis are as listed below:

- French Utility CFD methodology (presently not used in safety studies)
- Neptune CFD calculations of TOPFLOW-PTS Experiments
- ANSYS CFX Calculations of UPTF Experiments
- ANSYS Fluent used for CFD calculations for Czech PTS Studies

Many recent examples of the application of CFD to PTS related studies are found in open literature, highlighting that this is an area of active research. Studies have shown that the use of CFD can reduce some of the conservatism associated with the more traditional PTS analysis method. Examples of CFD simulations for both test facilities and operating reactors can be found and several of these have been presented. Both WWERs and PWRs are included in this list. For the most part, these examples are limited to cases where multi-phase CFD simulations are not required, e.g., SB-LOCA and MSLB. Examples of CFD simulations for more severe accidents such as MB-LOCAs and LB-LOCAs are quite scarce, due in part to the complexity and computational effort required. CFD methods and simulations are, however, not clearly established for complex multi-phase PTS transients and this is therefore an area of active research. The French utilities noted a lack of validation and consequently have prioritized R&D in this direction. Efforts to quantify the uncertainties in CFD simulations for PTS scenarios have also been started.

6.3.4   PTS Accident Scenarios

A large spectrum of postulated plant transients and accidents can lead to PTS (LOCA, stuck open safety relief valves, main steam line break, feed-and-bleed, etc.).

This subsection summarizes the scenarios that have been considered in the past or that are considered important for assessment. Moreover, this subsection provides information on the specific assumptions and methodologies that were applied in the past analyses and that should ideally be addressed in the future.

The International Comparative Assessment Study (ICAS) of Pressurized-Thermal-Shock (PTS) in Reactor Pressure Vessels (RPVs) was organized in 1996 to bring together an international group of experts from research, utilities and regulatory organizations in a comparative assessment study of integrity evaluation methods for nuclear RPVs under PTS loading. The postulated loading transients referred to a small-break loss-of-coolant accident typical for US PWR plants and transients due to leaks with different sizes typical for German PWR plants [26].

Report NUREG-1806, Vol. 1 [17] summarizes 21 supporting documents that describe the procedures used and results obtained in the probabilistic risk assessments, thermal hydraulic, and probabilistic fracture mechanics studies conducted in support of this investigation. The analyses considered transients in the following classes:

- primary side pipe breaks,
- stuck-open valves on the primary side,
- main steam line breaks,
- stuck-open valves on the secondary side,
- feed-and-bleed,
- steam generator tube rupture,
- mixed primary and secondary initiators.

In the IAEA-TECDOC-1627 on PTS in NPPs [6], which is the result of the Coordinated Research Pproject-9 (CRP-9), in which the benchmark deterministic calculations of a typical PTS regime were performed. Chapter 2 deals with selection of the overcooling transients and accidents to be analysed. Selection of the transients for deterministic analysis can be based on analysis and engineering judgment using the design basis accident analysis approach, combined with operational experience. An alternative approach to the selection of transients is the probabilistic risk assessment. It should be noted that

probabilistic PTS analysis is considered complementary to the deterministic analysis of the limiting scenarios.

At least the following groups of initiating events should be taken into account: (see subsection 6.3.1.1 for a more detailed description):

- Loss of Coolant Accidents (different sizes of both cold and hot leg loss of coolant accidents (LOCA) which are characterized by rapid cooldown should be considered);
- stuck open pressurizer safety or relief valve (after an overcooling transient caused by a stuck open pressurizer safety or relief valve, possible reclosure can cause a severe re-pressurization);
- primary to secondary leakage accidents (different sizes for both single and multiple steam generator tube ruptures up to the full steam generator collector cover opening should be considered);
- large secondary leaks (transients with secondary side de-pressurization caused either by the loss of integrity of the secondary circuit or by the inadvertent opening of a steam dump valve can cause significant cooldown of the primary side). Possible sources of secondary side de-pressurization are steam line break; main steam header break; spurious opening and stuck open of the turbine bypass valve, atmospheric dump valve and steam generator safety valve(s); feedwater line break.
- Inadvertent actuation of high-pressure injection or make-up systems (this kind of accident can result in a rapid pressure increase in primary system. Cold, hot, and cooldown initial conditions should be considered);
- accidents resulting in cooling of the RPV from outside (in some NPPs, there are several possible sources capable to flood the whole reactor cavity (e.g., break of the biological shield tank, ECCS or containment spray system actuation, loss of coolant from primary or secondary circuit, intentional cavity flooding, unintentional inadvertent actuation of a cavity flooding system — system installed in some plants for severe accident mitigation).

The above study from IAEA-TECDOC-1627 [6] also references NUREG-1806, Vol. 1 [17]. In Table A1 of [6] national practices have been presented. The critical transients are:

- China – PWR (SB-LOCA, LB-LOCA overcooling with re-pressurization based on PRA), WWER (SB-LOCA);
- Czech Republic – WWER (LB-LOCA, PRZ SV opening + reclosure);
- Finland – WWER and PWR (Large LOCA, Safety valve opening and reclosure, Cold pressurization, External cooling):
- France – PWR (LB-LOCA & SB-LOCA, SLB-SSLB);
- Germany – PWR (SB-LOCA and critical transient selected by fracture mechanics);
- Hungary – WWER (LB-LOCA, SLB, Overcooling with re-pressurization);
- Korea – PWR (SGTR, SB-LOCA, MSLB);
- Slovakia – WWER (Case to case, mainly transients with pressurization under low temperature as Small LOCA, Primary to secondary leakage);
- Russia – WWER-1000 (Primary Small LOCA, Primary to Secondary Leakage), WWER-440 (Primary Small LOCA, Secondary Leakage).

6.3.5   Other topics

No dedicated literature review on the topics below was included in the state-of-the-art report, and conclusions are instead based on the partner responses to the questionnaire.

6.3.5.1   Best-Estimate Plus Uncertainty (BEPU)

The application of uncertainty quantification (UQ) methods to the thermal-hydraulics analysis of PTS scenarios is relatively unexplored. The intent is to assess the status of thermal-hydraulics UQ methods, with a focus on PTS analysis.

6.3.5.2   Coupled Thermal-hydraulics/Fracture Mechanics Analysis

The purpose of thermal-hydraulics simulations for PTS is to provide boundary conditions for subsequent structural analysis simulations. The complete PTS analysis chain is therefore a multi-physics simulation where we need to propagate uncertainties downstream into the structural analyses. There are many approaches for multi-physics uncertainty propagation, and this topic has been the focus of several international projects in the past (OECD/NEA UAM benchmarks, etc.). The intent is to assess which methods are available to the partners for propagating uncertainties through the complete simulation chain.

6.3.5.3   Human Interactions

Many PTS scenarios are the direct result of human interactions with the system, e.g., feed-and-bleed, blowdown during SB-LOCA scenarios. Such interactions are often accounted for in probabilistic risk assessments, but accounting for them in deterministic simulations is less common. The intent is to assess to what extent human interactions are accounted for in PTS simulations and how this has been done in the past.

6.4   Conclusions

A literature review and collection of both experience and current practices have been carried out to define the current state-of-the-art and remaining gaps in thermal-hydraulic analysis for pressurized thermal shock (PTS) scenarios. In addition to an extensive literature survey, answers to a questionnaire distributed to all partners were compiled and assessed. These questions were focused on the topics of thermal-hydraulics analysis methodologies, relevant accident scenarios, best estimate plus uncertainty, multi-physics coupled thermal-hydraulics/fracture mechanics analysis and human interactions.

The thermal-hydraulic phenomena and factors important for PTS have been summarised based on several important PTS references and projects. In particular, attention was paid to available PIRTs in open literature and their evolution over time. The PIRTs and described phenomena will be assessed and used as a basis for the new PIRT to be developed within the APAL project.

An extensive survey of experimental facilities and experimental tests which may be used as data for PTS validation has been conducted and summarised.

6.4.1   Experimental Activities and Validation

As can be seen from the sections above, the experimental data base related to TH phenomena important for analysing PTS is huge. However, many of the experimental campaigns were conducted at a time when the used measurement techniques had not yet evolved into such a state of maturity as they are today.

For a detailed understanding of the flow and heat transfer behaviour, there still is a need for adequate experimental results to develop correlations and validate modelling approaches. Particularly, CFD techniques are showing great promise in this area, but more experimental data is needed, specifically in the area of multi-phase flow and DCC, in order to validate these tools and use them in safety assessment.

Different aspects of system and CFD codes and their physical models can be validated with the help of separate effects tests. The successful simulation of the single separated effects is a prerequisite for a complex industrial PTS flow simulation. In a validation test, the quality of the model is checked for a given flow situation. Validation tests are the only method to minimize and quantify modelling errors and to ensure that new models are applicable with confidence to certain types of flows. In an ideal case, a validation test case gives sufficient details to allow for an improvement of the physical models. The data are required in a high resolution in space and time for the whole domain of interest and

should include local and time-dependent information on interface between the phases, mean, and fluctuations (turbulence parameter) values for temperature and velocity [36].

The quality of data is of primary importance for a successful validation exercise. Error bounds/estimates are essential in evaluating the quality and suitability of data for validation purposes. Unfortunately, not all experiments provide this information. It is also desirable to have an overlap of experimental data to allow for testing of the consistency of the measurements. Experiments performed by different research groups in different facilities and possibly using different experimental techniques are thus beneficial for guaranteeing the quality of data used for code validation.

Although there are several experiments available where flow phenomena are investigated as separate effects and as integral effects, there is still a need for well instrumented validation data and demonstration experiments where experimental parameters are varied in order to investigate PTS phenomena. CFD methods use many turbulence and two-phase flow models which have a certain degree of empiricism. The accuracy and universal validity of these models must be assessed by comparison of the numerical results with experimental data. Depending on the suitability of the data, test cases are used for validation and calibration of statistical models as well as for demonstration of model capabilities [36]. CMFD codes are getting closer to experimental scenarios representative of industrial PTS. Some of them are already able to perform industrial computations, thus helping to improve the current status of safety technology [134]. Nevertheless, some strong differences in the results quality still exist between the different tools [135].

6.4.2   Thermal-hydraulic Analysis Methodologies

Thermal-hydraulics methodologies for the analysis of PTS have been described, including an overview of systems thermal-hydraulics codes, mixing codes and the current state-of-the-art for CFD. The ability of systems codes to adapt to different local flow conditions and yet model the entire primary side and large proportion of the secondary side of LWRs means that they are appropriate for modelling a large variety of transient scenarios. Systems thermal-hydraulics codes therefore remain the 'workhorse' of PTS analysis, predicting the system behaviour and providing boundary conditions to for the higher resolution mixing and CFD codes. In an effort to address the one-dimensional limitation, several systems codes now incorporate dedicated three-dimensional components. These components have shown some promise for PTS applications. The region mixing models as applied in several computer codes have been summarised. These codes can be used to perform many calculations in an acceptable amount of time, making them suitable for sensitivity analysis and uncertainty quantification.

Table 7 summarizes the Thermal-hydraulic Analysis Methodologies for solving PTS problem, systems and components considered in the models and V&V procedures for used codes. Based on the Table 7, it can be concluded that most partners use methodologies based on the standalone system codes (mainly RELAP5, TRACE, ATHLET) followed by mixing analysis codes (GRS-MIX, KWU-MIX, REMIX) using the boundary conditions obtained from the system code at the first step. Several of the partners use or plan to use CFD methods as an alternative to mixing codes mentioned above or in addition to these mixing analysis codes. Some of the partners consider coupling of system and CFD codes. As an example, in UJV the RELAP5-FLUENT coupling with CFD domain of reactor downcomer and cold legs is under development.

CFD currently provides an alternative to classic mixing codes, however CFD analysis of PTS scenarios remains an area of active research. CFD techniques show great promise, and their results suggest that the conservatism associated with traditional system and mixing code analyses can be reduced using CFD. The methodologies seem to be quite well established for "milder" scenarios where the coolant remains in single phase. Some recommendations for selecting the modelling domain, meshing and the selection of closure models and numerical schemes have been provided for such single-phase simulations. However, further developments are needed for multi-phase simulations which are required to accurately predict more severe transients. The lack of validation for multi-phase CFD simulations has also been highlighted; in the area of multi-phase flow and direct contact condensation,

high resolution experiments are needed in order to validate these tools and use them in RPV safety assessment.

6.4.3   Accident Scenarios

Table *8* shows a brief summary of the partner responses, particularly focusing on the:

- overview of the PTS scenarios, considered by the different organizations/countries
- applied methodologies for analysis of the PTS scenarios
- basic analysis assumptions that might affect the quality/validity of the predicted thermal-hydraulic parameters

As can be seen from Table 8, most of the partners/countries consider similar groups of initiating events, which include:

- spectrum of primary leaks (SB, MB, LB and DEGB LOCA)
- secondary leaks (isolated and non-isolated MSLB, MSH break, failures of steam dump valves)
- primary to secondary side leakages (SG heat exchange pipes rupture, PRISE with collector cover lift-up)
- other PTS related IE (such as inadvertent opening/stuck open of PRZ SV, false actuation of HA, HPIS or make-up systems leading to over-pressurization of primary side, feed & bleed by primary side)

Based on the partner's responses, it can be pointed out that among the LOCA accidents most representative ones are medium (MB) and large breaks (LB) LOCAs. Small breaks (SB) LOCAs of primary system are less representative than the LB and MB LOCAs from the PTS point of view. As for PRISE accidents, less detailed description (in comparison with LOCA) was provided in Table 8 in some cases. Nevertheless, some partners (in particular IPP, LUT) noted that it is expedient to perform also the analyses for rupture of several steam generator pipes and the collector cover lift-up, excluding the rupture of one SG heat exchange pipe. In the area of secondary leaks, some partners did not indicate the necessity of MSLB analysis (KIWA) or mentioned that large secondary breaks can be covered by LOCA (GRS) and have small or negligible contribution to PTS (OCI). As for other transients, the most unfavourable contribution, from the PTS point of view, are usually obtained in transients with PRZ SV failure (inadvertent opening/stuck open with reclosure) and feed & bleed by primary side accidents. Some partners (UJV, BZN, LUT, SSTC) also noted the necessity to analyse transients with false actuation of primary injection systems (HPIS, HA, make-up). The most common place of break location in case of LOCA is cold leg. At the same time, for large and double-ended breaks (DEB) hot leg is also used. PRISE accidents are more limited in terms of leak locations, therefore this information was not detailed in the report. Secondary leaks (MSLB) are covered by various steam line breaks (before MSIV, between MSIV and check valve, etc.) and main steam header break, which define break locations. As for NPP operational state only a few partners (UJV, IPP, JSI, SSTC) provided detailed description of PTS scenarios. It can be seen that PRISE and most of LOCA scenarios are analysed in the zero power (hot mode) of the NPP unit, which is determined by less coolant heat up during transients. At the same time some MSLB transients, large LOCA and failures of PRZ SV are also considered at full power.

Table 7: Summary of Partner Codes and Methodologies.

Partner	Methodology	Codes	Systems and Components to be Modelled	Verification and Validation
UJV	Standalone systems code -> Standalone CFD code	RELAP5	All important systems of the NPP are modelled. For downcomer 2D nodalisation is used	The 2D model of DC applied in RELAP5 modes was validated against more detailed full-2D/3D models of CATHARE and RELAP5-3D and later against CFD calculations. The FLUENT code was validated against tests from ROCOM facility. Also, a test of solution grid independence in typical mixing simulation, sensitivity of the results to the turbulence modelling and validation of CFD code ANSYS Fluent on mixing experiments in VVER reactor geometry were performed.
		ANSYS Fluent	Flow channels and solid walls of the following zones: cold legs of circulating loops, reactor downcomer and lower plenum. Models of cold legs with ECCS injections include loop seal and a simplified reactor coolant pumps (RCP)	
Framatome	Standalone systems code -> Mixing code	S-RELAP5	The entire primary-side coolant with most of the secondary-side coolant is simulated	The simulation of small-break LOCA with S-RELAP5 has been validated using experimental data from numerous research facilities. The validation of KWU-MIX has been performed by simulating the experiments in the UPTF facility, in addition to experiments at Creare and Battelle.
		KWU-MIX	Only the downcomer and lower plenum along with the cold legs and hot legs	
	Standalone CFD code as additional analysis	Not specified	Not specified	
PSI	Standalone systems code	TRACE	The complete primary side of the NPP and parts of the secondary side (steam generators and main steam line up to the turbine inlet valve) are modelled. Downcomer region modelled in cylindrical coordinates using a 3D component (in TRACE)	UPTF measurements were used to validate the RELAP5 and GRS-MIX coupled simulation for small-break LOCA scenarios.
	Standalone systems code + mixing code	RELAP5/TRACE + GRS-MIX	The complete primary side of the NPP and parts of the secondary side (steam generators and main steam line up to the turbine inlet valve) are modelled.	
	Standalone CFD code	ANSYS Fluent Star-CCM+ OpenFOAM	Cold leg, downcomer region and lower plenum	

Partner	Methodology	Codes	Systems and Components to be Modelled	Verification and Validation
IPP	Standalone systems code -> Mixing code	RELAP5	All important systems (complete primary side and partially the secondary side). The reactor is modelled in quasi-3D approximation and has 12 sectors in downcomer.	The RELAP 5 model verification and validation (V&V) was performed on the example of the transient process caused by the non-closing of the Pressurizer Valve (Unit #3 of Rivne NPP). Also, as a validation data for abnormal operation conditions of Unit #5 of Zaporizhzhya NPP were used.
		GRS-MIX	The sector with injection of cold emergency water is considered	
	Standalone CFD code *as additional analysis	ANSYS Fluent/CFX	Models for calculation the mixing effects in pipelines, taking into account reverse flows. Model for calculation the mixing in downcomer is under development.	
KIWA	Standalone systems code	RELAP5	Computations of separate components, integrated scale facilities and the whole PWR reactor. UPTF facility model.	Verification and validation (V&V) of the PTS specific case has not been conducted by our organization, i.e., no V&V specific for PTS was conducted.
GRS	Systems code + mixing code	ATHLET+ integrated ECC-MIX	System models for PTS analysis have included all major components in the primary circuit. The thermo-hydraulic model of the primary circuit consists of a closed loop. On the secondary side the steam generator is the minimum thermo-hydraulic modelling requirement based on internal conventions.	Numerous V&V based on experimental results of the UPTF-TRAM (C1/C2) for thermo-hydraulic results and the development of the mixing code GRS-MIX. Further GRS participated in several benchmark activities, e.g., FALSIRE and RPV PTS ICAS focused mainly on structural mechanical aspects of PTS analysis.
	Systems code -> Mixing code	ATHLET -> GRS-MIX		
	Standalone CFD code	Not specified		
BZN	Standalone systems code -> Mixing code	RELAP5, ATHLET	All major components for both primary and secondary plant systems are included in the model. The downcomer model was revised and divided into six azimuthal sectors and four axial volumes.	No specific V&V was made.
		REMIX	-	
JSI	Standalone systems code	RELAP5, TRACE	In RELAP5 system code all main systems and components of power unit are modelled (detailed description in paragraph 4.1.1) The one-dimensional TRACE plant input model was obtained from the RELAP5/MOD3.3 plant input deck. Additionally, three-dimensional RPV model (25 axial levels, 4 radial rings and 6 azimuthal sectors with an angle of 60 degrees) was created in TRACE.	The RELAP5 input model has been thoroughly validated for thermal-hydraulic safety analyses. No PTS specific verification and validation of the PTS methodology has been done.

Partner	Methodology	Codes	Systems and Components to be Modelled	Verification and Validation
IRSN	Systems code + mixing code	CATHARE/TDA/CICLAMEN chain	All major components for primary and secondary systems are included in the CATHARE model. 4 zones in the downcomer defined for CICLAMEN.	CATHARE is validated for LOCA simulations. TDA is validated against scaled experimental data.
	CFD code (in framework of R&D studies)	Code_Saturne/ Syrthes coupling or Neptune_CFD	The geometry represents a third of a PWR pressure vessel (Code_Saturne/Syrthes) or a simplified geometry as Topflow-PTS moke-up (Neptune_CFD).	Experimental data from Topflow-PTS is available.
LUT / Fortum	Standalone systems code -> Mixing code	Apros	The model covers modelling of all the main primary and secondary circuit systems, primary circuit auxiliary systems and limited scope of secondary circuit auxiliary systems. RPV vessel is divided into eight sectors azimuthally Axially each RPV sector is divided into a number of stacked-up nodalisation layers. RPV calculation nodes are connected to form 2D nodalisation scheme of RPV.	Codes are constantly V&V according to the established best practice. Codes are tested on a number of cases specified in V&V matrix, which cover local or integral phenomena that are important to PTS analyses.
		REMIX-LOVIISA		
SSTC	Standalone systems code	RELAP5	Model includes all important systems of the primary and secondary side of NPP. Depending on the task a four-sector model of reactor or a simplified one can be used. At the same time, both models contain a detailed downcomer, which consists of 12 vertical sectors (annulus type) with cross-flows.	V&V of the RELAP5 models is based (in most cases) on the simulation of incident at Unit 3 of Rivne NPP. As for GRSMIX, the code was verified and validated by the developer (GRS GmbH).
	Systems code + mixing code	GRS-MIX	Model is presented as a wide sector of downcomer with cold leg, connected to ECCS train, which supply cooling water.	
JAEA	Standalone systems code	RELAP5	A model of the PWR system including major components for both the primary and secondary plant systems and the nodalisation referring to the model of the LSTF system has been developed. The reactor vessel internals were modelled, such as core, downcomer, upper head, upper plenum, lower plenum, and core bypass are modelled. The downcomer was modelled with finely-divided nodes.	Comparisons of fluid temperature distributions (e.g. in downcomer and cold leg) between the experiments and post-test calculations under ECCS water injection during SBLOCA have been carried out in some OECD/NEA international joint projects, such as ROSA (rig-of-safety assessment) projects through the experiments using the JAEA's LSTF (large-scale test facility) as PWR accident simulator.

Partner	Methodology	Codes	Systems and Components to be Modelled	Verification and Validation
OCI	Standalone systems code	RELAP5	Model represents the power plant in detail and include all major components for both the primary and secondary plant systems. The downcomer model uses a two-dimensional nodalisation and is divided into six azimuthal regions for each plant	Existing experimental databases were reviewed, including integral system tests in the Loss-of-Fluid Test (LOFT) facility and the Rig of Safety Assessment (ROSA), as well as full-scale tests in the Upper Plenum Test Facility (UPTF), and reduced-scale mixing tests at Creare, Purdue University, and Imatron Voimy Oy (Finland)

Table 8 Summary of partner responses on accident scenarios, methodologies and assumptions for PTS analysis

Partner	PTS scenarios			Methodology	Basic assumptions that might affect results of analysis
	IE	Break location / ECCS configuration	Operational state		
UJV	LOCA: SB (DN 32, 60 mm) MB (DN 125, 210 mm) LB (DN 300 mm) LB DEGB (2x850 mm) Interfacing MSLB	Cold leg / max & min* Cold leg / max & min Hot & Cold leg / max & min -** / max close to SG / - upstream of MSIV / - between MSIV and MSH / - downstream of MSH / - MSH / -	zero power full / zero power full power zero power full/zero power full/zero power zero power full/zero power	1. Single-phase IE (MSLB, PRZ SV open, PRISE, SB-LOCA etc.): system code (RELAP5) + CFD (ANSYS Fluent) mixing 2. Two-phase EI (MB-LOCA, LB-LOCA): system code (RELAP5 or RELAP5-3D) with 2D modelling of downcomer	Too many to list here.
	Inadvertent opening of steam dump to atmosphere / condenser PRISE: 1,3 pipes rupture collector cover lift-up Inadvertent opening of PRZ SV (and its reclosure) Inadvertent actuation of HPIS Make-up system malfunction leading to increase of RCS inventory Feed & bleed by primary side Inadvertent start of HA injection	- / - - / max - / max & min - / max & min - / - - / - - / - - / -	zero power zero power zero power full/zero power various initial regimes - - -		
Fra-G	LOCA MSLB Stuck-open PRZ SV	- / -	-	Standalone system code (S-RELAP5) + mixing code (KWU MIX) / CFD calculation (part of additional analysis)	-
PSI	LOCA (SB, MB, LB) PRISE (SG tube rupture) Stuck-open PRZ SV MSLB	Hot & cold leg / - - / - - / - - / -	-	Standalone systems code (TRACE/RELAP5) + mixing code (GRS-MIX). Additionally CFD study (ANSYS Fluent, Star-CCM+)	-

Partner	PTS scenarios			Methodology	Basic assumptions that might affect results of analysis
	IE	Break location / ECCS configuration	Operational state		
IPP	LOCA: (DN 32, 279 mm) LB DEGB (2x850 mm) MSLB PRISE: rupture of 3 SG tubes collector cover lift-up Inadvertent opening of PRZ SV with reclosure	- / max & min hot leg / min close to SG / min - / max & min - / max & min - / -	zero/full power full power full power zero power zero power -	Standalone systems code (RELAP5) + mixing code (GRS-MIX) for the selected scenarios	-
Kiwa	LB LOCA SB LOCA at steam generator	- / -	-	Standalone systems code (RELAP5)	Conservative assumptions
Tecnatom	MB LOCA MSLB, etc.	- / -	-	-	-
GRS	LOCA MSLB Inadvertent opening of PRZ SV with reclosure	- / -	-	Systems code (ATHLET) with integrated mixing module (ECC-MIX); Systems code (ATHLET) with mixing code (GRS-MIX) Standalone CFD study	-
BZN	LOCA: DN 35, 73, 90, 111, 233, 492 mm DEGB (492 mm) MSLB PRISE (SG collector cover lift-up) Inadvertent opening of PRZ SV with reclosure Spurious operation of the SI	Hot & Cold leg / - Inside & outside the containment / - - / - - / - - / -	-	Standalone systems code (RELAP5, ATHLET) + mixing code (FLOOD and PLANE_PLUME_DECAY routines of the REMIX code)	-
IRSN	LOCA: SB, DN 3 to 6'' Additional studies performed for: MB-LOCA LB-LOCA MSLB	Several configurations were analysed (size and location of the break varied, as well as the set of hypotheses retained)	-	Systems code + mixing code (CATHARE/TDA/CICLAMEN chain) CFD code (in framework of R&D studies)	Conservative assumptions
JSI	MSLB (SB, LB, steam dump valves fail) PRZ PORV size break	- / - - / -	full / zero power zero power	Standalone systems code (RELAP5, TRACE with 3d vessel for mixing)	-

Partner	PTS scenarios			Methodology	Basic assumptions that might affect results of analysis
	IE	Break location / ECCS configuration	Operational state		
	PRISE (SG tube rupture) LOCA (DN 5.08, 6.35 cm) Feed & bleed by primary side Overfeed with auxiliary feedwater	- / - hot leg / - - / - - / -	full / zero power full / zero power full power -		
LUT / Fortum	LOCA (SB, LB) PRZ SV open with reclosure PRISE (multiple SG pipe rupture) MSLB Inadvertent actuation of HPIS or make-up system External RPV overcooling	Hot leg / - - / -	full power, zero power, heat-up etc.	Standalone systems code (Apros) + mixing code (REMIX-LOVIISA)	-
SSTC	LOCA: DN 10, 32, 63, 279 mm DN 105, 125, 209 mm LB LOCA DEGB (2x850 mm) MSLB Inadvertent opening of steam dump valve to atmosphere/condenser PRISE (rupture of 1 or 3 tubes, SG collector cover lift-up) Inadvertent opening of PRZ PORV with/without reclosure Inadvertent actuation of HPIS Feed & bleed by primary side	Cold leg / max & min Cold & hot leg / max & min Cold & hot leg / max & min SG side / min Between MSIV and check valve / min MSH / min - / min - / max & min - / max & min - / - - / -	zero power full / zero power full / zero power full / zero power full power zero power full / zero power zero power full / zero power zero power full power	Standalone systems code (RELAP5) + mixing code (GRS-MIX)	Conservative assumptions: - decay heat; - instrumentation measurement errors; - characteristics of ECCS pumps; - simplified modelling of HPIS without recirculation from the sump; - temperature of injected water
JAEA	LOCA (LB, MB, SB) Stuck-open valve events MSLB	- / -	-	Standalone system code (RELAP5)	-

Partner	PTS scenarios			Methodology	Basic assumptions that might affect results of analysis
	IE	Break location / ECCS configuration	Operational state		
OCI	LOCA Stuck-open valves on the primary side (with reclosure) Feed & bleed Steam generator tube rupture MSLB and stuck-open valves on the secondary side (has small or negligible contribution for PTS)	- / -	-	Standalone system code (RELAP5)	-
* "min" corresponds to ECCS configuration with minimum number of available ECCS trains (for instance, WWER minimum configuration of ECCS is 1/3 HPIS + 1/3 LPIS + 2/4 HA and additionally no make-up system), "max" means the maximum number of available ECCS trains; ** "– "means that data is absent or not clearly defined.					

6.4.4   Best-Estimate Plus Uncertainty (BEPU)

Table *9* shows a brief summary of the partner responses, particularly focusing on each partner's BEPU analysis methodology and any prior application to PTS analysis.

For general thermal-hydraulics applications, most countries have developed methodologies for uncertainty quantification. For the most part, this includes forward propagation of uncertainties and, in some cases, methods for calibration of prior uncertainties have been demonstrated. The general approach to selecting the influential parameters is through a phenomena identification and ranking table (PIRT). In some cases, the influential parameters are further filtered using sensitivity analyses. Uncertainty distributions are commonly derived through a combination of literature review and expert judgement. In some cases, methodologies for adjusting/calibrating the input uncertainties based on available separate-effects tests have been developed and demonstrated. The most common approach to forward propagation of uncertainties is the use of Wilks formula, which allows one to identify 95% confidence intervals with a relatively small number of random samples or code runs. Other approaches are, however, also used, e.g., Latin hypercube sampling and sampling of surrogate models.

In the specific area of PTS analysis, however, UQ methodologies are not well established, with relatively few countries having considered this. The US has perhaps the most comprehensive assessments of PTS that include UQ, which was used as a technical basis for revising the US NRC's PTS screening limits. In Europe, Germany appears to be the only country to have attempted best estimate plus uncertainty analysis for PTS. Both GRS and Framatome have derived input uncertainty distributions based on experimental data, literature review and expert judgement and GRS has applied this for PTS analysis.

6.4.5   Multi-Physics Thermal-Hydraulics/Fracture Mechanics Analysis

As in the case of best-estimate plus uncertainty (subsection 6.4.4), the passing of PTS thermal-hydraulics uncertainties to downstream structural mechanics codes is largely unexplored. In the US, this was done as part of the PTS Re-Evaluation project. Germany (GRS) has an established methodology based on the SUSA framework.

6.4.6   Human Interactions

In many cases, the effect of operator actions has been included in PTS analyses. These are typically at fixed times; UJV, for example assume realistic timing of operator actions, while IRSN and PSI select the time in accordance with DBA guidelines, and SSTC assume conservative timing of actions. The impacts of failure of the operator to successfully complete an action or the time required to complete the action are relatively unexplored in Europe. In the US, human reliability analysis (HRA) was included in the PRA portion of the PTS Re-Evaluation project. As an example, **Table *10*** listed the several general classes of human failures identified that were incorporated in the PRA model. **Table *10*** also details which of the primary functions was most affected by those failures.

This is an area where further research is needed within the context of the APAL and future projects, perhaps learning from efforts outside of Europe. In the case of operator actions, defining conservative assumptions for operator actions may be non-trivial; in some cases, the failure to initiate an event may be non-conservative, while initiating an action early could be conservative. Sensitivity analyses or more advanced uncertainty quantification, in which the uncertainty in operator actions is accounted for, are needed.

Table 9: Summary of Partner Status of BEPU for PTS.

Partner	Avail. BEPU Method	Parameter Ranking and Sensitivity Analysis	Derivation of Uncertainty Distributions	Application to PTS	V&V Status
UJV	Yes			Not yet applied (conservative input data only) Conservative only	
Fra-G	Yes	PIRT		Not yet applied	
PSI	Random sampling	PIRT Morris and Sobol SA methods	Open literature Expert judgement Bayesian calibration	Not yet applied	Demonstrated for core reflood
IPP	None	None			
Kiwa	Dakota	SUSA code		Conservative only	
Tecnatom					
GRS	GRS-Method	Open literature PIRT SUSA code	Open literature and prior experience	Applied to 4 loop PWR	PTS-specific verification based on ICAS
BZN	None				
IRSN	Random sampling	Sobol and FAST SA methods	Experimental data Inverse UQ Expert judgement	Not yet applied	
JSI	CSAU method and in-house tool	PIRT In-house SA tool		Not yet applied	SB-LOCA and LB-LOCA
LUT / Fortum	None				
SSTC	None	None	Open literature Expert judgement	Conservative only	
JAEA	Random Sampling	PIRT	Experimental data	Not yet applied	LSTF
OCI		PIRT Sensitivity analyses with binning	Experimental data Expert Judgement Statistical methods Open literature	PTS re-evaluation project	

Table 10: General Classes of Human Failure Considered in PTS Re-evaluation, from [17].

Primary Integrity Control	Secondary Pressure Control	Secondary Feed Control	Primary Pressure / Flow Control
I. Operator fails to isolate an isolable LOCA in a timely manner (e.g. close a block valve to a stuck open PORV) II. Operator indices a LOCA (e.g., opens a PORV) that induces/enhances a cooldown	I. Operator fails to isolate a depressurisation condition in a timely manner II. Operator isolates when not needed (may create a new depressurisation challenge, lose heat sink…) III. Operator isolates wrong path/SG (depressurisation continues) IV. Operator creates an excess steam demand such as opening turbine bypass/atmospheric dump valves	I. Operator fails to stop/throttle or properly align feed in a timely manner (overcooling enhanced continues) II. Operator feeds wrong (affected) SG (overcooling continues) III. Operator stops/throttles feed when inappropriate (causes underfeed, may have to go to feed and bleed possibly causing overcooling)	I. Operator does not properly control cooling and throttle/terminate injection to control RCS pressure II. Operator trips RCPs when not appropriate and/or fails to restore them when desirable III. Operator does not provide sufficient injection or fails to trip RCPs appropriately (failure to provide sufficient injection is modelled as leading to core damage; thus, such sequences are not PTS-relevant)

6.5   Recommendations

6.5.1   Experimental Activities and Validation

The main motivation for new experimental campaigns related to PTS is the better quality of data to be obtained by using modern sophisticated measurement techniques compared to the quality of data in the historical experiments conducted with traditional and often limited instrumentation. In particular, local measurements of void fraction, turbulent quantities and interfacial area in different geometries with precise, two-phase adapted and up-to-date experimental measurements techniques are needed.

6.5.2   Best estimate Plus Uncertainty

Several countries/partners admitted that the application of conservative assumptions and a generally conservative approach have large impact on the results of PTS analysis. This highlights the need to move towards BEPU methods in the future. In the area of best estimate plus uncertainty, many countries have established methodologies for general thermal-hydraulics problems. The general approach to selecting the influential parameters is through a PIRT. In some cases, the influential parameters are further filtered using sensitivity analyses. Uncertainty distributions are commonly derived through a combination of literature review and expert judgement. In some cases, methodologies for adjusting/calibrating the input uncertainties based on available separate-effects tests have been developed and demonstrated. The most common approach to forward propagation of uncertainties is the use of Wilks' formula. Other approaches are, however, also used, e.g., Latin hypercube sampling and sampling of surrogate models. Despite relatively well-established methods, it seems that few countries have applied BEPU for PTS analysis. Likewise, few partners have performed analysis of propagation of thermal-hydraulics uncertainties to downstream structural mechanics codes.

6.5.3   Human Interactions

On the topic of human interactions, and how these can affect PTS, most partners do include human interactions in their analyses, however these are generally at fixed times. The impact of failure of the operator to successfully complete an action or the time required to complete the action are relatively unexplored in Europe. This is an area where further research is needed within the context of the APAL and future projects, perhaps learning from efforts outside of Europe.

7 State-of-the-art of probabilistic PTS analysis and relevant statistical tools

7.1 Introduction

First application of probabilistic pressurized thermal shock (PTS) analysis was done in the US in 1980s and revised in the next decades. The risk-informed technical bases generated by the US Nuclear Regulatory Commission (USNRC) PTS Re-evaluation Project from 1999 through 2008 (using the advanced FAVOR) resulted in the promulgation of the Revised PTS Rule, 10 CFR §50.61a in February 2010. At the time of the release of the Revised PTS Rule by the USNRC in 2010, the FAVOR code represented the state of the art in the US for probabilistic assessments of the structural integrity of nuclear reactor pressure vessels (RPVs) challenged by PTS transients (ca. 2004).

In the EU the use of probabilistic PTS analysis in the scope of structural integrity assessment became of interest in the last two decades. However, current state-of-the-art for PTS analysis is the use of deterministic assessment based on conservative boundary conditions and methods for safety margin quantification. Nevertheless, also in the EU methods and tools used for probabilistic PTS analysis have been further developed and enhanced.

The main conclusions of Task 1.4 *State-of-the-art of probabilistic PTS analysis and relevant statistical tools* are summarized in this section. It may have an impact on the work to be performed in WP4 "*Probabilistic margin assessment*" and on the definition of the best-practice for advanced PTS analysis in WP5 "*Definition of best-practice for advanced PTS analysis*".

7.2 Overview

A collection of experience on probabilistic PTS analysis and on tools and software currently used for probabilistic assessments has been performed to identify the state-of-the-art. Therefore, a questionnaire was prepared to describe the currently used tools and software for probabilistic PTS analysis by the European and international partners.

Moreover, recommendations and conclusions were drawn as well as possible improvements identified for use of probabilistic PTS analysis.

7.3 Description of activities

To get an overview of the different types of assessment for probabilistic PTS analysis used by the partners a questionnaire was prepared, discussed among the partners and distributed for response. This questionnaire of Task 1.4 focuses on the following points:

- Methods for calculation of probability including convergence criterion
- Methods for sampling of distributed parameters
- Summary of distributed input data and basis for distribution parameters
- Consideration of the whole spectrum of PTS scenarios
- Scope of the assessment and treatment of RPV loading
- Events considered (Initiation, Failure, Arrest)
- Fracture mechanics models used
- Overview of performed applications

In total responses from 12 partners were obtained:

Country	Partner	Contributing Author
Czech Republic	UJV	Miroslav Posta, Vladislav Pistora and Katarina Siskova
Germany	Framatome	Ralf Tiete and Sebastien Blasset
Switzerland	PSI	Diego Mora
Ukraine	IPP-CENTRE	Maksym Zarazovskii and Yaroslav Dubyk

Country	Partner	Contributing Author
Sweden	KIWA	Peter Dillström
Spain	Tecnatom	Carlos Cueto-Felgueroso
Germany	GRS	Klaus Heckmann, Jürgen Sievers, Stefan Wenzel and Christoph Bläsius
Hungary	BZN	Judit Dudra and Szabolcs Szávai
Slovenia	JSI	Oriol Costa, Leon Cizelj and Andrej Prošek
France	IRSN	Jerome Roy and Bao Le Minh
Japan	JAEA	Jinya Katsuyama
USA	OCI	B. Richard Bass and Paul T. Williams

7.4   Main topics

7.4.1   Description of the tool/software for probabilistic assessment

Table *11* below lists the tools/software used by partners for probabilistic PTS analysis.

Table 11: Overview of tool/software for probabilistic PTS analysis.

Partner	Tool/Software	Remarks
UJV	PROVER (in-house)	Based on FAVOR and adjusted for VVER
FRA-G	In-House	modular based
PSI	FAVOR	v16.1
IPP	SIF-Master (in-house)	new version under development
KIWA	ISAAC	Probabilistic part = in-house
Tecnatom	FAVOR	v16.1
BZN	In-House	under development
JSI	FAVOR	v16.1
IRSN	In-House	under development
OCI	FAVOR	v16.1
JAEA	PASCAL	v4
GRS	PROST	

Complementary to the responses to the questionnaire, additional information has been requested and delivered by the partners:

- Why the FAVOR code results in CPI per Monte Carlo run
- Aleatory and epistemic uncertainties
- Description of FORM/SORM
- Analytical formula to account for plume effect

Moreover, a simple benchmark has been performed to demonstrate functionality, advantages, limitations and convergence of different probabilistic methods and influence of random number generators.

Czech Republic (UJV): PROVER software

a) For the probabilistic PTS assessments, the in-house software named PROVER is used. The program is implemented in accord with the Czech standard Normative Technical Documentation of Association of Mechanical Engineers, Section IV [8]. PROVER is based on FAVOR code, but it was adjusted for the VVER RPVs assessment. It consists of three main modules: VERLOAD, VERPFM and VERPOST. VERLOAD is used for thermal and mechanical FEM calculations on 1D mesh, VERPFM is used for probabilistic fracture mechanics calculations and VERPOST is a post-processing module which calculates the

frequency of fast fracture initiation (FI) as a final result of the assessment. Some of the flaw distribution parameters used in VERPFM module are generated a-priori in a standalone VERFDF module.

b) The PROVER code utilizes the Monte Carlo method for uncertainty modelling. The final result of the PTS assessment is the mean and the 95% quantile of FI. There is no convergence criterion built directly in the PROVER code, but the necessary number of Monte Carlo trials can be assessed by the user from the graphical evolution of the mean and 95% quantile of FI with respect to the number of Monte Carlo trials. Following the central limit theorem, the standard error of the FI mean can also be used as a reasonable measure of the results accuracy.

c) The standard [8] provides some guidance on crack arrest calculations in probabilistic assessment, but only the crack initiation is currently implemented in the PROVER code. A crack arrest model may be implemented in the future.

d) Sampling from random distributions is performed using the transformation method. Random numbers are initially sampled from the uniform distribution using the Mersenne Twister pseudorandom number generator. The random numbers are then transformed to values from other statistical distributions using the inverse transform method. Random samples from the standard normal distribution are generated using the Box-Muller transformation.

Currently, no variation reduction technique (like importance sampling) is implemented in PROVER. In other words, simple random sampling is used for all random parameters.

e) *Program Verification:* The VERLOAD module and accuracy of stress intensity factor (SIF) formulas implemented in the VERPFM module were verified against calculations performed by commercial FEM software Systus. Quality of random number generation and quality of generation of random samples from various statistical distributions were checked using quantile plots and statistical tests. Other parts of the software were checked by comparison of intermediate results with manual calculations. As PROVER is mostly implemented in Fortran, some parts of the program were later re-implemented in R-language for verification purposes.

Program Validation: The program was never validated on experimental data. Deterministic structural calculations (temperature and stress-strain fields, SIF calculation) were validated on problems from [64] benchmark. Probabilistic calculations were partially validated on tasks from [42] benchmark. Due to differences between the PROSIR definition and requirements in [8], the validation was possible only for the version of PROVER code modified for PROSIR tasks.

Germany (Framatome): In house tool

Framatome uses an in-house modular based EXCEL tool with routines and modules developed in Visual Basic code.

The main routine for calculation of initiation and failure probability is a Monte Carlo simulation. The main routine is used to calculate the initiation and failure probability for a single flaw (with distributed size) for a defined loading and embrittlement condition. Thus, a single stress and temperature distribution over wall thickness (usually from 3D FE calculation) in combination with a defined embrittlement state (e.g., RT_{NDT}) is taken into account in the main routine. Possible crack arrest will be considered but can be switched off if needed. The relevant methods and solutions (e.g., K_I solution or K_{IC}) are integrated as functions/modules and can be adopted due to specific application case. A flow chart for the main routine is presented in **Figure 25**.

The results for different types of flaws and different flaw locations (i.e., different loading and embrittlement conditions) can be combined to an overall RPV initiation and failure probability. This will be done by combination on several results from main routine within a post-procedure. The combination of results within the post-procedure is based on a defined flaw density distribution for assessed types of flaws. A flow chart of the post-procedure is given in **Figure 26**.
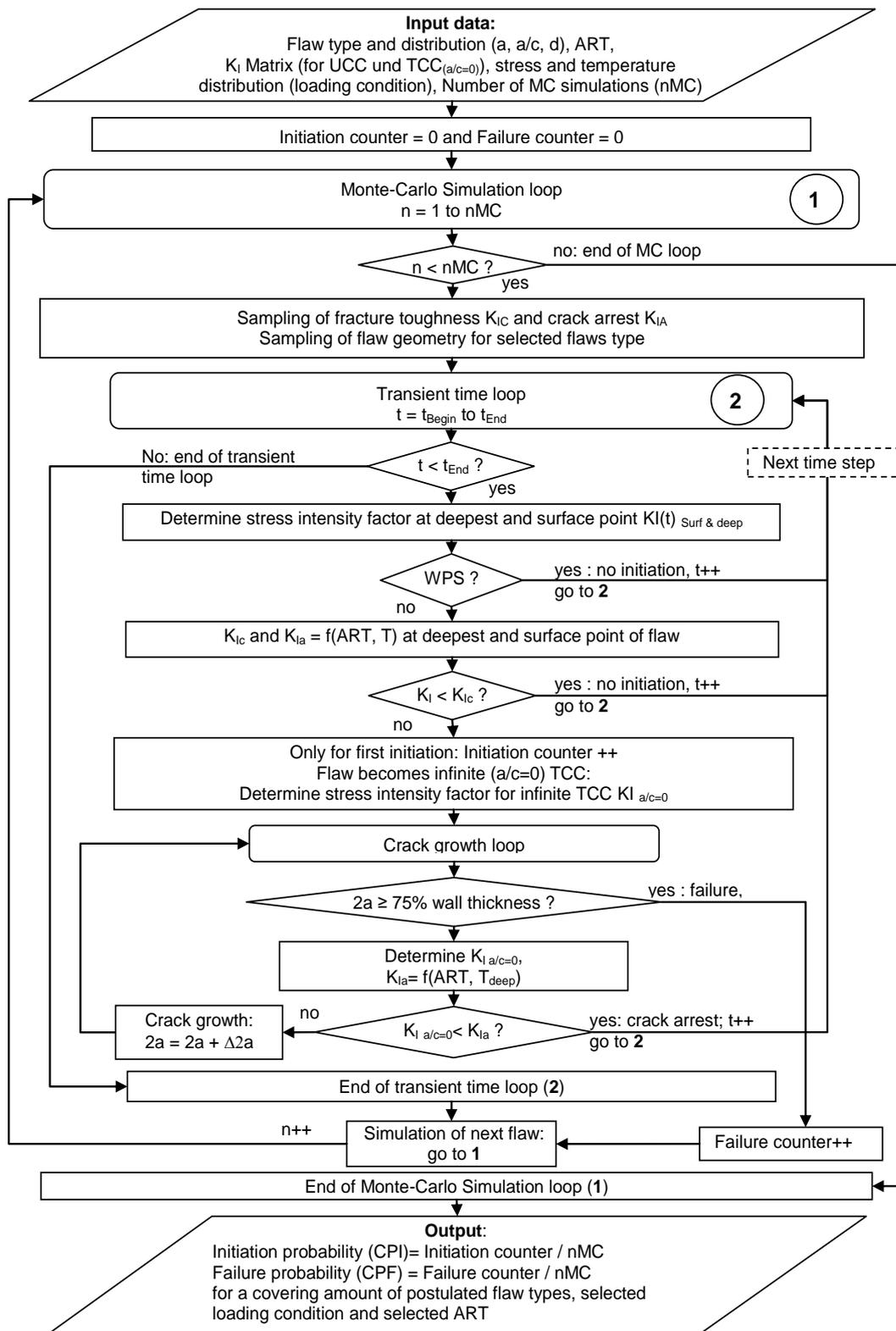
Figure 25: FRA-G in-house tool – Main routine.

The code of the in-house EXCEL tool has been verified. An explicit validation of several modules has been performed during the PROSIR benchmark, but in general we use individual methods and solutions that are validated to be appropriate for the case of interest. Moreover, it is common practice to use Monte Carlo simulations for calculation of initiation and failure probability.

An extension of the in-house code is foreseen to consider the K_{IC} as defined by the Master Curve as well as the $J_{0.2}$ as defined in ASME Code Case N-830 [176].
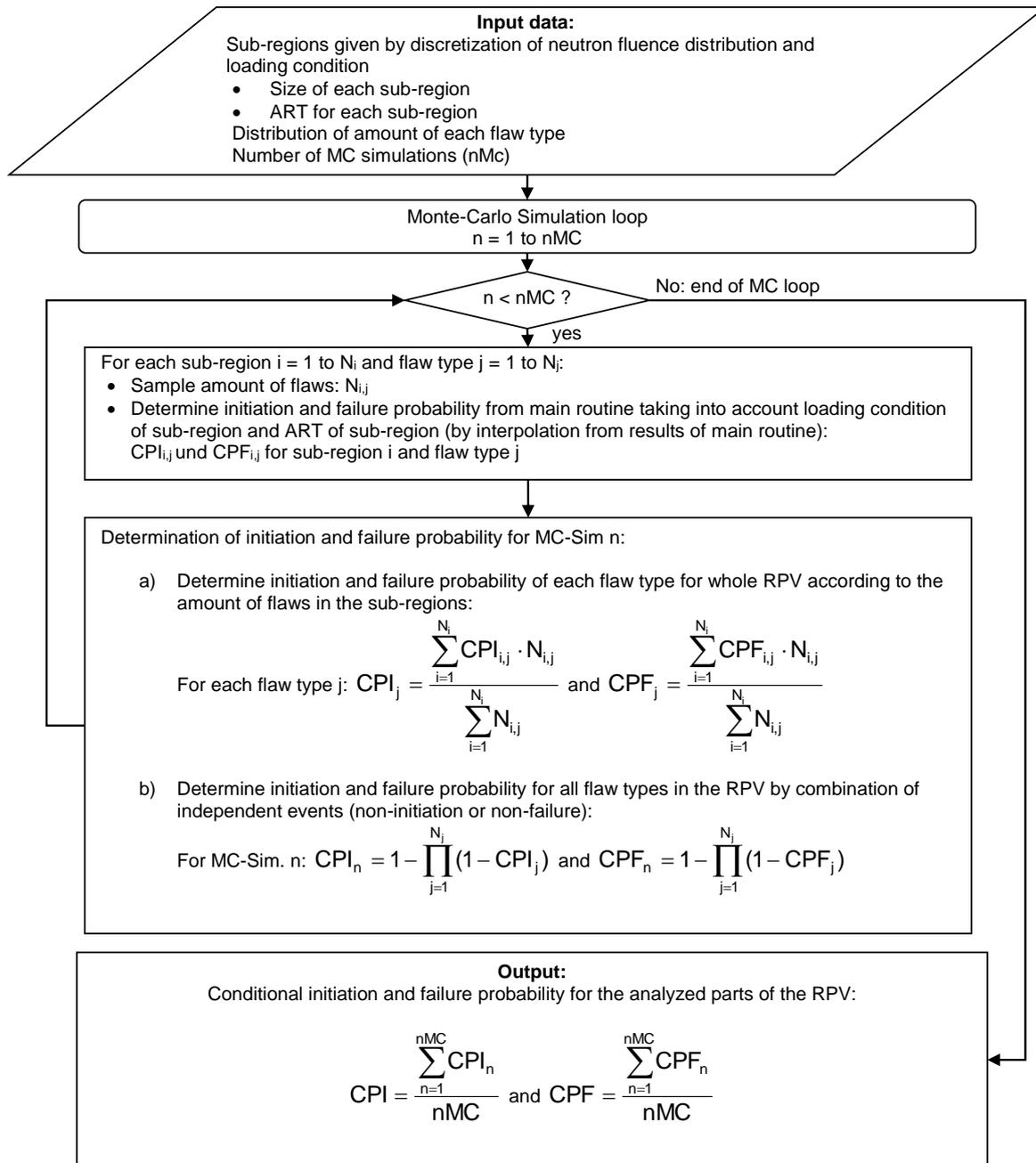
Figure 26: FRA-G in-house tool – Post-Procedure.

OCI, PSI, Tecnatom, JSI: FAVOR v16.1

Remark: The following description is compilation of OCI, PSI, Tecnatom and JSI responses.

OCI analyses a set of transients (provided to OCI by PRA experts) that represents a particular plant. These transients are identified using a PRA event-tree approach, in which many thousands of different initiating event sequences are "binned" together into groups of transients believed to produce similar TH outcomes. Judgments regarding which transients to put into which bin are guided by such characteristics as similarity of break size and similarity of operator action, resulting in bins such as "medium break primary system loss-of-coolant accidents (LOCAs)" or "Main Steam Line Breaks

(MSLB)". From each of the tens or hundreds of individual event sequences in each bin, a single sequence is selected and programmed into the Reactor Excursion and Leak Analysis Program (RELAP5) to define the variation of pressure, temperature, and heat transfer coefficient vs. time.

OCI then passes these TH transient definitions to the PFM code Fracture Analysis of Vessels – Oak Ridge (FAVOR) [13], [65], which estimates the conditional probability of through-wall cracking (CPTWC) for each transient. When multiplied by the initiating event frequency estimates produced by the PRA analysis, these CPTWC become through-wall-crack failure (TWCF) values, which, when rank-ordered, estimate the degree to which each bin contributes to the total TWCF of the vessel. At this stage many bins are found to contribute very little or nothing at all to the TWCF, and so receive little additional scrutiny. However, some bins invariably dominate the TWCF estimate. These bins are then further subdivided by partitioning the initiating event frequency of the bin and by selecting a TH transient to represent each part of the original bin. FAVOR is then used to analyse this refined model, and the bins that provide significant contributions to TWCF are again examined. This process of bin partitioning, and the selection of a TH transient to represent each newly partitioned bin, continues until the total estimated TWCF for the plant no longer changes significantly.

OCI employs the latest release of FAVOR, v16.1, which is composed of three computational modules (see Figure 27): (1) a deterministic load generator (FAVLoad), (2) a Monte Carlo PFM module (FAVPFM), and (3) a post-processor (FAVPost). **Figure 27** indicates the nature of the data streams that flow through these modules. The formats of the required user-input data files are discussed in detail in the FAVOR, v16.1, User's Guide [65].
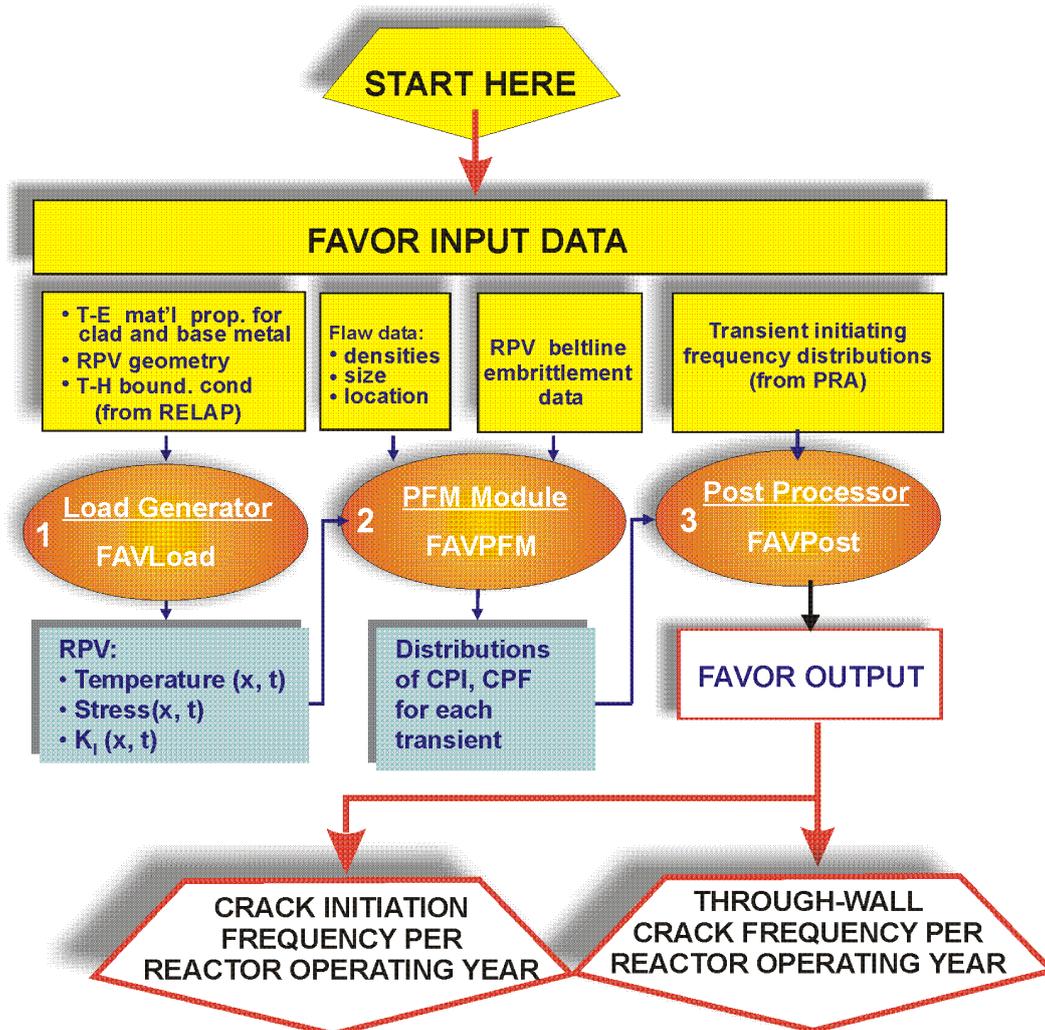

Figure 27: FAVOR data streams flow through three modules: (1) FAVLoad, (2) FAVPFM, and (3) FAVPost.

FAVLoad Treatment of RPV Loading

The functional structure of the FAVLoad module is shown in **Figure 28**, where multiple thermal-hydraulic transients are defined in the input data. For each transient, deterministic calculations are performed to produce a load-definition input file for FAVPFM. These load-definition files include time-dependent through-wall temperature profiles, through-wall circumferential and axial stress profiles, and stress-intensity factors for a range of axially and circumferentially oriented inner and external surface-breaking flaw geometries (both infinite- and finite-length).
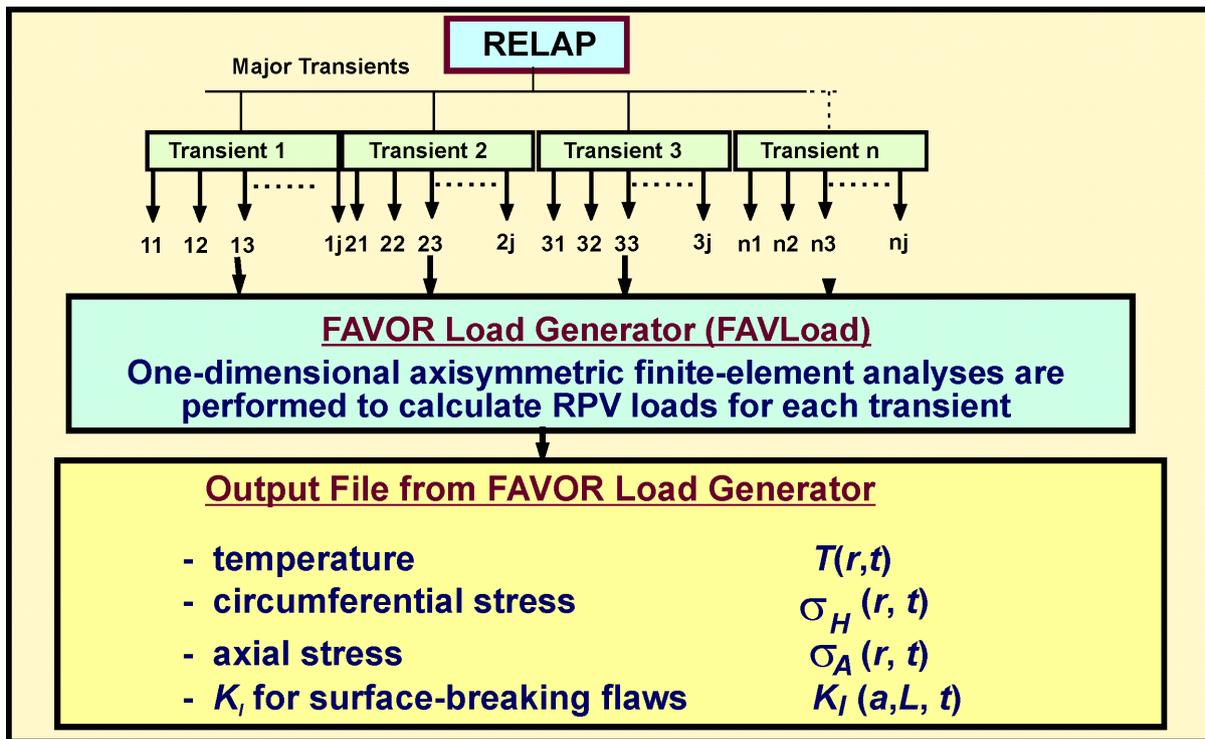
Figure 28: The FAVLoad module performs deterministic analyses for a range of thermal-hydraulic transients.

FAVPFM Treatment of Monte Carlo Fracture Mechanics

The functional structure of the FAVPFM module is shown in **Figure 29**. FAVPFM receives loading data determined by FAVLoad for a stack of TH transients along with flaw characterization data for pre-existing flaws embedded in rolled plates, forged rings, and welds. Data for pre-existing surface-breaking flaws in plates, forgings, and welds are also input. Radiation damage data in the form of an embrittlement map of material chemistry and fracture toughness parameters are also provided as input data.

Figure 30 presents a flowchart illustrating the essential elements of the nested-loop structure of the PFM Monte Carlo model – (1) RPV Trial Loop, (2) Flaw Loop, (3) Transient Loop, and (4) Time integration Loop. The outermost RPV Trial Loop is indexed for each RPV trial included in the analysis, where the number of RPV trials is specified by the user in the FAVPFM input stream.
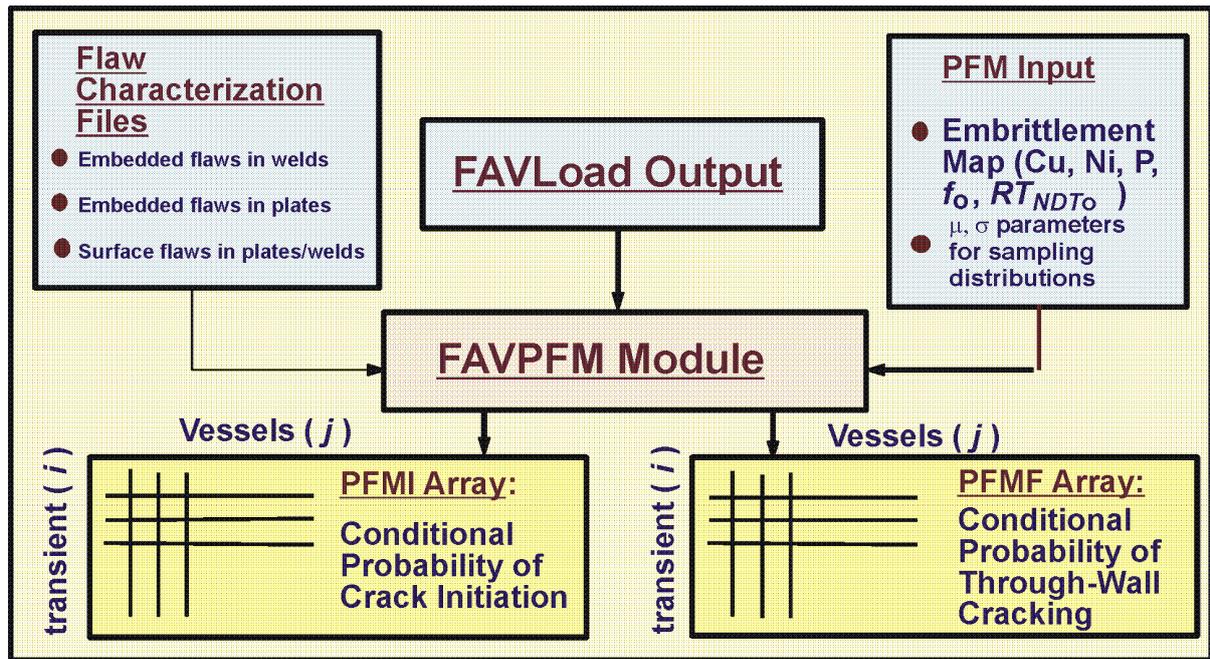
Figure 29: The FAVPFM module takes output from FAVLoad and user-supplied data on flaw distributions and embrittlement of the RPV beltline and generates PFMI and PFMF arrays.
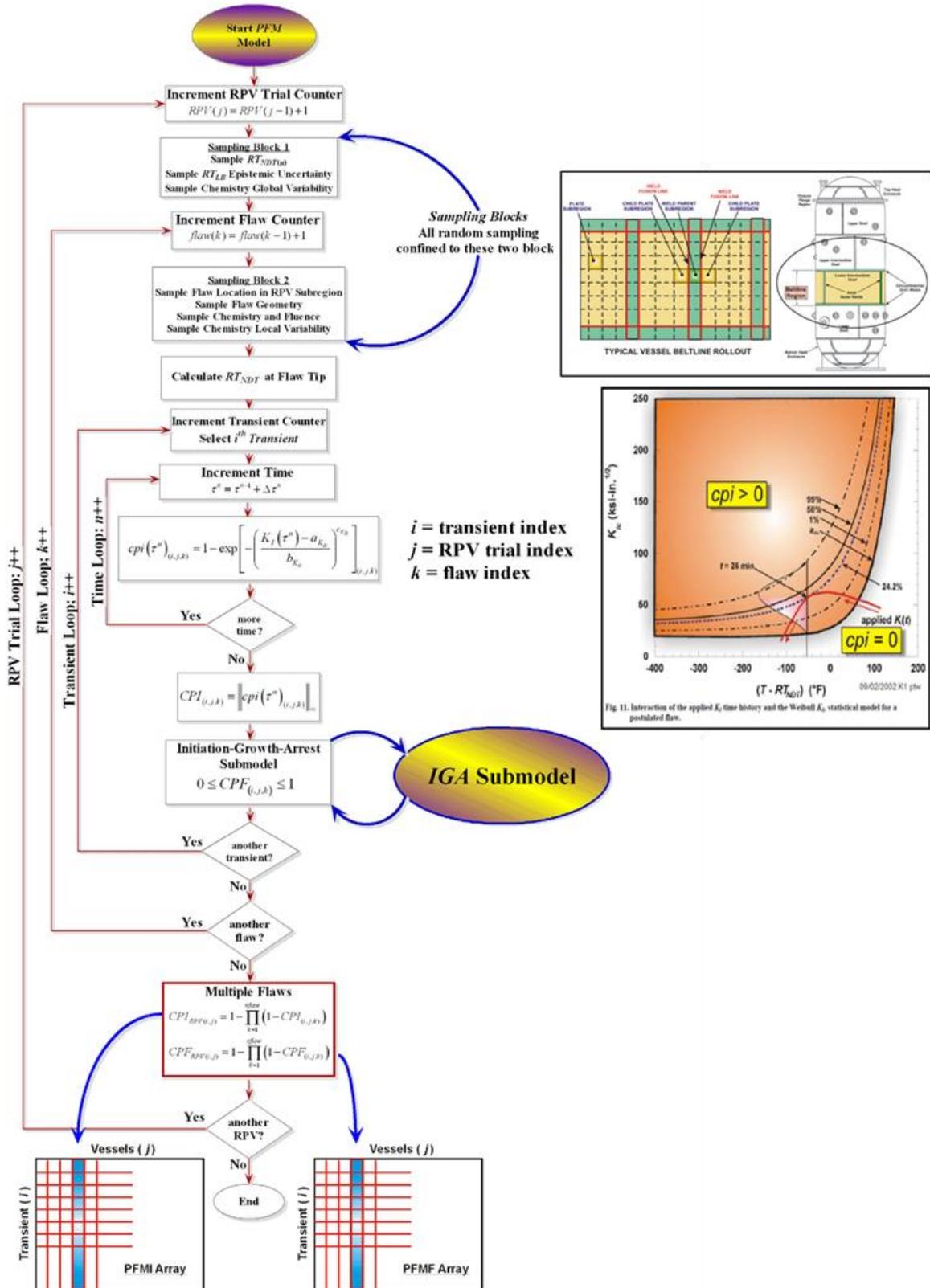
Figure 30: FAVPFM Module and interaction with IGA Submodel.

FAVPost Treatment of PRA

As shown in **Figure 31**, the FAVPost module combines the distributions of conditional probabilities of initiation and failure calculated by FAVPFM with initiating frequency distributions for all of the transients under study to create distributions of frequencies of RPV initiation of fracture and RPV failure by through-wall cracking.
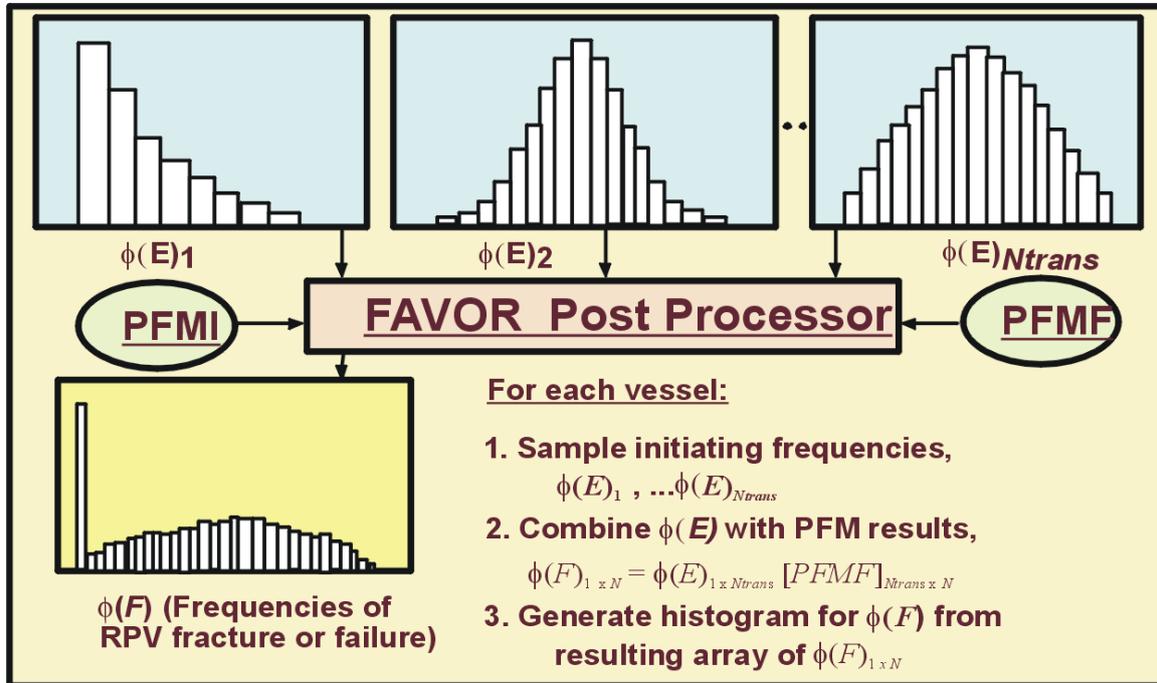
**Figure 31: The FAVPost module combines the distributions of conditional probabilities of initiation and failure calculated by FAVPFM with initiating frequency distributions for all of the transients under study to create distributions of frequencies of RPV initiation of fracture and RPV failure.**

Convergence of Monte Carlo Analysis

As shown in **Figure 32**, several metrics are used in FAVOR convergence studies, including tracking the running average and coefficient of variation for the conditional probability of vessel failure (CPF) by through-wall cracking. The FAVPost module is used to track the convergence of TWCF as a function of RPV realizations (see **Figure 33**) using the mean and higher percentiles.

Events Considered

All cracks (both surface-breaking and embedded) investigated by FAVOR are considered pre-existing manufacturing flaws. Crack initiation and growth by cleavage fracture, crack arrest of an advancing flaw, crack re-initiation and growth by either cleavage or ductile fracture, and crack re-arrest are fracture mechanics events treated by FAVPFM. Failure by through-wall cracking can occur by either net-section collapse of the remaining ligament or by flaw propagation to a user-defined fraction of the RPV wall thickness. Unstable ductile tearing is also a potential mode for vessel failure.
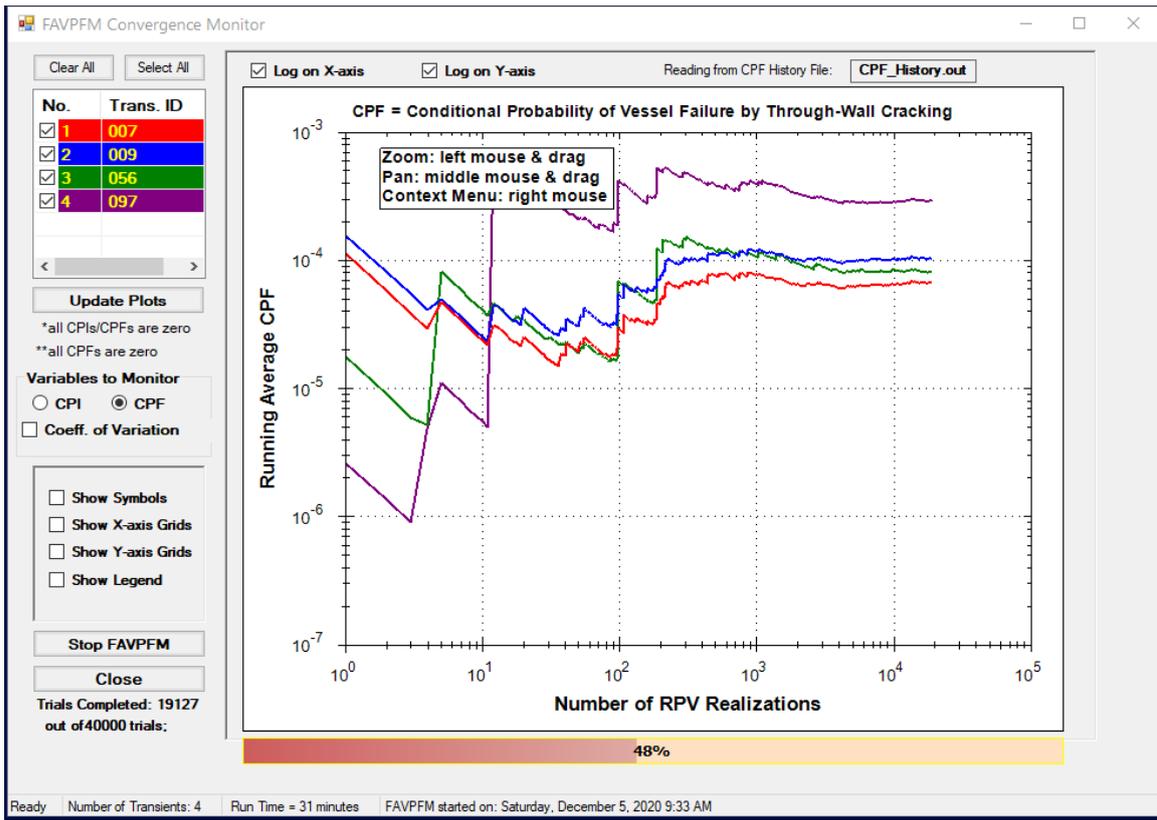
(a)
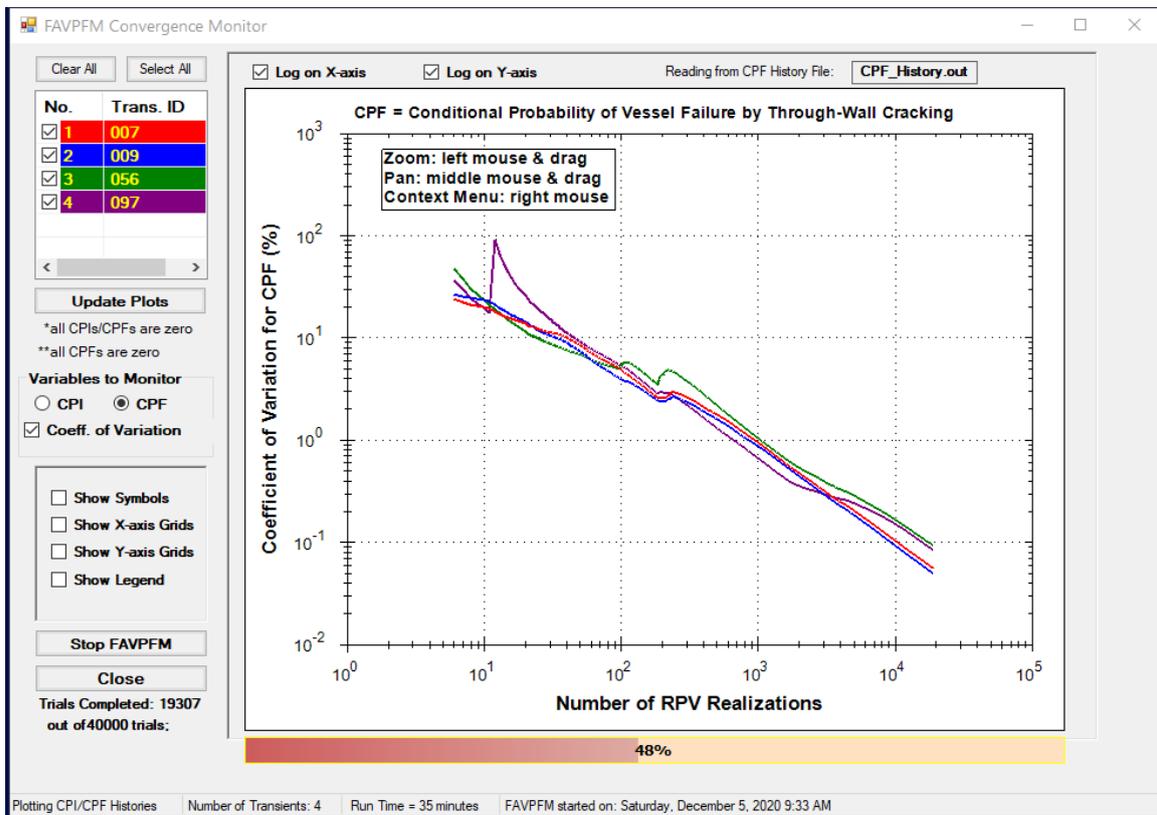
(b)

Figure 32: Tracking convergence as a function of RPV realizations: (a) running averages of CPF and (b) coefficient of variation of CPF for each transient.

113
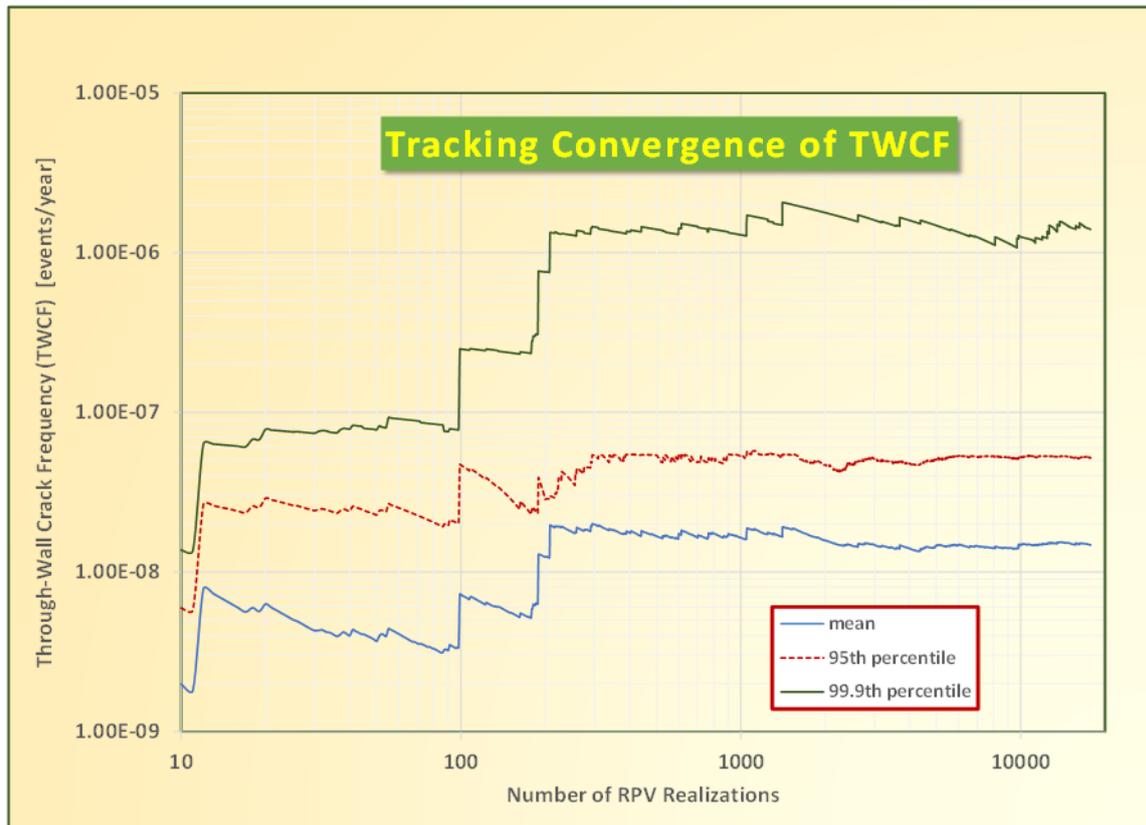
Figure 33: Tracking convergence of TWCF as a function of RPV realizations.

Assessed Phenomena

The following phenomena are simulated in a FAVOR analysis:

- temperature dependence of thermo-physical properties of clad and base metal of RPV wall
- warm pre-stress
- weld residual stress
- clad residual stress
- crack-face pressure loading
- cleavage initiation, re-initiation, and flaw advancement by brittle transgranular cleavage
- stable ductile tearing of an arrested flaw
- crack arrest
- net-section plastic collapse of remaining ligament leading to vessel failure
- unstable ductile tearing leading to vessel failure
- radiation embrittlement as a function of fast-neutron fluence, in-service time of RPV, temperature, and depth into wall (attenuation)

Distributed Input Data and Methods for Sampling

The uncertainty characterization and methods of sampling for all input data are described in detail in [65] [24].

Sampling methods are summarized in **Table 12**.

In FAVOR, the random number generator [66] [67] [68] is based on a composite of two multiplicative linear congruential generators using 32-bit integer arithmetic and has a reported theoretical minimum period of 2.3×10^{18}. This implementation was successfully tested by the HSST Program at ORNL for statistical randomness using the NIST *Statistical Test Suite for Random and Pseudorandom Number Generators* [69].

114

Table 12: Sampling methods used in FAVOR.

Sampling from a standard uniform distribution, U(0,1), is accomplished computationally with a Random Number Generator (RNG).
Sampling from standard normal distribution, N(0,1) uses the Forsythe's method
Sampling from a Two-Parameter Lognormal Distribution from a normal distribution with mean equal to the lognormal mean and standard deviation equal to the lognormal standard deviation.
Sampling from a Three-Parameter Weibull Distribution A random number is drawn from a uniform distribution on the open interval (0,1) and then transformed to a Weibull variate with the Weibull percentile function.
Sampling from a Two-Parameter Logistic Distribution A random number is drawn from a uniform distribution on the open interval (0,1) and then transformed to a logistic variate by the logistic percentile function.
Sampling from a Three-Parameter Log-Logistic Distribution A random number is drawn from a uniform distribution on the open interval (0,1) and then transformed to a log-logistic variate by the log-logistic percentile function.

IPP: SIF-Master

a) IPP uses the domestic SIF-Master software which is developed by IPP for probabilistic (versions 2.0, 2020) and deterministic (version 1.7, 2018) Fracture Mechanics calculations for pressure vessels and piping. The Linear-Elastic Fracture Mechanics is used.

b) Fracture probability is calculated based on probabilistic fracture mechanics by using the 1st order reliability method (FORM) which is embedded in SIF-Master versions 2.0 (2020) [70].

c) In the current SIF-Master versions only the brittle initiation of crack is considered.

d) Defect density is assumed to be a uniform distribution. Fracture Toughness, Critical temperature of brittleness T_k (Transition Temperature) and chemical factor are sampled from a normal distribution with its mean value corresponding to the best fit of experimental data. Defect depth is sampled from an exponential distribution law. Defect shape is sampled from a lognormal distribution law.

e) No verification or validation. The input data (such as: Fracture Toughness, Transition Temperature, chemical factor, defect depth, defect, shape and defect density) are validated based on the relevant experimental data.

KIWA: ISAAC

KIWA uses the ISAAC software that has been developed by KIWA for both deterministic (commercial version) and probabilistic (in-house version) safety assessment of components with defects.

The following numerical algorithms are implemented in ISAAC:

- Simple Monte Carlo Simulation (MCS).
- First/Second-Order Reliability Method (FORM/SORM).
- Monte Carlo Simulation with Importance Sampling (MCS-IS).

Within ISAAC, the probability of brittle initiation, ductile initiation or failure (determined by failure assessment diagram) can be analysed (arrest is not considered within ISAAC).

MCS-IS is an algorithm that concentrates the samples in the most important part of the integration interval. Instead of sampling over the entire probability density functions (MCS), one samples around the most probable point of failure (MCS-IS). This point, called MPP, is evaluated using information from a FORM/SORM analysis. The simulation outputs are weighted to correct for the use of a biased distribution, and this ensures that the new importance sampling estimator is unbiased.

The verification of ISAAC is presented in the SSM report 2018:18 [71].

GRS: PROST

GRS uses the PROST software being developed by GRS for probabilistic (and deterministic) fracture mechanics, together with GRS' in-house sensitivity and uncertainty analysis software SUSA. In the computation, the probability of brittle or ductile initiation or failure can be computed, as desired. Monte Carlo sampling is used to generate parameter sets in SUSA. SUSA is being developed by GRS to facilitate the implementation of uncertainty and sensitivity analyses based on Monte Carlo simulation methods. It uses established methods from probability theory and statistics and offers support to quantify the uncertainties probabilistically and to carry out the various steps of an uncertainty and sensitivity analysis. Different sampling approaches are available in SUSA depending on the demands of the investigation target. For the application of Wilks method to derive tolerance limits, simple random sampling is sufficient and will be applied.

Besides the coupling with SUSA, PROST can also compute the probability with a sampling method based on distributed input quantities. Various sampling algorithms are implemented in PROST, like Monte Carlo, Quasi Monte Carlo, Stratification, Design Point-based Importance Sampling, Vegas, and others. The PROST software is matter to a quality assurance plan with regression tests and a validation report; the guideline is the IAEA SSG-2 and ISO 9001.

BZN: In-house (under development)

In Hungary, nowadays probabilistic PTS assessment is not accepted for licensing. There is currently a project that will also cover even probabilistic PTS assessments within the framework of the EK (EK - Centre for Energy Research, Hungary).

The Thermal-Hydraulic and the Structural-Mechanics calculations are based on commercial and research software (for Structural Mechanics calculations, MSC.Marc is applied), the probabilistic fracture mechanics part will be implemented in an in-house EK's software. A Monte Carlo method is planned to be implemented, and initiation event frequencies will be considered for fracture probability calculations.

The organization of the software is planned as follows:

(1) Computation of the thermal and the mechanical fields on the whole model of the RPV, for each TH transient
(2) Generation of cracks on the basis of assumed distributions concerning dimensions and orientations, and using Monte Carlo method
(3) Calculation of the SIF for the defined cracks (applying an engineering stress intensity factor evaluation method [72], which is highly accurate and provides a fast working tool for considering many transients and postulated defect geometries/orientations, and which is also accepted and recommended in IAEA-TECDOC-1627 [6] and VERLIFE [27]), and the fracture toughness distributions of structural materials around the simulated cracks
(4) Calculation of fracture probability for a crack of assigned dimensions on the basis of a comparison of SIF and the fracture toughness following Weibull distribution
(5) Averaging fracture probability for each safety-critical, relevant part of the RPV
(6) Summing up fracture probabilities for all the TH transients, for each safety-critical, relevant component zone of the RPV
(7) The overall failure frequency of the RPV, is the integrated value of the fracture probabilities for all transients and all RPV zones.

IRSN: In-house (under development)

The probabilistic assessment that IRSN aims to perform in the frame of APAL is based on a deterministic calculation chain. It is an in-house chain, with CATHARE as system thermal-hydraulics code, TDA (Température Descente Annulaire) which is a simplified in-house code determining the fluid

temperature in the downcomer at the RPV wall, CICLAMEN (in-house code) in order to compute the heat exchange coefficient between fluid and RPV wall, and a MATLAB module to determine the stress in the wall, the stress intensity factor and the margin factor to the failure. The thermal-hydraulics part of the chain, including validation and verification, is described in the APAL D1.3 Document. The sampling tool for probabilistic evaluations will be a commercial tool based on OpenTurns software (with Simple Random Sampling (SRS) for Wilks method). The whole deterministic chain is described on the **Figure 34**.
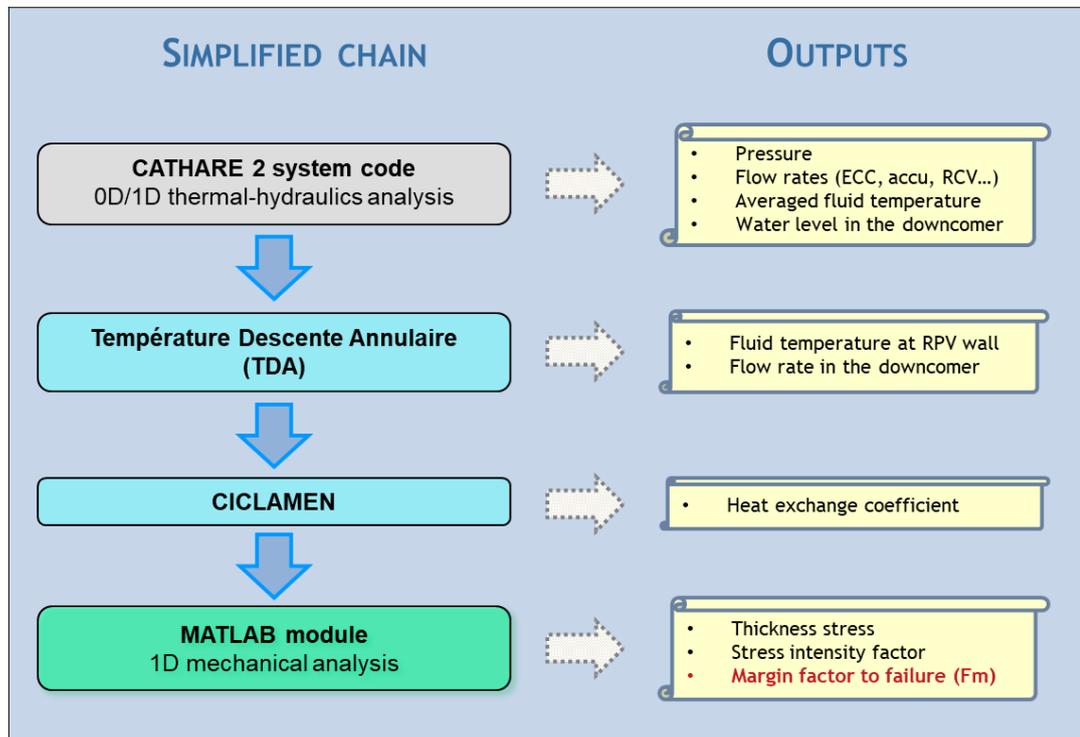
Figure 34: IRSN – In-house tool: Flowchart.

JAEA: PASCAL v4

JAEA will utilize PASCAL v4 in the APAL project. Main features of PASCAL v4 are listed as the below:

- The epistemic and aleatory uncertainties can be considered. Here only fracture toughness and crack arrest toughness are classified as the parameters with the aleatory uncertainties. The other parameters with epistemic uncertainties such as occurrence frequency of PTS events, initial RT_{NDT}, chemical compositions of RPV steel, neutron fluence, embrittlement prediction method, crack size and density can be taken into account.
- The parameters with the epistemic uncertainties are sampled by Latin hypercube sampling (LHS) method. The uncertainties of fracture toughness and crack arrest toughness are calculated based on a numerical integration method for reducing calculation time.
- Conditional probabilities of crack initiation (CPI) and failure (CPF) can be obtained by considering single crack and single PTS event. In addition, through a post-processing of CPI and CPF with several cracks and PTS events, failure frequencies (frequency of crack initiation and through-wall crack frequency considering multiple cracks and PTS events) can be obtained.
- WPS effect, crack arrest, weld residual stress for butt-welds and austenitic-stainless steel cladding, etc., can be considered.
- Not only PTS events corresponding to cooling events can be considered, but also heat-up events such as hydrostatic test and start-up of RPV.
- A flowchart of PASCAL v4 is given in **Figure 35**. There are three modules: (1) PrePASCAL, (2) PASCAL-RV, and (3) PASCAL-Manager. Pre-PASCAL is a 1D finite element analysis module used

117

for thermal-structural analysis. PASCAL-RV is a PFM analysis solver used for failure probability calculations. PASCAL-Manager is a post-processor for calculating failure frequency. Also, PASCAL-Manager can be used to automatically generate analysis files for PASCAL-RV and to run multiple analyses in parallel through the use of using multiple CPU cores.
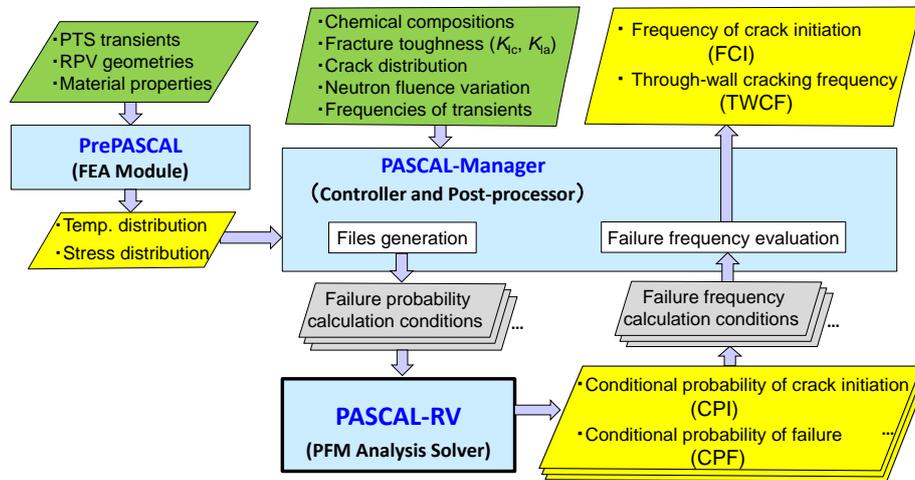
Figure 35: JAEA – PASCAL: Flowchart.

7.4.2   Description of the assessment of the whole spectrum of PTS scenarios

A probabilistic PTS analysis should cover the whole spectrum of possible scenarios leading to a PTS event. Therefore, the partners have described how they assess the whole spectrum of PTS scenarios, which should include:

  a. How are PTS events grouped together to cover the whole PTS spectrum?
  b. Where does the PTS event frequencies (probability of occurrence) come from? Probabilistic Safety Assessment (PSA) or other sources?
  c. How are the conditional probabilities of each analysed PTS transient combined together to get an overall failure frequency? (post-processing?)

UJV

a) All events potentially occurring in the nuclear power plant (NPP) that may lead to a pressurized thermal shock (PTS) are analysed within PSA (probabilistic safety analyses). For these events, event trees are developed and frequencies of scenarios leading to PTS are estimated. The relevant scenarios of similar variation of TH parameters are then aggregated into groups and the most conservative scenario within each group is selected as a representative scenario for the whole group. The selection of the representative scenario is based on engineering judgement. The minimal set of PTS scenarios that should be covered in PTS analyses is defined by the [8] standard.

In accordance with the NTD AME standard [8], the probabilistic assessment is performed only for PTS (emergency conditions). The hydrotest and normal operating conditions (p-T curves) are assessed only by deterministic calculations.

b) Frequencies of the scenarios leading to PTS are obtained from the PSA. Currently, the RiskSpectrum®PSA code is used in UJV for this purpose. The occurrence frequency of a whole group of scenarios is calculated as a sum of occurrence frequencies of each scenario (initiating event) included in the group. The frequencies are modelled as random variables (using histograms or lognormal distributions), therefore their mean values are estimated together with their uncertainties.

c) The overall failure frequency (FF) of the reactor pressure vessel (RPV) in expressed as

$$FF = \sum_{j=1}^{n} fr_j \cdot CPF_j,$$

where fr_j is the occurrence frequency of the j-th scenarios group, CPF_j is the conditional probability of failure due to the representative scenario belonging to the j-th scenarios group (on the condition that the scenario occurred) and n is the number of analysed scenarios groups. Both fr_j and CPF_j are random variables. The mean value and the 95% quantile of FF are calculated using random sampling from fr_j and CPF_j.

In a similar way, the overall frequency of fast fracture initiation in RPV is defined as

$$FI = \sum_{j=1}^{n} fr_j \cdot CPI_j,$$

where CPI_j is the conditional probability of fast fracture initiation for the representative scenario of the j-th scenarios group.

This post-processing is performed by the VERPOST module of the PROVER code.

FRA-G

The whole spectrum of PTS scenarios can be considered in two ways:

- The most penalizing PTS transient for the whole spectrum of PTS scenarios is assessed.
- The spectrum of PTS scenarios is divided into groups (e.g., SB-LOCA, MB-LOCA, LB-LOCA) and the most penalizing PTS transient for each group is assessed.

The conditional probability for an analysed PTS transient is then combined with the occurrence probability to get a failure frequency (failure probability per year). If the most penalizing PTS transient is assessed to cover the whole spectrum of PTS scenarios, the occurrence probability of all potential PTS scenarios should be summarized. If the most penalizing PTS transients is assessed for each group of PTS scenarios, then the occurrence frequency for the group (= sum of occurrence frequencies of all PTS scenarios of that group) should be used. The results from all groups are combined to get the overall failure frequency for the whole PTS spectrum.

The calculation of failure frequency for the whole PTS spectrum is done in a post-procedure after calculation of conditional probability for assessed PTS transients (as described in chapter 7.4.1).

OCI

A number of abnormal events and postulated accidents have the potential to thermally shock a reactor pressure vessel (RPV) (either with or without significant internal pressure); examples include a pipe break in the primary pressure circuit, a stuck-open valve in the primary pressure circuit, and breakage of the main steam line. During these events, the water level drops because of the contraction produced by rapid depressurization. In events involving a break in the primary pressure circuit system, the water level drops further because of leakage from the break. Automatic systems and operators must provide makeup water in the primary system to prevent the fuel in the core from overheating. The makeup water is typically much colder than that held in the primary cooling system.

Such overcooling events, where the temperature of the coolant in contact with the inner surface of the RPV wall rapidly decreases with time (possibly followed by late re-pressurization), can produce temporally dependent temperature gradients that induce biaxial stress states varying in magnitude through the heavy-section steel wall of the RPV. Near the inner surface and through a significant part of the wall thickness the stresses are tensile, thus presenting Mode I opening driving forces that can act on possible surface-breaking or embedded flaws. The combined thermal plus mechanical loading results in a transient condition known as a pressurized thermal shock (PTS) event. Concern with PTS results from the combined effects of (1) simultaneous pressure and thermal-shock loadings, (2) embrittlement of the vessel material due to cumulative irradiation exposure over the operating history

of the vessel, and (3) the possible existence of crack-like defects at the inner surface of or embedded within the RPV wall. The decrease in vessel temperature associated with a thermal shock could also reduce the fracture toughness of the vessel material and introduce the possibility of flaw propagation. Inner surface-breaking and embedded flaws near the inner surface are particularly vulnerable. In this region, the temperature is at its minimum, and the stress and radiation-induced embrittlement are at their maximum.

In general, a probabilistic risk assessment (PRA) event sequence analysis is performed to define the sequences of events that are likely to produce a PTS challenge to an RPV's structural integrity and to estimate the frequency with which such sequences can be expected to occur (The initial studies (see [73], [74] and [75]) that identified dominant plant-specific PTS overcooling events and their associated frequencies of occurrence were carried out at Oak Ridge National Laboratory (ORNL) in the early 1980s.). The event sequence definitions are then passed to a thermal-hydraulics (TH) model that estimates the temporal variation of temperature, pressure, and heat transfer coefficient in the RPV downcomer characteristic of each of the sequence definitions. These pressure, temperature, and heat transfer coefficient temporal histories are passed to a probabilistic fracture mechanics (PFM) model, which uses the TH output, along with other information concerning plant design and materials of construction, to estimate a time-dependent driving forces to fracture produced by a particular event sequence. The PFM model compares this estimate of fracture driving force to the fracture toughness, or fracture resistance, of the RPV steel. This comparison allows an estimate of the probability that a particular sequence of events will produce a crack all the way through the RPV wall if that sequence of events was to actually occur. The final step in the analysis involves a simple matrix multiplication of the probability of through-wall cracking (from the PFM analysis) with the frequency at which a particular event sequence is expected to occur (as defined by an event-tree analysis as discussed in the next section). This product establishes an estimate of the yearly frequency of through-wall cracking that can be expected for a particular plant after a particular period of operation when subjected to a particular sequence of events. The yearly frequency of through-wall cracking is then summed for all event sequences to estimate the total yearly frequency of through-wall cracking for the vessel. Performance of such analyses for various operating lifetimes provides an estimate of how the yearly through-wall cracking frequency (TWCF) can be expected to vary over the licensed service-life of the plant.

The post-processing module of FAVOR (FAVPost) combines the CPI and CPF matrices (of size #PTS transients x #RPV trials) obtained in FAVPFM with samples of the transient initiating frequencies generated from the input discrete distributions (size #PTS transients). The results are discrete distributions of (i) frequency of crack initiation and (ii) frequency of RPV failure (both of size #RPV trials). These output discrete distributions and their cumulative forms are then analysed to obtain relevant statistics such as mean, standard deviation, percentiles (5th, median, 95th, 99th and 99.9th) and several other measures for both, initiation and failure frequencies. Additionally, FAVPost also provides for each transient considered the conditional probabilities of both, initiation and failure, probabilities, namely their mean values and percentiles (5th, 95th and 99th).

JSI

JSI uses FAVOR Code v16.1. The PTS events considered in analysis are small break (SB-LOCA), medium break (MB-LOCA) and large break (LB-LOCA) loss of coolant accidents (3 cm^2 and 70 cm^2, 350 cm^2, respectively). The thermohydraulic transients are grouped into SB-LOCA, MB-LOCA and LB-LOCA, respectively. However, within the JSI research project several additional leak sizes (e.g., double guillotine break) were analysed.

b) The frequency of the MB-LOCA and SB-LOCA are 4.5×10^{-4}/year and 4.6×10^{-3}/year, respectively. The occurrence frequencies were calculated by PSA analyses and used, e.g., in [76].

c) The total cumulative failure frequency $\Phi(F)$ under several transients is determined from the summation of the products of the individual transient occurrence frequency and the corresponding conditional vessel failure probability, written as

$$\Phi(F) = \sum_i \Phi(E)_i \cdot P(P|E)_i$$

IPP

Identification of potential emergency scenarios, affecting on RPV brittle fracture, was performed using probabilistic models of Level 1 PSA for nominal and reduced power level of unit, and zero power. To identify PTS scenarios the following criteria were used: 150°C/hour and more coolant temperature drop; the state of emergency core cooling system; external flooding; fires. Further, all emergency sequences, which have been identified as affecting on RPV brittle fracture, were grouped to the corresponding groups (LOCA, PRISE, MSLB and OTHER). During the grouping of emergency sequences, types of initiating events, the mechanism of scenario occurrence, as well as the power level of a unit were considered.

b) Modelling and quantitative assessment of scenario occurrence frequencies were performed using the SAPHIRE or RiskSpectrum PSA computer code and modified model of Level 1 PSA. The sequences, which had frequency of occurrence less than 1.0E-08 1/year, were considered as of minor importance and they were removed from the sequence list of PTS cases.

c) The total risk of RPV brittle fracture $\Re$ is defined as the sum of the products of the frequency of occurrence for the *i*-th group of scenarios H_i and the conditional probability of brittle fracture P_i for this *i*-th group.

$$\Re = \sum_i P_i \cdot H_i$$

Usually, 6 to 9 most severe scenarios are considered as representative, which are identified from the results of deterministic calculations of RPV brittle fracture for the whole spectrum of PTS. Each group of PTS events is conservatively replaced by one of the representative scenarios.

BZN

The PTS events are grouped together in compliance with the recommendation of guidelines IAEA-EBP-WWER-08 [7]. PTS event frequencies come from PSA sources combined with international operating experience of existing NPPs. To elaborate an overall failure frequency of the RPV, the fracture probabilities for all transients and all RPV zones will be integrated.

IRSN

IRSN has not yet performed probabilistic PTS studies.

KIWA

The ISAAC software does not have this feature within the software. However, there is a possibility to deal with this independently of the software.

GRS

From regulatory perspective, it is not required to determine a RPV failure frequency due to PTS transients. Several PTS events are investigated with the aim to identify an enveloping scenario in the sense of a deterministic integrity assessment. The PTS event frequency itself originate from PSA.

JAEA

In deterministic methodology, such as codes and standards prescribing the structural integrity assessment method for reactor pressure vessel (RPV), two methods are provided. One is a simple method considering a PTS event which is the simplified LB-LOCA. The other is a detailed method considering multiple PTS events, such as LB-LOCA, SB-LOCA, and MSLB.

In Japan, the guideline which prescribes failure frequency calculation methodology for RPVs has been published by the Japan Electric Association. In the guideline, multiple PTS events which may contribute

121

to failure of RPV shall be taken into account. Based on PTS transients described in NUREG-1806 and failure frequency calculation results for Japanese model RPV, 13 PTS transients including LOCA, MSLB, SOV events are listed in the guideline. Occurrence frequency and its distribution for each PTS transient are determined in accordance with NUREG-1806.

7.4.3   Description of the scope of the assessment and treatment of RPV loading

Stress and temperature distribution in the RPV wall is of course an essential input to sub-sequent fracture mechanics analysis. Although the structural mechanics is usually not treated as probabilistic assessment, the treatment and consideration of RPV loading has a major impact on results of probabilistic PTS analysis. Therefore, the partners have described how the RPV loading is assessed within their probabilistic tool/software. The description includes:

  a)   Do you perform 1D, 2D or 3D temperature and stress calculations? Using elastic or elasto-plastic formulation? Using FEM mesh with or without crack?
  b)   What regions of RPV do you assess (RPV beltline welds and rings, possibly also nozzles and other regions)?
  c)   Do you consider regions of cold plume? (using simplified formula or full 3D calculation?)
  d)   Do you combine results from different regions to an overall probability? And if yes how?

UJV: PROVER

a) The VERLOAD module performs 1D FEM calculation of thermal and stress fields using linear elastic formulation on 1D (axisymmetric) mesh without a crack. Stress intensity factors are calculated by analytical formulas without plastic correction.

b) In the probabilistic assessment, only the beltline region of the RPV is assessed. The computational domain (for VVER-440 and VVER-1000 RPVs) includes two (circumferential) welds and three base metal rings close to the reactor core.

c) The PROVER code performs only 1D calculations of temperature and stress-strain fields without any analytical correction for the cold plume. If distinct cold plume and ambient temperatures are available from thermal-hydraulic calculations (e.g., from mixing calculations), it is preferred to use coolant temperature and HTC (or RPV inner surface temperature) from the cold plume as a boundary condition. This approach is conservative in the region outside of the cold plume because it leads to lower wall temperature and higher stresses than in a detailed 2D calculation. It is nevertheless somewhat non-conservative in the cold plume region due to lower stresses (but the wall temperature is correct).

PROVER considers spatial distribution of neutron fluence (in azimuthal and axial directions) and fluence attenuation in the through-wall direction.

d) For each PTS scenario (transient), we combine results from different RPV regions (see point b) to the resulting overall conditional probability of fast fracture initiation (CPI). It is assumed that all cracks sampled in the RPV are independent (i.e., that they do not interact mutually). This leads to the following formula for the probability that at least one crack will initiate:

$$CPI = 1 - \prod_{k=1}^{m}(1 - CPI_k)$$

where CPI_k is the conditional probability of initiation of the k-th crack sampled in the RPV, CPI is the overall conditional probability of fast fracture initiation in the RPV and m is the number of cracks postulated in the RPV (in one given trial of a Monte Carlo simulation). Currently we do not consider any crack interaction (proximity rules) in our calculations.

OCI, PSI, Tecnatom, JSI: FAVOR v16.1

a) The FAVLoad module is one-dimensional finite-element analysis, that calculates the RPV loads (temperature, axial and circumferential stress) through the wall. Moreover, stress intensity factors for surface-breaking flaws are calculated within the FAVLoad module.

The functional structure of the FAVLoad module is shown in **Figure 28**, where multiple thermal-hydraulic transients are defined in the input data. For each transient, deterministic calculations are performed to produce a load-definition input file for FAVPFM. These load-definition files include time-dependent through-wall temperature profiles, through-wall circumferential and axial stress profiles, and stress-intensity factors for a range of axially and circumferentially oriented inner and external surface-breaking flaw geometries (both infinite- and finite-length).

b) In FAVOR, the vessel beltline is treated as a collection of major regions of plates, forgings, and welds. These major regions are then discretized into sub regions, where, within a given sub region, flaws are analysed through Monte Carlo realizations of the RPV subjected to the PTS transients under study.

c) Cold plume effect is not considered within FAVOR. Special consideration on how to apply for plume effect by PSI and JSI are presented below.

PSI: Temperature calculation of the fluid was done performing 1D (RELAP5), 2D (GRS-mix), TRACE and 3D (CFD) calculations. Thermal and stress analyses in FAVOR used a one-dimensional axisymmetric model of the RPV wall, whereas the plume cooling was considered by using temperatures from GRS-MIX or CFD.

JSI: We mostly use RELAP/TRACE codes with a 1D RPV model. Therefore, cold plume is not considered unless a mixing code is used. Results of different regions are also not considered and we mostly focus on the middle of the core-height region where the highest fluence and, therefore, embrittlement is expected.

d) In FAVOR, the vessel beltline is treated as a collection of major regions of plates, forgings, and welds. These major regions are then discretized into sub regions, where, within a given sub region, flaws are analysed through Monte Carlo realizations of the RPV subjected to the PTS transients under study.

FRA-G: In-House Tool

The RPV will be divided into sub-regions defined by loading and embrittlement condition, see **Figure 36**. For the assessment of each sub-region, stress and temperature distributions will be used. The stress and temperature distributions are obtained usually from 3D FE analysis and consider plume effect as TH output resulting from a mixing code (like KWU-MIX). In the end, all areas with different loading and embrittlement conditions can be considered, but due to computation time it makes sense to define regions with covering loading and covering embrittlement (the more sub-regions, the more accurate value of the failure probability).

BZN: In-house (under development)

During PTS calculations, the RPV behaviour is calculated on full 3D geometry-model (including the beltline region and the nozzles) of the pressure vessel, using coupled thermal-mechanical calculations. Two types of calculations are used: (1) simplified, elastic calculations and (2) full elastic-plastic computations. The cold plume is considered using full 3D calculation.
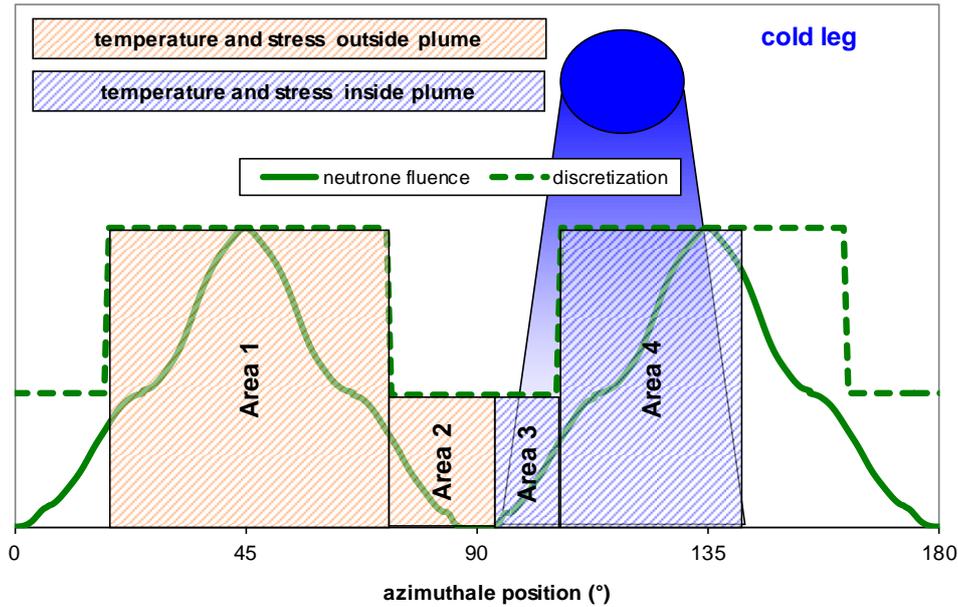
Figure 36: FRA-G In-house tool – Definition of sub-regions.

IPP: SIF-Master

a) To determine stress and strain fields the "indirect" solution method for the nonstationary temperature task in axisymmetric formulation with the method of further stress calculation is used [77]. Both methods are based on transfer matrix approach and use exact analytical expressions for the thick-walled cylinders. The accuracy of the model is improved by separate temperature calculations for "cold" plume and "hot" rest of the reactor. At every moment of time two thermal tasks are calculated: for the "cold" plume, on the base of coolant parameters at hypothetical crack zone (usually it is the coldest part of RPV) and for the "hot" part, on the base of the warmest coolant parameters or coolant parameters in the opposite to the "cold" zone. Then stress task for the "hot" part is calculated. Obtained axial "hot" strain is used as a constant loading for stress calculations of cold plume. The automatic time step determination method is implemented, which provides maximum calculation speed.

b) Only the RPV beltline welds and rings are considered.

c) The region of cold plume is considered (see a) and [77]).

d) The probability of brittle fracture P_i for the i-th group of scenarios is calculated as the sum of the probabilities for each element of estimation (RPV zone). The probability for each of the calculation element (RPV zone) is calculated as the sum of probabilities obtained for each of the calculation zones (see **Figure 38**). The probability of fracture for each of the "U" calculation zones is determined as the product of the probability of fracture for a single defect p_u (for the defect, whose conditional probability of which is the largest) and the number of defects in the zone. The quantity p_u is a sum of fracture probabilities $p_u(\alpha, \gamma)$ ($\alpha = a/t$, $\gamma = a/L$ for the whole set, where a is the crack depth; L is the half crack length and t is the thickness) for a whole array of defects sizes (α_k, γ_m), but with taking into account the probability of that size:

$$p_u = \sum_k \sum_m p_u\left(\alpha_{k+1}, \gamma_{m+1}\right) \cdot \int_{\alpha_k}^{\alpha_{k+1}} p_{at}\, d\alpha \int_{\gamma_m}^{\gamma_{m+1}} p_{al}\, d\gamma,$$

where the product of integrals is the probability of crack sizes being in range $[\alpha_k, \alpha_{k+1}]$, $[\gamma_m, \gamma_{m+1}]$ and $p_u(\alpha_{k+1}, \gamma_{m+1})$ is the maximum failure probability in the range.

The $p_u(\alpha, \gamma)$ is calculated on the base of the maximum allowable transition temperature value for the crack of corresponding size and based on material probabilistic parameters as schematically shown in **Figure 37**. Average safety margin is the maximum allowable transition temperature (T_{ka}) which is determined by deterministic calculations, and conditional probability is calculated using gamma function

$$\Gamma\left(\frac{\Delta}{\sqrt{\sigma_{SIF}^2 + \sigma_{FT}^2}}\right)$$
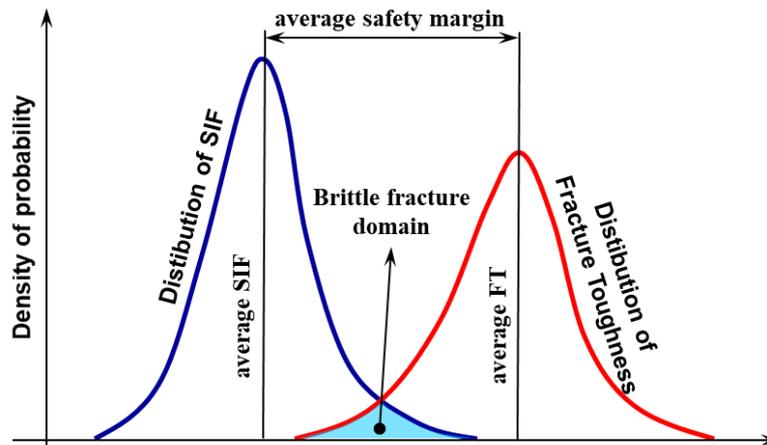
Figure 37: Scheme for conditional probability determination.

Note, that the calculation element is the zone of RPV wall thickness, which is selected in such a manner that the neutron fluence value from the border of one zone to the next another one is reduced (when moving from inner to outer RPV surface) by some step (discontinuously). In our practical calculations we usually define the zone with 0.1 neutron fluence step (SIF-Master proposes this value by default, but it can be changed by the user). The schematic WWER-1000 calculation zones are shown in **Figure 38**. In order to obtain conservative results from the RPV integrity probabilistic calculations, the fluence at any point in the zone is assumed equal to the maximum fluence of the zone (i.e., the value on outer line of the border).
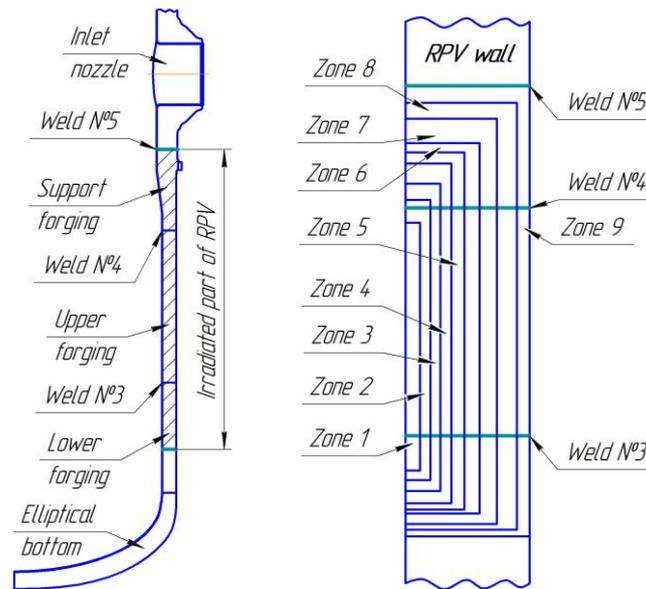
Figure 38: WWER-1000 RPV (without outlet nozzle and flange) and layout of its radiated part on estimated zones.

KIWA: ISAAC

To answer this question, one must distinguish between the calculation of temperatures and stresses and how these are then transferred to our software (ISAAC) that performs the probabilistic analyses.

In general, it can be said that the 3D calculation of temperatures and stresses may be very complex, for example in case of performing a complete analysis to determine weld residual and cladding stresses (with or without a crack included in the model). The results along a single path through wall thickness from these analyses are then transferred to ISACC, which is essentially a one-dimensional program (which, however, can take several dimensions into account in the calculations).

When carrying out probabilistic analyses of an RPV, different regions in the RPV are considered. As an example, in a recent analysis most welds in the RPV (also outside of the beltline region) were considered, including the most relevant nozzles (in total 32 welds and 20 nozzles).

As indicated above, ISAAC cannot deal with non-symmetrical loads in three dimensions. These loads must therefore be approximated in order to be specified as input to ISAAC.

In general, it can be said that we analyse the risk contribution from a particular weld. For this weld, a summation is made over all the load cases relevant for this weld.

GRS: PROST

GRS has performed a lot of RPV deterministic integrity analyses based on 2D/3D elastic-plastic FE calculations with postulated cracks in the beltline welds and nozzle regions. In this context asymmetric cooling conditions due to cold plumes and residual stresses have been considered. Analytical stress calculations are based on elastic analyses, using the temperature distributions. These stress computations are effectively 1D. The approaches for simplified formula have specific shortcomings, especially in case of non-symmetrical cooling, which would have to be resolved. The consideration of different regions would be a result of an a prior analysis for susceptibility of specific locations to damage or failure during a PTS; the combination of different locations also depends on the thermal-hydraulic assumptions.

IRSN: In-house (under development)

A 1D model is used to calculate the temperature and stress distributions through the RPV wall thickness. The mechanical model used is linear elastic. Plasticity effects are taken into account by the analytical formulations of RSE-M code.

The model has been developed for the RPV beltline welds and rings. Cold plume effect is evaluated by simplified formulations.

Results from different regions can be combined to assess an overall probability. The core shell can be divided into regions regarding the loading (heat transfer coefficient) and the material characteristics (toughness).

JAEA: PASCAL v4

PASCAL can consider spatial distribution of neutron fluence but not plume effect. Separate temperature and stress calculation results for plume and ambient can be taken into account by PASCAL v4.

7.4.4 Description of the fracture mechanics models used for probabilistic PTS assessment

A lot of information on the used fracture mechanics models has already been given in response to Section 7.4.1, but a more detailed description has been given by the partners due to:

 a. Damage Mechanisms Models (e.g., ductile crack growth)
 b. Stress intensity factor solutions and plastic correction, if applied
 c. Brittle and/or ductile crack initiation
 d. Crack arrest model
 e. Crack interaction and proximity rules, if multiple flaws are assessed
 f. Global/Local failure
 g. WPS model implemented in the software

UJV: PROVER

a) Ductile crack growth is not considered in the [8] guidance for probabilistic assessment and it is not implemented in the PROVER code. In the ductile region (the upper shelf), $J_{0.2mm}$ is used as a fracture toughness for crack initiation. The calculation of $J_{0.2mm}$ implemented in PROVER follows the approach introduced in the paper [78].

b) The plastic correction is not applied in the PROVER code. All calculations are performed using LEFM. Material plasticity effects are not considered.

Currently, only elliptical cracks embedded in the base and weld metals are modelled in PROVER. Underclad semi-elliptical cracks are modelled in a simplified way by replacing them with elliptical cracks of the same depth and length that touch the cladding from the side of base/weld metal.

Embedded cracks are postulated in the inner 40% of the wall thickness and only the point nearest to the inner surface is assessed, because this point has the lowest temperature (for PTS regimes) and highest SIF.

Surface-breaking cracks were originally implemented in FAVOR but they are currently not considered in PROVER, as they are not relevant for VVER RPVs due to cladding composed by several layers.

The SIF for embedded cracks is calculated using the following formula from ASME Code, Section XI, Appendix A [79], see also [80]:

$$K_I(a) = (M_m \sigma_m + M_b \sigma_b)\sqrt{\pi a/Q}.$$

Here σ_m and σ_b are membrane and bending stress determined by linearization of the opening stress component on the crack face, M_m and M_b are free-surface correction factors and Q is the flaw shape parameter. Plastic correction in the Q factor is not considered.

c) The statistical distribution of fracture toughness depends on the material temperature T and the Master curve reference temperature T_0. For temperatures in the transition region $T \leq T_{US}$, the fracture toughness is assumed to follow Weibull distribution in accord with the Wallin Master Curve theory. For temperatures in the ductile (upper-shelf) region $T > T_{US}$, the fracture toughness is calculated in accordance with the paper [78]. Following [78], T_{US} is defined by

$$T_{US} = 48.884 + 0.7985 \cdot T_0, \text{ in } °C.$$

In the transition region, $T \leq T_{US}$, the conditional probability of crack initiation is given by:

$$CPI(\tau) = 1 - \exp\left[-\left(\frac{K_I(\tau) - K_{min}}{K_0(\tau) - K_{min}}\right)^4\right],$$

where $K_{min} = 20 \, MPa \cdot \sqrt{m}$

$$K_0(\tau) = 20 + \left[11 + 77 \cdot \exp\left(0.019 \cdot (T(\tau) - T_0)\right)\right]\left(\frac{25}{L}\right)^{1/4}$$

L is the length of the crack front in mm and τ is the time.

To formulate the statistical distribution of fracture toughness in the upper-shelf region, the median fracture toughness in the brittle region (for 1 inch thickness) is expressed as:

$$K_{Ic,med}(T) = 30 + 70 \cdot \exp[0.019 \cdot (T - T_0)].$$

Converting $K_{Ic,med}(T)$ $[MPa \cdot \sqrt{m}]$ to the J-terms $[kJ/m^2]$:

$$J_{Ic}^{tran}(T) = 1000 \frac{(1 - v^2) \cdot K_{Ic,med}^2(T)}{E(T)},$$

where $E(T)$ is Young modulus in $[MPa]$ and v is the Poisson's ratio. Using the auxiliary function $f(T)$

$$f(T) = 1807.75 \cdot \exp\left[-(k_1 \cdot T + k_2)\right]$$

where $k_1 = 0.01022698$ and $k_2 = 2.793499$, we can define the mean fracture toughness on the upper-shelf in J-terms $[kJ/m^2]$:

$$J_{Ic}^{us,mean}(T) = f(T) + J_{Ic}^{tran}(T) - f(T_{US})$$

The fracture toughness in J-terms on the upper-shelf follows the normal distribution with the standard deviation σ $[kJ/m^2]$ dependent on the wall temperature T, [81]:

$$\sigma = 51.199 \cdot \exp(-0.0056 \cdot T).$$

Converting the stress intensity factor K_I $[MPa \cdot \sqrt{m}]$ to J-terms $[kJ/m^2]$:

$$J(\tau) = 1000 \frac{(1 - v^2) \cdot K_I^2(\tau)}{E(T(\tau))},$$

we come to the conditional probability of crack initiation in the upper-shelf region ($T > T_{US}$):

$$CPI(\tau) = \Phi\left(\frac{J(\tau) - J_{Ic}^{us,mean}(T(\tau))}{\sigma}\right) = \frac{1}{2}\left[1 + \text{erf}\left(\frac{J(\tau) - J_{Ic}^{us,mean}(T(\tau))}{\sqrt{2}\,\sigma}\right)\right],$$

where Φ is the cumulative distribution function of the standard normal distribution and erf denotes the error function. The conditional probability of crack initiation CPI over the entire PTS event is determined as the maximum over the entire time interval.

$$CPI = \max_{\tau} CPI(\tau).$$

d) The crack arrest is currently not implemented in the PROVER code, however, the [8] standard provides some guidance on crack arrest calculations. In the case of crack initiation, the crack shall be replaced by the surface-breaking crack of the same depth and infinite length.

The mean value of the fracture toughness for crack arrest K_{Ia} is given by

$$\text{mean } K_{Ia} = 30 + 70 \exp[0.019(T - T_{KIa})].$$

It is assumed that K_{Ia} has a lognormal distribution with the standard deviation of 18% of the mean value.

The reference temperature for crack arrest T_{KIa} is determined from the previously sampled value of T_0. The difference $T_{KIa} - T_0$ is assumed to have a lognormal distribution with

$$\text{mean}(T_{KIa} - T_0 | T_0) = \exp\left(5 - \frac{T_0 + 273}{136.3} + \frac{R_{p0.2}}{683.3}\right)$$

and a standard deviation of 19 ℃. This approach was adopted from [82].

e) The crack interaction is currently not considered. All cracks sampled in RPV are assumed to be mutually independent.

f) We currently do not assess crack growth and plastic collapse of the crack ligament. We also do not use local approach to fracture for probabilistic PTS assessment. Constraint effects (shallow crack effects) are also not considered.

g) The WPS approach is currently not implemented in the PROVER code. The WPS model that we use for deterministic calculations is described in Chapter 5.

FRA-G: In-House Tool

a) In the general, the events considered in the fracture mechanics assessment are, among others:

- Brittle fracture initiation (based on ASME K_{Ic}) followed by crack arrest
- Crack arrest (based on ASME K_{IR})
- Re-Initiation after crack arrest (during remaining time of transient)
- Crack arrest after re-Initiation
- In the end: No first Initiation, Stable Arrest (No Re-Initiation) or Failure (crack depth > 80% wall thickness)

b) Currently the following cracks and SIF solutions are implemented (analytical solutions):

- Surface flaw: K_I according to Raju/Newman, ASME XI, App. A or CEA/RCC-MRx solution (with explicit consideration of stresses in cladding and in base material)
- Underclad flaw: CEA/RSE-M solution with plastic correction according to RSE-M code (β correction factor, (see IRSN answer in this section)
- Embedded flaw: ASME XI, Appendix A

Due to modular based in-house tool any K_I solution can be implemented for specific case of interest.

c) Ductile crack initiation and stable ductile crack growth is not addressed until now but can be added as modules for specific application.

d) Crack arrest as indicated above.

e) Crack interaction and proximity rules for multiple flaws is not considered.

f) Failure as indicated above.

g) Two available WPS Models:

$dK/dt < 0 \rightarrow$ WPS, if $dK/dt > 0 \rightarrow$ initiation if $K_I \geq K_{IC}$

$dK/dt < 0 \rightarrow$ WPS, if $dK/dt > 0 \rightarrow$ initiation, if $K_I \geq K_{IC}$ and $K_I \geq K_{Imax,WPS}$ with $K_{Imax,WPS}$ is the previous non initiating maximum K_I (K_{Imax}) achieved previously during the time history at $t_{K_{Imax}}$ (so with $K_{Imax} < K_{IC}(t_{K_{Imax}})$)

OCI, PSI, Tecnatom, JSI: FAVOR v16.1

a) Damage Mechanisms Models

- cleavage initiation, re-initiation, and flaw advancement by brittle transgranular cleavage fracture
- stable ductile tearing of an arrested flaw
- crack arrest
- net-section plastic collapse of remaining ligament leading to vessel failure
- unstable ductile tearing leading to vessel failure
- radiation embrittlement as a function of fast neutron fluence, in-service time of RPV, temperature, and depth into wall (attenuation)

b) Stress-Intensity Factor Solutions

Based on the principles of linear-elastic fracture mechanics (LEFM), Mode I stress-intensity factor solutions are calculated by FAVOR for inside and external surface-breaking flaws and embedded flaws. The effects of inner surface cladding are included in the analysis.

Starting with the latest public release of FAVOR, v16.1, procedures for determining LEFM stress intensity factor influence coefficients for internal and external surface-breaking flaws were revised to incorporate new ASME Boiler and Pressure Vessel Code (BPVC 2015) methods [79]. Closed-form curve fits, based on tabular influence coefficient data from API 579/ASME FFS-1 (2007 edition) [83] for both infinite and finite axial flaws and 360° continuous and finite circumferential flaws (base material only), were developed by the ASME Working Group on Flaw Evaluation (WGFE) for the ASME BPVC 2015, Section XI, Appendix A, Article A-3000, *Method of K_I Determination,* Subsections A-3531 and A-3550 [79]. These curve fits [84] [85] were implemented into the FAVLoad, v16.1, module.

c) Brittle and/or ductile crack initiation

The statistical K_{Ic} model in FAVOR v16.1 consists of a family of 3-parameter Weibull distributions, where the *shape* parameter, $c_{K_{Ic}}$, is fixed, and the *location*, $a_{K_{Ic}}$, and *scale* parameters, $b_{K_{Ic}}$, are both functions of the normalized temperature $(T - RT_{NDT})$. The temperature, T, is scaled by a correlative material index called the reference nil-ductility transition temperature, RT_{NDT}. Note that the temperature at the crack tip resides within the RPV wall; therefore, T is a function of both radial distance into the wall and the elapsed time, τ, from the start of the transient of interest.

$$\Pr\left(K_{Ic} \leq K_I(\tau^n)_{(i,j,k)} = cpi(\tau^n)_{(i,j,k)} = \right.$$

$$\begin{cases} 0; & K_I(\tau^n)_{(i,j,k)} \leq a_{K_{Ic}} \\ 1 - exp\left\{ -\left[\dfrac{K_I(\tau^n)_{(i,j,k)} - a_{K_{Ic}}}{b_{K_{Ic}}} \right] \right\}; & K_I(\tau^n)_{(i,j,k)} > a_{K_{Ic}} \end{cases}$$

where

$a_{K_{Ic}} = 21.27 + 9.18 \cdot \exp\left(0.041 \cdot \left[\widehat{\Delta T_{RELATIVE}}\right]\right),$
$b_{K_{Ic}} = 17.16 + 55.10 \cdot \exp\left(0.014 \cdot \left[\widehat{\Delta T_{RELATIVE}}\right]\right),$
$c_{K_{Ic}} = 4,$
$\widehat{\Delta T_{RELATIVE}} = T_{wall}(r,t) - \widehat{RT_{NDT}},$
and $K_{IC}, K_I, a_{K_{Ic}}$ and $b_{K_{Ic}}$ are in $MPa\sqrt{m}$ and $\widehat{\Delta T_{RELATIVE}}$ in °C.

As shown in **Figure 39**, the location parameter, $a_{K_{Ic}}$, establishes a lower boundary to the K_{Ic} probability space. The orange region in **Figure 39** identifies the region in the probability space where the crack can initiate or re-initiate. For a given normalized temperature, $(T - RT_{NDT})$, any point within the orange region has an instantaneous conditional probability of initiation, cpi, corresponding to the percentile curve that the load path touches at a *point of tangency*. The *point of tangency* identifies where the

instantaneous *cpi* reaches a maximum along the load path. This maximum *cpi* is designated as the global *CPI* for this flaw and transient.
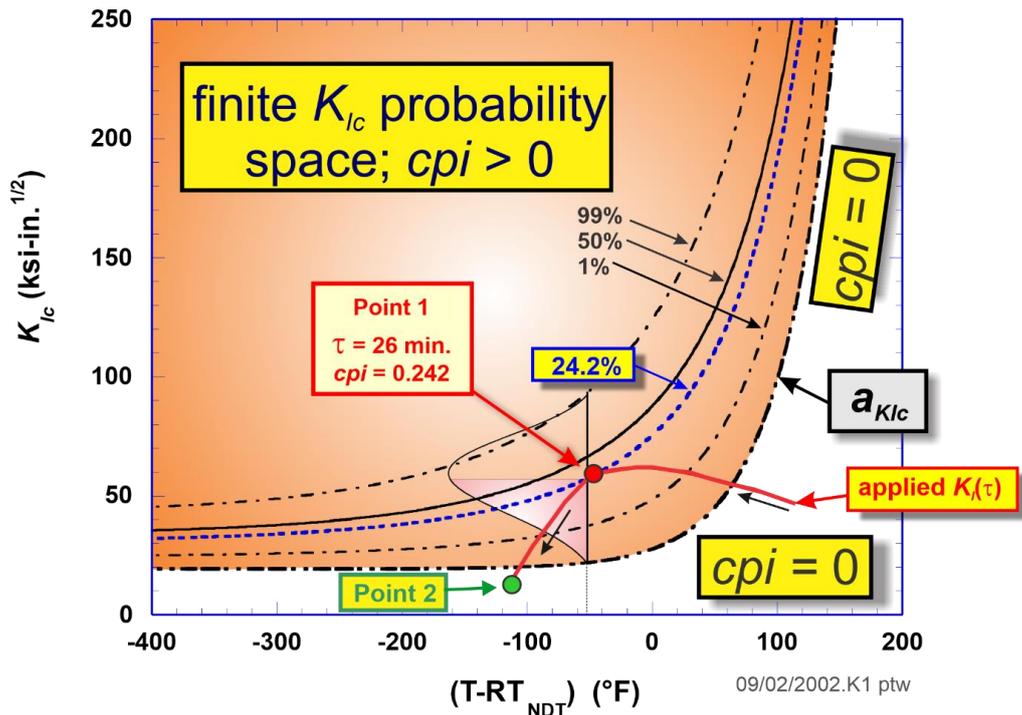
Figure 39: Interaction of the applied K_I time history and the Weibull K_{Ic} statistical model.

As an example, the solid red curve in **Figure 39** maps the load path of a fixed crack tip, where the elapsed time of the transient tracks from right to left along the load path curve. The crack is static and not propagating through the wall. Point 1 in **Figure 39** is located within the K_{Ic} probability space $\left(K_I > a_{K_{Ic}}\right)$, and, at 26 minutes into the transient, the load path touches at a *point of tangency* the 24.2% percentile curve generated by the K_{Ic} statistical model. Point 1, therefore, has a *cpi* = 0.242. After exiting the K_{Ic} space, Point 2 resides outside of the K_{Ic} probability space $\left(K_I \leq a_{K_{Ic}}\right)$; therefore, $cpi = 0$ at Point 2.

For transient index *i,* trial index *j,* and flaw index, *k,* the global conditional probability of initiation, *CPI*, is the sup-norm of the vector of *cpi* values calculated for all the time steps of the transient:

$$CPI_{(i,j,k)} = \left\| \{cpi(\tau^m)\}_{(i,j,k)} \right\|_\infty \text{ for } 1 \leq m \leq n \tag{1}$$

Where n is the number of time steps.

The ductile tearing models are activated if the crack tip temperature is higher than the ductile-tearing transition temperature $T_{DT} = 200$ °F (~93 °C). If it is not, the crack remains at arrest. If it is, $J_{applied}$ is computed from K_I assuming plane-strain as:

$$J_{applied} = \frac{(1 - \nu^2)}{E} K_I^2$$

and the tearing resistance parameters $\widehat{J_{IC}}$, $\hat{C}$ and $\hat{m}$ are sampled from one of the two ductile tearing models available. (Un)stable ductile tearing occurs if $J_{applied} > \widehat{J_{IC}}$ or $J_{applied} > J_R^*$. Otherwise, the crack remains at arrest. J_R^* is the value of $J_{applied}$ at the previous step were ductile tearing occurred.

Thus, $J_R^* = 0$ in first entry to the model or if cleavage re-initiation has occurred since last entry. If ductile tearing occurs, the crack is advanced to first nodal position (a^{**}) following the amount of crack growth produced by $J_{applied}$:

$$\Delta a = \exp\left[\frac{\ln(J_{applied}) - \ln(\hat{C})}{\hat{m}}\right]$$

$$a^* = a_0 + \Delta a$$

and at this new position the tearing resistance modulus T_R and the applied tearing modulus $T_{applied}$ are calculated:

$$\Delta a^{**} = a^{**} - a_0$$

$$T_R = \left(\frac{E}{\widehat{\sigma_{flow}}^2}\right)\hat{m}\hat{C}(\Delta a^{**})^{\hat{m}-1}$$

$$T_{applied} = \left(\frac{E}{\widehat{\sigma_{flow}}^2}\right)\frac{dJ_{applied}}{da}\Bigg|_{a=a^{**}}$$

If $T_{applied} > T_R$ the RPV fails due to unstable ductile tearing.

d) Crack arrest model

If the RPV has not failed, crack arrest is checked using the current chemistry content by calculating the arrest reference temperature $\widehat{RT_{ARREST}}$ as:

$$\widehat{RT_{ARREST}} = \widehat{RT_{NDT(0)}} - \Delta\widehat{RT_{epist-arrest}} + \Delta\widehat{RT_{arrest}} + \Delta\widehat{RT_{NDT}}$$

which is a function of the sampled unirradiated reference temperature $\widehat{RT_{NDT(0)}}$ for the subregion, the epistemic uncertainty in the arrest reference temperature $\Delta\widehat{RT_{epist-arrest}}$ and the sampled value of irradiation shift $\Delta\widehat{RT_{NDT}}$ determined from the embrittlement model applied for this flaw at its current position in the RPV wall. $\Delta\widehat{RT_{arrest}}$ is sampled from a lognormal percentile function and also depends on $\widehat{RT_{NDT(0)}}$ and $\Delta\widehat{RT_{epist-arrest}}$.

In welds, the wall-thickness is divided into quadrants to simulate in an approximate manner 4 different weld layers. If the crack belongs to a weld and has advanced into a new quadrant, the weld chemistry $(\widehat{Cu}, \widehat{Ni}, \widehat{Mn}, \hat{P})$ is resampled with the attenuated fluence $\hat{f}_0$. Then, the irradiation shift $\Delta\widehat{RT_{NDT}}$ and irradiated value of upper shelf energy $\widehat{USE_{(i)}}$ are updated, and the arrest reference temperature $\widehat{RT_{ARREST}}$ is re-calculated. Note that under ductile tearing model number 2, $\widehat{USE_{(i)}} = f(\widehat{USE_{(u)}}, \widehat{Cu}, \widehat{Ni}, \hat{P}, \hat{f}_0)$.

A value of arrest toughness K_{Ia} is drawn from its lognormal distribution with the following means and standard deviations under crack arrest model number 1 or 2:

1:      $K_{Ia(mean)} = 30 + 76.8772 \cdot \exp(0.01093 \cdot \Delta\widehat{T_{RELATIVE}}); [MPa \cdot \sqrt{m}]$

        $\sigma_{\ln(K_{Ia})} = 0.18$

2:      $K_{Ia(mean)} = 30 + 77.6880 \cdot \exp(0.016184 \cdot \Delta\widehat{T_{RELATIVE}}); [MPa \cdot \sqrt{m}]$

        $\sigma_{\ln(K_{Ia})} = 0.34$

with $\Delta\widehat{T_{RELATIVE}}[°C] = T_{wall}(r,t)[°C] - \widehat{RT_{ARREST}}[°C]$

e) Crack interaction and proximity rules

No crack interaction or grouping is considered, but re-sampling of chemistry is applied for multiple flaws.

Flaws are analysed independently. However, multiple flaw consideration in FAVOR is performed in a probabilistic manner by assuming that flaw initiations are independent (not interacting) events. Thus, the total probability that at least one of the flaws will initiate in a RPV trial (j) and transient (i) can be obtained as:

$$CPI_{i,j} = 1 - \prod_{k=1}^{nflaws} \left(1 - CPI_{i,j,k}\right)$$

where $CPI_{i,j,k}$ is the maximum cpi obtained during the transient for flaw No. k. The same method is used to compute CPF of multiple flaws.

f) Global/Local Failure

Assuming that a maximum $cpi > 0$ (CPI) occurs at time τ, the crack becomes a candidate for propagation at time $t \leq \tau$ only if cpi gradient is higher than 0 ($dcpi/dt > 0$). If this is the case, the crack is transformed into its infinite form and $K_{I-inf} > K_I$ is calculated. The applied infinite flaw K_{I-inf} is designated as $K_{I-initiation}$. With time frozen at t, the crack advances to its next position within the finer mesh of the propagation module. At this point, RPV failure by through-wall cracking is checked for the following 3 possibilities:

(1) Net-section plastic collapse: by comparing membrane stress due to pressure, $\sigma_m(t)$, with the sampled flow stress of the material:

$$\widehat{\sigma_{flow}} = \sigma_{flow(u)} + \gamma\widehat{\Delta T_{30}}$$

where γ is a constant that depends on the crack being placed in plate or weld, and $\widehat{\Delta T_{30}}$[7] is a sampled estimate of the material's ductile-to-brittle transition temperature shift between the unirradiated and irradiated Charpy V-notch curves at the $30\ ft-lbf$ ($41\ Joules$) energy level. Ductile tearing crack growth is not checked until the flaw has experienced its first arrest event. If the flaw has arrested and reinitiated in ductile tearing, then:

(2) unstable tearing is checked. If the flaw has re-initiated by cleavage, unstable tearing is not checked. Therefore, crack initiation by ductile tearing is not an event considered by FAVOR. Finally, RPV failure is also possible if:

(3) crack size is deeper than the user-specified fraction of the wall thickness.

The influence of multiple initiating flaws is included in the analysis as described in Sect. 4.3.10 of [13].

g) The WPS model is indicated in Section 5.2.

IPP: SIF-Master

a) No Damage Mechanisms considered (only irradiation embrittlement).

b) No plastic correction is applied. SIF is defined using linear-elastic solutions. For axial and circumferential surface and underclad cracks the solutions of the paper [86] and solutions of Appendix IV of VERLIFE–2008 [27] are used. For axial and circumferential embedded elliptical cracks, the solutions of APPENDIX IV of VERLIFE – 2008 [27] are used. Additional SIF-Master option is to use API 579 and ASME B&PVC SIF formulas for the above mentioned defects.

c) Only brittle crack initiation is considered.

d) In Ukrainian regulatory documents for safety assessment of RPV no crack arrest applied.

e) No crack interaction is considered.

f) Crack initiation event is assumed as global failure. No local failure is considered.

g) In SIF-Master only the tangent point (TP) approach is applied.

---

[7] See pp. 122-133 of the Favor, v16.1, Theory manual [13].

BZN: In-house (under development)

The fracture model for probabilistic assessments will be based on SIF solutions [72] with plastic corrections, taking into account brittle initiation. Other aspects have been described in previous sections.

KIWA: ISAAC

The fracture assessment procedure is based on the R6-method [87]. The procedure is described in the SSM report 2018:18 [71]. In comparison to the original R6-method this procedure contains a safety evaluation system which for the same set of loads gives similar safety margins against fracture initiation and plastic collapse as applied in the ASME Boiler and Pressure Vessel Code, Sections III and XI. Also, the handling of the secondary stresses is somewhat different (more detailed).

Stress intensity factor solutions are given in the SSM report 2018:18 [71]. It is possible to include ductile crack growth in the analysis. Neither crack arrest models nor multiple cracks are included. It is unclear what is meant by global/local failure. Often a local event is analysed that can have a global impact (failure/rupture).

No WPS model is included in ISAAC, so this is handled via pre- and post-processing.

GRS: PROST

The fracture mechanics models implemented in the PROST software for probabilistic fracture mechanical assessment include brittle crack initiation and ductile crack growth. Stress intensity factor solutions from IWM [88] , R6 [87] [87], ASME [79] and SINTAP [89] are implemented (depending on the actual crack geometry). For plastic corrections, the FITNET/SINTAP/R6 approach is used. The models can be applied for a brittle or ductile initiation value. Neither crack arrest models nor multiple cracks are included. PROST can distinguish between local and global failures, but this is rarely done in PTS analysis. A WPS model has not yet been implemented in PROST.

IRSN: In-house (under development)

The fracture mechanics model is a fast fracture analysis performed by comparing the stress intensity factor to the material facture toughness. Stress intensity factor is evaluated from elastic solutions with plastic correction. Both brittle and ductile crack initiation are assessed.

Crack arrest, WPS are not yet considered.

Proximity rules from the RSE-M code are considered for interaction between cracks (detected cracks only).

The fracture mechanics parameters are evaluated by influence coefficient method from RSE-M:

Evaluation of the "elastic" equivalent stress intensity factor K_{eq}:

- Polynomial regression of the thickness stress distribution:

$$\sigma\left(\frac{u}{L}\right) = \sigma_0 + \sigma_1\left(\frac{u}{L}\right) + \sigma_2\left(\frac{u}{L}\right)^2 + \sigma_3\left(\frac{u}{L}\right)^3 + \sigma_4\left(\frac{u}{L}\right)^4$$

- Evaluation of K_{eq}:

$$K_{eq} = K_I = \sqrt{\pi a}\left[\sigma_0 i_0 + \sigma_1 i_1\left(\frac{a}{L}\right) + \sigma_2 i_2\left(\frac{a}{L}\right)^2 + \sigma_3 i_3\left(\frac{a}{L}\right)^3 + \sigma_4 i_4\left(\frac{a}{L}\right)^4\right]$$

The influence coefficients are given in RSE-M, depending on the flaw geometry.
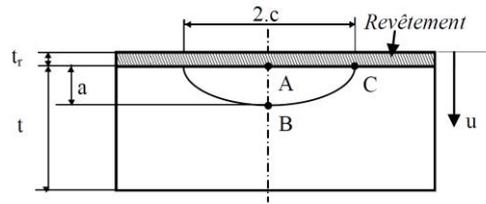
Plasticity Correction from RSE-M:

- Evaluation of radius of the crack tip plastic zone:

$$r_{yA} = \frac{1}{6\pi}\left[\frac{K_{eqA}}{\sigma_{yA}}\right]^2$$

- Stress intensity factor taking into account plasticity (plastic correction) at the crack tip:

$$\begin{cases} K_{cpA} = \beta_A . K_{eqA} & with\ \beta_A = 1 + C_A . th\left(\frac{36\,r_{yA}}{t_r}\right) \\ K_{cpA} = \beta_A . K_{eqA} & with\ \beta_B = 1 + C_B . th\left(\frac{36\,r_{yA}}{t_r}\right) \end{cases}$$

C_A and C_B are coefficients given in RSE-M, *th* is the thickness of the clad.

Evaluation of the margin factor:

$$F_m = \frac{K_{Ic}\ or\ K_{Jc}}{K_{cp}}$$

K_{Ic} or K_{JC} are based on ZG 6100 RCC-M curve [20] (modified ASME curve). This RT_{NDT} approach is used for deterministic calculation. For the probabilistic methodology performed in the frame of APAL, T_0 (or Master Curve) approach should be used.

Crack initiation occurs if the margin factor is less than 1: $F_m < 1$.

JAEA: PASCAL v4

Main features of PASCAL v4 are the following:

- Brittle crack initiation and arrest are judged by comparing the stress intensity factor with fracture toughness. Additionally, PASCAL v4 can evaluate ductile crack propagation based on J-T method (procedure based on J-integral and Tearing Modulus).

- The stress intensity factor can be calculated from the G (influence coefficient) solutions prescribed in the JSME and ASME codes. Weight function method can be applied to complicated distribution of weld residual stress.

- Global/Local failures cannot be distinguished. RPV failure is considered by plastic collapse and/or a critical user-defined crack depth ratio (e.g., $a/t > 0.8$).

7.4.5   What input data are distributed (with exception of flaws) and what is the basis for distribution parameters (standard/code or statistical data)

The input data that are assumed distributed in the tool/software are described by the partners, which includes:

  a. Summary of distributed input data
  b. Type of distribution and sources of distribution parameters
  c. Technical or statistical basis (such as operational experience, material testing, standards, engineering judgement and others) for type of distribution and distribution parameters

UJV: PROVER

Deterministic parameters and calculations

Temperature and stress fields in the RPV wall are calculated deterministically with fixed geometrical and material parameters. Material and thermo-mechanical properties of the base metal and cladding are considered as temperature dependent. For the weld metal the same material properties are used as for the base metal.

Residual stresses are treated deterministically. The stress intensity factor for a given sampled crack is also calculated deterministically.

Thermal-hydraulic parameters (pressure, temperature, heat transfer coefficient in reactor downcomer) for any given representative scenario are also assumed as deterministic.

Stochastic parameters

Stochastic parameters are summarized in **Table 13**.

Table 13: UJV – PROVER: Stochastic parameters.

Input data	Type of distribution	Distribution parameters	Technical or statistical basis for type of distribution and distribution parameters	Method for sampling, see also Section 7.4.1
Fast neutron fluence F ($> 0.5\ MeV$) Spatial distribution of mean fast neutron fluence in modelled region of RPV.	normal distribution	Mean value and standard deviation σ. Mean value depends on point coordinates in RPV. In PROVER, the fluence is approximated by the formula: $$F(r, z, \theta) = \mathrm{M} \cdot f_1(r) \cdot f_2(z) \cdot f_3(\theta),$$ where M depends on assessed lifetime of RPV. Typically, σ = 12% of the mean.	Calculation of fast neutron fluence by transport code (solving Boltzman transport equation or using stochastic methods) validated by neutron fluence monitors located outside RPV.	Fluence is sampled randomly for each flaw
Chemical composition P, Cu, Ni, Mn, Si [%wt]	Normal distribution	Mean value [%wt] and standard deviation [%wt].	Passport data	Chemical composition is sampled for each subdomain (weld or ring)
Initial Master curve reference	Normal distribution	Mean value and standard deviation σ.	Passport data, extended surveillance program (initial	Sampled separately for each

Input data	Type of distribution	Distribution parameters	Technical or statistical basis for type of distribution and distribution parameters	Method for sampling, see also Section 7.4.1
temperature $T_{0,init}$		The standard deviation is given by $$\sigma = [\sigma_1^2 + (1.64\Delta T_M)^2]^{1/2},$$ $$\sigma_1 = \frac{18}{\sqrt{n}},$$ $$\Delta T_M = 16\,°C,$$ where n is number of test specimens, ΔT_M characterizes material inhogomenity.	state material characterization) The value ΔT_M may be determined from material Qualification Tests.	subdomain (welds, rings)
Shift of Master Curve reference temperature ΔT_0 due to neutron fluence. Mean value is calculated from fluence and chemical composition.	Normal distribution	Mean and standard deviation σ Mean value of ΔT_0 depends on fluence and chemical composition. Standard deviation σ may be determined from experimental data or normative values may be used: VVER-440 base metal: $\sigma = 21,7\,°C$ VVER-440 weld metal: $\sigma = 22,6\,°C$ VVER-1000 base metal and weld: $\sigma = 25,0\,°C$	Best fit plus uncertainty estimates from surveillance programs or conservative normative curves. If sufficient amount of experimental data is not available, the ΔT_0 shift may be estimated from the shift of critical temperature of brittleness using $$\Delta T_0 = 1.1 \cdot \Delta T_k$$	
Fracture toughness K_{Ic} and J_{Ic}	Weibull distribution in transition region (for K_{Ic}), normal distribution in ductile region (for J_{Ic})	See detailed description in Section 7.4.4	Wallin Master Curve theory and papers [78] [81].	Fracture toughness is not sampled. Instead, the value of CPI is calculated directly from cumulative distribution function. See Section 7.4.4 for details.
Reference temperature	Lognormal distribution	See detailed description in Section 7.4.4	Ref [82]	Not implemented in PROVER

Input data	Type of distribution	Distribution parameters	Technical or statistical basis for type of distribution and distribution parameters	Method for sampling, see also Section 7.4.1
for crack arrest T_{KIa}				
Fracture toughness for crack arrest K_{Ia}	Lognormal distribution	See detailed description in Section 7.4.4	Ref [82]	Not implemented in PROVER

FRA-G: In-House Tool

Due to the modular structure of Framatome in-house tool, every required input data can be assumed distributed. A typical treatment of input data for a performed analysis with Framatome in-house tool is given in **Table *14***.

Table 14: FRA-G In-house tool – typical treatment of input data

Input data	Treatment
Geometry and dimension of RPV beltline region	Fixed
Flaws: Amount, Size and Location	Distributed
Fracture toughness	Distributed
Crack Arrest	Distributed
Occurrence of LOCA transients	Fixed
Loading of representative PTS transient	Fixed
Neutron fluence (axial and azimuthal distribution)	Fixed
Reference temperature	Distributed

For sampling of distributed input data several methods are applied, such as Box-Müller or inverse sampling. The statistical basis or technical background is based on either available material tests or NDE results, on state-of-the-art or on operational experience. The type of distribution and distribution parameter are estimated case by case and are not pre-defined.

OCI, PSI, Tecnatom, JSI: FAVOR v16.1

A summary of input data and uncertainty treatment for FAVOR is given in

Table *15*.

Table 15: Summary of input data and uncertainty treatment for FAVOR.

Input Category	Input Parameter	Uncertainty Classification	Uncertainty Distribution	References	Comments
RPV geometry	inner radius	constant	NA		
	wall thickness	constant	NA		
	clad thicknes	constant	NA		
base carbon steel	thermal conductivity	constant	NA	ASME BPV Code: Sect. II, Part D, Properties	
thermophysical	specific heat	constant	NA		
properties	Young's modulus	constant	NA		
	thermal expansion coeff.	constant	NA		
	Poisson's ratio	constant	NA		
caladding stainless steel	thermal conductivity	constant	NA	ASME BPV Code: Sect. II, Part D, Properties	
thermophysical	specific heat	constant	NA		
properties	Young's modulus	constant	NA		
	thermal expansion coeff.	constant	NA		
	Poisson's ratio	constant	NA		
thermal expansion	stress free temperature	constant	NA		
thermal-hydraulic	film coefficient	constant	NA	input from PRA studies	function of elapsed transient time
definition	coolant temperature	constant	NA	input from PRA studies	function of elapsed transient time
	coolant pressure	constant	NA	input from PRA studies	function of elapsed transient time
plate and forging	copper (Cu)	epistemic	normal	FAVOR Theory Manual: Sect. 5.2.9	
material	nickel (Ni)	epistemic	normal		
chemistries	phosphorous (P)	epistemic	normal		
	manganese (Mn) plate	epistemic	normal		standard deviation: Weibull
	manganese (Mn) forging	epistemic	normal		standard deviation: Johnson-SB
weld	copper (Cu)	epistemic	normal	FAVOR Theory Manual: Sect. 5.2.9	
material	nickel (Ni)	epistemic	normal		
chemistries	phosphorous (P)	epistemic	logistic		
	manganese (Mn) weld	epistemic	normal		standard deviation: Weibull
radiation damage	fast neutron fluence	epistemic	normal		
initiation	fracture toughness initiation, K_{Ic}	aleatory	Weibull		brittle transgranular cleavage
arrest	crack arrest, K_{Ia}	aleatory	lognormal		
	radiation shift	epistemic	Weibull		

Table *16* includes a summary of the distributed parameters in FAVOR. Note that sampling from normal distribution is performed in FAVOR with an extension of Forsythe's method. For other sampling methods see also Table 4 in Section 7.4.1.

Table 16: Distributions used in FAVOR.

Input data	Type of distribution	Distribution parameters	Technical or statistical basis for type of distribution and distribution parameters	Method for sampling, see also Section 7.4.1
$\widehat{Cu}, \widehat{Ni}, \widehat{Mn}, \widehat{P}$ content	Truncated normal distribution	Means and standard deviations. Std of Mn is a distributed parameter from	Table 15 in [13] Recommended SD values in plates and forgings:	

Input data	Type of distribution	Distribution parameters	Technical or statistical basis for type of distribution and distribution parameters	Method for sampling, see also Section 7.4.1
		Weibull (plates) and Johnson Sb (forgings) distributions. In welds, local variability is determined by sampling values from logistic, normal and Johnson Sb distributions.	$\sigma_{Cu} =$ 0.0073 wt% $\sigma_{Ni} =$ 0.0244 wt% $\sigma_{Cu} =$ 0.0013 wt% See equations 120-123 in [13]	
Fluence at the inside surface of the vessel $\widehat{f_0(0)}$	Truncated (2) normal distribution	Mean fluence of the subregion f_{subreg}. Global multipliers SIGFGL = 0.118 and SIGFLC = 0.056 which dictate a sample mean fluence and a sampled standard deviation		$\sigma_{global} = SIGFGLxf_{subreg}$ $\widehat{f_{mean}} \leftarrow N(f_{subreg}, \sigma_{global})$ $\widehat{\sigma_{local}} = SIGFLCx\widehat{f_{mean}}$ $\widehat{f_0(0)} \leftarrow N(\widehat{f_{mean}}, \widehat{\sigma_{local}})$
$\widehat{RT_{NDT(0)}}$	Normal distribution	Mean unirradiated $\overline{RT}_{NDT(0)}$ (recommended values of -8°F for welds and 0°F for plates and forgings) and $\sigma_{RT_{NDT(0)}}$.	$RT_{NDT(0)}$ is the heat estimate and it is not distributed if taken from the Reactor Vessel Integrity Database (RVID2) - ASME NB-2331 or MTEB 5-2. If Generic method is chosen, then it is sampled from normal distribution.	
$\widehat{\Delta RT_{epistemic}}$	Weibull percentile function (inverse CDF)	$\Phi \leftarrow U(0,1)$	Appendix F in [13]	$\widehat{\Delta RT_{epistemic}} = -29.5 + 78.0 \cdot [-\ln(1 - \Phi)]^{1/1.73}$ where $\Phi \leftarrow U(0,1)$
$\widehat{\Delta RT_{NDT}} = c \cdot \widehat{\Delta T_{30}}$ where $c = 0.99$ (welds) and $c =$	$\widehat{\Delta T_{30}}$ sampled from Eason 2000 [101] and Eason 2006 [102]	$\widehat{f_0(0)}, \widehat{Cu}, \widehat{Ni}, \widehat{Mn}, \widehat{P}, \tau_{exposure}(EFPY)$ $T_{coolant}$		

Input data	Type of distribution	Distribution parameters	Technical or statistical basis for type of distribution and distribution parameters	Method for sampling, see also Section 7.4.1
1.10 (plate and forgings)	embrittlement correlation			
$\widehat{cpi} = \Pr(K_{IC} < K_I)$	Weibull distribution	$a_{K_{Ic}}(\Delta T_{\widehat{RELATIVE}})$ $b_{K_{Ic}}(\Delta T_{\widehat{RELATIVE}})$ $c_{K_{Ic}}$. See eqns. in section 7.4.4 and eqns. below	If crack is in WPS state, $cpi = 0$.	
$\Delta RT_{\widehat{epist-arrest}}$ $= \Delta RT_{\widehat{epistemic}}$ $+ \Delta(\Phi)$	Shift of $\Delta RT_{\widehat{epistemic}}$ defined above	$\Delta RT_{\widehat{epistemic}}$ and Φ		
$\Delta \widehat{RT_{arrest}}$ $= 1.8$ $\cdot \exp\left[\hat{\sigma}_{ln(\Delta RT_{arres}} + \hat{\mu}_{ln(\Delta RT_{arrest})}\right]$	Lognormal percentile distribution	$RT_{\widehat{NDT(0)}}$, $\Delta RT_{\widehat{epist-arrest}}$ and $\hat{z}_{P_f} \leftarrow N(0,1)$ corresponding to $\widehat{P_f} \leftarrow U(0,1)$	See Eq. 139 in [13]. At this point: $RT_{\widehat{ARREST}}$ can be calculated acc. to Eq. in Section 7.4.4. $\Delta T_{RELATIVE}$ and $K_{Ia(mean)}$ acc. to Eq. in Section 7.4.4.	
$\widehat{K_{Ia}}$	Lognormal distribution	$\sigma_{\ln(K_{Ia})}$, $\hat{\mu}_{ln(\Delta RT_{arrest})}$ and fractile $\widehat{\Phi}_{K_{I-initiation}}$, which depend on $K_{I-initiation}$, $K_{Ia(mean)}$ and $\Delta T_{RELATIVE}$		
$\widehat{\sigma_{flow}}$	Calculated with Eqn. in section 7.4.4	$\widehat{\Delta T_{30}}$		
Alpha in best estimate WPS model (see section 5.3.1)	log-logistic distribution	a, b and c in distribution	SMILE project, Table 3 in [13]	
$\widehat{J_{IC}}, \hat{C}$ and $\hat{m}$ tearing resistance parameters in recommended Model 1	$\widehat{J_{IC}}$ truncated normal distribution. $\hat{m}$ normal distribution. $\hat{C}$ is derived from $\widehat{J_{IC}}$ and $\widehat{\sigma_{flow}}$	$\widehat{T_0}$ (1T) from a Weibull distribution using $RT_{\widehat{NDT(0)}}$, $\Delta \widehat{RT_{NDT}}$ and fractile Φ. Upper shelf $\widehat{T_{US}}$ using $\widehat{T_0}$. Mean $\overline{J_{IC}}$	NUREG experimental data, Tables 6-8 in [13]	

141

Input data	Type of distribution	Distribution parameters	Technical or statistical basis for type of distribution and distribution parameters	Method for sampling, see also Section 7.4.1
		and $\sigma_{J_{IC}}$ using all the above and T_{wall}		
$\widehat{USE_{(u)}}$	Normal distribution	Best-estimate value for unirradiated upper-shelf energy (mean-USE(u)) and standard deviation is sampled also from normal distribution with mean derived from mean-USE(u) and 2.2789 std.	Ductile tearing model number 2 [13]	
$\widehat{USE_{(i)}}$	Analytical expression	$\widehat{USE_{(u)}}, \widehat{Cu}, \widehat{Ni}, \hat{P}, \hat{f}_0$	Ductile tearing model number 2 [13]	Eq. (33) in [13]

$$\widehat{RT_{NDT}} = \widehat{RT_{NDT(0)}} - \widehat{\Delta RT_{epistemic}} + \widehat{\Delta RT_{NDT}} \qquad \text{(Eq. 104 in [13])}$$
$$\widehat{\Delta T_{RELATIVE}} = T_{wall}(r,t) - \widehat{RT_{NDT}} \qquad \text{(Eq. 136 in [13])}$$
$$\text{Arrest } \widehat{T_0} = \widehat{RT_{NDT(0)}} - \widehat{\Delta RT_{epist-arrest}} \qquad \text{(Eq. 139 in [13])}$$
$$\widehat{RT_{ARREST}} = \widehat{RT_{NDT(0)}} - \widehat{\Delta RT_{epist-arrest}} + \widehat{\Delta RT_{arrest}} + \widehat{\Delta RT_{NDT}} \qquad \text{(Eq. 109 in [13])}$$

In **Table 17** some distributed parameters are presented by PSI that differ from FAVOR recommendations.

Table 17: Distributed parameters from PSI.

Input data	Type of distribution	Distribution parameters	Technical or statistical basis for type of distribution and distribution parameters
ΔRT_{NDT} [°C]	Normal	ΔT_{41}	Parameters and distribution from RG 1.99 Rev. 2 [90]
K_{IC} reference curve (FAVOR) $K_{IC\,max}$=220 [MPa·m$^{0.5}$]	Weibull	FAVOR method	Parameters and distribution from FAVOR
K_{Ia} reference curve (FAVOR) $K_{Ia\,max}$=220 [MPa·m$^{0.5}$]	Lognormal	FAVOR method	Parameters and distribution from FAVOR
Cooper content Cu [wt. %]	Normal	$\mu = 0.092$ $\sigma = 0.01$	Parameters from internal report Distribution from PROSIR [42]

Input data	Type of distribution	Distribution parameters	Technical or statistical basis for type of distribution and distribution parameters
Nickel content Ni [wt. %]	Normal	$\mu = 0.71$ $\sigma = 0.05$	Parameters from internal report Distribution from PROSIR [42]
Phosphorous content P [wt. %]	Normal	$\mu = 0.014$ $\sigma = 0.001$	Parameters from internal report Distribution from PROSIR [42]
Neutron fluence f_o [10^{19} n/cm^2]	Normal	$\mu = [1 - 6.4]$ $\sigma = 10\% \mu$	Parameters from internal report Distribution from PROSIR [42]

IPP: SIF-Master

Table 18: IPP SIF-Master – Distributed input data

Input data	Type of distribution	Distribution parameters	Technical or statistical basis for type of distribution and distribution parameters
T_k	Normal	T_k or ΔT_k	Ukrainian surveillance database. Method is described in paper [91]
			Ukrainian surveillance database. Method is described in paper [92]
K_{IC}	Normal	T_k or ΔT_k	$K_{IC}(T) = 74 + 11 \cdot e^{0,0385(T+18,9-T_K)}$, $\sigma = 29,3$ºC – for base metal $K_{IC}(T) = 35 + 53 \cdot e^{0,0217 \cdot (T+23,8-T_K)}$, $\sigma = 18,8$ºC – for welds
Ni, Mn, Si	Normal	*Ni, Mn, Si*	Normal law is based on chemical composition measurement data for specific RPV

BZN: In-house (under development)

Not defined yet.

KIWA: ISAAC

In principle, any input data can be a probabilistic parameter of a stochastic nature. However, the most commonly used parameters to be included in an analysis are:

- Fracture toughness.
- Yield strength.
- Ultimate tensile strength.
- Primary stresses.
- Secondary stresses.
- Defect size (depth) given by NDT/NDE.

- Defect distribution.
- POD-curve.
- Constants in the fatigue crack growth law.
- Constants in the SCC crack growth law.

The choice of distribution for a parameter may depend on material testing, standard recommendations, simulations, and expert judgement. This means that a certain parameter can best be described by different distributions depending on the current conditions (a typical example is the fracture toughness). Some recommendations regarding distributions and input data can be found in the SSM report 2018:18 [71].

The description of fracture toughness given in DEFI-PROSAFE is not included in ISAAC, therefore a special version will be developed for the APAL project.

As for the "method of sampling" it is relevant for Monte Carlo simulation, but it is not relevant in a FORM/SORM analysis (which does not contain any sampling at all).

GRS: PROST

Nearly all parameters in PROST can be defined as distributed functions (Structure geometry, crack geometry, material parameters, damage mechanism characteristics, loads …). Different types of distribution functions are implemented.

IRSN: In-house (under development)

The input data that we identify as relevant to distribute randomly are mainly material characteristics: toughness, transition temperature, to a lesser extent tensile characteristics, and Young modulus. Their distributions have not been discussed yet but references such as the Master Curve concept shall be used.

JAEA: PASCAL v4

In PASCAL v4, the input data along with their distributions are summarized in Table 19. All of them were discussed and determined in a Japanese RPV structural integrity research committee.

<div align="center">**Table 19: JAEA PASCAL v4 – Distributed input data.**</div>

Item	Content/Description
Neutron fluence	Normal distribution based on Japanese data and expert judgement
Chemical compositions	
RT_{NDT}	
Flaw distribution	Data calculated from VFLAW by using the welding conditions (e.g., welding method and bead thickness) for Japanese RPVs
Occurrence of transients	Data refer to the US NUREG-1874 report [93]
Fracture toughness K_{Ic}	Weibull distribution based on Japanese data
Crack arrest toughness K_{Ia}	Lognormal distribution based on Japanese data

7.4.6   What flaw distribution (type, parameters) is used and what is the technical/statistical background

Special attention was paid to the description of flaw distribution used in probabilistic PTS analysis. The description of the partners should include:

a. Type of flaws to be addressed (surface, underclad, etc.)
b. Flaw size distribution and its technical/statistical background

    c. Flaw shape (aspect ratio) distribution, other flaw parameters (orientation) and their technical/statistical background

    d. Distribution of number of flaws (flaw density) and its technical/statistical background

    e. Role of NDE (if any) for determination and/or validation of flaw density, flaw size and other flaw parameters distributions.

UJV: PROVER

a) According to [8], the following types of cracks are included into the RPV probabilistic assessment:

- embedded cracks in welds (elliptical shape, circumferential orientation only)
- underclad cracks in base metal (semi-elliptical shape, axial orientation only)
- embedded cracks in base metal (elliptical shape, both circumferential and axial orientation)

The axial and circumferential orientations of the embedded flaws in the base metal are assumed to have the same probability.

Embedded flaws in the base metal are assumed to be uniformly distributed in the volume of the base metal. Flaws in welds are assumed to be uniformly distributed along the through-wall (radial) dimension of the RPV. Underclad cracks are assumed to be uniformly distributed beneath the interface between the base metal and cladding.

Surface breaking cracks are not postulated in the RPV probabilistic assessment because they were never detected in the Czech NPPs. In the PROVER code, semi-elliptical underclad cracks are replaced by elliptical cracks of the same depth for the sake of simplicity, therefore only the elliptical cracks are modelled.

b), c), d) Flaw density, number of flaws and flaw dimensions are modelled as random variables in PROVER. Parameters of the underlying statistical distributions are estimated from the results of ultrasound NDE of welds, base metal and cladding of the assessed RPV (or group of RPVs of the same type and manufacturer).

The statistical distributions presented below are recommended by [8]. Different distributions may be used if they represent available data better. Crack parameter estimation is based on Bayes approach using non-informative priors. The mathematical approach is similar to that of Appendix A of [94].

The number of flaws N in a particular material volume V (e.g., a RPV ring) is modelled by a Poisson distribution with the mean value $\lambda = \rho V$, where ρ is flaw density. The probability density function of the number of flaws N is given by

$$f(N \mid \rho) = \exp(-\rho V) \frac{(\rho V)^N}{N!}$$

The flaw density ρ is supposed to be gamma distributed. Under the assumption that all flaws were detected in a control volume V_0 (with 100% probability of detection) the probability density function for ρ is given by

$$f(\rho \mid M, V_0) = \frac{V_0^M \rho^{M-1} \exp(-V_0 M)}{(M-1)!},$$

where M is the number of flaws detected in the control volume V_0.

The flaw depth D is assumed to have an exponential distribution with parameter β_D

$$f(D \mid \beta_D) = \beta_D \exp(-\beta_D D).$$

The parameter β_D is supposed to be gamma distributed. Under the idealised assumption that the probability of detection is independent of the flaw depth and that all flaws are accurately sized, the probability density for β_D is given by

$$f(\beta_D \,|\, d, M) = \frac{d^M \beta_D^{M-1} \exp(-dM)}{(M-1)!},$$

where M is the number of detected flaws, d_i is the depth of the i-th flaw and $d = \sum_{i=1}^{M} d_i$.

The flaw lengths are modelled under the assumption that the flaw length L minus flaw depth D has exponential distribution with parameter β_{LMD}:

$$f(L \,|\, \beta_{LMD}, D) = \beta_{LMD} \exp\bigl(-\beta_{LMD}(L - D)\bigr) \quad \text{for } L \geq D$$

$$f(L \,|\, \beta_{LMD}, D) = 0 \quad \text{for } L < D$$

The parameter β_{LMD} is supposed to be gamma distributed. Under the idealised assumption that the probability of flaw detection is independent of $L - D$ and that all flaws are accurately sized, the probability density for β_{LMD} is given by

$$f(\beta_{LMD} \,|\, h, M) = \frac{h^M \beta_D^{M-1} \exp(-hM)}{(M-1)!},$$

where M is the number of detected flaws, l_i and d_i are length and depth of the i-th flaw, respectively, and $h = \sum_{i=1}^{M}(l_i - d_i)$.

e) The flaw density and dimensions are currently estimated only by ultrasound NDE and engineering judgement, because no destructive examination of relevant mock-ups has ever been made for RPVs of the Czech NPPs.

FRA-G: In-House Tool

Any kind of flaw can be assessed. Until now Framatome has addressed surface, underclad and embedded flaws. The underlying flaw distribution is either based on available NDE results (detailed UT records for RPV including also non recordable indications) or on generic flaw distributions given in NUREG/CR-6817 [94] and NUREG 1874 [93]. Several aspects need to be considered to estimate the distribution of flaws based on NDE results, such as NDE technique, detection limit, product form (plate, ring, weld) and manufacturing process.

OCI, PSI, Tecnatom, JSI: FAVOR v16.1

Remark: The following description is compilation of OCI, PSI, Tecnatom and JSI responses.

Description of flaw distributions in FAVOR

FAVOR has the user-specified optional ability to model three different flaw populations as follows:

Flaw population 1: All surface-breaking flaws (quantified in the surface flaw characterization input file) are internal surface breaking flaws and only those embedded flaws in the first 3/8 of the RPV wall thickness are included in the model. The primary application of this option is for modelling cool-down transients. Through-wall flaw propagation is included in this option.

Flaw population 2: All surface-breaking flaws (quantified in the surface flaw characterization input file) are external surface breaking flaws and only those embedded flaws in the outer 3/8 of the RPV wall thickness are included in the model. The primary application of this option is for modelling heat-up transients. Through-wall flaw propagation is not yet included in this option.

Flaw population 3: Includes internal and external surface-breaking flaws (double the number than that in options 1 or 2 and evenly divided between external and internal surfaces), and all of the embedded flaws are uniformly distributed through the RPV wall (approximately 8/3 times the number in options 1 or 2). The primary application of this option is for modelling transients where pressure induced loading is dominant such as hydro-testing. Through-wall flaw propagation is not yet included in this option.

Focusing on flaw population 1, three crack types are considered:

146

- **Crack type 1** is a surface-breaking crack.
- **Crack type 2** is an embedded crack, which has fully-elliptic geometry with inner crack tip located between the clad/base metal interface and 1/8 t from the inner surface.
- **Crack type 3** is an embedded crack, which has fully-elliptic geometry with inner crack tip located between 1/8 t and 3/8 t from the inner surface.

PSI also analysed flake-like cracks, as observed in the Belgian reactors; by means of XFEM analyses (see publication [95]).

Technical Background

Reference [94], authored by Pacific Northwest National Laboratory (PNNL) in the USA, provides comprehensive documentation regarding how a flaw-related input methodology was developed for the FAVOR probabilistic fracture mechanics code ([13] [65]). Through support provided by the USNRC, PNNL carried out a multi-year program to develop the structure of that flaw estimation model that can generate flaw input data essential for FAVOR PFM analyses of RPVs. As described in [94], the developmental process used by PNNL and the USNRC consisted of several key tasks:

1. Experimental work consisting of destructive and non-destructive examinations of RPV materials was performed to construct a database on fabrication flaws in welds, base metals, and cladding of RPVs fabricated from the late 1960s through the early 1980s. Included in the PNNL studies were the PVRUF vessel located at ORNL ([96], [97]) and the Shoreham vessel ([98]).
2. An expert solicitation process was used to augment gaps identified in the empirical database for RPV materials. Results from that expert judgment task were reported by the USNRC in [99].
3. Defect size distributions and densities for multi-pass welds were generated by applying the flaw simulation model in the PRODIGAL expert system (originally developed by Rolls-Royce [100]). For this task, the PRODIGAL system was updated to address the thick-section welds found in USA RPVs.
4. Data from the foregoing tasks 1-3 were used by PNNL to develop statistical flaw distribution functions for weld metal, base metal, and for surface-breaking flaws that reside in vessel cladding, respectively. Details of that statistical development are described in Chapters. 6-8 of [94].
5. The flaw estimation model from Task 4 was integrated into a PNNL FORTRAN computer algorithm that generates flaw-related input files for the FAVOR code (see Chapter 9 of [94]).

The following discussion provides:

- a brief overview of the flaw-related input data required by FAVOR to perform a PFM analysis of an RPV subjected to transient loading, and
- a summary of flaw-related files generated by the PNNL FORTRAN algorithm that meet those FAVOR requirements.

Input Files Required by the FAVOR Code

The flaw model employed in the FAVOR PFM code requires:

- three input files to simulate the size and location of each flaw for the following three categories of RPV regions:
    1) flaws in weld regions,
    2) flaws in base metal regions, and
    3) surface-breaking flaws in the RPV cladding and base material,
- user input data specifying the volume of metal for each RPV subregion; each subregion has its own specified embrittlement-related properties,

- the number of flaws per unit volume of material, or per unit area of weld fusion area, which are specified in numerical tables of data, and
- treatment of statistical uncertainties in flaw-related parameters, which is accomplished by generation of 1000 possible tables that reflect estimated uncertainties in the parameters of flaw distributions. Those tables describe the number of flaws per unit volume or area for defined ranges of depth dimension (as a percentage of RPV wall thickness), and for defined ranges of aspect ratios (length divided by depth). Locations of flaws in weld and base material regions are randomly distributed through the vessel thickness.

PNNL Computer Code for Generating FAVOR Flaw Input Files

The flaw input files required for a FAVOR PFM analysis can be generated using a FORTRAN compute program written by PNNL as part of their USNRC work, as referenced above. The PNNL code generates those FAVOR flaw input files using the following procedures:

- Calculations are based on three flaw distribution functions derived from PNNL studies:

    1) flaw densities,
    2) flaw depth dimensions, and
    3) flaw lengths or aspect ratios.

- The flaw distribution algorithm performs Monte Carlo calculations that simulate or sample from the uncertainty distribution for the parameters of the flaw distribution functions.
- The number of Monte Carlo simulations is typically set to specify 1000 simulations to generate 1000 samples for the uncertainty analysis
- The flaw distribution algorithm has three parts to individually address the three types of vessel regions, i.e., welds, base metal and cladding.
- Each run of the algorithm addresses one category of vessel region.
- An output file is generated by the PNNL code for use by FAVOR as an input file. This file is a relatively large file that is not intended to be printed as a hard copy.
- The output file contains flaw distribution tables for all the samples of flaw distribution that are calculated by the Monte Carlo simulations.
- The output file can be printed to provide the user with the first 10 of the large number (e.g., 1000) of samples.

Further details concerning construction of FAVOR flaw-related input files are beyond scope of the current document. The reader is referred to [13] [65] and [94] for an in-depth presentation.

IPP: SIF-Master

a) Semi-elliptical surface and underclad cracks as well as elliptical embedded (internal) cracks are considered as axial and circumferential.

b) Exponential function of defect depth distribution is used

$$f(x) = \frac{1}{a_0} \exp\left(-\frac{x}{a_0}\right)$$

where: a_0 - parameter of the exponential distribution (a_0=1,98 mm for base metal and a_0=2,05 mm – for welds). It is based on statistical data of NUREG report [103] (these parameters were verified using the data taken from the defect statistics of Ukrainian WWER-1000 RPVs (as result of NDE) – it was found that using these parameters is slightly conservative). These parameters were adjusted (if needed) depending on defect statistics of the specific RPV.

c) Shape of defect $\beta = L/a$ (half-length to depth ratio) is taken as probabilistic and is sampled from the lognormal distribution law according to [103]:

148

$$f(\beta) = \begin{cases} 0 & \beta < 1 \\ \dfrac{C}{\lambda\beta\sqrt{2\pi}}\exp\left[-\dfrac{1}{2\lambda^2}\left(\ln\beta/\beta_m\right)^2\right] & \beta \geq 1 \end{cases},$$

where the initial distribution parameters are taken as follows: λ=0,5382; C=1,419; β_m=1,136. It was assumed that this distribution law of the defect shape does not depend on the depth. Short defects ($\beta < 1$) are excluded from consideration.

d) Defect number is calculated using RPV dimensions and defect density according to Table 20.

Table 20: IPP SIF-Master – Defect density.

Zone	Crack type	Source	Defect density
Base metal	Internal (embedded)	[96]	620 def/m^3
	Surface or underclad	[104], [105]	150 def/m^2
Weld metal	Internal (embedded)	[96]	2730 def/m^3
	Surface or underclad	[104], [105]	70 def /running meter

e) The NDE results of specific RPV are used for validation of the laws distributions of both defects depth and defect shape, distribution and defect density as well.

BZN: In-house (under development)

Not defined yet.

KIWA: ISAAC

Surface or embedded cracks can be included in the analysis. Defect depth distributions are quite difficult to estimate reliably for any given application. This is because very few defects of significance have been observed by NDE of plain welds in pressure vessels. Some recommendations can be found in the SSM report 2018:18 [71]. These recommendations are based on results obtained from NDE in combination with simulation of the number and size of defects generated during the welding process.

GRS: PROST

Surface flaws of semi-elliptical shape with different depths and lengths are postulated according to the KTA standard KTA 3201.2 [9]. The actual size depends on the assumed load case. Typical positions of the postulated flaws are near core welds and the nozzle region of the main cooling line.

IRSN: In-house (under development)

The cracks characteristics were not distributed in former safety assessments analysed at IRSN: they were based on deterministic and conservative approaches.

The flaw position considered is the worst location regarding the fluence on the RPV wall and the flaw dimensions are the largest that cannot be detected considering the NDE used. Underclad defects are considered since they are the most critical ones. For the APAL project, we intend to consider only one underclad defect.

The flaw size and position are to be taken as distributed quantities.

JAEA: PASCAL v4

The information on flaws considered in PASCAL4 is given as follows:

- Several types of flaws can be considered, such as surface flaw, embedded flaw, underclad flaw, infinite-length flaw.

- For initial surface and embedded flaws, distributions of flaw size and density are generated from the VFLAW code [94] by using the welding conditions (e.g., welding method and bead thickness) for Japanese RPVs.

7.5 Conclusions

In the following sections the conclusions on state-of-the-art for probabilistic PTS analysis and relevant statistical tools are given. The conclusions are drawn from

- the evaluation of the questionnaire responses,
- the additional information provided and
- the discussions during the task meetings.

7.5.1 Methods for calculation of probability

In the following, the most common methods for calculation of probability in the scope of PTS analysis are summarized. A comparison of the different methods is presented in Annex 5.2 of Deliverable D1.4 [4] and will be assessed in WP4.

7.5.1.1 Monte Carlo Method

For probabilistic fracture mechanics, it is common practice to use Monte Carlo method for calculation of probability with the general approach that each Monte Carlo run gives either "failure" or "non-failure" and finally the probability of failure is simply the sum of number of failure runs divided by the total number of Monte Carlo runs. This is schematically shown in **Figure 40**.
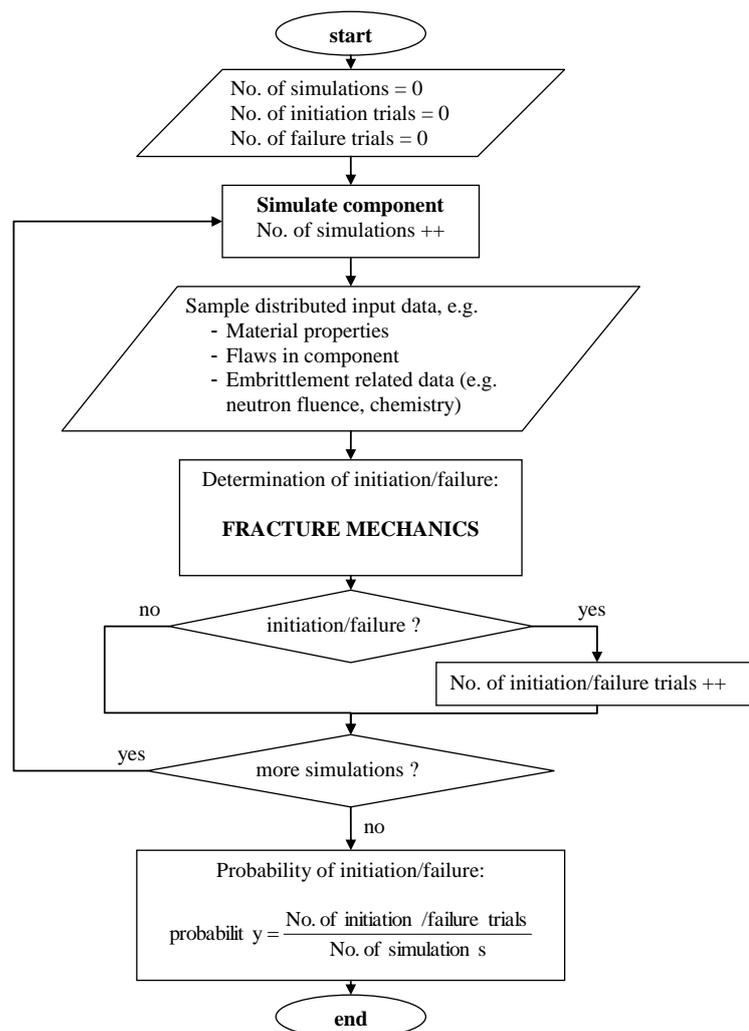
Figure 40: Flow chart of standard Monte Carlo method for fracture mechanics assessment.

For some tools (like FAVOR and PROVER) each Monte Carlo run gives a probability of failure (or initiation). This is due to the fact that fracture toughness and arrest toughness are not sampled, they remain as distributions, and this results in obtaining a probability of failure (or initiation) per one Monte Carlo run. Using this approach, mean value and standard deviation of failure and initiation probability related to aleatory uncertainties in fracture toughness and crack arrest are calculated (see also Section 7.4.1). It should be mentioned that the standard deviation related to these aleatory uncertainties is not an indicator for the convergence of the Monte Carlo method.

For a sufficiently large number of Monte Carlo runs the result of the standard Monte Carlo method (No. of failure runs divided by No. of Monte Carlo runs) is expected to coincide with the mean value of FAVOR's Monte Carlo simulations, if the underlying distributions for fracture toughness and crack arrest as well as for other sampled input data are the same. This has been shown in the simple benchmark in Annex 5.2 of Deliverable D1.4 [4].

The convergence of the Monte Carlo method is an important issue that needs to be addressed as it provides information on how accurate the result is. In this context, the convergence of Monte Carlo method is attained, if a sufficiently large number of runs are performed to get a stable result. Until now it is more or less common practice to arbitrarily select the number of Monte Carlo runs based on the expected probability or on an allowable value for the probability. Convergence criteria are not typically used in many cases.

To track run-time estimates of the convergence of the Monte Carlo method, FAVOR and PROVER use the visualization of the running-average and running coefficient of variation of the CPI and CPF over the current number of Monte Carlo trials as the solution evolves (see Figure 32 and Figure 33 Figure 33: Tracking convergence of TWCF as a function of RPV realizations.

in section 7.4.1). It is recommended to address the convergence of a Monte Carlo method by a quantification of the coefficient of variation, *CV*, and/or standard error, *SE*, of the Monte Carlo result, e.g.

- Coefficient of variation, *CV,* for the current number of completed MC trials, n_{trials}, or runs:

$$CV_{n_{trials}} = \frac{\sigma_{n_{trials}}}{\mu_{n_{trials}}}$$

  where $\mu_{n_{trials}}$ = running average at n_{trials} of the desired metric, e.g., *CPI* for a specified transient

  $\sigma_{n_{trials}}$ = running sample standard-deviation at n_{trials} of the desired metric

  n_{trials} = number of completed Monte Carlo trials

  Example: $\mu_{n_{trials}} = \sum_{j=1}^{n_{trials}} \frac{CPI_j}{n_{trials}}$; $\sigma_{n_{trials}} = \sqrt{\sum_{j=1}^{n_{trials}} \frac{\left(CPI_j - \mu_{n_{trials}}\right)^2}{n_{trials}-1}}$; $CV_{n_{trials}} = \frac{\sigma_{n_{trials}}}{\mu_{n_{trials}}}$

- Standard error, *SE*, for the current number of completed MC trials, n_{trials}, or runs:

$$SE_{n_{trials}} = \frac{\sigma_{n_{trials}}}{\sqrt{n_{trials}}}$$

  where $\sigma_{n_{trials}}$ = running sample standard-deviation at n_{trials} of the desired metric

  n_{trials} = number of completed Monte Carlo trials

  Example: $\mu_{n_{trials}} = \sum_{j=1}^{n_{trials}} \frac{CPI_j}{n_{trials}}$; $\sigma_{n_{trials}} = \sqrt{\sum_{j=1}^{n_{trials}} \frac{\left(CPI_j - \mu_{n_{trials}}\right)^2}{n_{trials}-1}}$; $SE_{n_{trials}} = \frac{\sigma_{n_{trials}}}{\sqrt{n_{trials}}}$

For Monte Carlo method with either "failure" or "non-failure" as result of each Monte Carlo run, the standard error is given by:

- Standard error:

$$e_n = \frac{\sigma}{\sqrt{n}}$$

$$\sigma = \sqrt{\frac{n \cdot \mu - n \cdot \mu^2}{n-1}}$$

with μ = mean value (i.e., result of Monte Carlo method)
        n = Number of MC runs
        σ = standard deviation

- To reduce the standard error by a factor of 10, 100 times more simulations are needed

As probabilistic PTS analyses are mostly dealing with very low probabilities (< 10^{-6}), an appropriate random number generator is needed to ensure an adequate result not impacted by the limitation of the sequence of random numbers. The choice of appropriate random number generator is always a question of sufficient length of random number sequence and of computation time. Commonly used is the Mersenne Twister Algorithm (https://en.wikipedia.org/wiki/Mersenne_Twister) and other self-made algorithms (see for example OCI's response in Section 7.4.1).

7.5.1.2   FORM/SORM

The first-order and second-order reliability methods (FORM and SORM) are commonly used probability estimation methods.

In the field of probabilistic fracture mechanics assessment FORM/SORM is used for different aspects:

- Determination of initiation or failure probability
- Sensitivity study to quantify the impact of different input data
- Importance Sampling

If FORM or SORM is used to calculate the probability of initiation or failure for PTS analysis, some inherent uncertainties due to the method remain:

- Find the most probable point (MPP): For PTS analysis the limit state for failure (or initiation) is usually not a closed form solution, mainly due to stress intensity factor solutions used (e.g., based on tabular influence functions). Therefore, the MPP has to be determined iteratively with a remaining error from the correct MPP. For simple approaches a closed form solution of the limit state can be formulated and mathematical methods, like Newton's method or Simplex algorithm, can be used to determine the MPP.
  Moreover, if a limit state function leads to multiple MPPs, the FORM/SORM cannot be assessed directly to determine the probability for $g(u) > 0$. Multiple MPPs make an adjustment of FORM/SORM necessary.
- FORM: Although the first-order approximation of the limit state function is not needed for determination of probability an error due to the goodness of the first-order approximation remains. For relatively small probabilities this error can usually be neglected because the approximation touches only the tail of the standard normal distributed data. But for higher probabilities the error might be of relevance.
- Transformation into standard normal space: Each distributed variable of the limit state function needs to be transformed into a standard normal variable, in order to give the limit state function in the standard normal space. The transformation of the distributions into equivalent standard normal distribution is either done directly (for log-normal or normal distribution) or by inverse sampling. If inverse sampling is applied an uncertainty in the resulting standard normal distribution remains. Moreover, a transformation of discrete sampled parameters (non-continuous distribution) into standard normal space is not intent a-priori and needs some additional approximation or simplification.

The description given in the report is valid if the input variables are independent of each other. If this is not the case, the random variables need to be transformed into independent variables in standard normal space. There are many efficient techniques available to conduct the required probability transformation, such as the Nataf transformation (used in ISAAC) or the Rosenblatt transformation. A description of these transformations can be found in most books on structural reliability (e.g., [123]).

- SORM: For the SORM the approximation of the limit state function by a second-order Taylor series around the MPP is needed. For limit state functions that cannot be formulated in a closed solution, the limit state function needs to be approximated in order to be able to determine the second-order Taylor series. This approximation is usually based on multiple regression with a remaining error to the exact limit state function.

In addition, FORM or SORM is also used for sensitivity study and for importance sampling. The idea and method of using FORM or SORM for sensitivity study is described in [124]. The idea of importance sampling in combination with Monte Carlo method is to sample around the MPP in order to reduce the number of runs. A more detailed description is given in section 7.5.1.3.

7.5.1.3 Monte Carlo with Importance Sampling

The Monte Carlo technique for the computation of the failure probability p_f can be seen as a numerical integration technique, integrating the distribution density functions ρ_i in the regions of failure $g(u(x)) < 0$ of the space of independent basic parameters.

$$p_f = \int_{g(u(x))<0} \prod_{i=1}^{n} \rho_i(x_i)\, d^n x$$

The Monte Carlo approach samples the points $x^{(j)}$ according to the distribution functions F_i. The approximation of the failure probability with the standard Monte Carlo technique can be written as follows, for N_{MC} sample points.

$$p_f \underset{\text{Carlo}}{\overset{\text{Monte}}{\approx}} \frac{1}{N_{MC}} \sum_{j=1}^{N_{MC}} \chi_{g(u(x))<0}(x^{(j)})$$

$\chi_{g(u(x))<0}$ is the characteristic function. For small failure probabilities, region of failure $\{x: g(u(x)) < 0\}$ is far from the median values, and the random sample points x only rarely fall into this subset. Therefore, for small failure probabilities, most of the evaluated sample points $x^{(j)}$ are not contributing to the sum since $\chi_{g(u(x))<0}$ is zero for most points. The importance sampling circumvents this problem by drawing the sample points $x^{(j)}$ from different distribution functions Ψ_i. This has to be compensated by correcting the weight of each contribution in the sum.

$$p_f \underset{\text{Sampling}}{\overset{\text{Importance}}{\approx}} \frac{1}{N_{IS}} \sum_{j=1}^{N_{IS}} \chi_{g(u(x))<0}(x^{(j)}) \prod_{i=1}^{n} \frac{\rho_i(x^{(j)})}{\rho_{\psi,i}(x^{(j)})}$$

There exist different choices of Ψ_i. Starting with the most probable failure point x^* computed during a FORM evaluation, it is a natural choice to sample around this point, using the formulation in standard normal space (u-space). This assumes a sample density $\rho_{\psi,i}(u_i) = \phi(u_i - u_i^*)$, where ϕ is the Gaussian density function.

$$p_f \underset{\text{Importance Sampling}}{\overset{\text{MPFP-centered}}{\approx}} \frac{1}{N_{IS}} \sum_{j=1}^{N_{IS}} \chi_{g(u)<0}(u^* + u^{(j)}) \prod_{i=1}^{n} \frac{\phi(u_i^{(j)} + u_i^*)}{\phi(u_i^{(j)})}$$

The advantage of this approach is the reduction of the number of the evaluation points needed for a given level of precision, $N_{IS} \ll N_{MC}$, which is favorable since each evaluation of the characteristic function requires the computation of the limit state function $g(u(x))$, which requires a deterministic fracture mechanical analysis with high numerical costs.

If done properly, the importance sampling method itself is a transformation of the Monte Carlo approach without inherent errors. The localization of x^* for this method does not even have to be determined with a high accuracy. However, the computational advantage is given if the most contributions to the failure integral come from the vicinity of x^*. In case of multiple x^* at different locations and with almost equal reliability index β, the method has to be adjusted.

7.5.2 Sampling of data

For sampling of data from a defined distribution the following methods are commonly used:

- Sampling from (standard) normal distribution: Box-Muller transformation (https://en.wikipedia.org/wiki/Box%E2%80%93Muller_transform)

- Sampling from log-normal distribution: Sampling the logarithm as normal distributed value

- Sampling from arbitrary distribution: Inverse transform method, i.e., $x = F^{-1}(p)$ with $F(x)$ distribution function and $p = U(0; 1)$ uniformly distributed between 0 and 1

As already described in section 7.5.1.1 an appropriate random number generator is needed to ensure randomness of distributed parameters for a large number of Monte Carlo runs.

In order to ensure a representative covering of all possible sets of distributed input data, sampling methods like Latin hypercube sampling or orthogonal sampling can be used. This becomes important, when the number of distributed input data is large and both aleatory and epistemic uncertainties are considered in combination with a relatively low number of Monte Carlo runs. For typical probabilistic PTS analysis with more than 10^6 Monte Carlo runs and less than 10 sampled input data, a random sampling is sufficient. A general comparison can be found here: https://analytica.com/latin-hypercube-vs-monte-carlo-sampling/. Moreover, JAEA performed comparison of results including Latin hypercube sampling vs. FAVOR Monte Carlo, see [125].

Nevertheless, a simple benchmark to investigate, if the interaction of Monte Carlo runs and number of sampled input data leads to a representative covering of all possible sets of distributed input data is recommended.

If uncertainties in the input data are separated into epistemic and aleatory the combination of both uncertainties is needed for sampling of the input data. In PASCAL v4 a numerical integration method is used to combine epistemic and aleatory uncertainties for sampling of fracture toughness and crack arrest.

7.5.3 Events considered

An overview of the different events considered is given in **Table 21**.

Table 21: Events considered by the different tools

Partner	Software/Tool	Initiation (brittle/ductile)	Arrest/Re-Initiation	Failure
UJV	PROVER (in-house)	yes/yes	no	no
FRA-G	In-house	yes/yes	yes/yes	yes
IPP	SIF-Master (in-house)	yes/no	no	no
KIWA	ISAAC (in-house)	yes/yes	no	yes[1]

JAEA	PASCAL v4	yes/yes	yes/yes	yes
GRS	PROST	yes/no	no	no
OCI, PSI, Tecnatom, JSI	FAVOR	yes/yes	yes/yes	yes

(1): If initiation and failure are independent events

It is obvious that brittle crack initiation for PTS analysis is always considered as an event. Some tools are assessing only brittle fracture initiation, resulting in probability of initiation, which can be treated as conservative for RPV failure probability. If so, no benefit of possible crack arrest is considered, which leads to inherent safety margin in the RPV failure probability. As the intention of a probabilistic assessment is always to reduce inherent safety margin, it is not advisable to use brittle fracture initiation probability equal to RPV failure probability.

For the determination of RPV failure probability it is common practice to assess crack arrest and possible re-initiation after arrest. This sequence of events should finally lead to stable arrest with no re-initiation (i.e., no failure) or failure of the RPV. Failure of the RPV is gained, if crack reaches a pre-defined fraction of the RPV wall (e.g., 80%). The use of an appropriate pre-defined fraction should be verified (e.g., instability of remaining ligament). Nevertheless, it is common understanding that a value in the range of 75% to 90% is appropriate for PTS assessment. The influence of values in the range of 75% to 90% could be analysed in WP4. Moreover, some tools assess net-section collapse of the remaining ligament directly in addition to the use of a pre-defined fraction of the RPV wall.

Although a potential ductile fracture initiation might be of minor importance for a PTS analysis, it should also be taken in account. It becomes more important when crack arrest is considered, because crack re-initiation may occur in warmer regions of the RPV wall, where ductile initiation becomes more relevant. The consideration should be done either by explicitly considering ductile fracture initiation as an event in the probabilistic tool or by a case-specific evaluation of relevance of ductile fracture initiation by a deterministic approach.

7.5.4   Fracture mechanics models

The use of appropriate fracture mechanics models is an important aspect for PTS analysis, both deterministic and probabilistic ones. For probabilistic PTS analysis it is common practice to use the well-established fracture mechanics models from deterministic analysis, concerning especially the stress intensity factor solutions for the cracks of interest, limit load analysis for cracked structures and ductile crack growth. Fracture mechanics models like brittle or ductile fracture initiation or crack arrest are more or less related to the distributions used for the material properties. Concerning the consideration of WPS effect the common practice has been defined in Deliverable 1.2 [2] (See also Section 5).

The use of different fracture mechanics models (e.g., stress intensity factor solutions or limit load solutions) has an impact on both deterministic and probabilistic results. It is common understanding that several solutions are adequate for the case of interest, but with different amount of inherent margin. The impact of different fracture mechanics models might be of interest for interpretation of the results from WP3 and WP4. Therefore, some effort should be made to investigate the different solutions used.

7.5.5   Treatment of loading

Temperature and stress calculations (3D or 1D) are usually pre-processing assessments for probabilistic PTS, and it is common practice to transfer transient temperature and stresses over wall thickness at relevant location to probabilistic fracture mechanics.

Most tools are assessing a single location of the RPV (e.g., core weld) with a representative stress and temperature distribution at that location. Only FAVOR, PROVER and FRA-G In-house tool assess the whole beltline region, but with different approach on loading:

- FAVOR and PROVER splits the beltline region into sub-regions with individual properties like chemistry, flaw population. But the loading condition is the same for all sub-regions.

- With the FRA-G In-house tool it is possible to combine results representative for various sub-regions of the RPV to an overall RPV result. With this approach it is also possible to address different loading conditions for the different sub-regions.

The consideration of cold plume effect for probabilistic PTS analysis is done in many different ways. For the most commonly used tools with 1D FE calculations, the use of coolant temperature and HTC in cold plume from mixing calculations leads to appropriate temperature for inside cold plume. But with 1D FE calculation it is not possible to determine thermal stresses in the region of the plume accurately. Using this simplified approach is realistic from the temperature point of view and non-conservative from stress point of view for plume region and it is conservative from both temperature and stress point of view for outside of plume region. The overall conservativeness of this approach is questionable. There are some methods and adjustments that can be used to ensure bounding stresses for cold plume region, but these methods and adjustments need to be verified and inherent margins remain. The common practice to calculate appropriate stresses inside the plume region is to use a 3D FE method with input from mixing codes or CFD analysis.

The impact of the different approaches for consideration of plume effect should be investigated in WP4.

The common practice on how to assess residual stresses due to welding and cladding in a PTS analysis has been investigated in Deliverable 1.1 [1] (see also Section 4). For probabilistic PTS analysis it is recommended to follow this common practice.

7.5.6 Combination of several PTS events

It is common practice to combine the results from several PTS events according to their occurrence probability (frequency). This leads to an overall frequency of initiation/failure (= initiation/failure probability per year):

$$FI = \sum_{j=1}^{n} f_j \cdot CPI_j \ \text{ and } \ FF = \sum_{j=1}^{n} f_j \cdot CPF_j,$$

(f_j= frequency of PTS transient j, CPI_j/CPF_j = conditional probability of initiation/failure))

The frequency for a PTS event is usually taken from PSA.

7.5.7 Distributed Parameters

In general, there exists a common understanding on which kind of distribution to be used for which kind of data. An overview for the most important input data is given in **Table 22**.

Table 22: Distribution used for most important input data.

Input data	Symbol	Distributed	Distribution
Neutron fluence	f	Mostly yes except SIF-Master, ISAAC	Normal
Chemical composition	Cu, P, Ni, Mn	Mostly yes except ISAAC	Normal
Reference temperature	RT_{NDT} or T_0	yes	Normal
Fracture Toughness	K_{IC}	yes	Mostly Weibull (Master-Curve)

			IPP, FRA-G: normal based on ASME K_{IC}
Upper shelf (ductile) crack initiation	J_{IC}	Mostly yes except SIF-Master	Normal
Crack arrest	K_{Ia}	FAVOR, FRA-G, PASCAL v4[1]	Lognormal

(1): Only FAVOR, FRA-G In-House and PASCAL v4 are assessing crack arrest

7.5.8 Flaw distribution and multiple flaws

For probabilistic PTS analysis it is common practice to assess inner surface (through clad), embedded and/or underclad cracks. An overview of the different flaw types assessed by the different tools is given in **Table 23**.

Table 23: Type of flaws to be assessed.

	Surface cracks	Underclad cracks	Embedded cracks
PROVER	no	yes	yes
FAVOR	yes	no	yes
ISAAC	yes	no	yes
SIF-Master	yes	yes	yes
FRA-G in-house	yes	yes	yes
PASCAL4	yes	yes	yes
PROST	yes	no	no

The general approach for flaw size distribution is as follows:

- Flaw depth: log-normal or exponential distribution
- Flaw length: log-normal or exponential distribution (Aspect ratio: log-normal or normal distributed)

When multiple flaws are assessed (FAVOR, PROVER and FRA-G In-house) flaw density and flaw orientation distribution is also required:

- Orientation: Uniform
- Density of surface and underclad cracks: Exponential distribution
- Density of embedded cracks: Poisson distribution

If multiple flaws are simulated in a probabilistic PTS analysis the interaction of the adjacent flaws is currently not considered.

8 Identification of further LTO improvements having an impact on PTS and selection for assessment

The objective of this chapter is to summarize the results of *Task 1.5 Identification of further LTO improvements having an impact on PTS and selection for assessment*, to highlight those relevant for PTS in European countries as well as those which will serve as an input for WP2, WP3 and WP4 within the APAL project.

Inputs from a number of European countries operating NPPs provide diverse views. The NPP improvements, such as heated emergency cooling water, fuel management strategies for reduction of neutron fluence, reduction of high-pressure injection flows during SB-LOCA and others, are included in this chapter.

8.1 Overview

The NPP modifications with an impact on the plant RPV resistance against pressurized thermal shock and reactor pressure vessel brittle fracture (that would result with high probability in core melt and severe accident) are categorized as follows:

- Plant modifications during designed plant lifetime

    o Post-Chernobyl actions
    o Activities of NPP designer and/or operator (heat-up of SI tanks etc.)
    o Refurbishing of safety injection pumps
    o Implementation of results of PTS studies (recommendations to modifications of SSC, EOP etc.)
    o Post-Fukushima actions

- LTO plant modifications
    o More stress on minimizing PTS risk due to ageing of RPV and other SSCs
    o Implementation of new measures reducing PTS risk
    o Quantification of improvements with help of state-of-the-art computational tools
    o Experience exchange in international projects

Major impact on PTS could have actuation of the Emergency Core-Cooling System (ECCS). Design of ECCS of the Gen II and III NPP's (in 1970s and '80s) was oriented mainly on core cooling (the PTS was not an issue at that time). Later, some NPP designers and operators implemented plant modifications to reduce the PTS risk. Generally, the ECCS design and parameters should be balanced to ensure emergency core cooling on one side and minimize PTS risk on the other side.

8.2 Description of activities

To achieve the objectives of *Task 1.5*, a questionnaire was prepared, discussed among the partners and distributed among them for their response. This questionnaire focuses on the following points:

- Improvements pertaining to PTS transients
- Improvements pertaining to RPV materials
- Improvements in plant software
- Improvements in plant procedures
- Improvements in methods of PTS analysis

The responses from the following partners were used for elaboration of Deliverable 1.5 [5]:

Country	Partner	Contributing Author
Czech Republic	UJV	Pavel Kral
Finland	LUT	Markku Puustinen
France	IRSN	Jerome Roy

Country	Partner	Contributing Author
Slovenia	JSI	Oriol Costa and Andrej Prošek
Switzerland	PSI	Diego Mora
Ukraine	IPP-CENTRE	Maksym Zarazovskii
Hungary	BZN	Szabolcs Szávai
Spain	Tecnatom	Carlos Cueto-Felgueroso
USA	OCI	B. Richard Bass and Paul T. Williams

The information from the individual partners on NPP improvements in their countries was the basis of Deliverable D1.5 [5]. It was further extended to comprehensively cover the topic and to prepare a valuable document and useful input for further tasks in the APAL project.

8.3 NPP improvements relevant for PTS in European countries

Based on the information provided by the partners, the main LTO improvements arisen from the Deliverable D1.5 [5] have been listed by each country and classified into five categories.

8.3.1 NPP improvements applied or planned in the Czech Republic

8.3.1.1 Improvements pertaining to PTS transients

- Heating of water in the HPSI tanks of VVER-440
- Potential heating of water in the LPIS tanks of VVER-440 (from room temperature to 550 °C). This measure would lead to increase of maximum allowable transition temperature by 28 °C, but it has not been implemented yet.
- Bypass of the ECCS heat exchanger, control of essential cooling water flow to HX etc. (VVER-1000)
- Optimization of accumulators parameters (lower pressure in VVER-440, [106])

8.3.1.2 Improvements pertaining to RPV material

- Fuel management strategies for reduction of the neutron fluence (low leakage cores, VVER-440, 1000)
- Advanced method for prediction of the ductile to brittle transition temperature (VVER-440, 1000) based on comprehensive surveillance specimens (SSs) programme
- Qualified NDT (leading to smaller postulated cracks in the PTS analyses, VVER-440, 1000)
- Annealing of RPVs (not yet applied)

8.3.1.3 Improvements in plant software

- Automatic cold over-pressurization protection (VVER-440, 1000)
- Setting of relevant protection signals (not yet applied)

8.3.1.4 Improvements in plant procedures

- Reduction of high-pressure injection flows during SB-LOCA (EOP in VVER-440, 1000)
- Changing of HPIS trains during SB-LOCA (EOP in VVER-1000)
- Opening of controllable PORV in course of "reclosure of inadvertently open PRZ SV"
- Putting stress on PTS scenarios in operators training on full scope simulator

8.3.1.5 Improvements methods of PTS analysis

- Elaboration of both deterministic and probabilistic PTS evaluations
- Application of 2D nodalization of reactor downcomer in all system TH analyses [107]
- Detailed models of ECCS systems to predict changes in temperature of injected water (instead of overly conservative boundary condition)
- Application of CFD for critical cases instead of regional mixing codes (VVER-440, 1000). An example is shown in Figure 41.
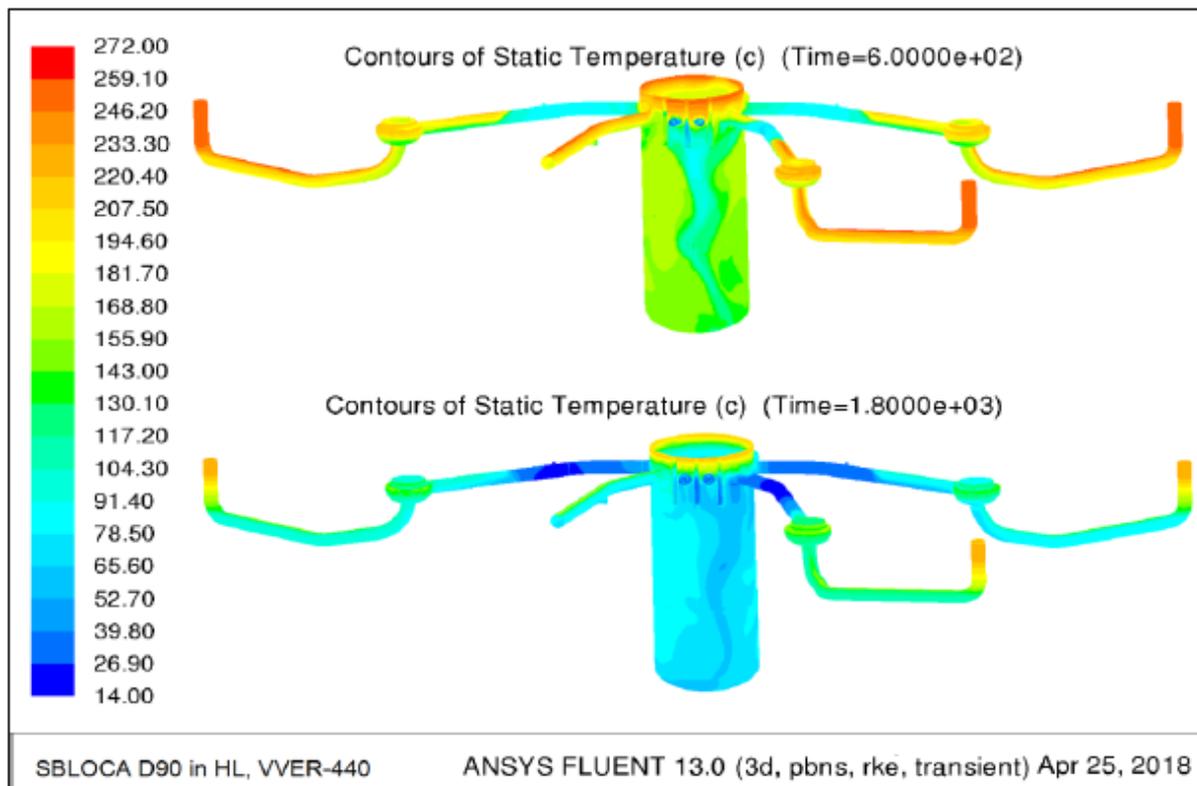
Figure 41: CFD mixing analysis of SBLOCA in VVER-440 [107].

8.3.2 NPP improvements applied or planned in Finland

8.3.2.1 Improvements pertaining to PTS transients

- Heating up the hydro accumulators and ECCS storage tank
- Decreasing the HPSI head and capacity
- Optimizing ECCS coolant temperature during recirculation from the sump

8.3.2.2 Improvements pertaining to RPV material

- Introduction of dummies to the core periphery to reduce neutron fluence
- Introduction of low-leakage core management to reduce neutron fluence
- Thermal annealing of the pressure vessel of Loviisa 1 unit

8.3.2.3 Improvements in plant software

- Additional I&C to improve plant protection system in case of overcooling transients from the secondary side
- Modifications to minimize containment spray system actuation

8.3.2.4 Improvements in plant procedures

- Introduction of new EOPs that take into account minimization of PTS risks
- Administrative instructions to prevent pressurization when primary temperature is below 50°C

8.3.2.5 Improvements methods of PTS analysis

- Experimental research to improve plant-specific thermal-mixing modelling (Figure 42)
- Significant improvements in stress analysis and fracture mechanics applied to Loviisa units
- Application of full-scale probabilistic assessment to complement deterministic design basis

Figure 42: Thermal mixing experiments for Loviisa reactor pressure vessel in scale 2:5.

8.3.3   NPP improvements applied or planned in France

8.3.3.1   Improvements pertaining to PTS transients

- Heating of water in ECCS tanks (20 °C)

8.3.3.2   Improvements pertaining to RPV material

- Fuel management strategies for reduction of neutron fluence (low leakage cores)
- Hafnium control rods for reduction of neutron fluence (low leakage cores)
- Heavy core reflector for reduction of neutron fluence (low leakage cores) for EPR
- Qualified NDT leading to smaller postulated cracks in PTS analyses
- Advanced method at nanometer scale for prediction of radiation embrittlement (not yet applied)

8.3.3.3   Improvements methods of PTS analysis

- Detailed models of flaws (specific detected flaws for some RPV) for prediction of margin factor
- Application of three-dimensional mechanical codes for critical cases instead of one-dimensional methods
- Application of system codes for all PTS cases instead of mixing correlations (not yet applied)
- WPS (not yet applied)

8.3.4   NPP improvements applied or planned in Slovenia

8.3.4.1   Improvements pertaining to RPV material

- "Low-leakage loading pattern" of the reactor core implemented from the 5th nuclear fuel cycle onwards to preventively reduce the neutron flux on the RPV wall
- Neutron shield around the core to prevent (reduce) irradiation embrittlement of the RPV beltline material

- Ex-vessel neutron dosimetry system implemented in 2010 to verify the analytically established neutron fluence used in determining the pressure-temperature operating limits at 60-year EOL. The last capsule withdrawal was in 2012
- Use of new and more sensitive non-destructive examination (NDE) techniques during RPV surveillance

8.3.4.2   Improvements methods of PTS analysis

- Detailed models of ECCS systems to predict change in temperature of injected water (instead of overly conservative boundary conditions)

8.3.4.3   Improvements pertaining to PTS transients, plant software/hardware and plant procedures

- Low-Temperature Overpressure Protection (LTOP) system implemented in 2001. The aim of the modification was to assure protection of the RCS against sudden rises of pressure when operating at low temperatures. Protection is requested in NUREG 0800, Chapter 5.5.2. For the over-pressure protection, the existing relief valves on the RHR lines were replaced with valves having greater relief capacity. Consequentially, the relief pipes and supports were modified also. The electrical interlock for the closure of RHR-to-RCS isolation valves was removed.

8.3.5   NPP improvements applied or planned in Switzerland

8.3.5.1   Improvements pertaining to PTS transients

- ECCS pre-heating to 30 °C in Beznau Unit 1

8.3.5.2   Improvements pertaining to RPV material

- Research on probabilistic analyses was carried out and reported to the regulatory bodies
- Low-leakage core loading since the 1980s to reduce the neutron fluence at the RPV wall
- External vessel neutron dosimetry was installed in Gösgen
- Introduction of Master Curve testing in addition to Charpy testing in the mid of the 2000s to improve the prediction of neutron embrittlement
- NDT for ensuring cladding integrity in Beznau NPP, to allow the exclusion of presence of a through-cladding crack

8.3.5.3   Improvements methods of PTS analysis

- Continued further development of PTS methodologies (starting from simple analytical two-dimensional models to three-dimensional FEA modelling)
- Extension of transient matrix
- Research was carried out using on three-dimensional analyses that were performed for small-, medium-and large-break loss-of-coolant accidents using CFD [53]
- Research was carried out on the applicability of TRACE analyses using three-dimensional techniques. Also, screening analyses were performed for different accident scenarios
- Research on finite-element model to analyse different crack geometries and locations. Plasticity and local approach to fracture were also investigated

8.3.6   NPP improvements applied or planned in Ukraine

8.3.6.1   Improvements pertaining to PTS transients

- Heating of water in ECCS hydro accumulators (VVER-440, VVER-1000)
- Regulation of the cooling water flow by installing control valves on the HPIS and LPIS pump head (VVER-1000/V-302, 338)
- Replacement of PRZ safety valves with valves that can operate in the over-pressure protection mode (VVER-440, VVER-1000)

8.3.6.2   Improvements pertaining to RPV material

- Fuel management strategies for reduction of neutron fluence (low leakage cores, VVER-440, VVER-1000)
- Annealing of RPV (VVER-440/Rivne NPP unit 1)
- Modernization of the SSs programs: reconstitution technology (VVER-440, VVER-1000), modernization of the SSs location as shown in Figure 43 (VVER-1000), (with this action, it is possible to smoothly adjust the average fluence in order to maximize the SSs irradiation to optimal conditions), implementation of the CT0,5T Fracture Toughness specimens (VVER-1000) and CT0,16T (VVER-1000– see Figure 44)
- Improvement methods of neutron fluence calculation for RPV and SSs (VVER-440, VVER-1000)
- Advanced method for prediction of radiation embrittlement (VVER-1000)
- Improved non-destructive ultrasonic testing of the RPV wall (VVER-440, VVER-1000)
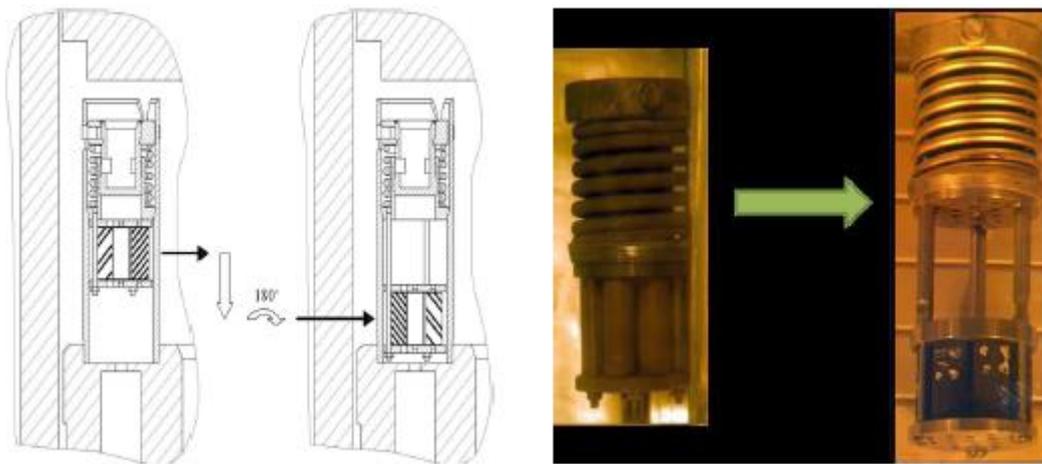
Figure 43: Modernization of the SS location for Ukrainian WWER-1000 RPVs.

Figure 44: Illustration of the CT0,16T specimens which can be made from broken pieces of Charpy and COD specimens

8.3.6.3   Improvements in plant software

- Automatic cold over-pressurization protection for PRZ safety valves and heaters (VVER-440, VVER-1000)

8.3.6.4   Improvements in plant procedures

- Adding procedures "Thermal shock" and "Threat of thermal shock" to EOP, where the operator is guided by the PT-diagram (VVER-440, VVER-1000)

163

8.3.6.5   Improvements methods of PTS analysis

- Detailed models for consideration of the air cooling of the RPV outer surface (VVER-1000)
- Application of CFD code for critical analyses of VVER-1000 instead of regional mixing codes (planned action)
- Development a normative document for probabilistic RPV brittle fracture assessment (planned action)

8.3.7   NPP improvements applied or planned in Hungary

8.3.7.1   Improvements pertaining to PTS transients

- Not relevant, all PTS events were considered (screening criterion: 10^{-5}/year)

8.3.7.2   Improvements pertaining to RPV material

- Determination of non-linear material properties of structural steels

8.3.7.3   Improvements in plant procedures

- Surveillance programme is continuously conducted until the end of the service life of the RPV

8.3.7.4   Improvements methods of PTS analysis
- Application of nonlinear fracture-mechanics theory

8.3.8   NPP improvements applied or planned in Spain

8.3.8.1   Improvements pertaining to RPV material

- "Low leakage loading pattern" of reactor core implemented about 5-10 years after start of operation to preventively reduce the neutron fluence on the RPV wall
- Ex-vessel neutron dosimetry system implemented in mid 2010s to control the neutron fluence, once the fourth irradiation surveillance capsule was retrieved and tested. The two remaining irradiation surveillance capsules were retrieved from the core and kept in the fuel pool for potential use in LTO
- Qualified NDE Techniques for ISI according to ENIQ methodology since early 2000s

8.3.8.2   Improvements pertaining to PTS transients, plant software/hardware and plant procedures

- Operating plant procedures to prevent the occurrence of overcooling scenarios that potentially lead to a PTS event
- Verification of compliance of the PTS screening limits established in US NRC 10 CFR 50.61 "Fracture Toughness Requirements for Protection against Pressurized Thermal Shock Events" (also known as PTS Rule). This verification accounts for:
    o The predicted neutron fluence at EOL based on irradiation surveillance program results and ex-vessel dosimetry
    o The predicted RT_{NDT} at EOL due to neutron irradiation
- Development of Pressure-Temperature (P-T) Limits for heatup/cooldown and hydrostatic tests according to Appendix G of Section XI of the ASME Code, with the minimum temperature requirements of 10 CFR 50 for the closure flange region highly stressed during tightening of bolts. The P-T limits are developed for the RPV extended beltline
- Two independent low-temperature over-pressure protection (LTOP) systems to prevent brittle fracture in the RPV:
    o One automatic system (named COMS) which commands the pressurizer power operated relief valves (PORVs) based on measurement of the RCS pressure and temperature. The opening setpoint of each pressurizer PORV consists of a specially calculated program of RCS pressure versus temperature

- o Qualification of residual heat removal (RHR) system relief valves for mitigating low-temperature over-pressure transients. For this purpose, the following modifications of plant technical specifications have been implemented:
  - Only one charging pump shall be operable whenever the RHR system is aligned
  - Restriction for restarting the reactor coolant pump (RCP) when the RCS is water solid

8.3.9   NPP improvements applied or planned in Germany

8.3.9.1   Improvements pertaining to PTS transients

- Increase of the water temperature in the storage tanks of the ECC system
- Increase of the water mixing in the RPV downcomer during safety injection

8.3.9.2   Improvements pertaining to RPV material

- NDT investigation of RPV base material (has been performed on some German plant due to Tihange/Doel hydrogen flakes) to increase confidence in postulated flaw size
- Direct determination of fracture toughness (Master Curve T_0) instead of indirect evaluation according to the RT_{NDT} concept
- Improvements in accuracy of neutron fluence calculations. These improvements are more important when measures such as RPV neutron shielding are implemented, as it would reduce the conservatism in fracture toughness estimation
- Consideration of ASME Code Case N-830 [176] for better description of the fracture toughness within the whole regime (brittle, tearing)

8.3.9.3   Improvements in plant software

- Transformation from analog to digital reactor protection system (TXS system)
- Surveillance monitoring of transient in the main coolant line, surge line (FAMOS)

8.3.9.4   Improvements in plant procedures

- Reactor protection system including limitation of cold over-pressure event (LTOP) based on fracture mechanics assessment
- Operator training in PKL (primary circuit test facility) in case of LOCA

8.3.9.5   Improvements methods of PTS analysis

- Investigation of extended transient matrix, see [108]
- Benefit of break exclusion concept for secondary side
- CFD analysis to reduce over conservative margins in safety assessments
- Consideration of Warm Pre-Stress (WPS) effect, constraint effect, and crack arrest in fracture mechanics assessments
- RPV nozzle detailed assessment, see IAEA Guideline TECDOC-1627 [6]

8.4 Conclusions

Section 8 summarizes NPP improvements having an impact on PTS and enabling long-term operation (already applied, or potential LTO improvements in hardware, software or procedures) for the nine European countries operating NPPs. This collection of improvements serves as a complex set of possible LTO improvements to minimize PTS risk and as an input for further tasks in the APAL project.

The findings documented in this report will be followed by other tasks and work packages within the APAL project:

- WP2: Only task T2.1 will analyse improvements on pertaining to PTS itself.

- WP3: Improvements in NDE (different crack sizes) will be assessed. It should be mentioned that material properties are assessed outside of deterministic PTS analyses (PTS analyses establish the margin).
- WP4: Improvements in fluence and consequently in material properties will be assessed.

8.5 Gaps

Possible new improvements or ideas relevant for PTS that might be further investigated are:

- Analysis of thermal-hydraulic transients during startup and shutdown considering mixing using modifications to the existing Framatome, GmbH, and KWU-Mix codes and detailed assessment of the p-T limit (with the goal to relax/increase p-T limit window) to avoid pressurized event at low temperature with limited thermal shock (cold over-pressurisation)
- PTS analysis of all relevant locations for LTO
- Locations with high degradation potential (thermal ageing, fluence)
- Locations with high loading during service
- Locations with higher potential of undetected flaws

- Hardware modification to allow safety injection in the hot leg (Countercurrent Flow in PWR Hot Leg) leading to PTS analysis considering injection of cold water into both hot and cold legs, see also NUREG IA 0116 [109]
- RPV annealing

9   References

[1]   APAL project Deliverable 1.1 "State-of-the-art for weld residual stress".

[2]   APAL project Deliverable 1.2 "State-of-the-art for warm pre-stress approach applied in the PTS".

[3]   APAL project Deliverable 1.3 "State-of-the-art for thermal-hydraulic (TH) analysis".

[4]   APAL project Deliverable 1.4 "State-of-the-art of probabilistic PTS analysis".

[5]   APAL project Deliverable 1.5 "Identification of further LTO improvements".

[6]   Pressurized Thermal Shock in Nuclear Power Plants: Good Practices for Assessment, IAEA TECDOC No. 1627 (https://www.iaea.org/publications/8237/pressurized-thermal-shock-in-nuclear-power-plants-good-practices-for-assessment).

[7]   IAEA-EBP-WWER-08 Rev.1. Guidelines on pressurized thermal shock analysis for WWER nuclear power plants. Revision 1, IAEA, Vienna, 2006.

[8]   Normative Technical Documentation of Association of Mechanical Engineers, Section IV. Lifetime Assessment of Components and Piping in VVER Nuclear Power Plants. Version 2020 (NTD AME).

[9]   Safety Standards of the Nuclear Safety Standards Commission (KTA) KTA 3201.2 Components of the Reactor Coolant Pressure Boundary of Light Water Reactors, Part 2: Design and Analysis.

[10]   G.G. Chell. Some Fracture Mechanics Application of Warm Pre-Stressing to Pressure Vessels, 4th International Conference on Pressure Vessel Technology Institution of Mechanical Engineers, Paper C22, 117-124, 1980.

[11]   BS 7910:2013. Guide to methods for assessing the acceptability of flaws in metallic structures.

[12]   PM-T.0.03.415-16. Standard program on technical state evaluation and life-time extension of reactor pressure vessels, upper heads and main flanges of WWER-1000 power units. Kyiv 2017.

[13]   P.T. Williams, T.L. Dickson, B.R. Bass, and H.B. Klasky, Fracture Analysis of Vessels – Oak Ridge, FAVOR, v16.1, Computer Code: Theory and Implementation of Algorithms, Methods, and Correlations, ORNL/LTR-2016/309 (Adams Access No. ML16273A033), Oak Ridge National Laboratory, Oak Ridge, TN (USA), September 2016.

[14]   Structural margin Improvements in Age-embrittled RPVs with Load History Effects (SMILE). Final report. Contract FIKS-CT2001-00131/ Editors: D.Moinereau and G.Bezdikian, 2008.

[15]   M.T. EricksonKirk and T.L. Dickson, The Sensitivity of Risk-Informed Reactor Structural Integrity Analysis Results to Various Interpretations of Warm Pre-stress, Paper number PVP2009-77127, Proceedings of the 2009 ASME Pressure Vessel and Piping Conference, July 26-30, Prague, Czech Republic.

[16]   D. Moinereau, A. Dahl, S. Chapuliot, T. Yuritzinn, Ph. Gilles, and B. Tanguy, "The demonstration of warm pre-stress effect in RPV assessment: some experimental results and their interpretation by fracture mechanics," presented at the 7th International ASTM/ESIS Symposium on Fatigue and Fracture Mechanics, 36th ASTM National Symposium on Fatigue and Fracture Mechanics, November 14-16, 2007, Tampa, Florida, USA.

[17]   M. EricksonKirk, M. Junge, W. Arcierci, B.R. Bass, R. Beaton, D. Bessette, T.H.J. Chang, T.L. Dickson, C.D. Fletcher, A. Kolaczkowski, S. Malik, T. Mintz, C. Pugh, F. Simonen, N. Siu, D. Whitehead, P.T. Williams, R. Woods, and S. Yin, *Technical Basis for Revision of the Pressurized Thermal Shock (PTS) Screening Limit in the PTS Rule (10 CFR § 50.61)*, NUREG-1806, Vol. 1, U.S. Nuclear Regulatory Commission, Washington, D.C. (USA), August 2007. (https://www.nrc.gov/docs/ML0728/ML072830076.pdf).

[18]   M. EricksonKirk, M. Junge, W. Arcierci, B.R. Bass, R. Beaton, D. Bessette, T.H.J. Chang, T.L. Dickson, C.D. Fletcher, A. Kolaczkowski, S. Malik, T. Mintz, C. Pugh, F. Simonen, N. Siu, D. Whitehead, P.T. Williams, R. Woods, and S. Yin, *Technical Basis for Revision of the Pressurized Thermal Shock (PTS) Screening Limit in the PTS Rule (10 CFR § 50.61) – Appendices*, NUREG-1806,

Vol. 2, U.S. Nuclear Regulatory Commission, Washington, D.C. (USA), August 2007. (https://www.nrc.gov/docs/ML0728/ML072820691.pdf).

[19]   Evaluation of brittle-fracture resistance of VVER-440/213 reactor pressure vessel for normal operation, hydrostatic test, pressurized thermal shock (PTS) and unanticipated operating occurrences, Regulatory Guide No 3.18 (Ver. 4), HAEA, Budapest, September.

[20]   Association Française pour les Regles de Conception et de Construction des Materiels de Chaudieres Electronucleaires, *Design and Construction Rules for Mechanical Components of PWR Nuclear Islands*, RCC-M.

[21]   Association Française pour les Regles de Conception et de Construction des Materiels de Chaudieres Electronucleaires, *In-Service Inspection Rules for Mechanical Components of PWR Islands*, RSE-M.

[22]   The Japan Electric Association, "Verification Method of Fracture Toughness for In-service Reactor Pressure Vessel", JEAC4206-2016, 2016.

[23]   The Japan Electric Association, "Guideline for calculating failure frequency of reactor pressure vessel based on probabilistic fracture mechanics", JEAG4640-2018, 2018.

[24]   M. EricksonKirk, B.R. Bass, T.L. Dickson, C. Pugh, C.T. Santos, and P.T. Williams, Probabilistic Fracture Mechanics – Models, Parameters, and Uncertainty Treatment Used in FAVOR, Version 04.1, NUREG-1807, U.S. Nuclear Regulatory Commission, Washington, D.C. (USA), June 2007.

[25]   Guidelines procedure for analysis of in-service brittle fracture resistance of WWER reactor pressure vessels (MRKR–SKhR –2004). RD EO 0606 – 2005.

[26]   Comparison Report of RPV Pressurised Thermal Shock International Comparative Assessment Study (PTS ICAS), NEA/CSNI/R(1999)3.

[27]   European Commission, 2008 "Unified Procedure for Lifetime Assessment of Components and Piping in WWER NPPs, "VERLIFE", Version 2008".

[28]   D.G.A. Van Gelderen, D. Lauerova, J. D. Booker, D.J. Smith Statistical Analysis and Monte Carlo Simulations of Warm Pre-Stressing of Irradiated Small Single Edge Notch Bend Specimens, Transactions, SMiRT-23, Paper ID 310.

[29]   Kostylev V. I., Margolin B. Z. Determination of residual stress and strain fields caused by cladding and tempering of reactor pressure vessels. International Journal of Pressure Vessels and Piping 77 (2000), 723-735.

[30]   D. A. Ferrill, P. B. Juhl, D. R. Miller: Measurement of Residual stresses in a Heavy Weldment Weld. Res., November 1966, 504-s.

[31]   Obermeier F., Nicak T., Meier G., Keim E., "*Analysis of residual stresses in a pressurizer surge – nozzle weldment*", Proceedings of the ASME 2011 Pressure Vessels & Piping Division Conference 2011, PVP2011-57506.

[32]   Qian G., González-Albuixech V.F., Niffenegger M. Effects of embedded cracks and residual stresses on the integrity of a reactor pressure vessel. Engineering Failure Analysis. 2018; 90: 451-62.

[33]   Typical program of technical condition estimation and lifetime prolongation for WWER-1000 type rector pressure vessel its upper block and flange. PM-T.0.03.415-16.

[34]   Safety Standards of the "National Nuclear Energy Generating Company "Energoatom". SOY NAEK 177:2019. Methodology for brittle fracture assessment of the WWER RPV.

[35]   Chapuliot S., Lauerova D., Brumovsky M. and Tanguy B., "*Information about WPS experiments performed in NRI REZ and their evaluation*" in Fontevraud 7, 2010.

[36]   D. Lucas, D. Bestion, E. Bodèle, P. Coste, M. Scheuerer, F. D'Auria, D. Mazzini, B. Smith, I. Tiselj, A. Martin, D. Lakehal, J.-M. Seynhaeve, R. Kyrki-Rajamäki, M. Ilvonen, J. Macek, "An Overview of the Pressurized Thermal Shock Issue in the Context of the NURESIM Project", Science and

Technology   of   Nuclear   Installations,   vol.   2009,   2009.
https://doi.org/10.1155/2009/583259583259.

[37]   Palmrose D., "Demonstration of Pressurized Thermal Shock Thermal-Hydraulic Analysis with
       Uncertainty," NUREG/CR-5452, U.S. Nuclear Regulatory Commission, March 1999.

[38]   Fletcher C.D., Prelewicz D.A. and Arcieri W.C., "RELAP5/MOD3.2.2 Gamma Assessment for
       Pressurized Thermal Shock Applications," NUREG/CR-6857, U.S. Nuclear Regulatory
       Commission, October 2004.

[39]   Bessette D.E., "Thermal-Hydraulic Evaluations of Pressurized Thermal Shock," NUREG-1809, U.S.
       Nuclear Regulatory Commission, May 2005.

[40]   Tiete R., Trewin R., Blasset S., Pistora V, Posta M., Niffenegger M., Qian G., "Presentation of DEFI-
       PROSAFE project: probabilistic methodology to assess margin in deterministic RPV integrity
       assessment and proposed benchmark", Proceedings of the ASME 2018 Pressure Vessels and
       Piping Conference PVP2018 July 15-20, 2018, Prague, Czech Republic, paper PVP2018-84615.

[41]   Comparison Report of RPV Pressurised Thermal Shock International Comparative Assessment
       Study (PTS ICAS), NEA/CSNI/R(1999)3.

[42]   Dillström P., "PROSIR Probabilistic Structural Integrity of a PWR Reactor Pressure Vessel", SSM
       2015:09 (2015) ISSN: 2000 0456.

[43]   Bolinder T., Eriksson A., Faleskog J., Linares Arregui I., Öberg M. and Nyhus B., "WRANC, Warm
       Pre-Stressing – Validation of the relevance of the main mechanisms behind Warm Pre-Stressing
       in assessment of nuclear components," NKS Nordic nuclear safety research, 2019.

[44]   Wallin, K., "Master curve implementation of the warm pre-stress effect", Engineering Fracture
       Mechanics, 70, pp. 2587–2602, 2003.

[45]   Chell G. G., Haigh J.R., "The effect of warm pre-stressing on proof tested pressure vessels",
       International Journal of Pressure Vessel and Piping, 23, pp. 121–132, 1986.

[46]   Lauerova D., Pištora V., Brumovský M. and Kytka M., "*Warm Pre-Stressing Tests for WWER 440
       Reactor Pressure Vessel Material*", ASME 2009 Pressure Vessels and Piping Conference. Paper
       No PVP2009-77287.

[47]   Margolin B., Rivkin E., Karzov G., Kostylev V., Gulenko A., "*New Approaches for Evaluation of
       Brittle Strength of Reactor Pressure Vessel*", SMiRT 17, Paper # G01-4, 2003.

[48]   Karzov G., Margolin B., Rivkin E., "*Analysis of structure integrity of RPV on the basis of brittle
       fracture criterion: new approaches*", Int. J. of Pressure Vessels and Piping 81 (2004), 651-656.

[49]   Shengjun Yin, Paul T. Williams, and B. Richard Bass, "NESC-VII: Fracture Mechanics Analyses of
       WPS Experiments on Large-Scale Cruciform Specimen," PVP 2011-57112 paper in ASME 2011
       Pressure Vessels & Piping Conference, Baltimore, Maryland, USA, 2011.

[50]   D. Moinereau, S. Chapuliot, S. Marie and C. Jacquemoud, "NESC VII synthesis: A European
       project for application of WPS in RPV assessment including biaxial loading," PVP 2014-28076
       paper in ASME 2014 Pressure Vessels & Piping Conference, Anaheim, California, USA, 2014.

[51]   F. M. Beremin, "A local criterion for cleavage fracture for a nuclear pressure vessels steels," Met.
       Trans., 14A, 2277–2287 (1983).

[52]   M. Kroon and J. Faleskog, "Micromechanics of cleavage fracture initiation in ferritic steels by
       carbide cracking," Journal of the Mechnics anf Physics of Solids, vol. 53, pp. 171-196, 2005.

[53]   González-Albuixech VF, Qian G, Sharabi M, Niffenegger M, Niceno B, Lafferty N. Comparison of
       PTS Analyses of RPVs based on 3D-CFD and RELAP5. Nucl Eng Des 2015; 291: 168-178.

[54]   Gonzalez-Albuixech VF, Qian G, Sharabi M, Niffenegger M, Niceno B, Lafferty N. Coupled RELAP5,
       3D CFD and FEM analysis of postulated cracks in RPVs subjected to PTS loading. Nucl Eng Des
       2016; 297: 111-122.

[55]   A. Bousbia Salah, S. C. Ceuca, R. Puragliesi, R. Mukin, A. Grahn, S. Kliem, J. Vlassenbroeck & H.
       Austregesilo (2018) Unsteady Single-Phase Natural-Circulation Flow Mixing Prediction Using 3-

D Thermal-Hydraulic System and CFD Codes, Nuclear Technology, 203:3,293-314, DOI: 10.1080/00295450.2018.1461517.

[56]   Chandesris M., Mazoyer M., Serre G., Valette M., "Rod bundle thermal hydraulics mixing phenomena: 3D analysis with CATHARE-3 of various experiments", Proceedings of 13th International Topical Meeting on Nuclear Reactor Thermal Hydraulics (NURETH-15), Pisa, Italy (2013).

[57]   K. Iyer, H. P. Nourbakhsh, and T. G. Theofanous, "REMIX: A Computer Program for Temperature Transients Due to High Pressure Injection After Interruption of Natural Circulation." U.S. Nuclear Regulatory Commission NUREG/CR-3701, 1986.

[58]   H.-G. Sonnenburg, "Phänomenologische versuchsauswertung des versuchs UPTF-TRAM C1 thermisches mischen im kaltstrang." GRS-A-2434, Gesellschaft für Anlagen und Reaktorsicherheit, 1997.

[59]   R. Hertlein, "Mixing and Condensation Models Based on UPTF TRAM Test Results." Jahrestagung Kerntechnik 2003, Berlin, pp. 97-133, June, 2003.

[60]   W. T. Sha, H. M. Domanus, R C Schmitt, J J Oras, and E I.H. Lin, "COMMIX-1: a three-dimensional transient single-phase component computer program for thermal-hydraulic analysis", NUREG/CR-0785, United States Nuclear Regulatory Commission, 1978.

[61]   L. L. Eyler, and D. S. Trent, "Pressurized thermal shock: TEMPEST computer code simulation of thermal mixing in the cold leg and downcomer of a pressurized water reactor.", NUREG/CR-3564, United States Nuclear Regulatory Commission, 1984.

[62]   B.J. Daly, and M.D. Torrey, "SOLA-PTS: a transient, three-dimensional algorithm for fluid-thermal mixing and wall heat transfer in complex geometries.", NUREG/CR-3564, United States Nuclear Regulatory Commission, 1984.

[63]   R. D. Cheverton, D. L. Selby, "A Probabilistic Approach to the Evaluation of the PTS Issue" Journal of Pressure Vessel Technology, Vol. 114. No. 4, pp. 396-404, November 1992.

[64]   Pistora V., Gillemot F., "*Evaluation of the second phase of benchmark results, 6th Framework Programme of EU, Project COVERS, Contract No. 12727 (FI60)*", Report No. COVERS-WP4-D4.4, 2008.

[65]   T.L. Dickson, P.T. Williams, B.R. Bass, and H.B. Klasky, Fracture Analysis of Vessels – Oak Ridge – FAVOR, v16.1, Computer Code: User's Guide, ORNL/TM-2016/310, Oak Ridge National Laboratory, Oak Ridge, TN (USA), August 2016.

[66]   B. W. Brown and J. Lovato, RANLIB – A Library of Fortran Routines for Random Number Generation, Department of Biomathematics, University of Texas, Houston, TX, 1994.

[67]   P. L'Ecuyer, "Efficient and Portable Combined Random Number Generators," Communications of the ACM 31(6), (1988) 742-774.

[68]   P. L'Ecuyer and S. Cote, "Implementing a Random Number Package with Splitting Facilities." ACM Transactions on Mathematical Software 17, (1991) 98-111.

[69]   A. Rukhin, et al., A Statistical Test Suite for Random and Pseudorandom Number Generators for Cryptographic Applications, NIST Special Publication 800-22, National Institute of Standards and Technology, Gaithersburg, MD, May 15, 2001.

[70]   Orynyak I., Zarazovskii M., Batura A., Borodii M., Danil'chuk E., 2014, "Brittle Fracture Probabilistic Assessment of WWER-1000 RPVs", PVP2014-28557, ASME 2014 Pressure Vessels & Piping Conference, ASME, Anaheim, California, USA.

[71]   Dillström P., Gunnars J., Unge P. v, and Mangard D., (2018), "Procedure for Safety Assessment of Components with Defects – Handbook Edition 5", SSM Report 2018:18, ISSN: 2000-0456, Swedish Radiation Safety Authority.

[72]   Marie S., Chapuliot S., "Improvement of the calculation of the stress intensity factor for underclad and trough-clad defects in a reactor pressure vessel subjected to pressurized thermal shock", Int. J. Pressure Vessels and Piping 85 (2008) p. 517-531.

[73]   Selby D.L. et al., Pressurized-Thermal-Shock Evaluation of the Calvert Cliffs Unit 1 Nuclear Power Plant, NUREG/CR-4022 (ORNL/TM-9408), Oak Ridge National Laboratory, Oak Ridge, TN, USA, September 1985.

[74]   Selby D.L. et al., Pressurized-Thermal-Shock Evaluation of the H. B. Robinson Nuclear Power Plant, NUREG/CR-4183 (ORNL/TM-9567), Oak Ridge National Laboratory, Oak Ridge, TN, USA, September 1985.

[75]   Burns T.J. et al., Preliminary Development of an Integrated Approach to the Evaluation of Pressurized-Thermal-Shock as Applied to the Oconee Unit 1 Nuclear Power Plant, NUREG/CR-3770 (ORNL/TM-9176), Oak Ridge National Laboratory, Oak Ridge, TN, USA, May 1986.

[76]   G. Qian, M. Niffenegger M, V. Gonzalez, 2013. "Probabilistic PTS analysis based on cracks statistics observed in Shoreham and PVRUF RPV".

[77]   Batura A.S., Bogdan A.V., Orynyak I.V., and Radchenko S.A., 2014, "Two Axisymmetric Models Application for Fast and Conservative Analysis of Cold Plumes in RPV at PTS Condition," PVP2014-28997, ASME 2014 Pressure Vessels and Piping Conference, ASME, Anaheim, California, USA.

[78]   EricksonKirk M., EricksonKirk, M., "*The relationship between the transition and upper-shelf fracture toughness of ferritic steels*", Fatigue & Fracture of Engineering Materials & Structures, vol. 29, issue 9-10 (2006), 672–684.

[79]   *ASME Boiler and Pressure Vessel Code*, *Section XI*, *Rules for Inservice Inspection of Nuclear Power Plant Components*, *Nonmandatory Appendix A, Analysis of Flaws*, Article A-3000, *Method for K_I Determination*, American Society of Mechanical Engineers, New York, 2015.

[80]   Cipolla R. C., "*Computational Method to Perform the Flaw Evaluation Procedure as Specified in the ASME Code, Section XI, Appendix A*", EPRI, Report NP-1181, 1979.

[81]   EricksonKirk, M., EricksonKirk M.: An upper-shelf fracture toughness master curve for ferritic steels, International Journal of Pressure Vessels and Piping 83 (2006), 571–583.

[82]   Wallin K., "Correlation Between Static Initiation Toughness KJc and Crack Arrest Toughness KIa 2024-T351 Aluminium Alloy", Fatigue and Fracture Mechanics, 32nd Vol, ASTM STP 1406, 2001.

[83]   API 579-1/ASME FFS-1 (API 579 Second Edition) American Petroleum Institute Practice 579 Fitness-for-Service, June 5, 2007 (Joint standard with ASME).

[84]   Cipolla R.C. and Lee D.R., "Stress Intensity Factor Coefficients for Circumferential ID Surface Flaws in Cylinders for Appendix A of ASME Section XI", PVP2013-97734, Proceedings of the ASME 2013 Pressure Vessels and Piping Conference, July 14-18, 2013, Paris, France.

[85]   Xu S.X., Scarth D.A., Cipolla R.C., and Lee D.R., "Closed-Form Relations for Stress Intensity Factor Influence Coefficients for Axial ID Surface Flaws in Cylinders for Appendix A of ASME Section XI", PVP2014-28222, Proceedings of the ASME 2014 Pressure Vessels and Piping Conference, July 20-24, 2014, Anaheim, CA (USA).

[86]   Orynyak I. V., Borodii M. V., "Point Weight Function Method Application for Semi-elliptical Mode 1 Cracks", Int. J. of Fracture, 70, pp. 117-124, 1995.

[87]   R6, "Assessment of the Integrity of Structures Containing Defects", R6–Revision 4, Up to amendment record No.11, EDF Energy Nuclear Generation Ltd (2015).

[88]   Busch, M., Petersilge, M. and Varfolomeyev, I., "KI-Factors and Polynomial Influence Functions for Axial and Circumferential Surface Cracks In Cylinders". IWM-Report T18/94, Fraunhofer Institut Werkstoffmechanik, Halle, Germany, 1994.

[89]   Zang, W., "Stress Intensity Factor Solutions for Axial and Circumferential Through-Wall Crack in Cylinders". SINTAP/SAQ/02, Technical Report, 1997.

[90]   US NRC Regulatory Guide 1.99 "Radiation Embrittlement of Reactor Vessel Materials" Revision 2, May 1988.

[91]   Orynyak I., Radchenko S. "Methodological Features of WWER RPV Metal Critical Temperature of Brittleness Prediction on the Base of the Data Scatter and the Chemical Composition", PVP2015-45679, ASME 2015 Pressure Vessels and Piping Conference, ASME, Boston, Massachusetts, USA.

[92]   Zarazovskii M., Revka V., Chyrko L., "Regression Analysis of Transition Temperature Shift Database for the Core Region Beltline Welds of WWER-1000 RPVs", PVP2020-21748, ASME 2020 Pressure Vessels & Piping Conference, ASME.

[93]   EricksonKirk M.T. and Dickson T.L., NUREG-1874 "Recommended Screening Limits for Pressurized Thermal Shock (PTS)". US NRC. 2007.

[94]   Simonen F.A., Doctor S.R., Schuster G.J., and Heasler P.G., "A Generalized Procedure for Generating Flaw-Related Inputs for the FAVOR Code", NUREG/CR-6817, Rev 1, PNNL-14268, Rev 1, Pacific Northwest National Laboratory, Richland, Washington, October 2003.

[95]   González-Albuixech, V.F., Qian, G., Niffenegger, M., Integrity analysis of a reactor pressure vessel with quasi laminar flaws subjected to pressurized thermal shocks, (2014) Nuclear Engineering and Design, 280, pp. 464-472.

[96]   Schuster G.J., Doctor S.R., Crawford S.L., and Pardini A.F., "Characterization of Flaws in U.S. Reactor Pressure Vessels: Density and Distribution of Flaw Indications in PVRUF", NUREG/CR-6471, Vol. 1, U.S. Nuclear Regulatory Commission, Washington, D.C, 1998.

[97]   Schuster G.J., Doctor S.R., and Heasler P.G., "Characterization of Flaws in U.S. Reactor Pressure Vessels: Validation of Flaw Density and Distribution in the Weld Metal of the PVRUF Vessel", NUREG/CR-6471, Vol. 2, U. S. Nuclear Regulatory Commission, Washington, D.C., 2000.

[98]   Schuster G.J., Doctor S.R., Crawford S.L., and Pardini A.F., "Characterization of Flaws in U.S. Reactor Pressure Vessels: Density and Distribution of Flaw Indications in the Shoreham Vessel", NUREG/CR-6471, Vol. 3, U. S. Nuclear Regulatory Commission, Washington, D.C., 2000.

[99]   Jackson D.A. and Abramson L., "Report on the Results of the Expert Judgment Process for the Generalized Flaw Size and Density Distribution for Domestic Reactor Pressure Vessels", U.S. Nuclear Regulatory Commission Office of Research, FY 2000-2001 Operating Milestone 1A1ACE, 1999.

[100] Chapman O.J.V., Simonen F.A., "*RR-PRODIGAL—A Model for Estimating Probabilities of Defects in Welds*", NUREG/CR-5505. US Nuclear Regulatory Commission, Washington, DC, 1998.

[101] M.T. Kirk, C.S. Santos, E.D. Eason, J.E. Wright, and G.R. Odette, "Updated Embrittlement Trend Curve for Reactor Pressure Vessel Steels," Paper No. G01-5, Transactions of the 17th International Conference on Structural Mechanics in Reactor Technology (SMiRT 17), Prague, Czech Republic, August 17-22, 2003.

[102] E.D. Eason, G.R. Odette, R.K. Nanstad, and T. Yamamoto, A Physically-Based Correlation of Irradiation-Induced Transition Temperature Shifts for RPV Steels, Oak Ridge National Laboratory, ORNL/TM-2006/530,2006.

[103] NUREG/CR-6986. Evaluation of Structural Failure Probabilities and Candidate Inspection Programs. United States Nuclear Regulatory Commission. 2009.

[104] Energoatomizdat, "PNAE G-7-010-89. Equipment and pipelines of nuclear energy facilities. Welded joints and beads. Testing rules", Moscow, 1989.

[105] GP NAEK "ENERGOATOM", "Typical program for periodical in service inspection of base metal, welds and claddings of components and piping in WWER-1000 NPPs, (AIEY-9-04), PM-T.0.03.061-04", Kyiv, 2004.

[106] Král P., Macek J., Meca R., Hofmann E., Trnak M.: Thermal Hydraulic Analyses for Optimization Hydroaccumulator Parameters in VVER-440, NURETH-14, September 2011.

[107] Kral P., Vyskocil L.: Thermal Hydraulic Analyses for PTS Evaluation. Comparison of Temperature Fields at RPV Predicted by System TH Code and CFD code, ICONE 26, July 2018.

[108] Keim E. et al., "*Brittle Fracture Safety Analysis of German RPVs Based on Advanced Thermal Hydraulic Analysis*" PVP2008-61188, ASME 2008 Pressure Vessels & Piping Conference, ASME.

[109] NUREG/IA-0116, "*Assessment of RELAP/MOD3/V5m5 Against the OPTF Test No. 11 (Countercurrent Flow in PWR Hot Leg)*", May 1993 (https://www.nrc.gov/docs/ML0625/ML062550491.pdf)

[110] B. Richard Bass, Terry L. Dickson, Paul T. Williams, Hilda B. Klasky, and Robert H. Dodds, Jr., The Effect of Shallow Inside-Surface-Breaking Flaws on the Probability of Brittle Fracture of Reactors Subjected to Postulated and Actual Operational Cool- Down Transients: A Status Report, ORNL/TM-2015/59531/REV-01, Oak Ridge National Laboratory, February 2016, NRC ADAMS ML16043A170.

[111] J. Sievers, H. Schulz, R. Bass, C. Pugh: Final Report on the Reactor Pressure Vessel Pressurized Thermal Shock International Comparative, Assessment Study, GRS – 152.

[112] H. Rathbun, L. Fredette, P. Scott, A. Csontos: NRC Welding Residual Stress Validation Program International Round Robin Program and Findings,   ASME 2011 Pressure Vessels and Piping, PVP 2011-57642.

[113] ENPOWER – Management of nuclear plants operation by optimising weld repair, Final Technical Summary Report, FIKS-CT-2001-00167.

[114] ASME Boiler and Pressure Vessel Code, Section XI, Appendix G, "*Fracture Toughness Criteria for Protection Against Failure*", New York, 2004.

[115] T. L. Dickson, B. R. Bass, and W. J. McAfee, "The Inclusion of Weld Residual Stress in Fracture Margin Assessments of Embrittled Nuclear Reactor Pressure Vessels," PVP-Vol. 373, Fatigue, Fracture, and Residual Stresses, ASME Pressure Vessels and Piping Conference, (1998) 387-395.

[116] J. A. Keeney, et al., Preliminary Assessment of the Fracture Behavior of Weld Material in Full-Thickness Clad Beams, NUREG/CR-6228 (ORNL/TM-12735), Oak Ridge National Laboratory, Oak Ridge, TN, October 1994.

[117] B. Richard Bass, Paul T. Williams, Terry L. Dickson, and Hilda B. Klasky, "Assessment of a Stress-Free Temperature Model for Residual Stresses in Surface Cladding of a Reactor Pressure Vessel," PVP2017-65255, Proceedings of the ASME 2017 Pressure Vessels and Piping Conference, PVP2017 July 16-20, 2017, Waikoloa, Hawaii.

[118] Czech large experimental programme, which was conducted in 2006 – 2008 within a large research project focussed on WPS, funded by the Czech national regulatory body (SONS, State Office for Nuclear Safety).

[119] V. V. Pokrovsky, V. T. Troshchenko, G. A. Kopcmsky, V. G. Kaplunenko, V. G. Fiodorov, and Yu. G. Dragunov. The Influence of Plastic Prestraining on Brittle Fracture Resistance of Metallic Materials with Cracks // Fatigue & Fracture of Engineering Materials & Structures. 1995. – Vol. 18, No. 6. – pp. 731-746. https://doi.org/10.1111/j.1460-2695.1995.tb00897.x.

[120] P.V. Yasnii, Plastically Deformed Materials: Fatigue and Crack Resistance, [in Ukrainian], Svit, Lviv 1998.

[121] IAEA, 1997, "Guidelines on Pressurized Thermal Shock Analysis for WWER Nuclear Power Plants", IAEA-EBP-WWER-08. Vienna.

[122] V.F. Gonzalez-Albuixech, G. Qian, M. Sharabi, M. Niffenegger, B. Niceno, N. Lafferty, Integrity analysis of a reactor pressure vessel subjected to a realistic pressurized thermal shock considering the cooling plume and constraint effects, Engineering Fracture Mechanics, 2016.

[123] Robert E. Melchers, Andre T. Beck, "Structural Reliability Analysis and Prediction, 3rd Edition, 2018.

[124] K. Heckmann, R. Alzbutas, M. Wang, T. Jevremovic, B. O.Y. Lydell, J. Sievers, X. Duan, "Comparison of sensitivity measures in probabilistic fracture mechanics", International Journal of Pressure Vessel and Piping, Vol. 192, 2021.

[125] Li Y., Uno S., Masaki K., Katsuyama J., Dickson T., Kirk M., "Verification of probabilistic fracture mechanics analysis code through benchmark analyses", PVP2018-84963.

[126] J.P. Boris. New insights into large eddy, Fluid Dynamics Research, Vol. 10, No. 2, pp. 199-228, 1992.

[127] J. Mahaffy et al., Best Practice Guidelines for the Use of CFD in Nuclear Reactors Safety Applications, NEA/CSNI/R(2007)5.

[128] F.R. Menter. Two-equation eddy-viscosity turbulence models for engineering, AIAA Journal, Vol. 32, No. 8, pp. 1598–1605, 1994.

[129] C. Boyd, Pressurized Thermal Shock, THICKET 2008, pp. 463-472, 2008.

[130] H. P. Nourbakhsh and T. G. Theofanous, A Criterion for Predicting Thermal Stratification Due to High-Pressure Injection in a Circulating Reactor Loop, Nuclear Science and Engineering, Vol. 94, No. 1, pp. 77-79, 1986.

[131] ROSA V Large Scale Test Facility (LSTF) System Description for the Third and Fourth Simulated Fuel Assemblies, Tokai Research Establishment, Japan Atomic Energy Research Institute, 2003.

[132] JAERI, Final Data Report of OECD/NEA ROSA Project Test 1-1. Thermohydraulic Safety Research Group, Nuclear Safety Research Centre, Japan Atomic Energy Agency, 2008.

[133] S. Kliem, T. Sühnel, U. Rohde, T. Höhne, H.-M. Prasser, F.-P. Weiss, Experiments at the mixing test facility ROCOM for benchmarking of CFD codes, Nucl. Eng. Des. 238, 566-576, 2008.

[134] N. Mérigoux, J. Laviéville, S. Mimouni, M. Guingo, C. Baudry, S. Bellet, 2015. Verification, validation and application of NEPTUNE_CFD to two-phase pressurized thermal shocks. In: Proc. NURETH-16, Chicago, August 30–September 14, 2015.

[135] N. Mérigoux, P. Apanasevich, J.-P. Mehlhoop, D. Lucas, C. Raynaud, A. Badillo, CFD codes benchmark on TOPFLOW-PTS experiment, Nuclear Engineering and Design 321, 288–300, 2017. http://dx.doi.org/10.1016/j.nucengdes.2016.10.030.

[136] F. X. Dolan, J. A. Valenzuela, Thermal and Fluid Mixing in 1/2-Scale Test Facility, Facility and Test Design Report, NUREG/CR-3426, EPRI NP-3802, Creare TN-384, Vol.1, R4.

[137] J. A. Valenzuela, F. X. Dolan, Thermal and Fluid Mixing in 1/2-Scale Test Facility, Data Report, NUREG/CR-3426, EPRI NP-3802, Creare TN-384, Vol.2, R4.

[138] Transient Cooldown in a Model Cold Leg and Downcomer, Interim Report, EPRI NP-3118, May 1983.

[139] H. Tuomisto, P. Mustonen, Thermal Mixing Tests in a Semiannular Downcomer With Interacting Flows From Cold Leg, NUREG/IA-0004, 1986.

[140] T.G. Theofanous, K. Iyer, H.P. Nourbakhsh, P. Gherson, Buoyancy Effects in Overcooling Transients Calculated for the NRC Pressurized Thermal Shock Study, (1986), NUREG/CR-3702.

[141] L. Wolf, U. Schygulla, F. Gorner and G.E. Neubrech, Thermal mixing processes and RPV wall loads for HPI-emergency core cooling experiments in the HDR-pressure vessel, Nuclear Engineering and Design 96, 337-362, 1986.

[142] L. Wolf, U. Schygulla, W. Häffner, K. Fischer and W. Baumann, Results of thermal mixing tests at the HDR-facility and comparisons with best-estimate and simple codes, Nuclear Engineering and Design 99, 287-304, 1987.

[143] J.N. Reyes, J.T. Groome, A.Y. Lafi, D. Wachs, C. Ellis, PTS thermal hydraulic testing in the OSU APEX facility, International Journal of Pressure Vessels and Piping 78, 185-196, 2001.

[144] J.N. Reyes, et al., Final Report for the OSU APEX-CE Integral Test Facility, NUREG/CR-6856, U.S. Nuclear Regulatory Commission, 2004.

[145] P. Weiss, R. Emmerling, R. Hertlein, J. Liebert, UPTF experiment refined PWR LOCA thermal-hydraulic scenarios: conclusions from a full-scale experimental program, Nuclear Engineering and Design 149, 335 347, 1994.

[146] K. Umminger, W. Kastner, J. Liebert, T. Mull, Thermal hydraulics of PWRS with respect to boron dilution phenomena. Experimental results from the test facilities PKL and UPTF, Nuclear Engineering and Design 204, 191–203, 2001.

[147] P. S. Damerell, J. W. Simons, 2D/3D Program Work Summary Report, NUREG/IA-0126, 1993.

[148] M. Scheuerer, M. Weis, Transient computational fluid dynamics analysis of emergency core cooling injection at natural circulation conditions, Nuclear Engineering and Design 253, 343–350, 2012. http://dx.doi.org/10.1016/j.nucengdes.2011.08.063.

[149] U. Rohde, S. Kliem, B. Hemstr€om, T. Toppila, Y. Bezrukov, The European Project FLOMIX-R: Description of the Slug Mixing and Buoyancy Related Experiments at the Different Test Facilities (Final Report on WP 2), FZR, Forschungszentrum Rossendorf, 2005.

[150] H.M. Prasser, Basic test section design and parameters, Deliverable D1-02 of the TOPFLOW-PTS Experimental Program, Revision 4, 2010.

[151] A. Martin, C. Raynaud, P. Péturaud, C. Heib, F. Dubois, F. Huvelin, A. Barbier, Pre test calculations on TOPFLOW PTS experiment with Neptune_CFD code, Proceedings of the ASME 2011 Pressure Vessels & Piping Division Conference PVP2011, Baltimore, Maryland, 2011.

[152] P. Péturaud, U. Hampel, A. Barbier, J. Dreier, F. Dubois, E. Hervieu, A. Martin, H.M. Prasser, General overview of the TOPFLOW-PTS experimental program, Proceedings of NURETH-14, Toronto, Ontario, 25-30 September, 2011.

[153] C. Vallée, D. Lucas, M. Beyer, H. Pietruske, P. Schütz, H. Carl, Experimental CFD grade data for stratified two-phase flows, Nuclear Engineering and Design 240, pp. 2347–2356, 2010. http://dx.doi.org/10.1016/j.nucengdes.2009.11.011.

[154] R. Kadi, S. Aissani, A. Bouam, Numerical simulation of the direct contact condensation phenomena for PTS-related in single and combined-effect thermal hydraulic test facilities using TransAT CMFD code. Nuclear Engineering and Design 293, 2015.

[155] D. Orea, R. Vaghetto, T. Nguyen, Y. Hassan, Experimental measurements of flow mixing in cold leg of a pressurized water reactor. Annals of Nuclear Energy 140, 2020.

[156] P. Coste, J. Laviéville, J. Pouvreau, C. Baudry, M. Guingo, A. Douce, Validation of the Large Interface Method of NEPTUNE CFD 1.0.8 for Pressurized Thermal Shock (PTS) applications. Nuclear Engineering and Design 253, 2012.

[157] A. Janicot, D. Bestion, Condensation modelling for ECC injection. Nuclear Engineering and Design 145, pp. 37-45, 1993.

[158] P. Coste, A. Ortolan, Two-phase CFD PTS validation in an extended range of thermohydraulics conditions covered by the COSI experiment. Nuclear Engineering and Design 279, 2014.

[159] S. Kliem, B. Hemström, Y. Bezrukov, T. Höhne, U. Rohde, 2007. Comparative evaluation of coolant mixing experiments at the ROCOM, Vattenfall, and Gidropress test facilities. Sci. Technol. Nucl. Install. 2007.

[160] M. Gavrilas und T. Höhne, OECD/CSNI ISP NR. 43 Rapid Boron Dilution Transient Tests for Code Verification Post Test Calculation with CFX-4, Forschungszentrum Rossendorf, FZR-325, 2001.

[161] K.T. Kiger, F. Gavelli, Boron mixing in complex geometries: flow structure details, Nucl. Eng. Des. 208, pp. 67–85, 2001.

[162] M. Iguchi, K. Okita, F. Yamamoto, Mean velocity and turbulence characteristics of water flow in the bubble dispersion region induced by plunging water jet. Int. J. Multiphase Flow 24 (4), pp. 523–537, 1998.

[163] H. Tuomisto: Overcooling Transient Selection and Thermal Hydraulic Analyses of the Loviisa PTS Assessment, IAEA Specialists on Methodology for PTS Evaluation, 1997.

[164] D. Lucas, D. Bestion, P. Kral et al: Identification of Relevant PTS Scenarios, State of the Art of Modelling and Needs for Model Improvements, NURESIM, 2008.

[165] D. Lucas, Deliverable D2.1.1: Identification of Relevant PTS-Scenarios, State of the Art of Modelling and Needs for Model Improvements, European Commission, 6th Euratom Framework Programme 2005-2008.

[166] G. Qian, M. Niffenegger, M. Sharabi, N. Lafferty, Effect of non-uniform reactor cooling on fracture and constraint of a reactor pressure vessel, Fatigue and Fracture of Engineering Materials and Structures, 41(7), pp. 1559-1575, 2018. https://doi.org/10.1111/ffe.12796.

[167] X. Ruan, K. Morishita, Pressurized thermal shock analysis of a reactor pressure vessel for optimizing the maintenance strategy: Effect of asymmetric reactor cooling, Nuclear Engineering and Design 373, 2021. https://doi.org/10.1016/j.nucengdes.2020.111021.

[168] Sam J., Oliver Residual Stresses in Clad Nuclear Pressure Vessels and Their Interaction with Thermal and Mechanical Load, PhD Thesis, Department of Mechanical Engineering, University of Bristol, 2018.

[169] Carsten Ohms, Residual Stresses in Thick Bi-metallic Fusion Welds: a Neutron Diffraction Study, PhD Thesis, Delft University of Technology, 2013.

[170] Daniel Mångård and Jens Gunnars, Weld Residual Stress through a Strip Cladded Block - Experimental Measurements (to appear as an SSM-report), 2021.

[171] Mechanical behaviour of materials in case of postulated incipient cracks in pressurized components with pre-loaded crack tip due to loadings caused by rapid cooling processes; point of interest: influence of varying material properties and specimen sizes MPA Final Report 86 67 00 000, 1997.

[172] Mechanical behaviour of materials in case of postulated incipient cracks in pressurised components with pre-loaded crack tip due to loadings caused by rapid cooling processes; point of interest: influence of crack length and strain rate, IWM Final Report T3/98, Freiburg, 1998.

[173] Mechanical behaviour of materials in case of postulated incipient cracks in pressurised components with pre-loaded crack tip due to loadings caused by rapid cooling processes, BAM Final Report 234, Berlin, 2000.

[174] Mechanical behaviour of materials in case of postulated incipient cracks in pressurised components with pre-loaded crack tip due to loadings caused by rapid cooling processes; point of interest: influence and importance of microstructure and micro-geometry Final Report 03/98, Otto-von-Guericke University, Magdeburg, 1998.

[175] MPA/VGB Research Project 5.1 Investigation of Warm Prestress Effect. Final Report 944 705 100 (12/1998).

[176] ASME Boiler and Pressure Vessel Code Case N-830 "*Direct Use of Master Fracture Toughness Curve for Pressure-Retaining Materials of Class 1 Vessels Section XI, Division 1*", 2014.

10 Annexes

Annex A.   Task 1.1 Partner Questionnaire

1. **In what cases do you take into consideration RS for RPV integrity assessment in case of PTS?**

    Please, cover the following points mainly and feel free to add any other information:

    a. What are the critical locations and environments where RS should be considered? (We suggest distinguishing welds, HAZ due to weld, cladding, HAZ due to cladding.)

    b. For what PTS analyses should RS be considered? (We suggest different consideration of RS for normal operating conditions and for emergency conditions. Please, consider not only brittle fracture but also stable crack growth (upper-shelf fracture toughness)).

2. **Describe your methodology to determine RS focusing on three main topics:**

    2a. RS taken from standards (or other literature)

    2b. RS calculations (maybe distinguished to detailed and simplified)

    2c. RS based on measurement

    Please, cover the following points mainly and feel free to add any other information:

    a. What are the basic assumptions?

    b. What kinds of inputs are needed? (e. g. duration of tempering and tempering temperature; not only for detailed FEM simulation of welding and heat treatment, but also for determination of the residual stress profiles from the standards)

    c. Do you use predefined residual stress (strain) profiles from standards (or based on testing) or detailed FEM modelling of residual stresses for PTS assessment?

    d. Which software, code, procedure, in-house solution is used?

    e. How do you take into consideration the RS redistribution due to pressure test and/or operational load?

    f. How have the uncertainty distributions been derived?

    g. How do you validate your method?

    h. Do you have any published work/result or suggested references related this point?

3. **Do you have any experimental experience?**

    Please, cover the following points mainly and feel free to add any other information:

    a. Which parts of the RPV have been tested?

    b. Did you have any measurements on real components?

    c. Please, describe the geometry of the mock-ups used for residual stress testing (e. g. plate or cylindrical geometry).

    d. How did you measure the RS (measurement method)?

    e. What are your conclusions from the tests?

    f. Do you have any published work/result or suggested references related this point?

4. **How do you take into consideration RS for PTS assessment of RPV?**

   (e.g. direct introduction of stresses to FEM, direct introduction of strains to FEM, artificial RPV loading to introduce stresses similar to RS, supplement to KI determined analytically, …)

   Please, cover the following points mainly and feel free to add any other information:

   a. Do you consider RS for ageing? If yes, be so kind to introduce it shortly!

   b. RS effect on crack initiation, propagation, arrest and stable crack growth

   c. Do you use the same approach for deterministic and probabilistic assessment in what regards residual stresses?

   d. How do you treat stresses due to different thermal expansion coefficient of the base (weld) metal and cladding? Are they included in your residual stress profiles?

   e. Please, describe your method to include residual stresses (residual stress profiles) into the assessment in case you use nonlinear (elasto-plastic) calculations of the stress-strain field (on mesh with crack). (mostly relevant for deterministic PTS assessment only)

   f. How are the uncertainties in residual stresses treated in your probabilistic PTS calculations? (Do you use any statistical distribution for residual stress magnitude or spatial distribution?)

5. **What are the knowledge gaps concerning RS based on your opinion? Please, give information about your national or international projects related to RS!**

   Please, cover the following points mainly and feel free to add any other information:

   a. Completed

   b. Ongoing

   c. Planned

6. **What is your overall point of view concerning role of residual stress in LTO focusing on RPV and PTS?**

   Please, cover the following points mainly and feel free to add any other information:

   a. Importance

   b. Relevance

   c. Any other issues

Annex B.   Task 1.2 Partner Questionnaire

A) National approach to WPS application in PTS assessment

1. Is WPS applied in your country?
    If the answer is no – give the reasons, please.

2. Which standard do you use, where WPS is implemented?

3. Describe the WPS approach (and WPS model on which the WPS approach is based) used in your country for PTS assessment
    The answer should include restrictions for WPS application (for instance monotonic/non-monotonic, Case 1-3, additional safety margins, additional restrictions for WPS application) and the list of references.

4. Describe experimental data related to the WPS effect based on which the WPS approach was implemented into your national standard (e.g. materials, irradiated/non irradiated specimens, types of specimens, WPS regimes, approximate number of specimens).

5. WPS and constraint effect (shallow crack effect and/or biaxial loading effect), are they applicable simultaneously in PTS assessment (according to your national standard)?

6. WPS and crack arrest, are they applicable simultaneously in PTS assessment (according to your national standard)?

7. According to your national standard, can WPS approach be applied to irradiated (embrittled) material? Is there any limit on ductility, embrittlement or fluence with regard to WPS applicability?

B) Other WPS issues

8. What is your overall opinion concerning WPS consideration in the RPV PTS assessment?

    The answer should cover: WPS importance, relevance and any other issues.

9. Which of the WPS models or national regulatory WPS approaches do you find as the most sophisticated (most suitable) one and why? E.g. from the point of view of physical relevance (accordance with WPS experiments, conservativeness but not overconservativeness, simplicity of application, theoretical justification, etc.)

10. Do we need to perform variative TH calculations for one and the same transient in order to obtain different K^{max} and K^{min} values with subsequently obtaining the most conservative maximum allowable transition temperature?

11. Should a WPS approach be applied in probabilistic calculations of RPV brittle fracture?
    If yes, do we need to give the WPS model a probabilistic nature?

12. Can we use WPS approach in case of loading path (K^{max} or K^{WPS}) exceeding the upper shelf of fracture toughness (FT) curve (e.g. 200 MPa*$^{m0.5}$)?

13. Is it necessary to change the approach to conservative selection of PTS scenarios and input parameters for TH analyses, if WPS approach is applied?

C) Additional requests

14. Can you provide some of your national experimental data related to the WPS effect and/or results of international projects you participated in?

15. Can you provide the SIF versus temperature data for two or three representative transients (according to your opinion) to be evaluated using different WPS models?

16. In case the SIF versus temperature data are provided (in relation to point 15), can you evaluate RPV brittle fracture margin (i.e. maximum allowable transition temperature) for these representative transients with using WPS approaches that are already implemented in your calculation tools?

Annex C.   Task 1.3 Partner Questionnaire

1. Methodology for Thermal-Hydraulics Analysis of PTS

Several options are available for the thermal-hydraulic analysis of the system thermal-hydraulics and detailed flow distribution in the downcomer for PTS scenarios. These include system thermal-hydraulics analysis codes, CFD analysis codes, and mixing codes. The purpose of this question is to assess which methods are most commonly used for PTS analysis and whether any special techniques or methodologies have been developed to improve predictions. Finally, the question also aims to assess the current state of validation of the different simulation codes.

   a. Please provide a description of your organisation/country's current approach (methodology) for thermal-hydraulic analysis of PTS scenarios. Describe the type of codes used (e.g. system, mixing code, CFD) and how the data is exchanged in the case of coupled analyses.
   b. Please provide a basic description of what systems and components have been included in your organisation/country's analysis models and provide a basic description of the nodalisation.
   c. What PTS-specific verification and validation (V&V) of this methodology has been carried out by your organisation/country?

2. PTS Accident Scenarios

A large spectrum of postulated plant transients and accidents can lead to PTS (LOCA, stuck open safety relief valves, feed-and-bleed, etc.). The purpose of this question is to determine which scenarios have been considered in the past, which scenarios are considered important, and whether any specific assumptions and methodologies have been applied in the past analyses that should ideally be addressed in the future.

   a. Please provide an overview of the PTS scenarios that have been considered by your organisation/country in the past.
   b. What methodology has been used for which scenarios?
   c. What basic analysis assumptions have been applied that might affect the quality/validity of the predicted thermal-hydraulic parameters?

3. Best-estimate Plus Uncertainty Methodology for Thermal-Hydraulics Analysis of PTS

The application of uncertainty quantification (UQ) methods to the thermal-hydraulics analysis of PTS scenarios is relatively unexplored. The purpose of this question is to assess the status of thermal-hydraulics UQ methods, with a focus on PTS analysis.

   a. Does your organisation/country have a well-established uncertainty quantification (UQ) methodology and has this been applied successfully to PTS TH analysis in the past? If so, please provide a description of the methodology.
   b. What methodology has been used to identify and rank the most important uncertain parameters?
   c. How have the uncertainty distributions been derived?
   d. What PTS-specific V&V of this methodology has been carried out by your organisation/country?

4. Coupled TH/Fracture Mechanics UQ Methodology

The purpose of thermal-hydraulics simulations for PTS is to provide boundary conditions for downstream structural analysis simulations. The complete PTS analysis chain is therefore a multi-physics simulation where we need to propagate uncertainties downstream to the structural analyses.

There are many approaches for multi-physics uncertainty propagation, and this topic has been the focus of several international projects in the past (OECD/NEA UAM benchmarks, etc.). The purpose of this question is to assess what methods are available to the partners for propagating uncertainties through the complete simulation chain.

   a. Does your organisation/country have an established methodology for multi-physics uncertainty propagation? If so, please describe your basic methodology for propagating uncertainties from one code to the next.
   b. Has this methodology been successfully applied for PTS analysis in the past? If yes, please elaborate on the outcomes of this work.

5. Human Interactions

Many PTS scenarios are the direct result of human interactions with the system, e.g. feed-and-bleed, blowdown during SB-LOCA scenarios. Such interactions are often accounted for in probabilistic risk assessments, but accounting for them in deterministic simulations is less common. The purpose of this question is to assess to what extent human interactions are accounted for in PTS simulations and how this has been done in the past.

   a. Has your organisation/country considered the impact of human interactions (e.g. timing of operator actions, erroneous operator actions) on PTS TH analysis?
   b. If so, please give a short summary of what human interactions were considered and the methodology used to incorporate the uncertainty in human interactions. If applicable, please elaborate on the outcomes of this work.

Annex D.   Task 1.4 Partner Questionnaire

1. Describe your tool/software for probabilistic PTS assessment

The description should include:
   a. Name and kind (Commercial/in-house) of software
   b. Method for calculation of probability including convergence criteria (e.g. for Monte Carlo)
   c. Events considered (initiation, arrest, failure) for probability calculation
   d. Methods for sampling of distributed parameters
   e. Validation and Verification of software

A flow chart will be very helpful to understand and compare the tools/software

2. Describe your assessment of the whole spectrum of PTS scenarios

Remark: Only relevant if you are able to combine results from several PST transients to an overall failure frequency.
The description should include:
   d. How are PTS events grouped together to cover the whole PTS spectrum?
   e. Where does the PTS event frequencies (probability of occurrence) come from? Probabilistic Safety Assessment (PSA) or other sources?
   f. How are the conditional probabilities of each analysed PTS transient combined together to get an overall failure frequency? (post-processing?)

3. Describe the scope of the assessment and treatment of RPV loading
   a. The description should include:
   b. Do you perform 1D, 2D or 3D temperature and stress calculations? Using elastic or elasto-plastic formulation? Using FEM mesh with or without crack?
   c. What regions of RPV do you assess (RPV beltline welds and rings, possibly also nozzles and other regions)?
   d. Do you consider regions of cold plume? (using simplified formula or full 3D calculation?)
   e. Do you combine results from different regions to an overall probability? And if yes how?
   f. How are residual stresses (due to cladding and welds) quantified and modelled?

4. Describe the fracture mechanics models used in your tool/software for probabilistic PTS assessment

The description should include:
   h. Damage Mechanisms Models (e.g. ductile crack growth)
   i. Stress intensity factor solutions and plastic correction, if applied
   j. Brittle and/or ductile crack initiation
   k. Crack arrest model
   l. Cracks interaction and proximity rules, if multiple flaws are assessed
   m. Global/Local failure
   n. WPS model

5. What input data are distributed (with exception of flaws) and what is the basis for distribution parameters (standard/code or statistical data)

The answer should include:
    d. Summary of distributed input data
    e. Type of distribution and sources of distribution parameters
    f. Technical or statistical basis (such as operational experience, material testing, standards, engineering judgement and others) for type of distribution and distribution parameters

Answer:

Input data	Type of distribution	Distribution parameters	Technical or statistical basis for type of distribution and distribution parameters	Method for sampling, see also 1. d)

6. What flaw distribution (type, parameters) is used and what is the technical/statistical background

The answer should include:
- Type of flaws to be addressed (surface, underclad, etc.)
- Flaw size distribution and technical/statistical background
- Flaw shape (aspect ratio) distribution, other flaw parameters (orientation) and their technical/statistical background
- Distribution of number of flaws (flaw density) and technical/statistical background
- Role of NDE (if any) for determination and/or validation of flaw density, flaw size and other flaw parameters distributions.

7. Describe performed applications

The answer should include:
    a. Brief description of performed probabilistic PTS analysis performed by your organization (e.g. for licensing of a NPP, support for NPP LTO, only research projects)
    b. Main results (initiation/failure probability or frequency)
    c. Recommendations for further assessments
    d. What acceptance criteria were used in your analyses?
    e. Description of normative requirements and/or recommendations that are applicable in your country for probabilistic PTS assessment.

8. Describe identified improvements for further applications

The answer should include:
    a. Identified improvements from performed assessments (see also question #6)
    b. Identified improvements due to lack of information
    c. Identified improvements due to enhanced probabilistic methods
    d. Identified improvements due to customer needs
    e. Identified improvements in the software tool